

TRANSPORTATION RESEARCH
RECORD

No. 1495

*Highway Operations, Capacity,
and Traffic Control*

**Traffic Control Devices,
Visibility, and
Railroad Grade Crossings**

A peer-reviewed publication of the Transportation Research Board

**TRANSPORTATION RESEARCH BOARD
NATIONAL RESEARCH COUNCIL**

NATIONAL ACADEMY PRESS
WASHINGTON, D.C. 1995

Transportation Research Record 1495

ISSN 0361-1981

ISBN 0-309-06160-1

Price: \$35.00

Subscriber Category

IVB highway operations, capacity, and traffic control

Printed in the United States of America

Sponsorship of Transportation Research Record 1495

**GROUP 3—OPERATION, SAFETY, AND MAINTENANCE OF
TRANSPORTATION FACILITIES**

Chairman: Jerome W. Hall, University of New Mexico

Facilities and Operation Section

Chairman: Jack L. Kay, JHK & Associates

Committee on Traffic Control Devices

Chairman: Jonathan Upchurch, Arizona State University

Rahim F. Benekohal, Arthur H. Breneman, Linda L. Brown, E. Nels Burns, Benjamin H. Cottrell, Jr., Daniel J. Gilliam, H. Gene Hawkins, Jr., Joseph L. Henderson, Bahman Izadmehr, Feng-Bor Lin, John J. Logan, Richard W. Lyles, Martin T. Pietrucha, A. Essam Radwan, Stephen H. Richards, Michael Robinson, Robert K. Seyfried, Steven R. Shapiro, Howard S. Stein, Dwight L. Stevens, Gerald L. Ullman, W. Scott Wainwright

Committee on Visibility

Chairman: John B. Arens, Federal Highway Administration

Peter G. Contos, Eugene Farber, Mark Freedman, Donald C. Harris, S. Allen Heenan, Ronald J. Hensen, Antanas Ketvirtis, L. Ellis King, Ken F. Kobetsky, David A. Kuemmel, Douglas J. Mace, Marc B. Mandler, Richard A. Mather, Herbert A. Odle, Richard Arnold Olsen, Justin J. Rennilson, Duco A. Schreuder, Richard N. Schwab, Richard E. Stark, Robert R. Wylie, Helmut T. Zwahlen

Committee on Railroad-Highway Grade Crossings

Chairman: Dr Brian L Bowman, Auburn University

Anya A. Carroll, Daniel B. Fambro, Bruce F. George, Lawrence E. Jackson, Susan J. Kirkland, Charles Raymond Lewis II, Richard A. Mather, Linda J. Meadow, G. Rex Nicholson, Jr., William T. O'Brien, Ernie Oliphant, Hoy A. Richards, Stephen H. Richards, Frank Donald Roskind, Eugene R. Russell, Sr., Timothy A. Ryan, John M. Schercinger, Cliff Shoemaker, Thomas D. Simpson, Robert C. Winans, Bing L. Wong, Thomas R. Zeinz

Transportation Research Board Staff

Robert E. Spicher, Director, Technical Activities

Richard A. Cunard, Engineer of Traffic and Operations

Nancy A. Ackerman, Director, Reports and Editorial Services

Sponsorship is indicated by a footnote at the end of each paper. The organizational units, officers, and members are as of December 31, 1994.

Transportation Research Record 1495

Contents

Foreword	vii
Effective Use of Variable Message Signs: Lessons Learned Through Development of Users' Manuals	1
<i>John S. Miller, Brian L. Smith, Bruce R. Newman, and Michael J. Demetsky</i>	
Motorist Interpretation of Yellow X and Yellow Diagonal Arrow in Freeway Lane Control Signal Array	9
<i>Steven D. Wohlschlaeger, Gerald L. Ullman, and Conrad L. Dudek</i>	
Effects of Pavement Markings on Driver Behavior at Freeway Lane Drop Exits	17
<i>Kay Fitzpatrick, Marty Lance, and Torsten Lienau</i>	
Comparative Study of Advance Warning Signs at High Speed Signalized Intersections	28
<i>Prahlad D. Pant and Yuhong Xie</i>	
Evaluation of Strobe Lights in Red Lens of Traffic Signals	36
<i>Benjamin H. Cottrell, Jr.</i>	
High-Volume Pedestrian Crosswalk Time Requirements	41
<i>Mark R. Virkler, Sathish Elayadath, and Geethakrishnan Saranathan</i>	
Empirical Analysis of Traffic Characteristics at Two-Way Stop-Controlled Intersections in Alaska	49
<i>Jian John Lu and B. Kent Lall</i>	
Evaluation of Proposed Minimum Retroreflectivity Requirements for Traffic Signs	57
<i>Cletus R. Mercier, Charles Goodspeed, Carole J. Simmons, and Jeffrey F. Paniati</i>	

Detectability of Pavement Markings Under Stationary and Dynamic Conditions as a Function of Retroreflective Brightness	68
<i>Gregory F. Jacobs, Thomas P. Hedblom, T. Ian Bradshaw, Neil A. Hodson, and Robert L. Austin</i>	
<hr/>	
Visibility of New Yellow Center Stripes as a Function of Obliteration	77
<i>Helmut T. Zwahlen, Toru Hagiwara, and Thomas Schnell</i>	
<hr/>	
Effects of Lateral Separation Between Double Center-Stripe Pavement Markings on Visibility Under Nighttime Driving Conditions	87
<i>Helmut T. Zwahlen, Thomas Schnell, and Toru Hagiwara</i>	
<hr/>	
Curve Radius Perception Accuracy as Function of Number of Delineation Devices (Chevrons)	99
<i>Helmut T. Zwahlen and Jin Young Park</i>	
<hr/>	
Knowledge-Based Personal Computer Software Package for Applying and Placing Curve Delineation Devices	107
<i>Helmut T. Zwahlen and Thomas Schnell</i>	
<hr/>	
Visibility of New Pavement Markings at Night Under Low-Beam Illumination	117
<i>Helmut T. Zwahlen and Thomas Schnell</i>	
<hr/>	
Loss of Visibility Distance Caused by Automobile Windshields at Night	128
<i>Helmut T. Zwahlen and Thomas Schnell</i>	
<hr/>	
Traffic Sign Reading Distances and Times During Night Driving	140
<i>Helmut T. Zwahlen</i>	
<hr/>	
Yellow Pavement Markings with Yellow Nighttime Color	147
<i>Gregory F. Jacobs and Norbert L. Johnson</i>	

**Application of Geographic Information Systems Rail-Highway Grade
Crossing Safety** 156
Ardeshir Faghri, and Sriram Panchanathan

**Evaluation of Accuracy of U.S. DOT Rail-Highway Grade Crossing
Accident Prediction Models** 166
M. I. Mutabazi and W. D. Berg



Foreword

The papers contained in this volume are primarily from the 74th Annual Meeting of the Transportation Research Board and the Symposium for Improving Visibility for the Night Traveler, which was held in May 1994 in Washington, D.C. They concern traffic signs and signals, highway visibility, and rail-highway grade crossing safety and research, addressing some of the problems and issues facing urban engineers as they grapple with the ever more complex traffic system.

Readers with a specific interest in traffic control devices will find papers related to effective uses of variable message signs, comprehension of various types of traffic control devices and their effects on driver behavior, pedestrian crosswalk time requirements, and empirical analysis of two-way stop-controlled intersections.

Readers with an interest in delineation and illumination will find papers on minimum retroreflectivity requirements, pavement marking visibility and detectability, curve delineation, traffic sign reading distances at night, and apparent nighttime color of pavement marking products.

Closing out this Record are papers addressing the application of GIS to rail-highway crossing safety and the accuracy of U.S. Department of Transportation rail-highway grade crossing accident prediction models.

All papers were peer reviewed and sponsored by the Committee on Traffic Control Devices, the Committee on Visibility, and the Committee on Railroad Highway Grade Crossings.

Effective Use of Variable Message Signs: Lessons Learned Through Development of Users' Manuals

JOHN S. MILLER, BRIAN L. SMITH, BRUCE R. NEWMAN,
AND MICHAEL J. DEMETSKY

In an effort to improve the operations of both portable and permanent (fixed-site) variable message signs (VMSs) in Virginia, a comprehensive research effort to develop operational guidelines was undertaken. These guidelines, presented in the form of users' manuals, were based on information obtained from the literature, VMS operators, and motorists. Issues addressed by the manuals include whether to use a VMS, where to place a portable VMS, and how to design a VMS message. The manuals are not simply a list of predefined messages; instead, they are composed of concise, readable modules designed to guide an operator through the thought process required to use a VMS effectively. An operator follows a logical decision tree as each module is completed, allowing effective use of the VMS as well as training the operator for use of the device. Key lessons learned in developing two such manuals for portable and permanent VMSs are highlighted. On the basis of theoretical calculations and motorists' experiences, it is strongly recommended that a VMS use no more than two message screens. A single message screen is preferred. VMSs should be used only to advise drivers of changed traffic conditions and to convey specific traffic information concisely. Because of limited information capabilities, VMSs should be used in conjunction with other means of communication such as highway advisory radio and static signs. Most importantly, it is crucial that credibility be maintained. Incorrect information can have disastrous consequences on VMS effectiveness.

The need to provide drivers with real-time information has spawned a dramatic increase in the use of variable message signs (VMSs). VMSs are programmable traffic control devices that display messages composed of letters, symbols, or both, and may be either permanently mounted or portable units. The VMS allows transportation officials to quickly inform motorists of abnormal traffic conditions. Although the ability of VMSs to display messages that describe current traffic conditions has made the signs popular, this added flexibility results in increased operational responsibility to ensure that the signs are used to their maximum benefit. Some VMSs are difficult to understand because word choices are confusing, messages contain too much information or are ambiguous, or placement of portable VMSs is poor.

This research sought to develop user's manuals that provide Virginia Department of Transportation (VDOT) field personnel sufficient detail to effectively use VMSs on the basis of the type of situation, predominant travel speed, time of day, goal of message, and type of sign (1). These manuals address questions such as

- Under what circumstances should VMSs be utilized?
- Where should a portable VMS be placed?

- What are the limits of the quantity of information that can be displayed?
- What information should be given to drivers?

Although a significant amount of VMS research has been conducted nationally, most of it has dealt with physical specifications of the signs rather than operational issues. The focal question of this research has been, Given the existing technology, how should VMSs be operated?

METHODOLOGY

Three information-seeking strategies were used for this project: a literature search, surveys of VDOT personnel, and discussions with drivers in the Commonwealth of Virginia. The literature review provided the base of the study, as a significant amount of VMS research had been conducted and needed to be assimilated into a concise format (2-6). Additional ideas were gleaned from other states' VMS guidelines (7-11). VDOT personnel played an important role because they are the primary users of the manuals, and their participation ensured the development of a product that meets their needs. Finally, motorists' reactions provided recommendations for improvements that make VMSs more useful to the driving population, the ultimate "customer" of traffic information.

RESULTS

The literature addressed the theoretical operation of VMSs, which provided a solid basis from which to construct the manuals. For example, one FHWA publication defined the components of an advisory message to be (a) a problem statement, (b) an effect statement, (c) an attention statement, and (d) an action statement. Such message deconstruction proved useful for understanding how to develop effective VMS messages and for forming the message design modules of the manuals. VMS usage was also addressed. For example, static signs should be used to complement the VMS and should be considered before the decision to use a VMS is made. Working with VDOT VMS operators, it became clear that previous research was not in an easily used form.

The outcome of the literature review, focus groups, and discussions and surveys involving VMS operators yielded six key lessons:

1. VMS operators need a user's manual—not a set of canned messages. Operators need final responsibility for how the VMS is used as well as the ability to respond to unforeseen applications. A list of suggested messages is ineffective, as variations in traffic conditions and available information are numerous. Clearly the operators need a product that is not overly restrictive but is much more substantive than simply authorizing the use of "engineering judgment." The product needs to take the form of a user's manual, which will assist operators but not replace their judgment.

2. VMSs should be used to advise the motorist of changed traffic conditions. Operators' field experience showed that VMSs should be used only to convey information about traffic abnormalities such as lane closures, delays, or sudden stoppages. VMS operators noted that motorists ignored greetings and general safety statements (e.g., "Please drive safely").

3. VMSs must meet motorist information needs. Specifically, the VMS should tell motorists what action is required of them. Messages such as "LANE CLOSED AHEAD" need to indicate which lane is being closed and the distance to that closure. General messages such as "SLOW SLOW SLOW" or "CAUTION" are useless, as they do not inform motorists about traffic conditions. Finally, word choice has a powerful impact. Motorists noted that the word "DETOUR" meant static signs would guide them along the alternate route, whereas the phrase "ALTERNATE ROUTE" means they must find that route on their own.

4. VMSs have limited information capabilities. VMSs can provide effective alternative route guidance for unfamiliar drivers only if used in conjunction with another information medium, such as static signs or highway advisory radio.

5. Credibility is crucial. Failure to confirm the message displayed by a VMS can have disastrous consequences in terms of the public's faith in future VMS messages. Motorists recalled instances in which the information was clearly wrong, such as warnings of construction activity at night when no construction was taking place.

6. VMSs should use no more than two message screens. Even though portable VMSs may display up to six different message screens, it is difficult at high speeds 88.6 kph (55 mph) for motorists to read a message with only two screens.

Motorists cited difficulties reading multiple screen messages because large vehicles blocked the line of sight, visibility conditions were poor, there were other distractions, or the sign was placed on the opposite shoulder. Messages longer than two screens can easily confuse motorists if they encounter such a VMS in midmessage, and VMS operators need to allow for this possibility.

Dudek's technique for determining the amount of time motorists have to read a VMS demonstrates that a portable VMS should employ only one or at most two message screens (3). For example, a portable three-line, eight-character-per line, flip-disk VMS will cease to be comfortably readable when the motorist gets very close to it. An equation to account for this distance from the VMS to the point at which it becomes unreadable is given as

$$\text{Unreadable Distance} = [S + (N - 0.33)*L + 0.5*W]*5.67 \quad (1)$$

where

- S = distance from the side of the road to the VMS [m (ft)],
- N = number of lanes,
- L = width of the lanes [m (ft)], and
- W = width of the VMS [m (ft)].

This unreadable distance may then be subtracted from the legibility distance, which is the distance at which the VMS becomes legible, to yield the distance for which the VMS may be read by the motorist. This calculation is shown in Equation 2.

$$\text{Readable Distance} = \text{Legibility Distance} - \text{Unreadable Distance} \quad (2)$$

The resultant readable distance may then be divided by the travel speed to compute the time for which the VMS is readable, as shown in Equation 3.

$$\text{Readable Time} = \frac{\text{Readable Distance}}{\text{Travel Speed}} \quad (3)$$

For example, suppose a VMS is mounted such that, as calculated by Equation 1, it has an unreadable distance of 61 m (200 ft). The literature states that in daylight conditions, a flip-disk VMS has a legibility distance of approximately 198 m (650 ft) (2; P. Garvey, unpublished data). Therefore, from Equation 2, one may compute the readable distance to be

$$198 \text{ m} - 61 \text{ m} = 137 \text{ m (450 ft)}$$

Substitution of this value and a travel speed of 88.6 kph (55 mph) into Equation 3 yields a readable time of about 6 sec.

Manual on Uniform Traffic Control Devices (MUTCD)-proposed guidelines specify that motorists must be able to read the entire VMS twice while traveling at the posted speed (12). Using Dudek's approximation that motorists need 1 sec to read each eight-character line, it will take 3 sec to read a screen once or 6 sec to read a screen twice. Thus for this particular example, an operator should ideally use a message with only one screen. (Even if one decides to display each screen for only 1.5 sec these computations show that no more than two message screens should be used.)

DISCUSSION

The most challenging task of this project was synthesizing the results into easy-to-read operator's manuals. The features of these manuals are discussed.

Use of Modules

The manuals were divided into separate modules designed to step an operator through the thought process involved in using a VMS (Figures 1 and 2). A module is a distinct thought process in the overall VMS message development. Each module serves as a check-point for ensuring that the correct decisions have been made, such as whether to use or where to place the VMS.

Using a logical flow of decision points, which is accomplished by dividing the manuals into modules, ensures that the VMS is used correctly. For example, one problem that operators often face is how to convey location information to motorists. Depending on the type of route, driver familiarity with the area, and amount of signing, it may be better to tell motorists that there is an accident at a particular exit near a well-known landmark or a certain number of miles away. If an operator is faced with this decision, Module 10, as indicated in Figure 2, quickly guides the operator to the correct usage. Furthermore, a progression of decision points allows an inexperienced operator to become familiar with the choices that should be

1. SHOULD A VMS BE USED?

A VMS is a tool for grabbing the motorist's attention. Therefore it should be used only when there is a specific message that needs to be conveyed to motorists: overuse of a VMS will cause motorists to ignore it and lessen its effectiveness.

All of the following statements should be true if a VMS is to be used.

- T F** Drivers are required to do something in response to the message such as:
- change travel speed,
 - change lanes,
 - divert to a different route, or,
 - be aware of a change in traffic conditions either now or in the future.
- T F** Where applicable, static signs which can effectively convey this message are not readily available.
- VMSs should be used to supplement, *rather than replace*, static signs that are required by law.
- T F** The VMS does not tell drivers something they already know.
- T F** Message accuracy can be confirmed from a reliable source such as State Police, a credible commercial traffic reporter, or visual inspection.
- T F** Traffic conditions may be monitored to detect significant changes such that the VMS may be removed or the message may be changed as soon as necessary.

IF all answers are True then proceed to 2.

IF any answers are False then stop.

FIGURE 1 Module 1.

made when using a VMS, thereby providing a training opportunity parallel with a VMS operation.

It is believed that the use of modules offers distinct advantages. First, modules facilitate the updating of the manuals, which must occur if they are to become and remain a useful tool. Second, modules streamline the VMS decision process: operators need only complete those modules that are necessary. Often, a decision in one module will eliminate the need to go through certain subsequent modules. Finally, modules present the information in a concise, user-friendly manner.

The example modules, shown in Figures 1 and 2, illustrate the diversity of input requirements and purposes for the modules. For example, the first module's purpose is to determine whether a VMS should be used; thus it should always be completed, and if successful then the result is to simply continue with the second module. However, the tenth module should be completed only if the operator needs to convey a distance or a location, and the tenth module's result is a recommended choice of words.

Integration of Modules: An Example Application

The portable VMS manual is divided into 17 modules, as shown in Figure 3, with each module designed to help the operator answer

one basic question: "Where should the VMS be located?" Figure 3 outlines the purposes and some considerations of each module as well as how the modules are integrated to guide the operator through the VMS decision process.

An example scenario briefly illustrates how the operator moves through these modules. Suppose an operator receives notification from the supervisor that a truck has crashed on a rural two-lane Interstate highway, resulting in a traffic queue and blockage of the left lane, although traffic can pass in the right lane. The goal of the first module (Figure 1) is to help the operator decide whether to use the VMS. In this case, the operator makes the decision to use the VMS; drivers are required to do something (change lanes); static signs that can inform motorists of an accident are not available; the VMS conveys new information to drivers (to merge right); message accuracy can be confirmed (by the supervisor); and the VMS operator will be on the scene to monitor traffic conditions. In the second module, the operator decides that the purpose of the VMS will be "current incident advisory." The operator then proceeds to the third module to determine the location of the VMS, considering factors such as access to the VMS, major decision points (in this case, Interstate exits), and the effect of future traffic backups. The VMS is thus placed upstream of an Interstate exit before the crash, and the VMS is placed off the shoulder in conjunction with Group II channelization devices (e.g., orange barrels) such that the VMS itself is not a

10. HOW SHOULD DISTANCES AND LOCATIONS BE CONVEYED?

IF a distance or a location is part of the message, then complete this module.
OTHERWISE go to 11.

When using a location or distance, the question arises as to whether the operator should give a distance ("ACCIDENT IN 3 MI"), an exit number ("ACCIDENT AFTER EX 100"), or the name of a prominent landmark ("ACCIDENT AT BROAD STREET"). In order to make this decision, complete this module.

T F The message applies **ONLY** to familiar drivers.

IF True, then consider the use of cross-streets, landmarks, and exit numbers and select the term that is best known by the local population. Go to 11.
IF False, then continue with this module.

T F The route is an interstate.

IF True, then continue with this module.
IF False, then give a distance in miles. Go to 11.

T F The exits are numbered sequentially (i.e. they do not correspond to mile markers).

IF True, then give a distance in miles. Go to 11.
IF False, then continue with this module.

T F At least one of the following are located within one mile after the VMS:

- an exit, or
- a static sign indicating a distance to an exit

IF True, then give the location as an exit number. Go to 11.
IF False, then give a distance in miles. Go to 11.

FIGURE 2 Module 10.

safety hazard. Had this been an urban area, the operator would have considered moving the VMS even further from the crash depending on previous experience with traffic congestion. In the fourth module, with traffic flowing past at 55 mph (88.6 kph), the operator decides to try and keep the message to one screen. Module 5 shows that because this is a "current incident advisory" type of usage, the operator should complete Module 6, which is the design of the current incident advisory message. In Module 6 the message is synthesized on the basis of the three components of a current incident advisory message: the problem component (an accident blocking the left lane), the *location* component [the incident is about 3 mi (4.9 km) away], and the *instruction* component (motorists should move out of the left lane and into the right lane or exit from the Interstate altogether). The operator tentatively envisions a message such as "accident—left lane closed—3 mi ahead—merge right." Note that this module discourages peripheral information, such as a description of the crash (e.g., "truck overturned"); instead, the goal is to establish the essential message elements.

The operator is now sent to Module 10, which is shown in Figure 2. Because the message applies to drivers both familiar and unfamiliar with the route and it is an Interstate, the operator arrives at the third true/false statement shown in that module. If the exit numbers were according to mile marker, then the operator would change the phrase "3 mi ahead" to refer to an exit, such as

"after exit 100." In this case, however, suppose exit numbers are sequential. Because there are travelers using the Interstate who might not be familiar with the distances between exits, Module 10 advises the operator to give a distance in miles and then proceed to Module 11. In Module 11, the operator realizes the word "ahead" is not necessary in the phrase "3 mi ahead." Module 12 is not applicable as the word "next" has been avoided in the message, so the operator proceeds to Modules 13 and 14, where the message is divided into multiple screens, abbreviations are considered, and the necessity of each screen is scrutinized. Supposing a three-line, eight-character-per-line VMS, the operator's first attempt might be as follows:

screen 1	screen 2
ACCIDENT	3 MILES
LEFT LANE	MERGE
CLOSED	RIGHT

The operator then uses abbreviations and develops the following message:

screen 1	screen 2
ACCIDENT	MERGE RIGHT
LEFT LN	3 MI
CLOSED	

Module	What operator accomplishes in this module	Some factors considered in completing the module
1. Should a VMS be used?	If successful, then goes to module 2. If unsuccessful, then stops.	Change in driver response required, ability of operator to confirm and maintain message accuracy, and inability of static signs to accomplish the task.
2. What is the purpose of the VMS?	Selects ONE of these four categories: (a) current incident or work zone advisory (b) diversion to an alternate route (c) guidance for a current special event. (d) advisory for a future event	Expected purpose of message.
3. Where should the VMS be located?	Determines an acceptable location with respect to the roadway and the condition being conveyed.	Roadway geometry, presence of major decision points, access to the VMS, sight distance, and future traffic backups.
4. What is the maximum number of screens that may be used?	Conveys to operator that 1 screen is ideal, two screens are acceptable, and 3 screens should be used only if absolutely necessary.	Driver inattention, MUTCD guidelines, amount of time required to read a VMS, legibility distance of a flip-disk VMS, and calculations detailed in Appendix A.
5. What is the message type?	Selects ONE of the following modules to complete: 6, 7, 8, or 9.	Category identified in module 2.
6. What is the message? (current incident or work zone advisory)	Designs a message considering problem, location, and instruction components.	Example message components, effect of sensationalist messages, and need to convey specific information to the motorist.
7. What is the message? (route diversion)	Designs a message considering audience, time saved, and instruction components.	Example message components, distinction between "alternate route" and "detour", and the need for "time saved" statement to be accurate or avoided.
8. What is the message? (guidance for a special event)	Designs a message considering audience and instruction components.	Example message components and names or events that motorists will recognize.
9. What is the message? (advisory for a <u>future</u> event)	Designs a message considering condition & location, time, and instruction components.	Example message components and time requirements (such as not describing future conditions more than one week in advance).
10. How should distances and locations be conveyed?	If locations or distances are needed, decides whether to use landmarks, exit numbers, or distances in the message.	Type of exit numbering scheme (sequential or by mile marker), familiarity of the driver population, and proximity of static signs.

FIGURE 3 Overview of portable VMS modules.

(continued on next page)

11. Are the words "TRAFFIC" and "AHEAD" used correctly?	If applicable, then verifies that these words are used correctly. For example, the message "BEACH TRAFFIC USE EXIT 5" may be shortened to "BEACH USE EXIT 5".	Readability of the message and number of screens used.
12. Is the word "NEXT" used only as necessary?	Ensures that use of the word "next" is not confusing when referring to an exit or turn. Considers options such as naming the exit or turn or replacing the word "next" with "first" or "this".	Whether the exit or turn is visible once the message is read, whether the road is an Interstate, and how well the exit or turn is marked with static signs.
13. How should the VMS message be sequenced?	If message is longer than 1 screen, then determines how message should be divided.	Motorists' comprehension of individual screens if read by themselves.
14. Is the message acceptable?	Verifies that message wording is effective.	Abbreviations, local signing, order of message information, and necessity of all screens.
15. How should the message be displayed?	Determines how to display the message with respect to font and amount of time each screen is shown.	Speed of traffic, increased legibility distances associated with single stroke fonts and upper case letters, and avoidance of blank screens.
16. Does the VMS pass the drive-through test?	Drives past the VMS at least once to verify its effectiveness.	Visibility of VMS, readability of message, driver environment, and the necessity of information conveyed.
17. When should the message be updated, modified, or discontinued?	Determines when to change the message or remove the VMS.	Message accuracy, timeliness of the message, current or expected changes in traffic conditions, and motorists' reaction to the VMS.
Appendix A: Why should a VMS use no more than two screens?	Steps through calculations showing how motorists have a very limited amount of time to assimilate VMS messages.	Limited flip-disk VMS legibility distance, concept of VMS being outside of driver's field of vision when the VMS is very close to driver, prevailing traffic speed, and amount of time required to read a message.
Appendix B: How should the VMS be maintained when not in use?	Understands suggestions for cleaning the screen, removing VMS from the road when not in use, and charging the battery if necessary.	Need to reduce glare (by cleaning the Lexan screen), need to remove VMS when there is no message to be displayed, and the need to charge the battery for VMSs which have not been used recently.
Appendix C: What abbreviations are recommended?	Reads a list of recommended abbreviations (such as "ln" for "lane").	Commonly used words and abbreviations obtained from the literature.

FIGURE 3 (continued)

The operator then realizes that not all screens are necessary: on the two-lane road, "left lane closed" and "merge right" imply the same message. The operator concludes Modules 14 and 15 with a one-screen message: "ACCIDENT|3 MI|MERGE RT." In Module 16, a drive past the VMS verifies its effectiveness: this drive-through can reveal simple mistakes, such as the view of the VMS being blocked by a pole or roadway curve. Finally, the last module ensures that the operator either changes the message or removes the VMS as soon as traffic conditions have returned to normal to ensure VMS accuracy.

In the previous scenario a variety of approaches could have been considered that were not mentioned in the interests of time. For example, had the major problem not been for motorists to merge but instead for motorists to divert from the Interstate, the operator also would have completed Module 7, which helps design a message for diverting motorists to an alternate route. In that case the operator also would have examined the need to use static signs for motorists unfamiliar with the area. The emphasis of this example, however, is to show how the modules can help the operator design an effective VMS message for a particular situation.

Two Sets of Manuals

A separate operator's manual was developed for permanent VMSs. This manual is similar to the portable VMS manual, and in many cases the modules are the same. However, the two manuals have distinct differences.

The permanent VMS manual has only 16 modules because it does not include a module describing where to place the VMS. In addition, although portable and permanent VMSs both become unreadable when the motorist drives close to them, the methods differ for computing the distance at which the VMS becomes unreadable. As shown in Equation 1, lateral distance is the key factor for portable VMSs, whereas for permanent VMSs the problem is vertical distance (3,13). Thus, the appendixes that describe these calculations are different for portable and permanent VMSs. Furthermore, additional message purposes have been included for permanent VMSs, as they have greater display capabilities. Finally, example message components for the two manuals differ because of their variance in display formats. For example, if one wants to convey that the two left lanes are closed, then a permanent VMS with twelve characters per line can display a message such as "2 LFT LANES | CLOSED" whereas a portable VMS with only eight characters per line might use a message such as "2 LEFT | LANES | CLOSED."

Consistency and Readability Built into Manuals

The single most important aspect of the manuals is that they are users' manuals rather than mandates or a laundry list of messages. They are essentially a training tool that encourages the creativity of the operator and allows him or her to have the final decision in the application of the VMS.

The manuals are simple and effective. They are highly readable but substantial enough to help the operator ensure that the VMS is used properly. Decision boxes placed in the same location on each page step an operator through the manuals. The use of a "true-or-false" procedure enables the operator to easily determine whether each guideline has been met. For example, Figure 3 shows the third module as determining the location of a VMS. Several requirements

are included within that module, such as placing the VMS before major decision points in the most level area possible and where it is accessible to maintenance vehicles. If any of the requirements are not met, the operator is advised to consider either a different location for the VMS or an alternative form of communication, such as a static sign, a flagger, or highway advisory radio.

Figure 2 demonstrates the power of the manuals' guidelines for assisting an operator with a complex decision: how to relay distance information to the motorist. The operator is presented with each piece of information in a binary decision format. By following this decision tree an operator quickly learns whether a landmark, exit number, or distance in miles should be used.

A few key concepts are emphasized throughout the manuals. For example, the idea of giving the motorists a message that they can read twice is repeated in several modules: first, the maximum number of screens is established on the basis of traffic conditions; second, the message is designed such that only essential components are retained; third, the operator is asked to verify the message if it is longer than one screen. In this manner, operators can be sure that they have met basic VMS usage requirements without being prevented from using the VMS innovatively and effectively.

Mechanisms for Feedback from VMS Operators

The authors realize that these manuals must evolve to accommodate the needs of VMS operators if this work is to be useful. During training courses based on the manuals, therefore, comments will be solicited from VMS operators. One comment that has already been received from VDOT traffic engineers is that these manuals are more useful as a training tool and reference document than as a pamphlet that should be carried to the field each time a VMS is used. To reflect this change in emphasis, the guidelines are now formally known as a user's *manual*. A second comment that has been received is that the computational methods for determining the maximum number of screens could be expressed as some simple rules: one message screen is ideal, two are acceptable, and three should be used only under extreme circumstances. Thus, although the calculations for determining the amount of time a VMS is legible were used in the development of these manuals, it was not necessary for operators to redo those computations each time a VMS is used in the field.

The traffic engineers also recommended the addition of a "drive-through" module, explicitly stating that the operator should drive past the VMS to assess its effectiveness, with attention to such details as traffic or other obstructions that might hamper the view of the VMS, the amount of time each message screen is displayed, and a motorist's reaction if a VMS is not expected. Finally, a fourth comment illustrates the importance of keeping the manuals consistent with VDOT practices in other areas. The engineers noted that the word "next" had the potential to be confusing, as is the case with static signs. Therefore an additional module was developed that followed practices outlined in previous research and the current MUTCD guidelines (14). Additional comments of this nature will be sought and used to improve the manuals.

CONCLUSIONS

It is critical to consider the needs of both operators and motorists to maximize the effectiveness of VMSs. In developing VMS opera-

tors' manuals designed to help achieve this objective, essential lessons were learned. Operators need a set of guidelines rather than an extensive list of messages to fully use the capabilities of VMSs. The manuals developed through this research are in a format easily followed by an operator and they assist rather than replace the operator's decisions. Because they outline the thought process an operator should employ when using a VMS, the manuals may also serve as a training tool.

Credibility must be maintained to maximize the effectiveness of VMSs. VMSs should be used only to transmit essential information about changed traffic conditions. Information limitations of VMSs, confirmed by the literature and motorists, demonstrate that VMSs should use no more than two screens, and use of only one screen is preferred. Therefore VMSs should be used in conjunction with other communications mediums if it is necessary to convey detailed information to motorists. Finally, these manuals should be updated as additional feedback from VMS operators and motorists becomes available.

ACKNOWLEDGMENTS

This research report was supported by the Virginia Transportation Research Council.

REFERENCES

1. Miller, J. S., B. L. Smith, B. R. Newman, and M. J. Demetsky. *Development of Manuals for the Effective Use of Variable Message Signs*. Virginia Transportation Research Council, Charlottesville, 1995.
2. Upchurch, J., J. D. Armstrong, M. H. Baaj, and G. B. Thomas. Evaluation of Variable Message Signs: Target Value, Legibility, and Viewing Comfort. In *Transportation Research Record 1376*, TRB, National Research Council, Washington, D.C., 1992, pp. 35-44.
3. Dudek, C. L. *Guidelines on the Use of Changeable Message Signs*. Report FHWA-TS-90-043. FHWA, U.S. Department of Transportation, 1991.
4. Dudek, C. L. *Manual on Real-Time Motorist Information Displays*. Report FHWA-IP-86-16. FHWA, U.S. Department of Transportation, 1986.
5. Smith, S. A. *INFORM Evaluation, Volume I: Technical Report*. Report FHWA-RD-91-075. FHWA, U.S. Department of Transportation, 1991.
6. Dudek, C. L. *Guidelines on the Use of Changeable Message Signs-Summary Report*. Report FHWA-TS-91-002. FHWA, U.S. Department of Transportation, 1991.
7. *Guidelines for Use of Portable Changeable Message Signs*. Michigan Department of Transportation, n.d.
8. *Guidelines for the Use of Portable Changeable Message Signs in Work Zones*. Minnesota Department of Transportation Work Zone Safety Committee, St. Paul, 1994.
9. Commonwealth of Pennsylvania Department of Transportation. *S.R. 0095, Section Eye: Basic Message Library for the Variable Message Sign System*. Urban Engineers, Inc. and Ebasco Infrastructure, 1993.
10. Blodgett, F. J. *Changeable Message Sign, I-5, Vancouver Freeway*. (Experimental Feature WA75-02). Washington State Department of Transportation, 1987. Available from National Technical Information Service, Springfield, Va.
11. Voza, A. *Standard Guidelines for Variable Message Sign Operation, Version 1.0*. New Jersey Turnpike Authority, New Brunswick, 1993.
12. *Notice of Proposed Amendments to the Manual on Uniform Traffic Control Devices*, Part 6. FHWA, U.S. Department of Transportation, 1993, pp. 56-59.
13. Armstrong, J. D. *An Evaluation of Human Factors Aspects of Variable Message Signs on Freeways*, pp. 60-62. Arizona State University, Tempe, 1991.
14. Perfater, M. A. *Motorist Understanding of Directional Messages*. Virginia Transportation Research Council, Charlottesville, 1981.

The contents of this paper reflect the research of the authors but not necessarily the official views of VTRC.

Publication of this paper sponsored by Committee on Traffic Control Devices.

Motorist Interpretation of Yellow X and Yellow Diagonal Arrow in Freeway Lane Control Signal Array

STEVEN D. WOHLSCHLAEGER, GERALD L. ULLMAN, AND CONRAD L. DUDEK

Licensed driver interpretation of the Manual of Uniform Traffic Control Devices (MUTCD)-approved and experimental transition symbols in a lane control signal (LCS) array is documented. The two symbols tested were the yellow X (MUTCD approved) and the yellow downward diagonal arrow (experimental). These two symbols were displayed in a scene depicting a three-lane freeway section containing one LCS array. The various LCS arrays were representative of typical LCS configurations for a median lane closure. Each transition symbol was tested in combination with two green down arrows and in an array containing one red X and one green down arrow. Overall, the study showed the yellow downward diagonal arrow to be interpreted more consistently and "correctly" given its intended use than the yellow X. Subject responses varied more for the yellow X than for the yellow downward diagonal arrow when a red X was included in the LCS array. In addition, subjects were more likely to interpret the yellow X in a manner that was considered "incorrect" given the intended use of the yellow transition symbols—a problem that was magnified when a red X was incorporated into the LCS array. Subject interpretation of the yellow transition symbols was also affected by the introduction of a red X into the LCS array. The most preferred subject interpretation of the yellow X and yellow downward diagonal arrow was the same when the transition symbols were displayed in an LCS array either with or without a red X. The meaning offered most frequently by subjects was "lane closed, blocked, or closing." The second most common interpretation of both the yellow X and yellow downward diagonal arrow varied somewhat, however. When displayed with two green down arrows "lane ends physically" was the second most frequent interpretation, whereas introduction of a red X into the LCS array altered subject perception and "lane is congested" became the second most popular meaning.

The Manual on Uniform Traffic Control Devices (MUTCD) (1) defines lane use control signals (LCSs) as special overhead signals having symbols that are used to indicate whether the use of a specific lane or lanes of a street or highway is permitted or prohibited, or to indicate the impending prohibition of use. In the United States LCSs have most commonly been used for reversible-lane control. However, the MUTCD also points out several instances in which LCS may be appropriate where there is no intent or need to reverse traffic flow. Most of these applications involve freeways and include the following (1):

1. On a freeway, where it is desired to keep traffic out of certain lanes at certain hours to facilitate the merging of traffic from an entrance or exit ramp or other freeway;
2. On a freeway near its terminus, to indicate a lane that ends; and

3. On a freeway or long bridge to indicate a lane that may be temporarily blocked by an accident, a breakdown, or some other incident.

The MUTCD (1) currently specifies only one symbol for use when transitioning the status of a lane from open (green down arrow) to closed (red X). A steady yellow X may be used to indicate to a driver that he or she should prepare to vacate the lane above which it is displayed because a signal change is being made to a red X. Previous research has indicated that motorists may not fully understand the intended meaning of and proper response to the yellow X, especially if it is displayed concurrently with a red X in the same LCS array (2, 3). Although motorist understanding of the yellow X appeared to be somewhat limited, an outdoor laboratory study conducted by Lavallée et al. (4) and Engel et al. (5), using actual LCS heads, found that 85 percent of the observers identified yellow downward diagonal arrows pointing right or left as meaning merge right or merge left, respectively.

Questions raised as a result of these studies have prompted the Texas Department of Transportation, in cooperation with FHWA, to sponsor research to determine the suitability of another transition symbol, the yellow downward diagonal arrow, for use in place of the yellow X. This paper presents the results of a laboratory study conducted to document motorist interpretation of MUTCD-approved and experimental transition symbols in a lane control signal array. Whereas all approved and several experimental LCS symbols were tested, this report focuses primarily on motorist interpretation of the yellow X and yellow downward diagonal arrow. The term array as used here refers to a combination of two or more lane control signals facing one direction of traffic at a single location.

BACKGROUND

Although several reports documenting motorist comprehension of green down arrow and red X LCS symbols were identified in the literature review, only a few were found that chronicle motorist interpretation of and reaction to a yellow transition symbol. Of the three yellow transition symbols identified in the literature review (that is the yellow X, the yellow down arrow, and the yellow downward diagonal arrow), studies examining motorist understanding of the yellow X were found to be the most prominent.

Using slightly different survey instruments, Forbes et al. (6), Carlson and Lari (7), and Ullman et al. (3) found that subject interpretations of the yellow X were somewhat inconsistent. Both Ullman et al. and Forbes subjects were shown full-color pictorial representations of LCS arrays in a freeway environment, whereas

S. D. Wohlschlaeger, Texas Transportation Institute, The Texas A&M University System, 701 North Post Oak, Suite 430, Houston, Tex. 77024-3818.
G. L. Ullman and C. L. Dudek, Texas Transportation Institute, The Texas A&M University System, College Station, Tex. 77843.

Carlson and Lari subjects were presented with black and white graphical depictions of LCS symbols on the questionnaire they were asked to complete. Although no attempt was made by Carlson and Lari to depict the LCS symbols in a freeway environment, most of the survey subjects had been exposed to them in the field while driving through the Lowry Hill Tunnel on I-94 in Minnesota.

Subject interpretations of the yellow X in the three studies included "do not drive in this lane"; "warning (take caution) in lane"; and "drive slow in lane" among others, indicating that there may be some confusion about the proper driving response required. In addition, Ullman et al., observed that driver interpretation of the yellow X was further influenced by the presence of a red X in the LCS array, making the interpretation less consistent with that intended by MUTCD.

Carlson and Lari (7) and Ullman et al. (3) also surveyed motorists to determine their interpretation of the yellow down arrow. Although further research may reveal a more appropriate use for this particular symbol, subject interpretations suggest that it would perform no better than a yellow X given the objective of encouraging motorists to exit the lane above which it is displayed. Carlson and Lari also conducted operational tests of the yellow down arrow and the yellow X in the I-94 Lowry Hill Tunnel. During normal operations on this facility, green down arrows were displayed above all travel lanes. However, when an incident occurred, a red X was displayed above the obstructed lane(s) and a flashing yellow X or yellow down arrow was displayed above any other lane(s) which was affected by the incident but not blocked. (Steady yellow symbols were used to transition LCS indications from the green down arrow to the red X.) Green down arrows remained over the lanes that were not affected by the incident or the resulting congestion. Results of these studies indicated that drivers do respond to information conveyed by LCSs by shifting from incident to nonincident lanes. No field studies were found that documented motorist reaction to the yellow downward diagonal arrow.

For a more detailed review and critique of the previously mentioned studies or for information about motorist interpretation of the red X, green down arrow, and additional experimental LCS symbols, the reader is encouraged to refer to Wohlschlaeger (8) and Ullman et al. (3).

OBJECTIVES

Three objectives were identified for this study:

1. To determine the degree to which the interpretation of and reaction to the yellow X and yellow downward diagonal arrow vary with respect to the other symbols present in the LCS array.
2. To identify the yellow symbol with the most consistent driver interpretation over the various freeway LCS arrays investigated.
3. To determine the urgency with which drivers expect action to be required when presented a yellow transition symbol in a freeway driving situation.

STUDY METHOD

To address the objectives of this study, a laboratory experiment was constructed to evaluate motorist response to, interpretation of, and perceived urgency of response to MUTCD-approved and experimental transition symbols in an LCS array. The investigation con-

sisted of person-to-person surveys of licensed motorists solicited from the patronage of a San Antonio, Texas, Department of Public Safety (DPS) Drivers' License Station. As such, subjects were limited to licensed drivers who were present at the drivers' license station on the days of the study and who agreed to participate.

Each subject was required to sit through a 2-min introduction. Including the introduction, each survey took approximately 10 min to conduct. Slightly more than 240 usable questionnaires were collected over a 2-wk period.

Survey Stimuli

The LCS array configurations investigated are indicated in Table 1. Figures 1 and 2 illustrate the visual stimuli presented to motorists. The actual drawings used were color reproductions and were larger [27.5 by 21.25 cm (11 by 8.5 in.)]. They have been modified to black and white for reproduction purposes. An identical three-lane section was used for each freeway scene. Four different LCS arrays were created by varying the symbols presented and the lanes over which they were positioned. Numbers were placed in the freeway travel lanes for use as a reference during survey administration. Vehicles were intentionally left out of the drawing to eliminate subject confusion when answering survey questions.

Upon presentation of a particular LCS array, subjects were asked (a) what they would do in response to the LCS symbol shown above a certain lane, and (b) what they felt that particular symbol indicated about the condition or status of that lane, or both. In addition, if they indicated that a response other than "continue in lane" would be appropriate, subjects were asked to provide an estimate of how far downstream they would expect to have to respond. Survey participants were also asked to identify what differences, if any, they felt were implicit in the use of the two yellow transition symbols. An open-ended response format was used to avoid biasing the subjects.

Experimental Plan

Each participant was shown all four freeway scenes; however, the order in which they were presented was varied for each group. The arrays shown and the order in which they were shown to each of four groups can be seen in Table 2.

The first scene shown to all subjects (Scene A) consisted of one of the yellow transition symbols (yellow X or yellow downward diagonal arrow) along with two green down arrows. The second scene (Scene B) provided subjects with the opportunity to make a side-by-side comparison of the two yellow transition symbols. The two LCS arrays shown in Scenes A and B (Arrays 1 and 2) are indicative of displays that a transportation agency may use to indi-

TABLE 1 Lane Control Signal Arrays

Array No.	Inside Lane (Lane 1)	Middle Lane (Lane 2)	Outside Lane (Lane 3)
1	yellow x	green ↓	green ↓
2	yellow ↘	green ↓	green ↓
3	red X	yellow X	green ↓
4	red X	yellow ↘	green ↓

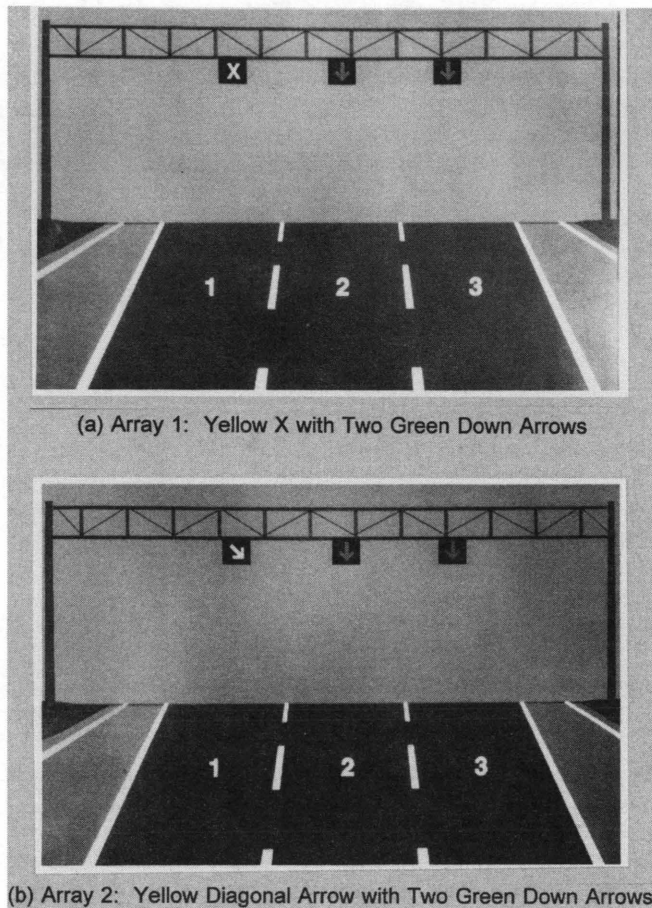


FIGURE 1 Freeway scenes shown to subjects participating in survey: Arrays 1 and 2.

cate that the inside lane (Lane 1) of a freeway will be closed ahead because of an incident.

The LCS array shown in Scene C contained one of the yellow transition symbols in conjunction with a red X and green down arrow. The LCS array shown in Scene D was similar to that shown in Scene C but exposed the subject to the candidate yellow symbol not shown in Scene C. These two LCS array configurations (Arrays 3 and 4) might be used by a transportation agency to inform motorists that the inside lane (Lane 1) was already closed and that incident conditions required the closure of the middle lane (Lane 2) further downstream.

Data Reduction

The answers to the survey questions were categorized by the authors and entered into a spreadsheet by group number, scene, symbol, question, and response. After compiling these answers, the percentage of response was calculated for each group number, scene, symbol, and question. Although answers varied slightly because of the survey format (i.e., open-ended response), it was not difficult to compile answers into larger-answer categories. Subject answers that did not clearly fit into one of the more definitive answer categories were categorized as "other." After determining that

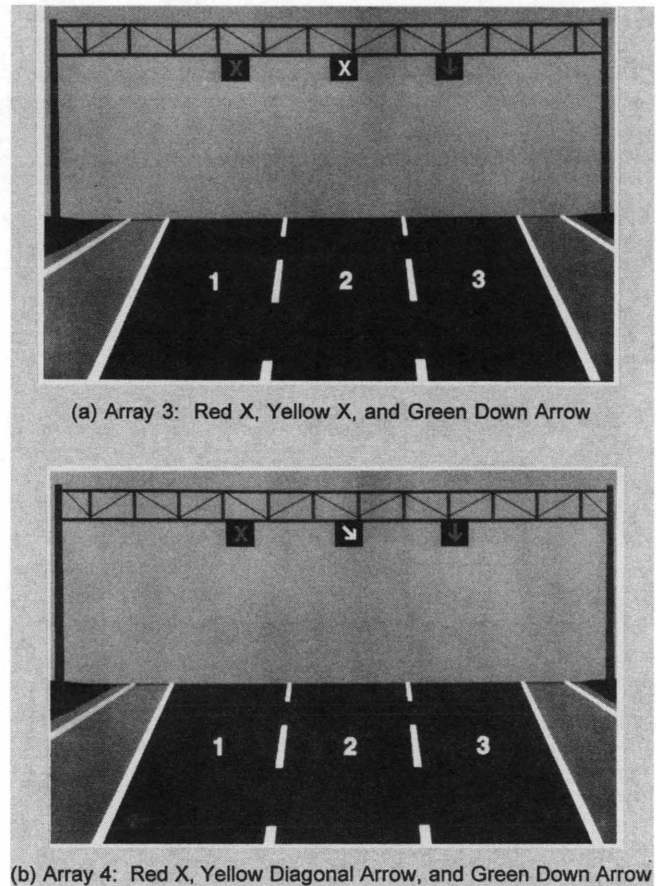


FIGURE 2 Freeway scenes shown to subjects participating in survey: Arrays 3 and 4.

answers did not vary significantly across subject groups or as a result of the LCS array exposure order, the subject groups were combined and then separated into four categories corresponding to the four LCS arrays shown in Figures 1 and 2. The four categories included the following:

1. Yellow X without a red X present in the LCS array (YX);
2. Yellow downward diagonal arrow without a red X present in the LCS array (YDA);
3. Yellow X with a red X present [YX(RX)]; and
4. Yellow diagonal arrow with a red X present [YDA(RX)].

Test of proportions analyses were then conducted on the percentage of response in each answer category to determine whether subject answers about the candidate yellow symbols (a) varied with respect to the yellow symbol shown in the LCS array or (b) varied with respect to the other symbols shown in the LCS array (i.e., the presence or absence of the red X). Each test of proportions analysis conducted took on the following basic structure:

1. $H_0: p_1 = p_2$
2. $H_1: p_1 \neq p_2$
3. Level of significance: $\alpha = 0.005$
4. Critical region: $|z| > z_{\alpha/2} = 2.81$
5. Test statistic:

TABLE 2 Lane Control Signal Array Sequence Groupings

Group No.	Array Sequence by Scene			
	Scene A	Scene B	Scene C	Scene D
I	Array 1	Arrays 1 and 2	Array 3	Array 4
II	Array 2	Arrays 2 and 1	Array 3	Array 4
III	Array 1	Arrays 2 and 1	Array 4	Array 3
IV	Array 2	Arrays 1 and 2	Array 4	Array 3

$$z = \frac{\hat{p}_1 - \hat{p}_2}{\sqrt{\hat{p}\hat{q}[(1/n_1) + (1/n_2)]}} \quad (1)$$

Where p_1 and p_2 are the two population proportions of the attribute under investigation and

$$\left(\hat{p}_1 = \frac{x_1}{n_1}\right), \left(\hat{p}_2 = \frac{x_2}{n_2}\right), \text{ and } \left(\hat{p} = \frac{x_1 + x_2}{n_1 + n_2}\right) \quad (2-4)$$

where

x_i = the number of subjects whose answers fit within the indicated category i ;

n_i = the total number of subjects in the sample population for the indicated category i ; and

$$\hat{q} = 1 - \hat{p}.$$

The very low significance level ($\alpha = 0.005$) was selected to account for the multiple comparisons made with the same set of data. For example, did the responses to the yellow x differ (a) between subject groups, (b) because of LCS array exposure order, (c) from the responses given for the yellow diagonal arrow, or (d)

from the responses indicated to the yellow X when it was displayed in conjunction with the red X? The lower level of significance, therefore, was used so that the experiment-wide level of significance would be statistically acceptable ($\alpha \leq 0.5$). No statistical analyses of the subjects' perceived urgency of response were performed.

STUDY RESULTS

Demographics

Table 3 summarizes the basic demographic distribution of subjects recruited to participate in this study. Overall, the 240 survey subjects included more men and Hispanics and were younger and more educated than both the Texas and U.S. averages. Although some of the more unusual answers may or may not be given if another 240 subjects were surveyed, it is felt, given the sample size, that the overall breakdown of responses into the various answer categories would remain essentially the same.

There is no apparent explanation for the higher percentage of men participating in the study. One possible factor contributing to this may have been that the person soliciting subjects to participate

TABLE 3 Comparison of United States, Texas, and Survey Subject Demographics

Question	Response	Percent of Drivers (9, 10)		
		U. S.*	Texas*	Study Subjects
Gender	Male	51.3	51.5	60.6
	Female	48.7	48.5	39.4
Age Category	Less than 25	15.1	15.2	34.4
	25 to 39	35.4	37.2	31.5
	40 to 54	24.9	25.2	26.6
	Over 55	24.6	22.4	7.5
Ethnic Background	European-American	73.8	60.1	63.9
	African-American	11.1	9.5	5.8
	Latin-American/Hispanic	8.1	20.2	27.0
	Pacific-American	2.7	1.5	1.2
	American Indian/Eskimo	0.7	0.3	1.2
	Other	3.6	8.4	0.9
Education	Less than high school	24.6	28.1	12.0
	High school graduate	30.1	26.0	22.4
	Some College	20.8	22.9	29.9
	College Graduate	24.5	23.1	35.7

*Information on ethnicity and education includes general population (not just licensed drivers)

in the survey was a woman. Perhaps men were more willing to participate because of this, or it may have been that women were less likely to participate given that the survey administrator was a man.

The higher percentage of subjects in the youngest age category was not totally unexpected because drivers licensed in the state of Texas can renew their drivers' license by mail if they have an unblemished driving record. Because older drivers are usually safer drivers and can therefore renew their license by mail, it was not surprising that more younger than older drivers would be patronizing the DPS Drivers' License Station. The high percentage of Latin-American drivers participating in the survey was not surprising either. San Antonio, Texas, is known for its rich Hispanic heritage, and many of the residents are of Mexican descent.

The fact that more of the survey subjects had received a college education than was evident in both the Texas and national averages was a bit unanticipated. Although outside comments were rare and highly discouraged by the survey administrators, it may have been that the DPS patrons who chose not to participate in the study were concerned that family members or others standing nearby might be critical of their answers.

Subjects' Indicated Response to Yellow Transition Symbols

Freeway LCSs should convey a clear message and produce a consistent response from all drivers if they are to be truly effective tools for managing freeway traffic at major interchanges or during incidents, or both. Table 4 summarizes the percentage of subject responses in each of the yellow transition symbol categories.

When viewing the two LCS arrays that contained one of the yellow transition symbols and two green down arrows only (Arrays 1 and 2), a significantly higher percentage of subjects indicated that they would respond to the yellow downward diagonal arrow by moving to the lane with the green down arrow (98.8 percent) than would respond similarly to the yellow X (93.8 percent).

After a red X was added into the LCS array, 97.9 percent of the subjects responding to the yellow downward diagonal arrow con-

tinued to indicate that they would respond by moving to the lane with the green down arrow (a decrease of less than 1 percent). On the other hand, only 89.2 percent of the subjects indicated that they would respond similarly to the yellow X after the addition of a red X into the freeway LCS array (a decrease of about 4.5 percent). This difference between the two candidate yellow symbols was also found to be statistically significant. Introduction of the red X into the LCS array containing the yellow X also seemed to create some confusion among survey respondents causing them to be "unsure" of the proper driving response.

Subjects' Interpretation of Yellow Transition Symbols

Not only was it important to understand how subjects were likely to respond to the yellow transition symbols, it was also important to understand why subjects chose their particular response. Thus, subject interpretation of the yellow transition symbols was also explored. A summary of subject interpretations of the yellow symbol categories can be found in Table 5.

The interpretation given most frequently for all of the yellow symbol categories was that the "lane is closed, blocked, or closing." Excluding the "other" category, the interpretation offered second most frequently for both yellow transition symbols without the red X was that the "lane ends physically," an interpretation survey subjects felt was slightly more appropriate for the yellow downward diagonal arrow than for the yellow X.

After adding a red X into the LCS array, the most frequent interpretation for both yellow transition symbols remained "lane is closed, blocked, or closing." However, the second most preferred subject interpretation of both yellow transition symbols changed to "lane is congested," an increase that was found to be statistically significant. In addition, the percentage of subjects who offered the interpretation "lane ends physically" decreased significantly for both yellow transition symbols after the addition of a red X into the LCS array. When a red X was added to the LCS array, the yellow transition symbol was moved to the center lane. It seemed logical then that with three travel lanes visible, survey subjects were less

TABLE 4 Subjects' Indicated Response to Yellow Transition Symbol Categories

Response to Symbol	Percent of Subjects Responding to Candidate Yellow Symbol Category							
	YX		YDA		YX(RX)		YDA(RX)	
Move to the lane with the green arrow	90.5		96.3		82.6		94.6	
Slow and move to the lane with green arrow	3.3	93.8	2.5	98.8	6.6	89.2	3.3	97.9
Stay in lane	2.5		0.8		1.7		0.4	
Slow and stay in lane	2.9		0.4		6.6		1.3	
Stop	0.8		--		--		--	
Stop and continue slowly	--	6.2	--	1.2	0.4	10.8	--	2.1
Unsure	--		--		1.7		--	
Other	--		--		0.4		0.4	
Total	100.0		100.0		100.0		100.0	

YX = Yellow X; YDA = Yellow Diagonal Arrow; YX(RX) = Yellow X with red X; YDA(RX) = Yellow Diagonal Arrow with red X

TABLE 5 Subjects' Interpretation of Yellow Transition Symbol Categories

Meaning of Symbol	Percent of Subjects Responding to Candidate Yellow Symbol Category			
	YX	YDA	YX(RX)	YDA(RX)
Lane is closed or blocked	57.3	51.5	50.2	57.3
Lane closing ahead	1.7	3.7	7.5	5.8
Lane ends physically	12.4	17.0	5.0	5.8
High occupancy vehicle lane	1.2	--	--	--
Contraflow lane	1.7	0.8	0.8	--
Exit lane	1.2	0.4		0.4
Lane is congested	2.9	2.5	13.7	13.3
Road splits	--	--	0.4	0.8
Pavement damage in lane	0.9	--	1.2	--
Unsure	3.7	0.8	2.5	2.1
Other	17.0	23.3	18.7	14.5
Total	100.0	100.0	100.0	100.0

YX = Yellow X; YDA = Yellow Diagonal Arrow; YX(RX) = Yellow X with red X; YDA(RX) = Yellow Diagonal Arrow with red X

likely to indicate that the yellow transition symbol indicated that the lane would be physically ending.

Subjects' Perceived Urgency of Response to Yellow Transition Symbols

Subjects' perceived urgency of response was also studied to discern the differences in subject understanding of the two yellow transition symbols. This was determined by asking subjects how soon they felt action was required in response to the yellow transition symbols.

Only those subjects who indicated that they would respond to the yellow transition symbols by "moving to the lane with the green arrow" were used in this analysis (sample sizes for other responses were not large enough to draw meaningful conclusions from them). This included those subjects who gave the response "move to lane with green arrow," as well as those subjects who responded "slow and move to lane with green arrow."

Figure 3 shows the cumulative proportion of subjects' perceived distance to the lane change maneuver for each of the four yellow transition symbol categories. Although most subjects (around 93 percent) felt they would respond within 1.61 km (1 mi), there were slight differences between perceived distances to the lane change maneuver for the four LCS arrays studied.

When displayed with green down arrows only, the yellow X appeared to command a more urgent response by survey participants. Approximately 35 percent of the subjects indicated that it would be appropriate to respond to the yellow X "as soon as possible," and 56 percent indicated that it would be appropriate to respond within 0.40 km (1/4 mi) or less. The yellow downward diagonal arrow was a relatively close second. Approximately 26 percent stated that a lane change maneuver should be initiated "as soon as possible," whereas 52 percent said 0.40 km (1/4 mi) or less. The yellow X and the yellow downward diagonal arrow shown with a red

X tied for third (18 percent of the subjects asserted that it would be appropriate to respond "as soon as possible" to the yellow X (17 percent for the yellow downward diagonal arrow) and 43 percent indicated 0.40 km (1/4 mi) or less for the yellow X (45 percent for the yellow downward diagonal arrow)).

Figure 4 shows the frequency with which subject responses fell into the various distance groupings for each of the yellow transition symbol categories. The majority of subjects (36 percent) who indicated that they would respond to the yellow X by moving to the lane with the green down arrow, indicated that they would do so as soon as possible. Those subjects responding similarly to the yellow downward diagonal arrow with two green down arrows however, were equally as likely (26 percent) to respond as soon as possible as they were to respond at a distance less than or equal to 0.40 km (1/4 mi).

While subjects appeared to assign more urgency to the yellow X when the yellow transition symbols were displayed with green down arrows only, this trend was reversed when a red X was introduced into the LCS array. The majority of subjects (29 percent) who offered the response "move to the lane with the green down arrow" for the yellow X with a red X shown concurrently, indicated they would do so at a distance greater than 0.40 km (1/4 mi) yet less than or equal to 0.81 km (1/2 mi). Subjects responding to the yellow downward diagonal arrow with the red X present in the LCS array, on the other hand, were most likely (28 percent) to initiate a response that was not immediate but was at a distance less than or equal to 0.40 km (1/4 mi).

Although both the yellow X and yellow downward diagonal arrow were affected by the introduction of a red X into the LCS array, the yellow X was again affected to a greater degree. As explained previously, it seemed that when subjects viewed an array with one of the yellow transition symbols and two green down arrows, they tended to focus on the symbol being displayed. However, when the yellow transition symbol was displayed in the LCS

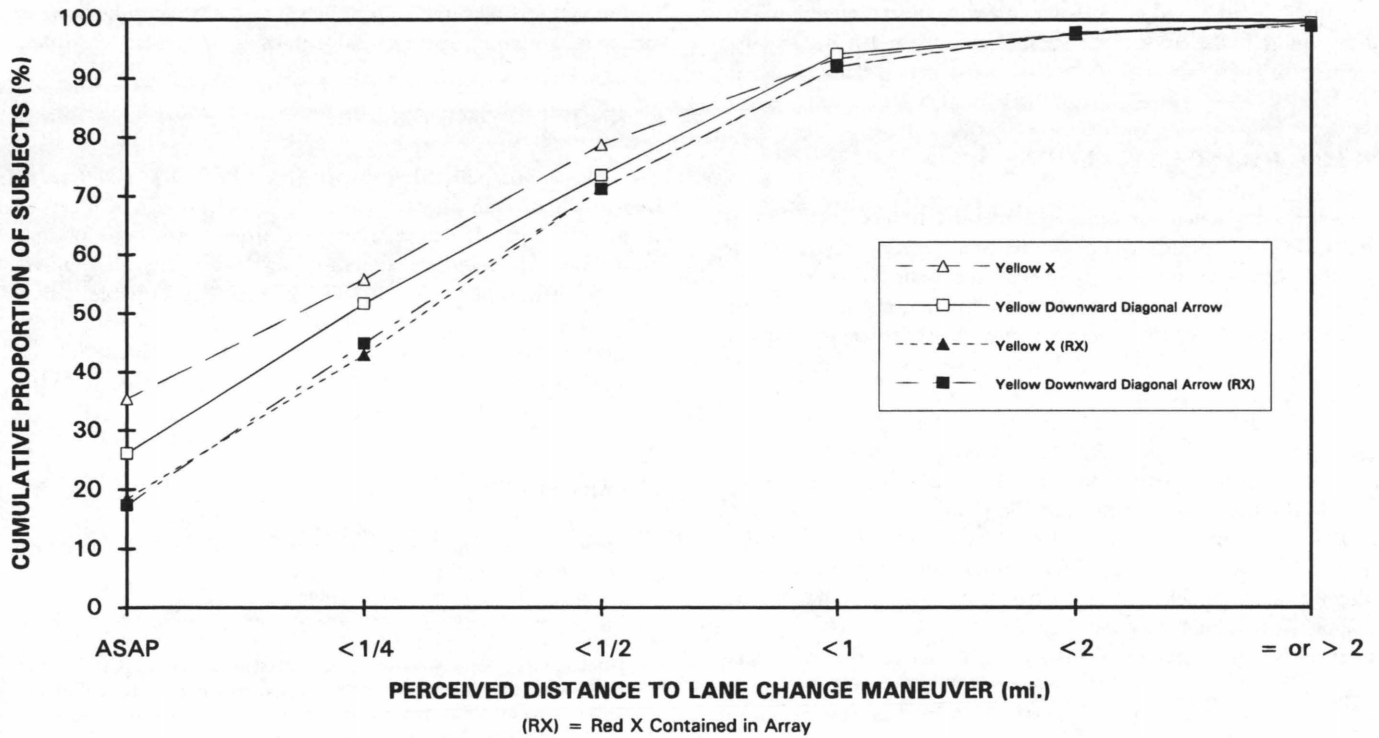


FIGURE 3 Cumulative proportion of subjects responding to "move to the lane with the green arrow" for the yellow transition symbol category indicated.

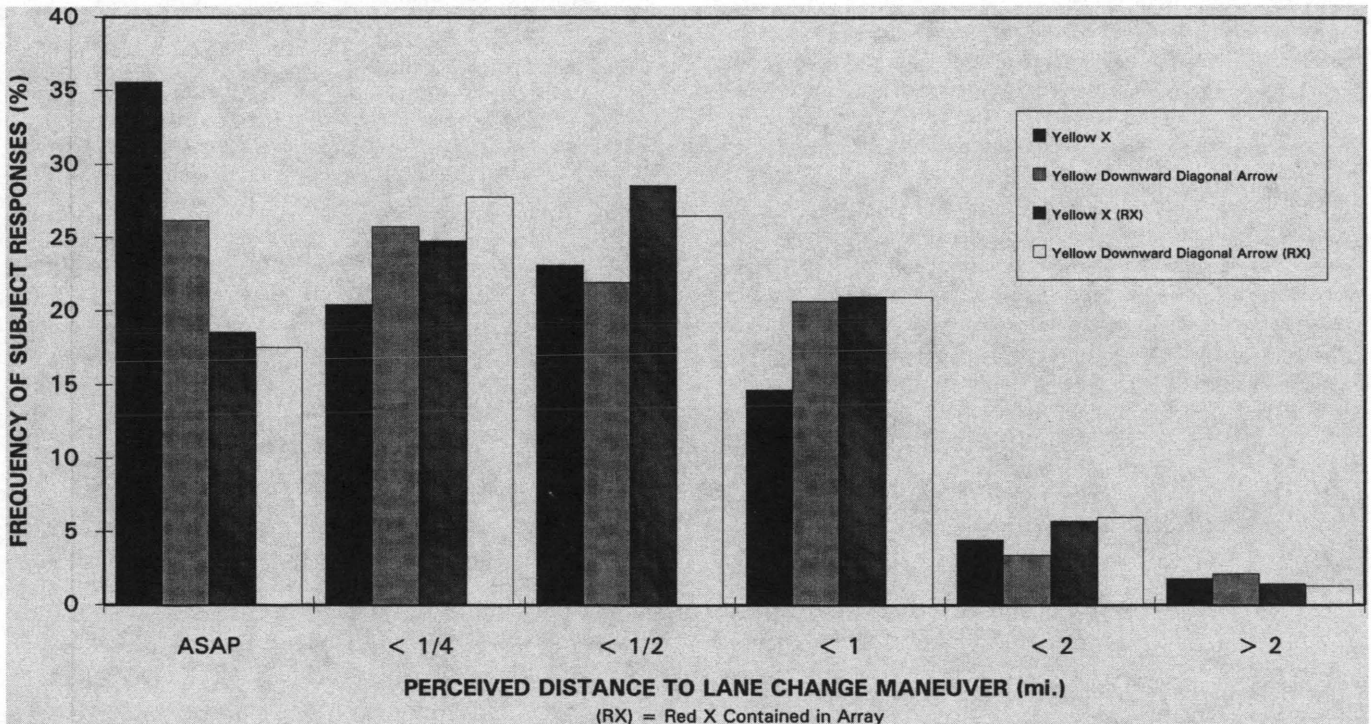


FIGURE 4 Frequency of subject responses for subjects responding to "move to the lane with the green arrow" for the yellow transition symbol category indicated.

array with a red X and green down arrow, subjects' attention was drawn more to the color of the symbols and the red X became the worse case.

SUMMARY AND CONCLUSIONS

This study has documented motorist interpretation of the yellow X and yellow downward diagonal arrow in a freeway LCS array. In general, the results of this study indicate that both yellow transition symbols are affected somewhat by the introduction of a red X into the LCS array. However, although the majority of subjects indicated a reaction that was considered "correct" given the intended meaning of the yellow transition symbols, the frequency with which subjects indicated an "incorrect" reaction for the yellow downward diagonal arrow was significantly lower than it was for the yellow X. Of the two yellow transition symbols investigated, the yellow downward diagonal arrow appeared to produce the least variation and confusion among survey subjects. There was also less of a disparity in subject perceived distance to the lane change maneuver after the red X was added to the LCS array for the yellow downward diagonal arrow than there was for the yellow X.

Truly effective freeway LCS symbols should convey a clear message and elicit a consistent response from all motorists if they are to be useful tools for managing freeway traffic at major interchanges or during incidents, or both. This should be true whether drivers have been educated about their use, or if they are seeing them for the first time.

The results of the study of subjects' indicated reaction to the yellow transition symbols showed that the yellow downward diagonal arrow was better than the yellow X for persuading subjects to initiate a lane change maneuver. Therefore, the yellow downward diagonal arrow is recommended for evaluation as a suitable alternative to the yellow X for use when changing the status of a freeway lane from open (green down arrow) to closed (red X). Further research is needed to determine whether these relationships will indeed hold true for drivers who are actually traveling on the mainlanes of a freeway.

As a result of the studies conducted by the Texas Transportation Institute (TTI), The Texas Department of Transportation (TxDOT) is currently seeking approval from FHWA to initiate field experiments using the yellow downward diagonal arrow in freeway LCS systems. TxDOT is also working with researchers at TTI to determine scenarios appropriate for LCS use and their corresponding LCS array configurations and to solve legibility issues about LCS displays. In addition to these, research should be conducted with the aim toward standardizing symbolic information signs in the hopes

of eliminating driver confusion as they transfer between the freeway main lanes, high-occupancy-vehicle transitways, and toll facilities.

ACKNOWLEDGMENTS

This study was conducted in cooperation with TxDOT and the U.S. Department of Transportation, FHWA. Ray Derr of TxDOT served as technical panel chairman of this project; his contributions throughout the study are gratefully acknowledged. The authors thank R. Dale Huchingson of TTI for furnishing valuable human factors expertise to the study. The authors also recognize Henry Hutchinson, the troopers, and employees of the DPS Babcock Road Drivers' License Station for their cooperation and assistance during this research effort.

REFERENCES

1. *Manual on Uniform Traffic Control Devices*. FHWA, U.S. Department of Transportation, Washington, D.C., 1988.
2. Ullman, G. L. Motorist Interpretations of MUTCD Freeway Lane Control Signals. In *Transportation Research Record 1403*, TRB, National Research Council, Washington, D.C., 1993, pp. 49-56.
3. Ullman, G. L., S. D. Wohlschlaeger, C.L. Dudek, and P. Wiles. *Driver Interpretation of Existing and Potential Lane Control Signal Symbols for Freeway Traffic Management*. Research Report FHWA/TX-93/1298-1. Texas Transportation Institute, College Station, Nov. 1993.
4. Lavallée, P., D. Sims, S. Stewart, and M. Lau. Multimessage Fiber-Optic Lane-Control Signs for Freeway Applications. In *Journal of Transportation Engineering*, Vol. 116, No. 6, Nov./Dec. 1990, pp. 725-733.
5. Engel, G. R., M. Townsend, and W. Dougherty. *Preliminary Evaluation of Prototype Lane Control Signs*. Research and Development Branch, Ontario Ministry of Transportation, Downsview, Ontario, Canada, July 1988.
6. Forbes, T. W., E. Gervais, and T. Allen. Effectiveness of Symbols for Lane Control Signals. In *Bulletin 244*, HRB, National Research Council, Washington, D.C., 1960, pp. 16-29.
7. Carlson, G. C., and A. Z. Lari. *Evaluation of the Use of Downward Yellow Arrows in the I-94 Lane Control Signal System*. Minnesota Department of Transportation, Traffic Systems and Research Section, St. Paul, Aug. 1982.
8. Wohlschlaeger, S. D. *Motorist Interpretation of Potential Transition Symbols in a Freeway Lane Control Signal Array*. M.S. thesis. Texas A&M University, College Station, May 1994.
9. *Highway Statistics 1991*. U.S. Department of Transportation, FHWA, Administration, Washington, D.C., 1991.
10. *1990 U.S. Census of Population and Housing*. Bureau of the Census, U.S. Department of Commerce, Economics and Statistics Administration, Washington, D.C., 1990.

Publication of this paper sponsored by Committee on Traffic Control Devices.

Effects of Pavement Markings on Driver Behavior at Freeway Lane Drop Exits

KAY FITZPATRICK, MARTY LANCE, AND TORSTEN LIENAU

Field studies were designed to measure the effects of pavement markings on driver behavior at freeway lane drop exits. Number and location of lane changes and erratic maneuvers upstream of three lane drop exits were the measures of effectiveness used to describe driver behavior. The data from two sites directly revealed—and the data from a third site indicated—that drivers are moving into or out of the exiting lane further upstream of the lane drop gore in the after period than in the before period. The before-and-after studies also revealed that the number of erratic maneuvers within the entire study segment decreased with the installation of the markings. The largest decrease was in the number of one-lane lane changes through the gore.

A lane drop exit occurs when one or more lanes are eliminated from a freeway at an exit. This treatment is used when traffic demand decreases or when high volumes are exiting to another facility. Lane drop exits can cause driver confusion when the driver does not expect the lane to exit; rather, the driver expects the lane to continue with the freeway main lanes. Without proper notification of the impending exit, drivers can find themselves performing erratic maneuvers to prevent exiting at undesirable locations. Exit-only signs are the predominant type of traffic control device used to communicate the existence of a lane drop exit. A pavement marking treatment is included in the national and Texas Manual on Uniform Traffic Control Device (1,2) as an optional MUTCD treatment.

Because of interest in determining more effective methods of communicating lane drop exits to motorists, the Texas Department of Transportation (TxDOT) commissioned a study (3) to determine the effects of pavement markings on motorists. The pavement markings, which are generally known as lane drop markings, consist of larger-width lane striping that begins approximately 0.8 km (0.5 mi) in advance of the theoretical gore point and a solid white channelizing line 203 mm wide (8 in.) extending approximately 91.5 m (300 ft) upstream from the theoretical gore point. The larger-width lane striping is 203 mm wide by 0.9 m long (8 in. wide by 3 ft long) separated by 3.7-m (12-ft) gaps. White pavement marking arrows can also be included as part of a pavement marking treatment.

Previous studies on pavement markings at exit and entrance ramps focused on the effectiveness of different color markings and on raised pavement markers. One study (4) specifically investigated signing and pavement markings at lane drop exit locations. The study compared the lane changes and erratic maneuvers occurring within 152.5 to 213.5 m (500 to 700 ft) of the gore on a matched 15-min interval basis. The results were mixed; one site showed improvements in all times studied, whereas the other two sites

showed decreases in lane changes only during certain times. Because the study focused only on the section 152.5 to 213.5 m (500 to 700 ft) immediately upstream of the gore, researchers designed this TxDOT study to gather data (a) for a longer distance upstream of the gore, (b) in smaller increments [say every 30.5 m (100 ft)], and (c) to separate the lane changes into those vehicles moving into the exit lane and those vehicles moving out of the exit lane.

FIELD STUDIES

Field studies were designed to measure the effects of lane drop markings on driver behavior at three freeway lane drop exits. Number and location of lane changes and erratic maneuvers upstream of a lane drop exit were the measures of effectiveness (MOEs) used to describe driver behavior. With these MOEs the influence of the markings could be seen in the number of lane changes (or erratic maneuvers) and in the position in which those changes are occurring.

Before-and-after data were collected at the following sites: Site A, I-820 northbound (NB) to White Settlement Road; Site B, I-35E southbound (SB) to I-20 west; and Site C, I-45NB to I-610 west. Table 1 provides a summary of the characteristics for each site, whereas Figures 1 through 3 show the signs and markings present at the sites during the before-data collection. These sites were selected because the exiting lane existed for a mile or more before being dropped, and they had minimal potential influences, such as entrance ramps or poor geometry, which could affect the quantity and location of lane changes and erratic maneuvers. Figures 4 through 6 illustrate the markings installed at each site.

Video cameras recorded several days of operations at each site. Three to four cameras were installed at each site on overhead sign structures. Videotapes in videocassette recorders located in ground-VCR level controller cabinets mounted specifically for this project were replaced every 6 hr during daylight conditions. The videotapes provided the following information: number and location of lane changes; number, location, and type of erratic maneuvers; and volumes. The roadway sections studied were divided into 30.5-m (100-ft) zones. The location of an event was defined as the zone in which a vehicle's front wheel first crossed a lane line. Erratic maneuvers included one-lane lane changes through the gore; two-lane lane changes; swerving in and out of a lane or the shoulder; riding between two lanes on the solid white line; and others.

Once the lane change and erratic maneuver data were obtained, the data were then summarized in 15-min increments by zone for the time periods available for all zones. Graphic representations of the values calculated were valuable tools in evaluating the findings. The findings were plotted by the 30.5-m (100-ft) increments used to reduce the data. These plots, while revealing the trends in the data, also showed the variability that exists between such short

K. Fitzpatrick and T. Lienau, Transport Operations Program, Texas Transportation Institute, College Station, Tex. 77843-3135. M. Lance, Civil Engineering Department, North Carolina State University, Raleigh, N.C. 27695-7908.

TABLE 1 Study Site Characteristics

Characteristics	Site A	Site B	Site C
Exit Name	I-820 NB to White Settlement Road	I-35E SB to I-20 West	I-45 Northbound to I-610 West
Location	west Ft. Worth	south Dallas	south Houston
Description	One-lane exit	One-lane exit	One-lane, left exit
Length of lane drop	approximately 1.6 km	over 11.3 km	greater than 8.1 km
Dates of filming	Before: Jan 1993 After: June 1993	Before: June 1993 After: June 1993	Before: March 1993 After: November 1993
Markings installed	May 1993	June 1993	August 1993
Number of lanes after exit	three	two	three
Potential Influences (distance upstream from gore)	Entrance ramp (610 m)	Exit ramp--I-20 E (275 m) Exit ramp (550 m)	Two-lane with optional lane lane drop exit (183 m)
AADT on freeway (1992 AADT Maps)	47,000	75,000	202,000

Conversion factors: 1.61 km = 1 mile and 0.305 m = 1 ft

increments—a driver can traverse the 30.5-m (100-ft) increment in 1.2 sec when driving 89 kph (55 mph). Figures 7 through 9 illustrate the number of lane changes by zone location for Sites A, B, and C, respectively.

Four hourly values were sought for each site: the number of lane changes and erratic maneuvers for the entire study length, and the number of lane changes and erratic maneuvers for the 91.5-m (300-ft) segment closest to the gore. The hourly values for the entire study length reflected the quantity of lane changes (or erratic maneuvers) occurring at the site. Because of concern with inappropriate driving behavior near gore areas, the 91.5-m (300-ft) segment closest to gore value was also determined. The hourly values were calculated by dividing the total number of lane changes for a zone, or for all zones, by the number of 15-min intervals reduced and then

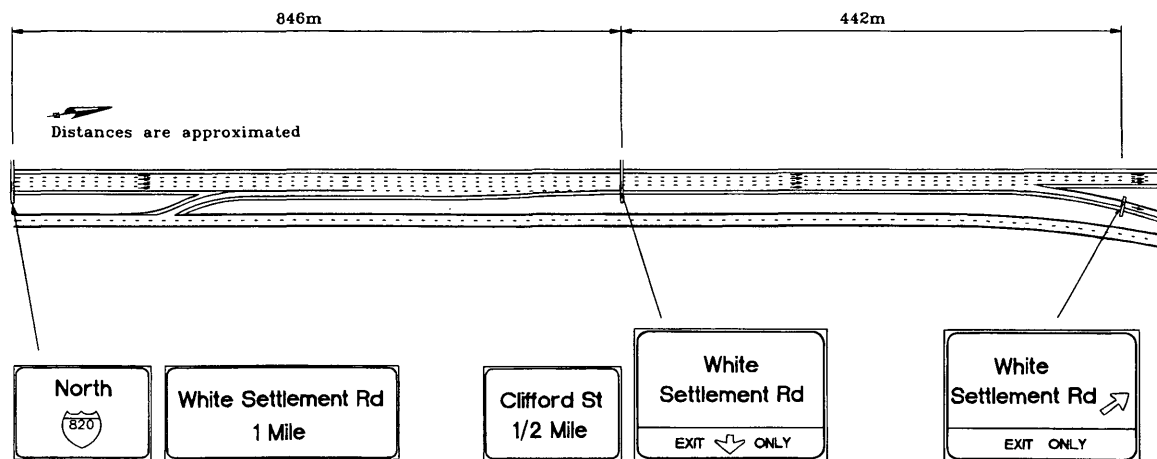
multiplying by 4 to obtain an hourly value. Table 2 lists the findings for each site.

The concluding step of the evaluation used all available resources, such as site characteristics, plots, numeric values, and results from statistical evaluations, to draw observations and then conclusions for the project.

BEFORE-AND-AFTER FINDINGS

Volumes

When comparing changes in driver behavior in a before-and-after study, potential influences, other than the item studied (which in this



Conversion factor: 0.305m = 1ft

FIGURE 1 Site A before condition.

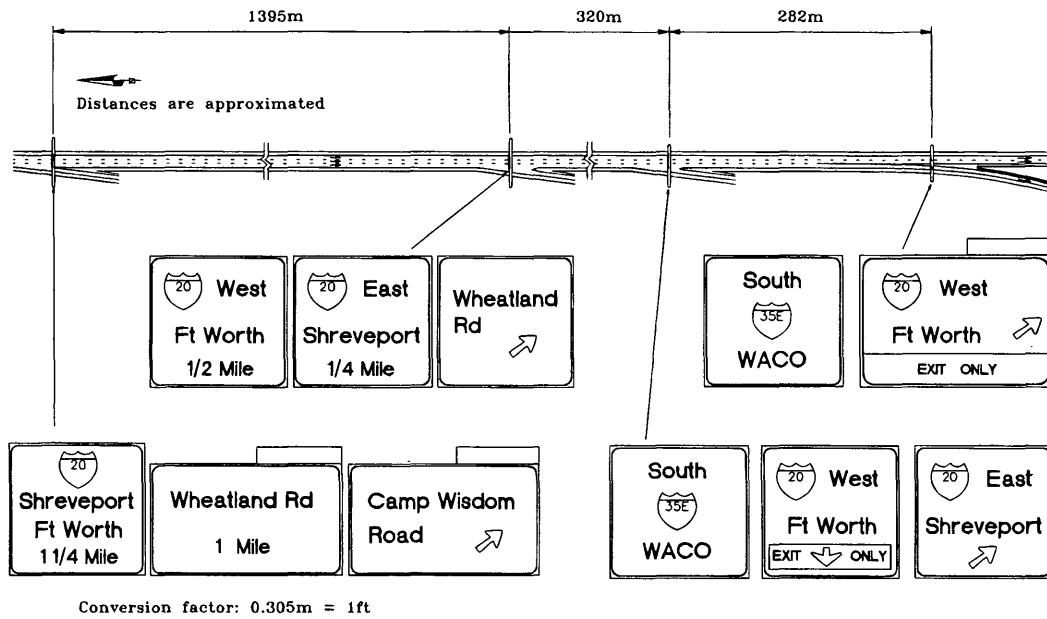


FIGURE 2 Site B before condition.

project is the lane drop markings), should be investigated to determine whether they affect the results. From observations and information from the TxDOT, nonrecurrent congestion or construction did not influence the data. Another item to investigate is whether traffic volumes are similar from the before period to the after period. To compare the before-and-after traffic volumes, an analysis of variance statistical model was used. The test showed that there were no differences in before-and-after traffic volumes for any given site.

Lane Changes

The next statistical test determined if the values of lane changes per hour (as listed in Table 2) were statistically different from the changes from the before to the after period. A test of equality of proportions (also known as the comparison of two binomial parameters test) determined whether the overall percentage of total lane changes or erratic maneuvers before the treatment was equal to the

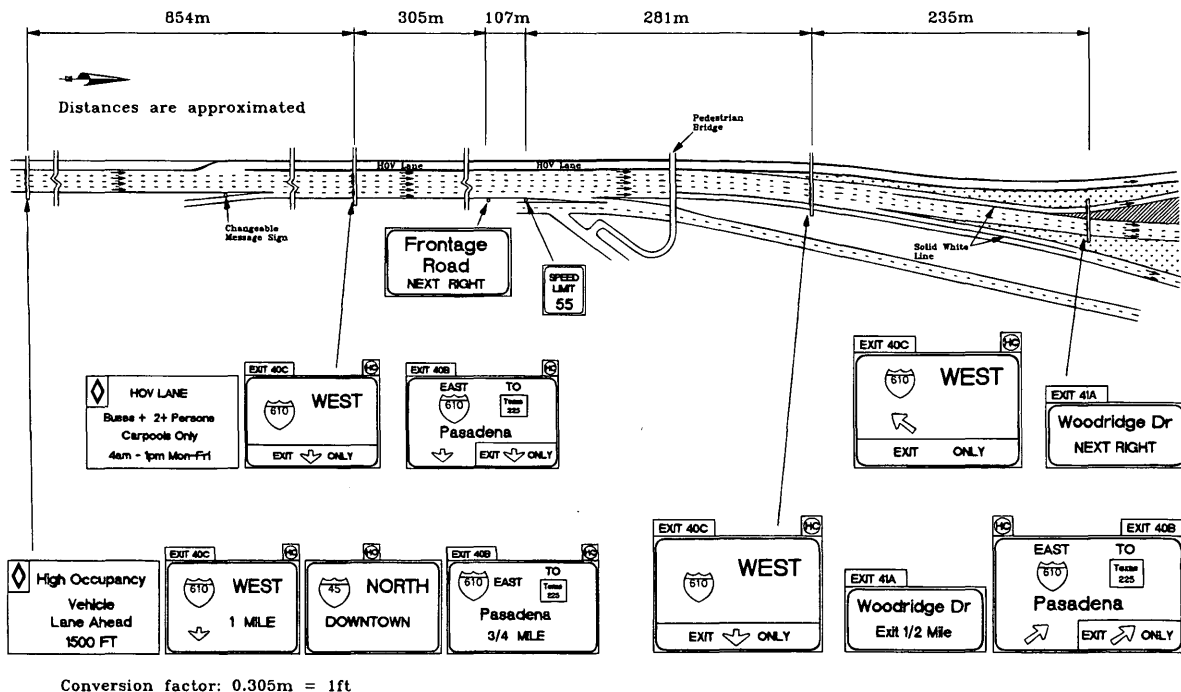
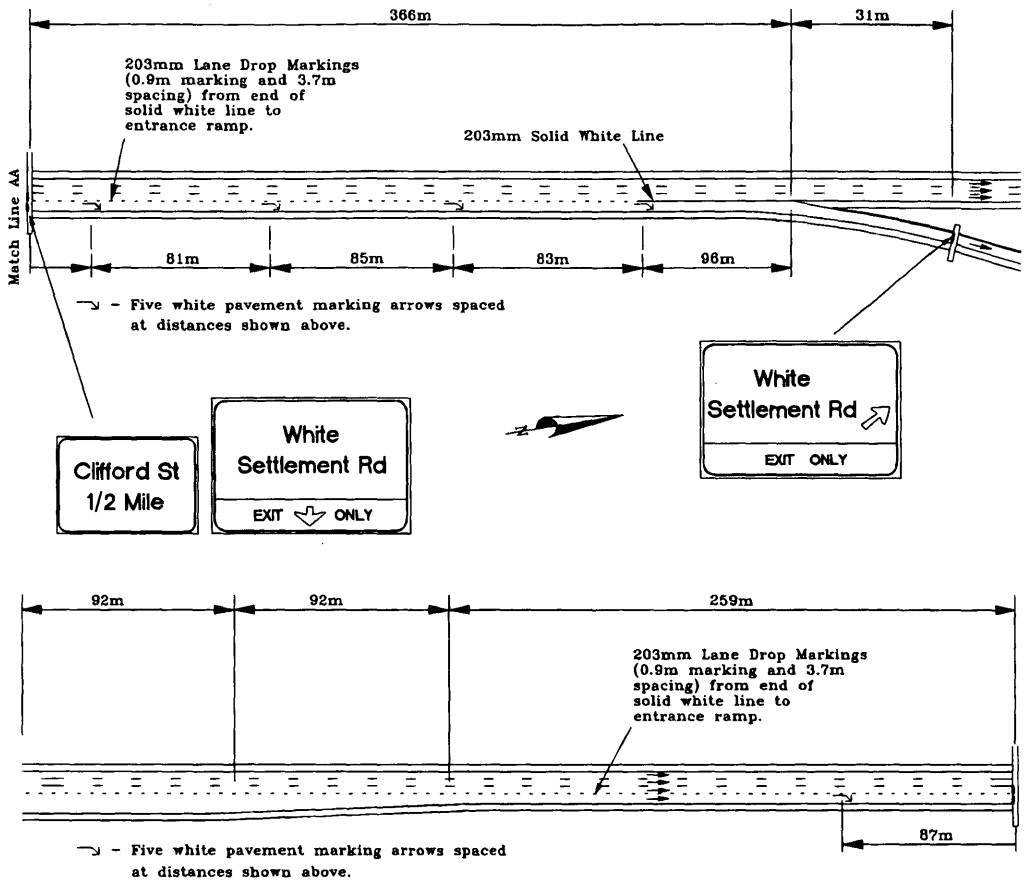
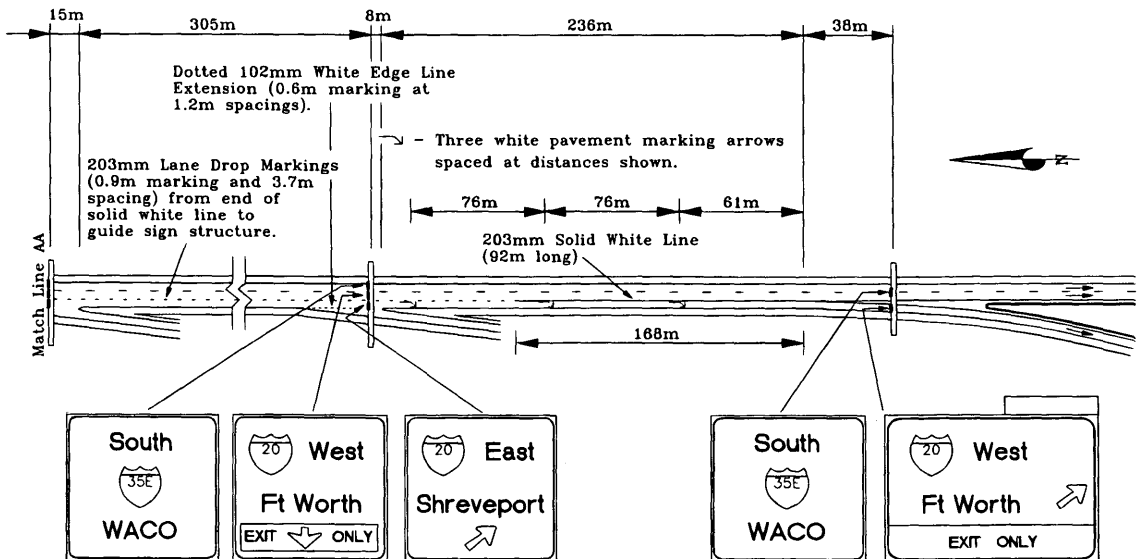


FIGURE 3 Site C before condition.



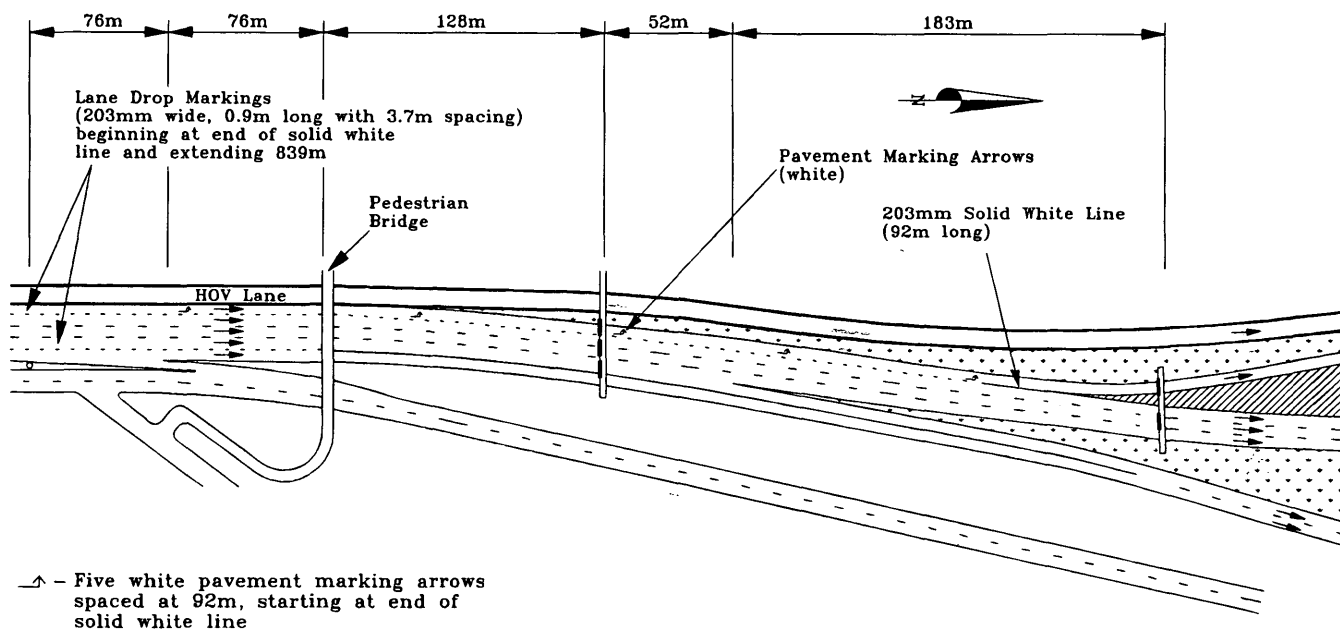
Distances are approximated
 Conversion factor: 0.305m = 1ft and 25.4mm = 1in

FIGURE 4 Pavement markings installed at Site A.



Distances are approximated
 Conversion factor: 0.305m = 1ft and 25.4mm = 1in

FIGURE 5 Pavement markings installed at Site B.



Distances are approximated

Conversion factor: 0.305m = 1ft and 25.4mm = 1in

FIGURE 6 Pavement markings installed at Site C.

percentage after treatment. For example, for Site A, the percent of the total lane changes was 58.3 before and 41.6 after. The statistical test compares these numbers to 50 percent. Table 3 shows the results. In each case, the decrease in the number of lane changes at a site was statistically significant.

Erratic Maneuvers

The number of erratic maneuvers at all sites decreased from the before period to the after period for both the entire study length and the 91.5-m (300-ft) segment closest to the gore and over 33 percent for the entire study length. Substantial decreases in the number of one-lane lane changes through the gore and swerves into a lane and backout (attempted lane change) were the prime contributors to the reduction in number of erratic maneuvers at Sites B and C. The largest decrease in the erratic maneuver type at Site A was the two-lane lane change. The statistical test revealed that only the erratic maneuvers at Site A (see Table 3) did not have a statistically significant difference between the before-and-after periods.

Location of Lane Changes

To determine whether a "shift" in lane change locations is occurring, plots of percent of lane changes per zone were used. Percent lane change demonstrates where lane changes are occurring within the study site. If lane changes are uniform and the study site has ten zones, one would expect each zone to experience approximately 10 percent of the lane changes. If in the after period of the hypothetical situation the five zones furthest from the gore now each have 20 percent of the lane changes and the five zones closest to the gore now have no lane changes, a conclusion that the markings created

a "shift" in where the lane changes occurred could be made, that is, one would conclude that drivers change lanes further upstream of the gore.

Because of the variations present when the data were distributed in the 30.5-m (100-ft) increments, the data were collapsed into 61-m (200-ft) zones to better illustrate the findings. When these plots were reviewed, a shift in where lane changes occurred was revealed for certain situations. The plot of percent of lane changes per zone for Site A indicates that the distribution of lane changes in the before period is similar to the distribution of lane changes in the after period. In other words, no shifting of lane changes from one area of the study segment to another occurred (see Figure 10).

Site B and C plots, however, did show a shift in where vehicles were changing lanes, with the most noticeable shift occurring for vehicles moving out of the exit lane. Figure 11 illustrates the percent lane changes by zone for the vehicles moving from the exit lane into the through lane for Site B. For the eight zones closest to the gore [representing approximately 244 m (800 ft) upstream of the gore], fewer vehicles left the exit lane in the after period than in the before period, whereas for Zones 10 through 17 more vehicles left the exit lane in the after period than in the before period. In summary, Site B drivers are leaving the exit lane further upstream of the gore after the lane drop markings were installed. Site C also showed a similar trend. As indicated in Figure 12, fewer vehicles in the after period than in the before period left the exiting lane in the 183 m (600 ft) closest to the gore.

To statistically validate the suspected shift, the percentage distribution for the before-and-after time periods were tested for equality using the chi-square test for independence. The overall chi-square value for total lane changes at Site A was not significant, indicating that there was no significant variability in the lane change percentage distribution before-and-after treatment for any zones. For Sites B and C, the overall chi square was significant, which indi-

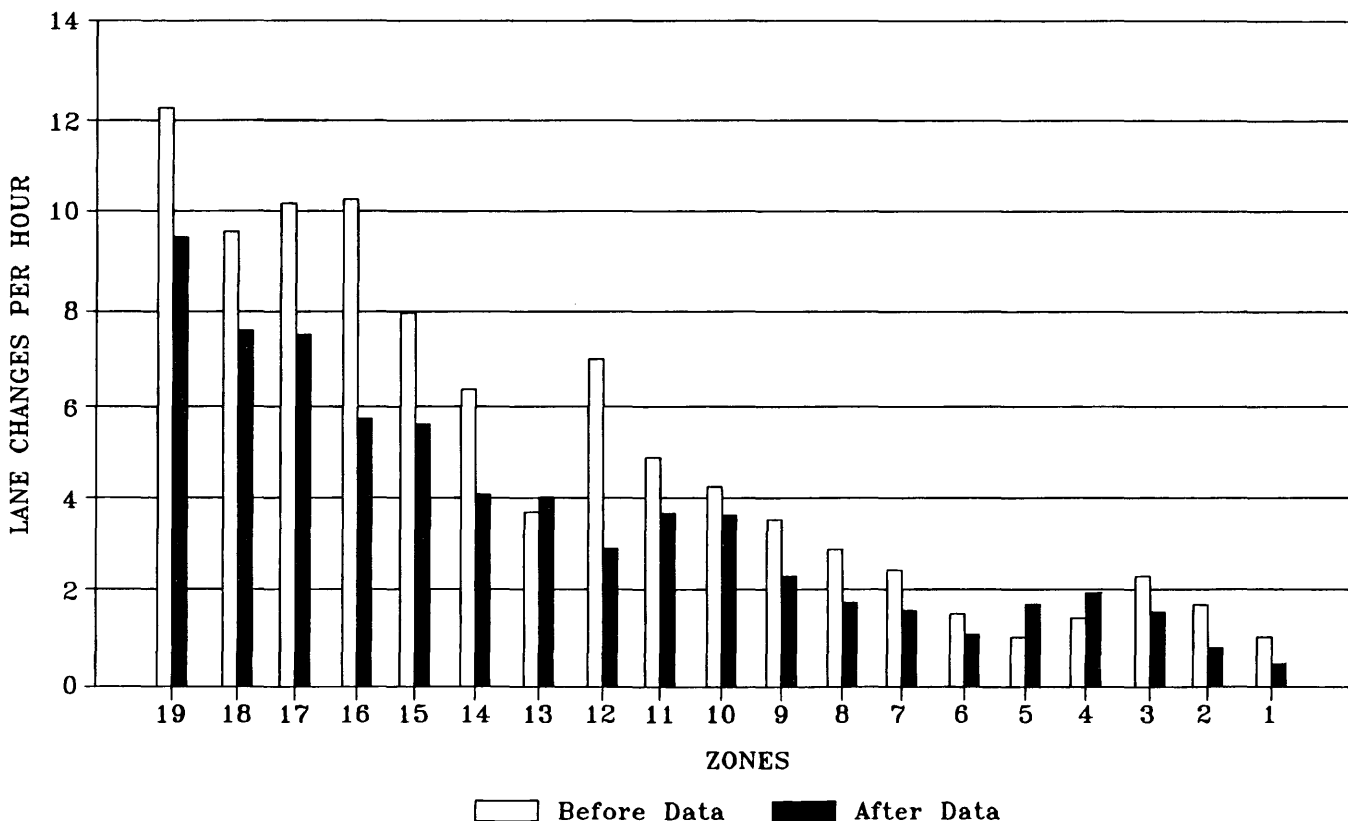
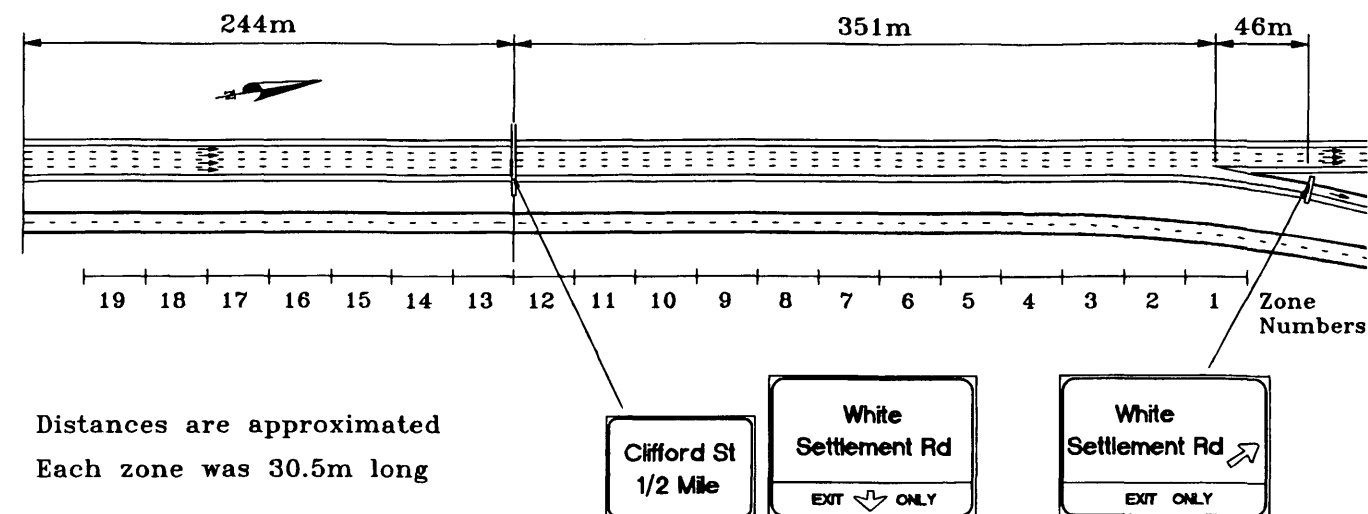


FIGURE 7 Site A layout and lane changes per hour per zone.

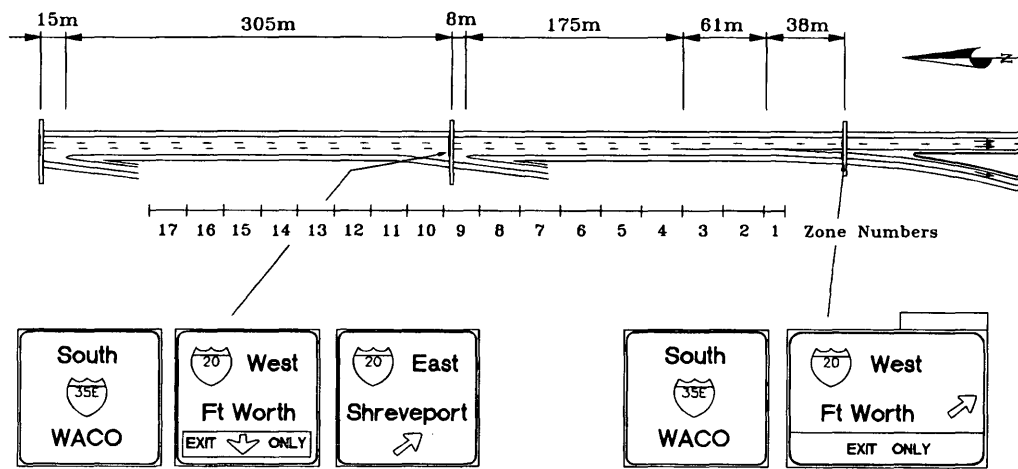
icates that there was a difference in at least one zone. All three sites had a statistically significant difference for the exit-to-through maneuver.

To determine the zones that were statistically different, the individual standardized cell chi squares were tested. All tests were completed at the 0.05 level of significance. Figures 11 and 12 illustrate the findings from the statistical test for the exit-to-through lane changes. The zones that showed a significant difference in percentage distribution of lane change before and after treatment are high-

lighted. The statistical tests confirmed that the lane drop markings caused a shift in where lane changes occurred at Sites B and C.

Combining Findings

Another observation on the reduction and shifting of lane changes is appropriate. Although the lane drop markings have caused a shift in where motorists are leaving the exit lane in Sites B and C but not



Distances are approximated

Each zone was 30.5m long except zone 1 which was 15.3m long

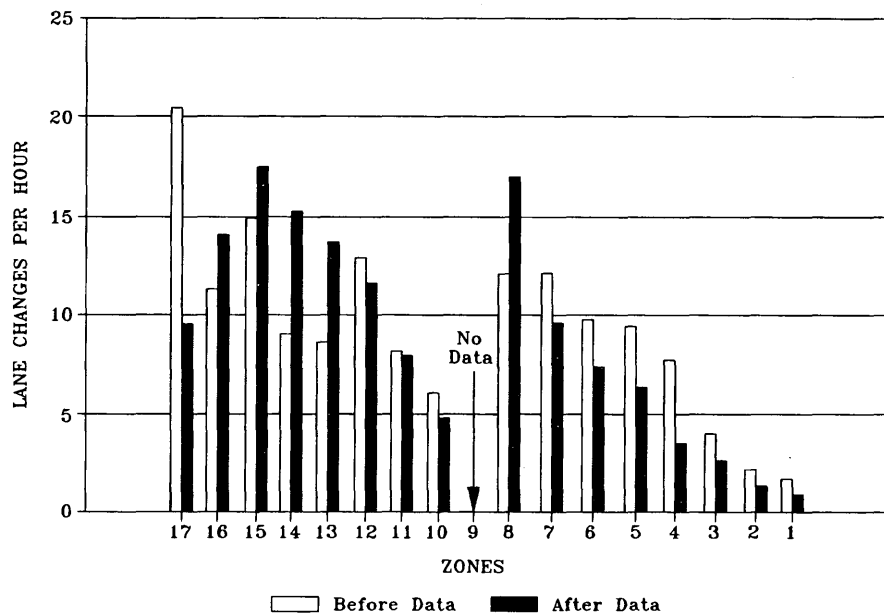
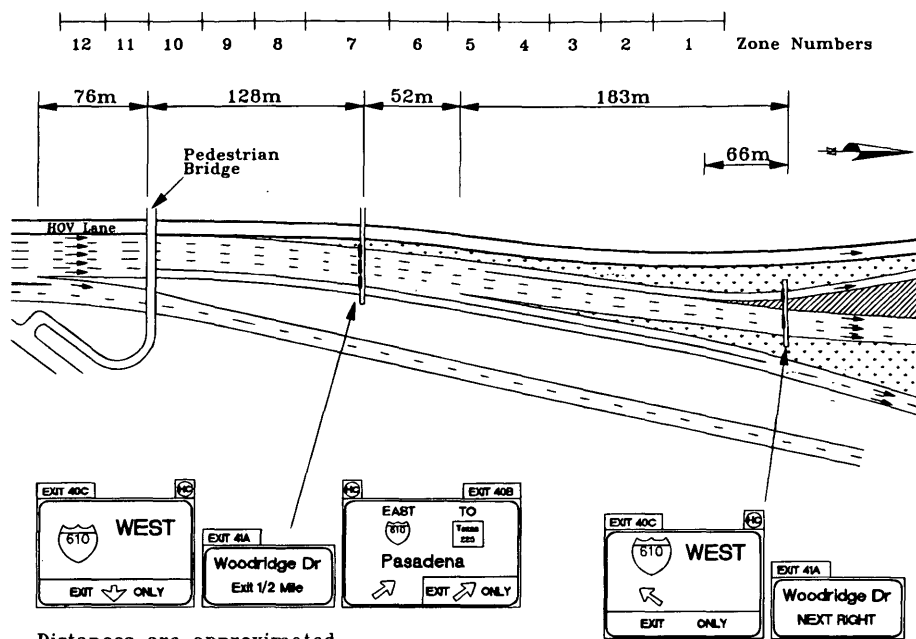


FIGURE 8 Site B layout and lane changes per hour per zone.

in Site A, this finding may be a function of the length of the study segment and the presence of upstream entrance and exit ramps. For example, Site A could have experienced a shift in where lane changes occurred, with the shift occurring upstream of the study segment. An entrance ramp is located approximately 762 m (2,500 ft) upstream of the gore. The large reduction in lane changes at Site A (29 percent drop) could be a reflection that when vehicles enter the freeway on the entrance ramp and see the lane drop markings, they are moving from the entrance ramp through the exit lane to a through lane before entering the study segment. If so, then a shift in where motorists are changing lanes at Site A could also be occurring. However this region was beyond the study sections and therefore could not be tested.

SUMMARY AND CONCLUSIONS

The field studies demonstrated that the installation of lane drop markings can cause a shift in where motorists make lane changes in advance of a lane drop. The distribution data from Sites B and C (see Figures 11 and 12) revealed that drivers are exiting the lane further upstream of the lane drop in the after period than in the before period. For the area immediately upstream of the gore [e.g., the 183 to 244 m (600 to 800 ft) closest to the gore], fewer vehicles left the exit lane in the after period than in the before period (both in terms of percentages and absolute values). For the area upstream of the gore, more vehicles left the exit lane in the after period than in the before period [between 241 and 366 m (700 and 1,200 ft) or 305 to



Distances are approximated

Each zone was 30.5m long except zone 7 (53m) and zone 1 (37m)

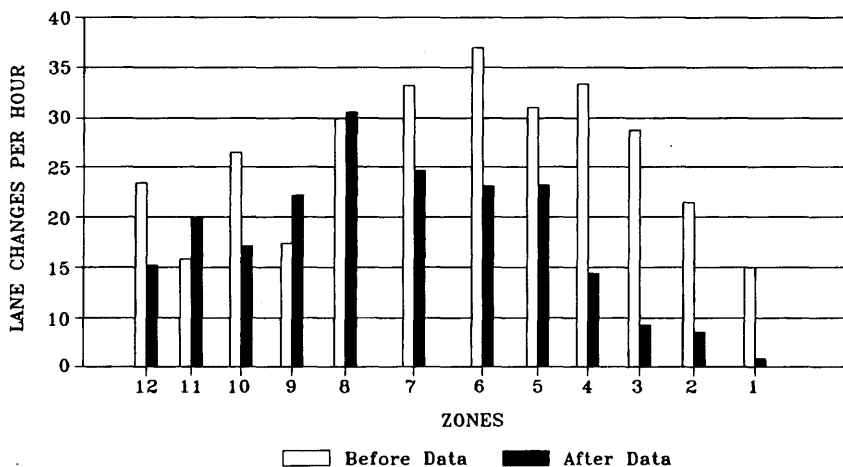


FIGURE 9 Site C layout and lane changes per hour per zone.

519 m (1,000 and 1,700 ft) upstream of the gore, depending on the site].

Similar analysis at the other before-and-after study site (Site A) did not produce the same results. The distribution data (see Figure 10) showed that a shift was not occurring within the study segment [which was approximately 488 m (1,600 ft) long]. Other evidence, such as the statistically significant reduction in the number of lane changes, indicates that a shift may be occurring upstream of the study segment limit. An entrance ramp is located approximately 762 m (2,500 ft) upstream of the gore, and the large reduction in lane changes within the study segment could be a reflection that vehicles entering the freeway on the entrance ramp and seeing the lane drop markings are moving from the entrance ramp through the exit lane to a through lane before entering the study segment.

The before-and-after studies also revealed that the number of erratic maneuvers within the entire study segment decreased with the installation of the markings. Decreases over 50 percent were observed at two of the three sites for the area within 91.5 m (300 ft) of the gore. The largest decrease was in the number of one-lane changes through the gore.

RECOMMENDATIONS

Government agencies should use lane drop markings and arrows at exit lane drops for the following reasons: (a) the field studies demonstrated that the installation of the lane drop markings caused a shift in where motorists are making lane changes in advance of a

TABLE 2 Comparison of Before-and-After Data

Characteristics	Site A			Site B			Site C		
Exit Name	I-820 NB to White Settlement			I-35E SB to I-20 West			I-45 Northbound to I-610 West		
Time used in comparison	7:30 a.m. to 5:45 p.m.			6:45 a.m. to 6:00 p.m.			7:15 a.m. to 6:00 p.m.		
Zones used in comparison	Zones 1 to 19			Zones 1 to 17 (except 9)			Zones 1-12		
Equil. length of study site	580 m			488 m			378 m		
	Before	After	Change	Before	After	Change	Before	After	Change
Freeway hourly volume ^a	1436	1453	1%	1405	1374	-2%	5851	5761	-2%
Hourly volume exiting ^a	280	231	-18%	158	165	4%	1708	1720	1%
Total study length									
Lane Changes ^b	95.2	67.8	-29%	149.6	141.1	-6%	315.0	217.0	-31%
Erratic Maneuvers ^b	5.1	4.2	-18%	12.9	8.6	-33%	47.5	28.4	-40%
For 91.5 m nearest to gore									
Lane Changes ^b	5.4	3.1	-42%	7.8	4.4	-44%	66.0	24.0	-64%
Erratic Maneuvers ^b	0.7	0.5	-29%	5.6	2.0	-64%	25.2	12.6	-50%
Rate ^c (10 ⁻⁶ /ft/veh)									
Lane Changes	114.3	80.7	-30%	218.0	210.5	-4%	142.4	99.68	-30%
Erratic Maneuvers	6.2	4.9	-19%	18.7	12.8	-32%	21.5	13.0	-39%

^a Freeway hourly volumes were measured prior to gore and represent the average of the time periods used in the comparison

^b Values represent an average 60-minute period for the time periods used in the comparison.

^c Rates were determined by dividing the number of lane changes, or erratic maneuvers, in an hour by study length and freeway hourly volume, and multiplying by 1,000,000.

Conversion factor: 0.305 m = 1 ft

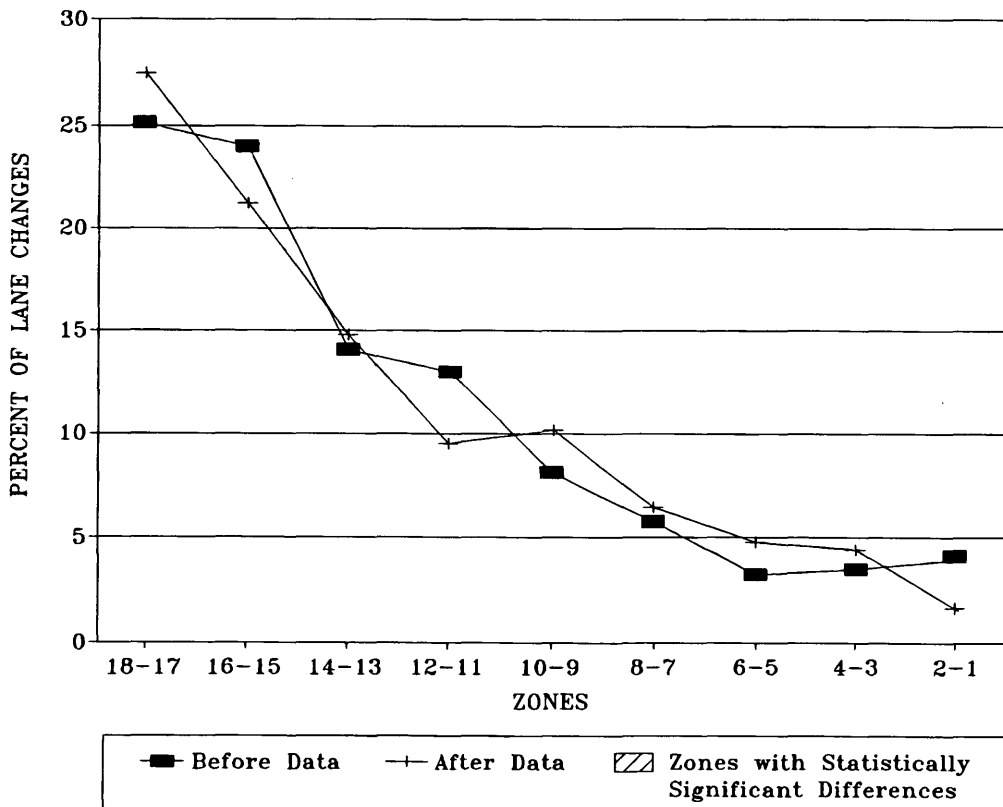


FIGURE 10 Site A exit-to-through lane changes.

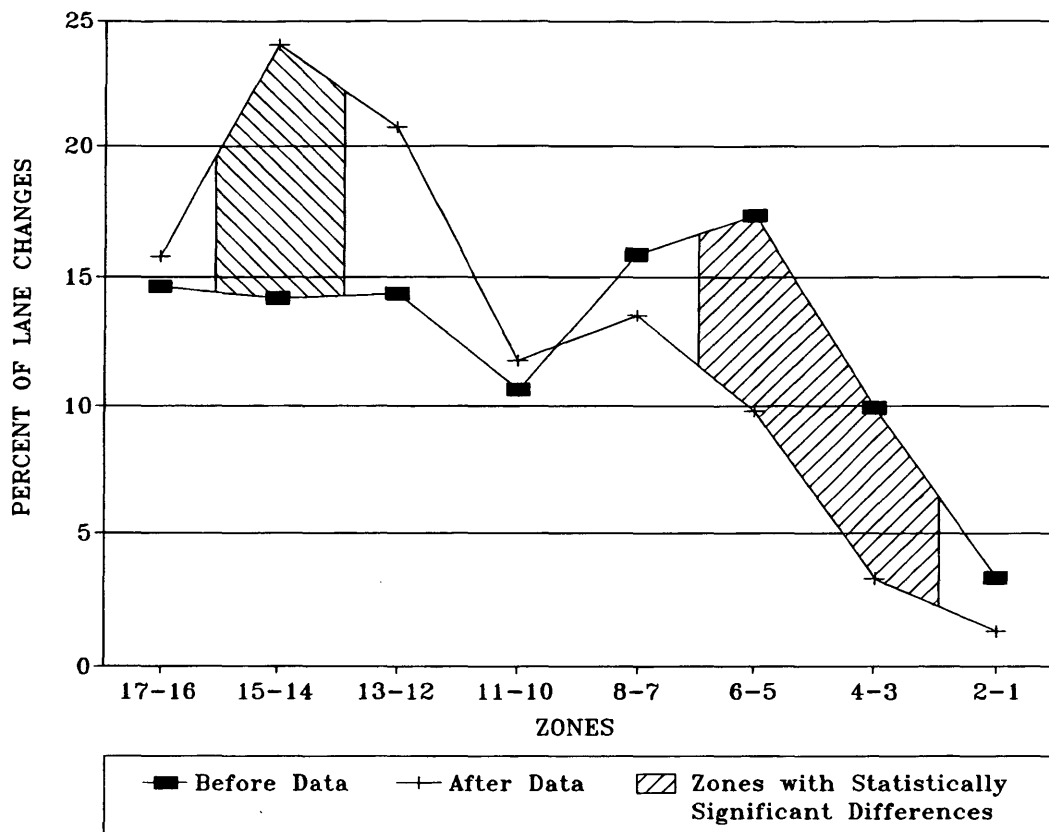


FIGURE 11 Site B exit-to-through lane changes.

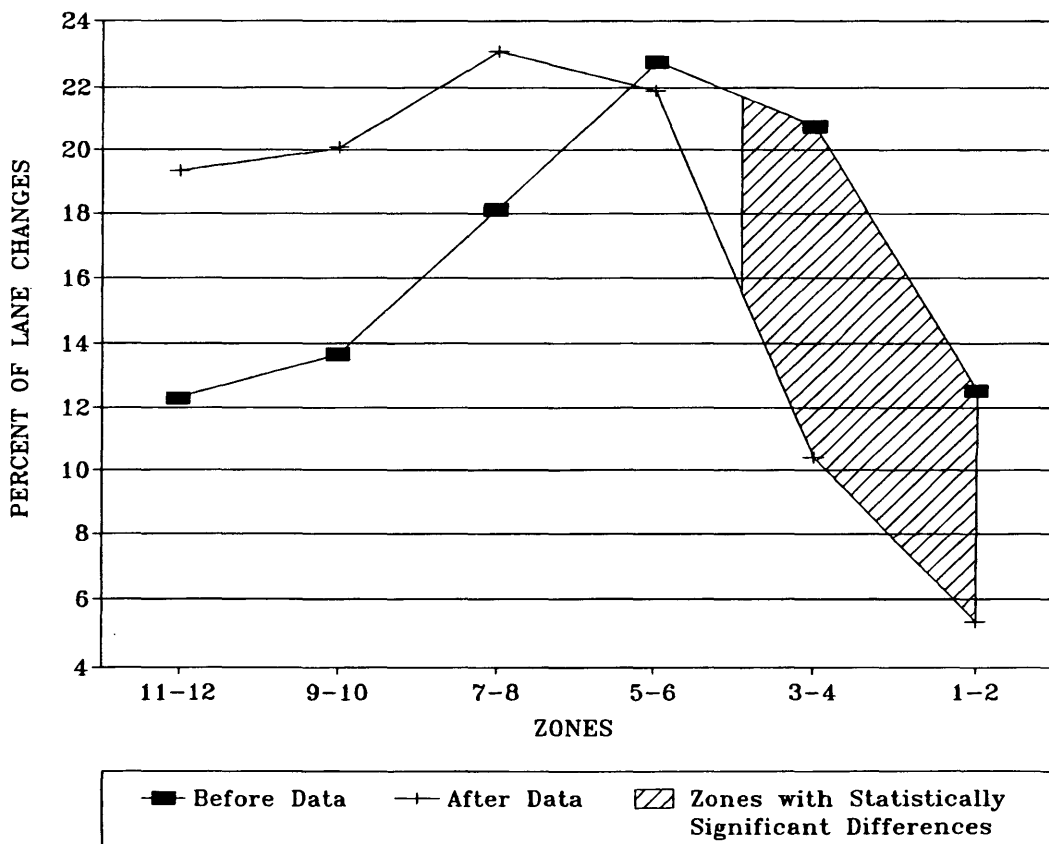


FIGURE 12 Site C exit-to-through lane changes.

TABLE 3 Results of the Equality of Proportions Tests

	Site A		Site B		Site C	
	Before	After	Before	After	Before	After
Number of Lane Changes for Study Segment ^a	976	696	1683	1587	3386	2333
Lane Change Proportion	.58	.42	.51	.49	.59	.41
Z statistic ^b Significant/Not Significant?	9.72 Significant		2.36 Significant		19.70 Significant	
Number of Erratic Maneuvers for Study Segment ^a	52	43	145	97	511	305
Erratic Maneuvers Proportion	.55	.45	.60	.40	.63	.37
Z statistic ^b Significant/Not Significant?	1.34 Not Significant		4.40 Significant		10.17 Significant	
Number of Lane Changes for Gore Area ^a	55	32	88	50	710	258
Lane Change Proportion	.64	.36	.64	.36	.73	.27
Z statistic ^b Significant/Not Significant?	3.57 Significant		4.62 Significant		20.53 Significant	
Number of Erratic Maneuvers for Gore Area ^a	7	5	63	23	271	135
Erratic Maneuvers Proportion	.58	.42	.74	.26	.67	.33
Z statistic ^b Significant/Not Significant?	0.83 Not Significant		6.19 Significant		9.50 Significant	

^a for an average day of observations

^b If the calculated Z statistic is greater than 1.645, then one can conclude that the difference is significant.

lane drop and (b) erratic maneuvers decreased. The consistent use of the marking treatments can provide other benefits, such as consistency in communicating lane drops to motorists and improved driver expectancy at exit lane drops.

This research studied the effects of the markings on one-lane drop exits. Additional research is needed to determine the effects of lane drop markings on motorist behavior at two-lane exits with an option lane and an exit-only lane.

ACKNOWLEDGMENTS

The authors recognize the fellow researchers who contributed to this research: Mike Ogden, Tom Urbanik, and Olga Pendleton. They also express their appreciation to the students who reduced the large quantity of data from the videotapes. This research was sponsored by TxDOT and FHWA. Data for this paper are from two TxDOT projects. The efforts and guidance provided by members of the projects' technical panels are recognized.

REFERENCES

1. *Texas Manual on Uniform Traffic Control Devices*. State Department of Highways and Public Transportation, Austin, 1980.
2. *Manual on Uniform Traffic Control Devices*. U.S. Department of Transportation, FHWA, Washington, D.C., 1988.
3. Fitzpatrick, K., T. Lienau, M. A. Ogden, M. Lance, and T. Urbanik. *Freeway Exit Lane Drops in Texas*. FHWA/TX-94/1292-IF. Texas Transportation Institute, College Station, Nov. 1993.
4. Ogden, M. A., and S. Albert. *Analysis of California Striping to Be Utilized in Texas, Exit Lane Striping Proposal*. Technical Memorandum. Texas SDHPT, May 1989.

The contents of this paper reflect the views of the authors, who are responsible for the opinions, findings, and conclusions presented. The contents do not necessarily reflect the official views or policies of TxDOT of FHWA. This paper does not constitute a standard, specification, or regulation.

Publication of this paper sponsored by Committee on Traffic Control Devices.

Comparative Study of Advance Warning Signs at High Speed Signalized Intersections

PRAHLAD D. PANT AND YUHONG XIE

The effects of two dynamic signs that begin to flash a few seconds before the onset of the yellow interval and a static sign that flashes all the time were examined at rural, high-speed signalized intersections. The dynamic signs included (a) a PTSWF (prepare to stop when flashing) sign, and (b) an FSSA (flashing symbolic signal ahead) sign with green, yellow, and red circles. The static sign was a CFSSA (continuously flashing symbolic signal ahead) sign with the three circles. The effects of these signs on vehicular speeds at different segments of the intersection approach including the dilemma zone were analyzed as were the vehicle conflict rates and the responses from the drivers' surveys. The study revealed that the PTSWF and FSSA signs generally have similar effects on driver behavior. It is advantageous to consider the CFSSA sign before using the PTSWF sign because the PTSWF and FSSA signs have a few undesirable effects on vehicular speeds, unlike the CFSSA sign. The use of a PTSWF sign at a tangent approach to a high-speed signalized intersection is discouraged.

High-speed signalized intersections at unexpected or hidden locations generally pose a potentially hazardous situation for drivers when the signal indication changes from green to yellow. A dilemma or decision zone exists on the intersection approach upstream of the stopline, which makes it difficult for the drivers to decide whether to stop during the yellow interval or go through the intersection before the beginning of the red interval. Traffic engineers generally have used advance warning signs and inductive loop detectors to warn drivers of the existence of the signalized intersection or to adjust the green time to minimize dilemma zone problems.

This paper presents the final outcomes of a study in Ohio, the earlier results of which were previously published (*1*). The following advance warning signs with flashers were examined. The signs were ground mounted and diamond shaped.

SIGNS

Prepare To Stop When Flashing Sign

As indicated in Figure 1, the prepare to stop when flashing (PTSWF) sign has two flashers (one at the top and the other at the bottom) that begin to flash a few seconds before the onset of the yellow interval and continue to flash until the end of the red interval. Meanwhile the loop detectors, if any, are temporarily shut down until the beginning of the next green phase.

Currently, Ohio Department of Transportation (ODOT) uses a passive symbolic signal ahead (PSSA) sign in advance of the

PTSWF sign at signalized intersections. The PSSA sign is a passive advance warning sign that has the green, red, and yellow circles. The purpose of installing a PSSA sign is to inform the drivers of the existence of the signalized intersection because the PTSWF sign is not necessarily capable of conveying this message.

Flashing Symbolic Signal Ahead Sign

The flashing symbolic signal ahead (FSSA) sign is similar to the PTSWF sign except that the words are replaced by the green, red, and yellow circles. The two flashers operate in the same manner as the PTSWF sign.

Continuously Flashing Symbolic Signal Ahead Sign

The continuously flashing symbolic signal ahead (CFSSA) sign, as the name suggests, has flashers that flash all the time. The flashers are not connected to the signal controller.

The overall objective of the study was to perform a comparative evaluation of these signs relative to their effects on driver behavior. These signs were installed at high-speed signalized intersections in rural areas where signals are normally unexpected or hidden because of curvature.

STUDY DESIGN AND DATA COLLECTION

The study was performed by collecting traffic flow and related data at the following study sites.

Intersection with Tangent Approach: US-33 at US-127 in Mercer County

The study site is a two-lane highway located in a rural area. The PSSA sign was located at 397 m (1,303 ft) upstream of the intersection and the PTSWF sign (and later the FSSA or CFSSA sign) existed at 200 m (655 ft) upstream of the intersection. The signs at the study sites are listed in chronological order:

- 1988: PSSA sign with no flashers. This sign was used for reference purposes only.
- 1989–1991: PTSWF and PSSA signs,
- 1992: FSSA sign (Because the FSSA sign has the green, yellow, and red circles, the PSSA sign was removed from the site.), and
- 1993: CFSSA sign.

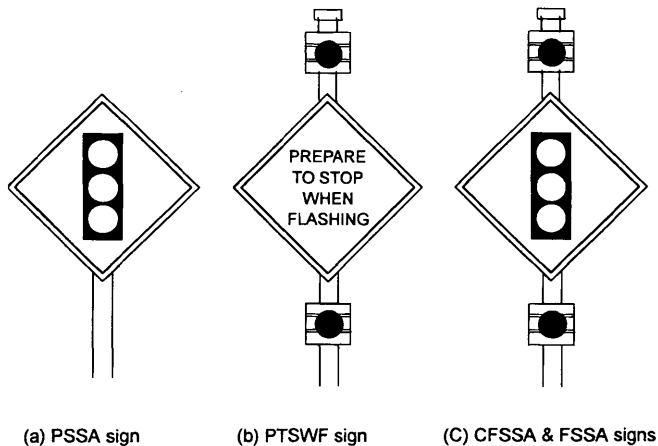


FIGURE 1 Advance warning signs with flashers.

Intersection with Curved Approach: SR-37 at US-40 in Licking County

The study site is a curved approach with one lane and no exclusive left turning lane at the intersection. In 1988, there was a CFSSA sign with only one flasher at 312 m (1,024 ft) upstream of the intersection. In 1989, it was replaced by a PSSA sign, and a PTSWF sign was installed at 202 m (664 ft) upstream of the intersection. In 1992, the PTSWF sign was replaced by an FSSA sign and the PSSA sign was removed. In 1993, a CFSSA sign with two flashers replaced the FSSA sign. The discussions below refer to the CFSSA sign installed in 1993. The following intersections were used as control sites: (a) intersection with tangent approach: US-36 and SR-235 in Champlain County; and (b) intersection with curved approach: US-127 and SR-725 in Preble County.

When a new sign was installed at an intersection, a minimum of 6 months was allowed for the drivers to become familiar with the sign before the data were collected. Because of time and financial constraints, it was not possible to counterbalance the order of the various treatments at the study sites. The driver learning effects, if any, could not be directly examined in this study.

The following data were collected at the study and control sites

Vehicle Speed

The intersection approach on which the data were collected was divided into the following four zones.

- Zone 1—The roadway segment in advance of the PSSA sign (US-33 at US-127) or the old CFSSA sign with one flasher (SR-37 at US-40);
- Zone 2—The roadway segment, downstream of Zone 1, measured from the existing sign to the PTSWF (or FSSA or CFSSA) sign;
- Zone 3—The roadway segment from the PTSWF (or FSSA or CFSSA) sign to the beginning of the decision zone;
- Zone 4—The roadway segment from the beginning of the decision zone to the stopline.

The data were collected by five observers who recorded the arrival time of sampled vehicles at various positions along the inter-

section approach. Other information recorded by the observers included vehicle type (passenger vehicles or trucks), flasher and signal indications when the vehicle arrived at selected positions, and whether the vehicle stopped at the intersection. The vehicles were sampled for several hours during various periods from 7:00 a.m. to midnight.

Vehicle Conflict

All vehicles moving through the intersection were observed for the following types of conflicts: (a) run red light, (b) stop abruptly, and (c) accelerate through yellow. The turning movements (through, right, or left turn) were also recorded.

Driver Survey

A questionnaire was prepared to obtain drivers' subjective responses to the advance warning signs. Copies of the questionnaire were mailed to area residents or distributed to visitors or employees at nearby business facilities.

A more detailed description of the method for data collection and the location of the signs appear elsewhere (1). The speed patterns were examined relative to the following conditions:

1. Flasher conditions (on or off) when the vehicles arrived at the locations of the existing sign as well as the PTSWF (or FSSA or CFSSA) sign, as applicable;
2. Signal indications (green, yellow, or red) when the vehicles arrived at the beginning of the decision zone and at the stopline; and
3. Vehicle status at the stopline (stop or go).

Vehicles were categorized according to several combinations of flasher and signal conditions and whether the vehicles stopped at the intersection, as follows:

1. Off-Off-Green-Green-Go,
2. Off-Off-Green-Yellow-Go,
3. On-Off-Green-Green-Go,
4. On-On-Red-Green-Go,
5. On-On-Red-Red-Stop, and
6. Off-On-Red-Red-Stop.

The first condition (off or on) refers to the status of the flashers when the vehicles arrived at the existing sign. Similarly, the second condition (off or on) refers to the status of the flashers when the vehicles arrived at the PTSWF (or FSSA or CFSSA) sign. The next two conditions (green-green, green-yellow, etc.) refer to the status of the signal indication when the vehicles arrived at the beginning of the dilemma zone and the stopline, respectively. The final condition (go or stop) refers to the status of the vehicle at the stopline, that is, whether the vehicle stopped.

STUDY RESULTS

Speed Study

The speed data were analyzed separately for the passenger vehicles and trucks in the through direction. The speed variables included in the analysis were the mean, 85th percentile, and 95th percentile speeds.

Condition: Off-Off-Green-Green-Go

Passenger Vehicles. When the PTSWF sign was installed on the tangent approach, the mean speeds in Zones 3 and 4 were almost equal (Figure 2). Similarly, when the FSSA sign existed on the tangent approach, the results indicated a similar speed pattern in Zones 3 and 4. However, when the CFSSA sign existed on the tangent approach, the mean speed in Zone 4 dropped by 11 kph (7 mph) from that in Zone 3. The result showed that the impacts of the dynamic (PTSWF or FSSA) and static (CFSSA) signs on the speed behavior of the drivers in Zone 4 were different. (The differences in mean speeds reported in this paper are based on *t*-tests at 0.05 level of significance.)

An analysis of the 85th percentile speeds demonstrated more noticeable changes in the speed patterns when the dynamic advance warning signs existed on the tangent approach. It showed that the PTSWF and FSSA signs caused an increase in the 85th percentile speeds in Zone 4, whereas the CFSSA sign caused a decrease. An analysis of the 95th percentile speed showed a similar speed pattern among the three signs.

The speed patterns on the curved approach are shown in Figure 3. The mean speed in zone 1 remained almost unchanged at 75 kph (47 mph) for the three signs, perhaps because of the existence of the roadway curvature. The difference between the mean speeds in Zones 3 and 4 was 10 and 11 kph (6 to 7 mph), with the speeds in Zone 4 being lower than that in Zone 3. Because it was a curved

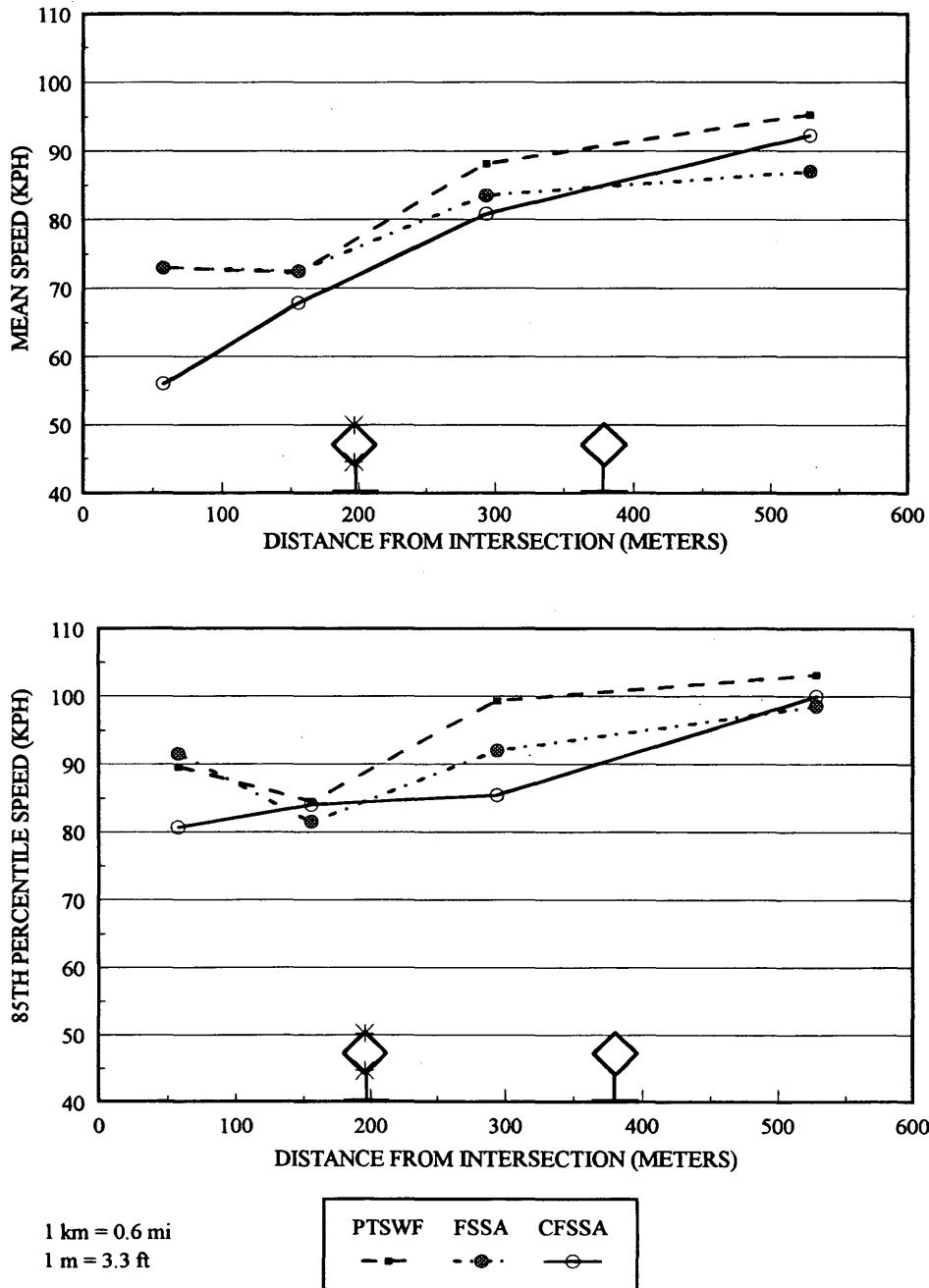


FIGURE 2 Speeds of passenger vehicles at tangent approach: Condition Off-Off-Green-Green-Go.

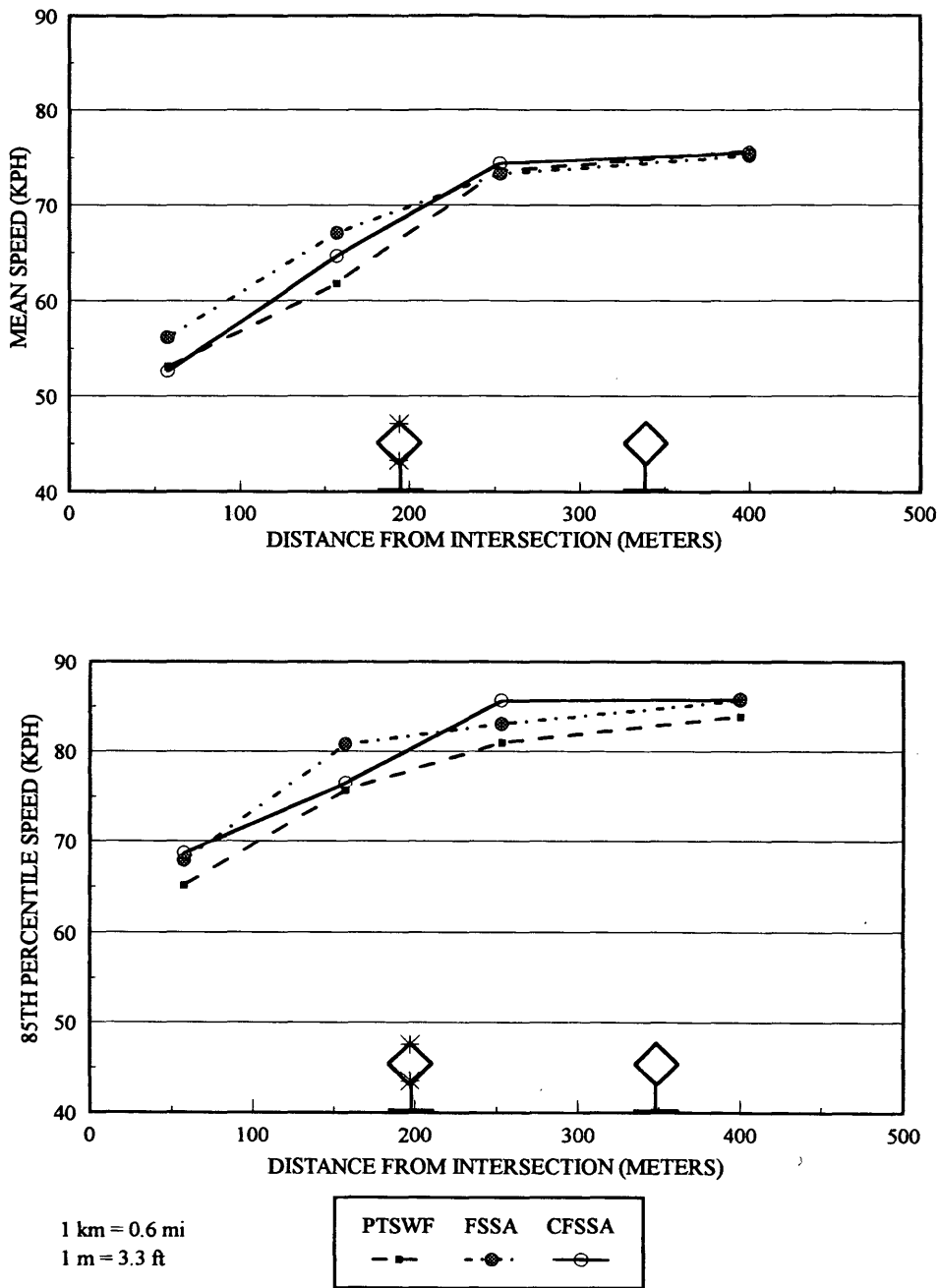


FIGURE 3 Speeds of passenger vehicles at curved approach: Condition Off-Off-Green-Green-Go.

approach, drivers were constrained on the selection of their speeds. The 85th and 95th percentile speeds also showed a diminishing pattern from Zone 1 to Zone 4. Overall, there was little difference on the speed pattern because of the existence of the PTSWF, FSSA, or CFSSA signs. The result is quite in contrast with that found in the tangent approach. It shows that roadway geometry is an important variable in the determination of the vehicular speeds as are flasher and signal indications.

Trucks. The speed data for trucks were separately analyzed (Figure 4). When the PTSWF sign existed on the tangent approach,

the mean speeds in Zones 3 and 4 were almost equal. When the FSSA sign existed on the tangent approach, the trucks increased their mean speed by 5 kph (3 mph) when they traveled from Zone 3 to Zone 4. On the contrary, with the CFSSA sign on the tangent approach, the mean speeds in Zones 3 and 4 were almost equal.

The effects of the signs on vehicular speeds on the tangent approach were more noticeable when the data for the 85th percentile speeds were analyzed. When the PTSWF or FSSA sign existed on the tangent approach, the 85th percentile speeds increased when the trucks traveled from Zone 3 to Zone 4. On the other hand, there was no change in the 85th percentile speed in Zone 4 when the CFSSA sign existed on the tangent approach. The analysis of the 95th per-

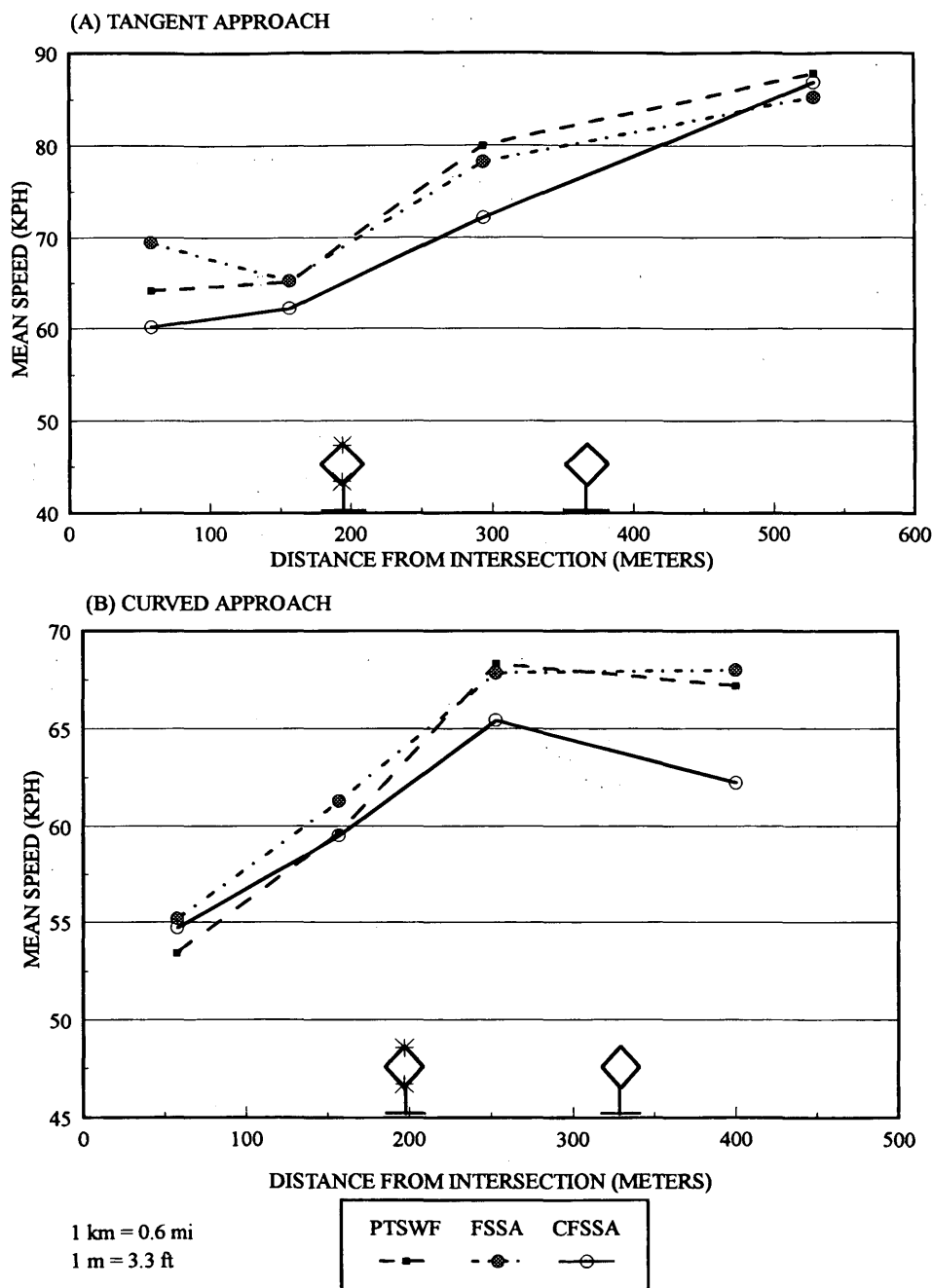


FIGURE 4 Speeds of passenger vehicles at tangent and curved approaches: Condition Off-Off-Green-Green-Go.

centile speeds of the trucks showed similar speed patterns on the approach.

The trucks on the curved approach showed a diminishing speed pattern as they traveled from Zone 1 to Zone 4 (Figure 4). Because the drivers were constrained by the roadway curvature on the selection of their speeds, there was no appreciable difference in their mean speeds in each zone when the PTSWF, FSSA, or CFSSA signs existed on the approach. The difference in the mean speeds between zones 3 and 4 was smaller (5 to 6 kph or 3 to 4 mph) for trucks than for the passenger vehicles (10 to 11 kph or 6 to 7 mph)

Condition: Off-Off-Green-Yellow-Go

Passenger Vehicles. Under the "off-off-green-yellow-go" condition, the signal indication changed from green to yellow when the vehicles traveled from the beginning of the decision zone to the stopline. When the PTSWF or FSSA sign existed on the tangent approach, the drivers of the passenger vehicles increased speed by 10 kph (6 mph) for the PTSWF sign and 6 kph (4 mph) for the FSSA sign when they traveled from Zone 3 to Zone 4 (Figure 5). On the contrary, a decrease of 7 mph in the mean speed was observed when

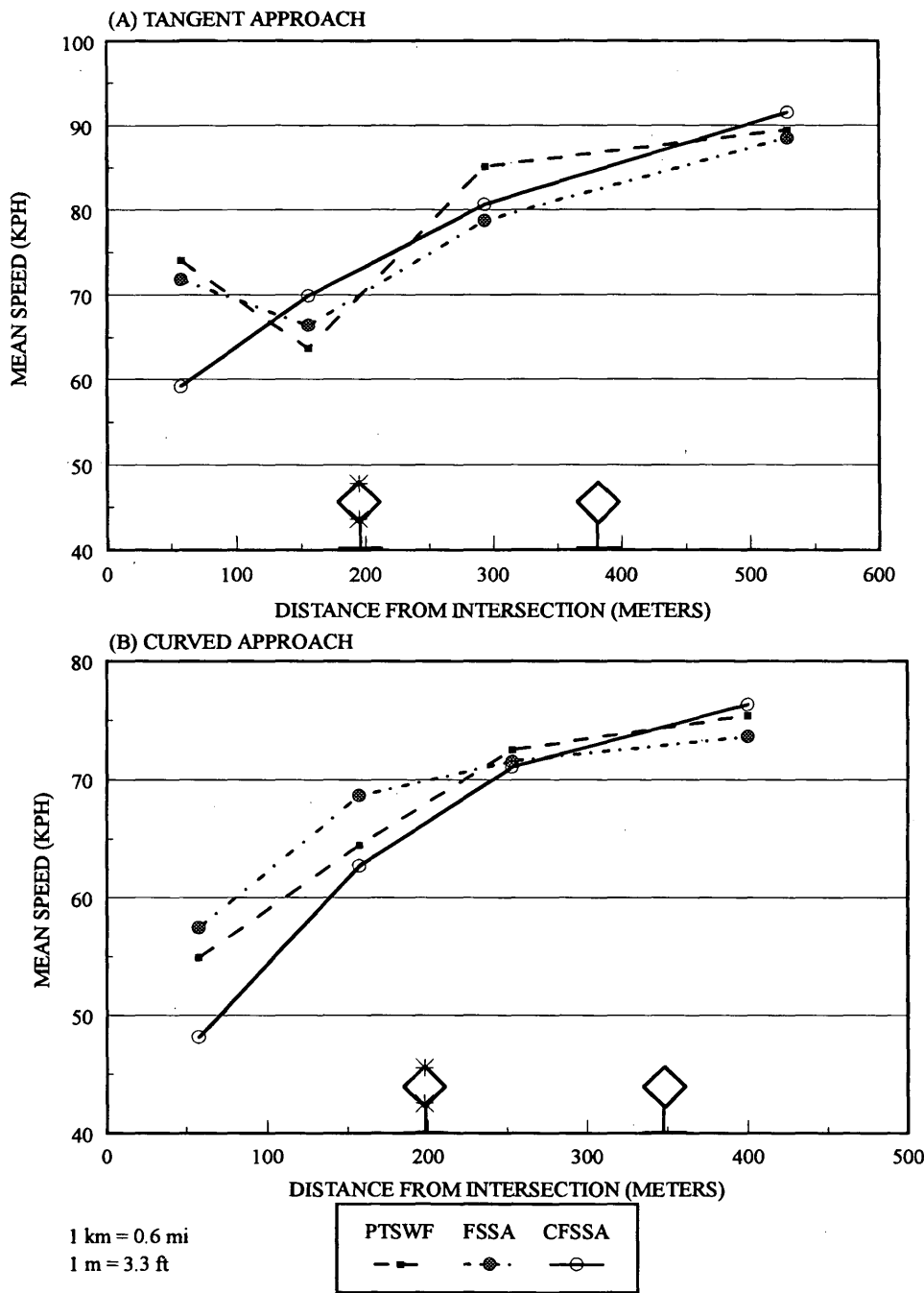


FIGURE 5 Speeds of passenger vehicles at tangent and curved approaches: Condition Off-Off-Green-Yellow-Go.

the CFSSA sign existed on the tangent approach. Although this result should be read with caution because of the small sample size, it indicates that the drivers were speeding up during the yellow interval when the PTSWF and FSSA signs existed on the tangent approach.

At the curved approach, the mean speeds in Zone 1 for the PTSWF, FSSA, or CFSSA signs indicated only a small difference because of the constraints caused by the roadway curvature (Figure 5). The speed showed a diminishing pattern when the vehicles trav-

eled between Zone 1 and Zone 4. The result showed that the drivers drove through the curved intersection at a relatively lower speed when the CFSSA sign existed at the intersection. If reducing speed during the yellow interval is an objective of an advance warning sign, the CFSSA sign could be more effective than the PTSWF or FSSA sign.

Trucks. The results are not reported because of insufficient sample size.

Condition: On-On-Red-Red-Stop

Passenger Vehicles. The results showed that the mean speed in Zone 4 was the lowest for the PTSWF sign, indicating that the drivers reduced the speeds at a higher rate when the PTSWF sign existed on the curved approach. The 85th percentile speeds in Zone 4 were lower for the PTSWF and FSSA signs than for the CFSSA sign.

Trucks. The results for vehicular speeds at the curved approach indicated that the lowest mean speed in Zone 4 was associated with the PTSWF sign. A similar pattern was observed with the 85th percentile speeds. It showed that drivers could relate the flashers on the PTSWF sign with the likelihood of stopping at the intersection. Although the flashers on the FSSA sign operated in a manner similar to those on the PTSWF sign, the FSSA sign was less effective in reducing speed at the curved approach.

Other Conditions

The speed data for other flasher, signal, and stop conditions as previously listed were analyzed. However, no unusual speed patterns were found.

Conflict Analysis. The vehicle conflict data are indicated in Table 1. The total conflict rate for the PTSWF, FSSA, and CFSSA signs at the tangent approach varied between 28 and 34 conflicts per 1,000 vehicles. The number of vehicles running red lights were 2.4 per 1,000 vehicles for the PTSWF and FSSA signs and 4.7 per 1,000 vehicles for the CFSSA sign, indicating that the CFSSA sign had the highest rate of "running red light." It indicates that the PTSWF and FSSA signs were more effective in reducing the "running red light" problem than the CFSSA sign at the tangent approach.

No significant difference among the three signs in the number of vehicles speeding up on yellow light was found at the tangent approach. The number of vehicles with abrupt stop was slightly higher for the PTSWF sign.

The result of the vehicle conflict analysis at the curved approach showed that the CFSSA sign had the overall lowest conflict rate at 28 conflicts per 1,000 vehicles. However, the CFSSA sign also had the highest rate of vehicles running red light (4.7 per 1,000 vehicles). On the other hand, the CFSSA sign had the lowest number of vehicles (21 per 1,000 vehicles), speeding up during yellow interval. The number of vehicles making an abrupt stop was slightly higher (3.1 per 1,000 vehicles) for the PTSWF sign than for the CFSSA sign (2.4 for 1,000 vehicles).

TABLE 1 Vehicle Conflict Rates

Intersection	Sign	Number of Vehicles	Conflicts Per 1000 Vehicles			Total
			Run Red	Speed Up on Yellow	Abrupt Stop	
US 33 & US 127	PTSWF	1389	1.9	27.4	1.9	31.2
	FSSA	861	2.5	25.3	1.1	28.0
	CFSSA	1485	4.7	27.6	1.3	33.6
SR 37 & US 40	PTSWF	3737	2.4	31.6	3.1	37.2
	FSSA	1465	1.8	31.8	2.7	36.3
	CFSSA	1695	4.7	20.6	2.4	27.7

Driver Survey. During the survey performed in 1993, drivers were asked to indicate their preferences among the PTSWF, FSSA, and CFSSA signs. Among the 89 drivers who responded to the survey questionnaire concerning the signs at the tangent approach, almost half of them preferred the PTSWF sign. The percentage of respondents in favor of each sign was as follows: PTSWF, 48 percent; FSSA, 13 percent; CFSSA, 29 percent; and No preference, 10 percent.

Many respondents who preferred the PTSWF sign at the tangent approach indicated that the sign helped them to stop. Other respondents indicated that the CFSSA sign had little effect on local drivers because it was always flashing. One respondent indicated that the CFSSA sign would benefit out-of-state drivers. Although the FSSA sign operated in a manner similar to that of the PTSWF sign by activating the flashers a few seconds before the onset of the yellow interval, a large percentage of respondents preferred the PTSWF sign.

Similarly, of the 71 respondents who returned the questionnaire about signs on the curved approach, about two-thirds of the respondents preferred the PTSWF sign. The preferences of the respondents for the different signs were as follows: PTSWF, 65 percent; FSSA, 13 percent; CFSSA, 13 percent; and No preference, 9 percent.

The respondents indicated that the PTSWF sign helped them stop at the intersection or to learn in advance when the signal indication was going to change. They also indicated that the flasher on the CFSSA sign was likely to be ignored by local drivers because they knew it flashed all the time.

CONCLUSIONS AND RECOMMENDATIONS

The study revealed that the impacts of the PTSWF, FSSA, and CFSSA signs vary among intersections with tangent and curved approaches. It is evident that roadway geometry and flasher and signal indications are important parameters, based on which drivers adjust their speeds on an intersection approach. The PTSWF and FSSA signs are designed to prepare the drivers to stop, if necessary, at the intersection. However, the CFSSA sign, which is a static device, provides no clue about the possible state of signal indication or stop.

The study has shown that the PTSWF and FSSA signs generally have similar effects on driver behavior. The effects of the CFSSA sign generally resemble those of the PSSA sign, but the CFSSA sign has the added advantage of the flashers. Drivers in Ohio generally are familiar with the PTSWF sign because ODOT has been using it for several decades. The study did not find any advantage in replacing the PTSWF sign with the FSSA sign. Any use of the FSSA sign will require a long period of driver familiarization without any obvious operational benefit. If engineers are concerned that the PTSWF sign provides no prior information about the existence of the signal, the intersection can be equipped with a PSSA sign as in the study sites described before.

It seems advantageous to consider the CFSSA sign before using the PTSWF sign because the PTSWF and FSSA signs have a few undesirable effects on vehicular speeds. When flashers are off and the signal indication is green or yellow, drivers on an approach with PTSWF or FSSA sign generally increase their speeds in an apparent attempt "to beat the light." This behavior is particularly more evident on intersections with a tangent approach than on intersections with a curved approach because the roadway curvature provides restrictions to the drivers on the selection of their speeds. The effect of the CFSSA sign on vehicular speed is generally similar to

that of the PSSA sign, which shows a diminishing pattern along the entire length of the intersection approach. The use of the CFSSA sign may also allow a more effective use of detection techniques to minimize dilemma zone problems.

At an intersection approach with a PTSWF sign, drivers generally increase speed when the flashers are inactive and the signal is green or yellow. At a curved approach, however, the PTSWF sign may help drivers reduce speed during a red interval.

On the basis of the findings of the study, the recommendations are listed below:

1. The PTSWF sign is preferable to the FSSA sign in Ohio. The FSSA sign should not be used as a replacement for the PTSWF sign.
2. At any potential location for an advance warning sign with flashers, the CFSSA sign should be considered for selection prior to the PTSWF sign.
3. The use of the PTSWF sign at a tangent approach to a high-speed signalized intersection is discouraged.

ACKNOWLEDGMENTS

The study was funded by ODOT in cooperation with FHWA. The authors express their sincere appreciation to Mohammad Khan and Rodger Khan of the Bureau of Traffic and William Edwards of the Bureau of Research and Development for their valuable assistance. The authors are solely responsible for the opinions expressed in this paper.

REFERENCES

1. Pant, P. D., and X. H. Huang. Active Advanced Warning Signs at High Speed Signalized Intersections: Results of a Study in Ohio. In *Transportation Research Record 1368*, TRB, National Research Council, Washington, D.C., 1992, pp. 18–26.

Publication of this paper sponsored by Committee on Traffic Control Devices.

Evaluation of Strobe Lights in Red Lens of Traffic Signals

BENJAMIN H. COTTRELL, JR.

Strobe lights are used as a supplement to the red lens to draw the attention of the driver to a traffic signal. Strobe lights have been used in situations in which (a) the signal is unexpected, (b) the signal may be difficult to see, and (c) there is an accident problem or potential accident problem. The Barlo strobe light, a horizontal bar positioned across the middle of the red lens with about 60 flashes of white light per minute, was used at all of the sites. A study was undertaken to evaluate the effectiveness of the strobe light in the red lens of traffic signals and, if appropriate, to recommend guidelines for the use of strobe lights. Only applications of the Barlo strobe light were studied. The use of strobe lights by the Virginia Department of Transportation was examined and accident analyses were performed. On the basis of the trend analysis, there was no consistent evidence that strobe lights are effective in reducing accidents. The limitations of the analyses were identified in the study. There is no basis for recommending the use of strobe lights unless there are other bona fide measures of effectiveness that can be used to justify their installation.

Strobe lights have been used as a supplement to the red lens to draw the attention of drivers to a traffic signal. Strobe lights have been used in situations in which (a) the signal is unexpected, (b) the signal may be difficult to see, and (c) there is an accident problem or potential accident problem. Specific applications of the strobe light include

1. Isolated, high-speed, rural intersections,
2. First signalized intersection into an urbanized area following travel on an extended road section without a signal,
3. First signalized intersection following a transition from a grade-separated or limited-access highway to an at-grade highway with intersections, and
4. Where the background lighting and signs (visual noise) are a problem.

There have been limited applications of strobe lights in the red indication in the United States. Consequently, few studies have been conducted that evaluate the effectiveness of strobe lights. The limited study results that are available are inconsistent and inconclusive (1). In many cases, especially in North Carolina, strobe lights are included among multiple safety improvements at intersections, making it impossible to determine the effectiveness of the strobe lights. A similar situation exists at new signal installations with strobe lights.

In June 1987, there were three intersections with strobe lights in two Virginia Department of Transportation (VDOT) districts. In

April 1994, there were 22 intersections with strobe lights in six VDOT districts. Apparently, the interest in and popularity of strobe lights have increased in Virginia. The Barlo strobe light, a horizontal bar positioned across the middle of the red lens with about 60 flashes of white light per minute, was used at all of the sites.

According to FHWA (2), there is insufficient evidence to support the inclusion of strobe lights in the *Manual on Uniform Traffic Control Devices (MUTCD)* (VDOT, unpublished data, 1985). Other concerns about the strobe light include whether (a) it distracts the drivers from other traffic control devices and other vehicles, and (b) its attention-getting value diminishes with time. There is a need for an evaluation of the use of strobe lights in the red lens of traffic signals.

OBJECTIVES AND SCOPE

The objectives of this study were to evaluate the effectiveness of the strobe light in the red lens of the traffic signals and, if appropriate, to recommend guidelines for the application of strobe lights. Only applications of the Barlo strobe light were studied.

METHODS

Two activities were conducted to accomplish the study objectives:

1. Data collection. A questionnaire survey was sent to the nine VDOT district traffic engineers to compile information on strobe light use, including an inventory of strobe light installations, maintenance experiences, and reasons for installing the strobe. Accident data were collected for selected sites.

2. Data analysis and evaluation. The collected data were summarized and analyzed to assess the use and performance of strobe lights. The evaluation plan for the strobe lights focused on a trend analysis of accidents.

RESULTS AND DISCUSSION

VDOT District Traffic Engineers Survey Results

There are 22 intersections with strobe lights in the seven districts that responded to the survey. Most of the strobe lights (19 of 22, or 86 percent) are in the western part of the state. At 17 intersections (77 percent), the Barlo strobe light is in the red signal indicator over the left through lane. This position was selected on the basis of the notion that the strobe light would be detected at a greater distance in the left through lane signal because horizontal curves and possi-

bly foliage on the right shoulder might block the view of the right through lane. At four intersections in one western district, strobe lights are in the red signal indicator over both through lanes. It is suspected that two strobe lights were used to enhance the visibility of these devices. In an eastern district, the strobe light is in a separate red signal head next to the traffic signal over the right lane. Staff from this district had observed this arrangement in North Carolina and the city of Virginia Beach. At 18 intersections, strobe lights were installed on both directions of the major roadway; at four intersections these devices were needed in only one direction. Strobe lights were installed on all approaches at only one intersection.

At nine intersections, the strobe lights were installed with a new traffic signal; at seven intersections, strobe lights were installed less than 12 months after a signal installation. Of the remaining six intersections, five of them had a traffic signal in place at least 3 years before the strobe light was installed.

Reasons for installing the strobe lights included one or more of the following: (a) high truck volumes and high speed, (b) accident experience, (c) road geometrics, especially grades (downgrade), horizontal curves, and other features resulting in limited sight distance, and (d) an isolated intersection where a signal is unexpected.

Maintenance of the strobe lights has not been a problem in general. At least three districts initially had problems. In one district, the problem of a strobe light exploding because it failed to release stored energy was solved by using a strobe from a different manufacturer. In another district, the number of failures with the control circuits decreased after several discussions with the supplier and manufacturer. A third district had problems with a transformer exploding when the side street strobe lights were flashing; these strobes were removed to solve the problem. One district noted that any malfunction is usually caused by the power pack, which is relatively expensive (about \$110). It costs about \$765 for a red signal head with a Barlo strobe light. The annual preventive maintenance routine typically includes cleaning the explosion guards, lenses, and reflector, replacing the incandescent lamp, and inspecting the seals for leaks that could result in water damage. Extreme care must be taken because of the high voltage of the strobe apparatus.

When asked when strobe lights should be used, the responses were (a) isolated intersections, (b) limited sight distance, (c) high speed, and (d) one or more of the following: poor alignment, curves,

or grades. One potential concern was that many requests would be made for strobe lights. However, the district offices have received few requests for strobe lights. There were 0 to 3 requests for strobe lights during a 3-year period.

Some potential uses of strobe lights suggested by district personnel include (a) use with a hazardous indication beacon for a warning sign, (b) school flashing lights, and (c) emergency vehicles. In a western district, a strobe light in an amber lens has been installed above a sign warning of "trucks crossing highway 800 ft" (245 m) near a truck stop on an arterial (the flashing lights are actuated); there is limited sight distance [less than 180 m (600 ft)] southbound because of an upgrade.

Accident Analysis and Evaluation

A review of accident trends of the six sites with 3 years of accident data before and after the strobe light installation was performed. Rear-end, angle, and total accidents that involved at least one vehicle on the strobe light approaches were examined.

Traffic and geometric data on the sites are listed in Table 1. All of the six sites had a four-lane divided highway as a main approach with strobe lights. Sites 1, 4, and 5 intersect with a two-lane road. Sites 2 and 6 intersect with a four-lane divided road on one side and two lanes on the other side; Site 3 intersects with a four-lane divided road. Site 4 is the only T-intersection.

Before-and-after accident data are presented in Table 2 for six sites. The percentage changes in accidents are discussed next. For rear-end accidents, there was no change at four sites, and an increase of 100 percent or more at two sites. Three sites had a decrease between 38 and 75 percent in angle accidents, whereas there was an increase of 25 and 400 percent at two sites, and no change at one site. For total accidents, one site had no change, one had a 5 percent increase, two sites had an increase of at least 80 percent, and two had a decrease of at least 25 percent. The accident experience at Site 5 is identical for both periods, and the number of accidents is the lowest of all the sites. The finding that two sites had an increase in accidents, two sites had a decrease, and two sites had little or no change suggests no conclusion or no consistent impact as a result of using the strobe lights. Additional review produced some explanations for the findings, however.

TABLE 1 Study-Site Traffic and Geometric Data

Site	No. Strobe Lights Per Approach	+ or T	Major Route		Minor Route	
			Speed Limit kph (mph)	Estimated ADT	Speed Limit kph (mph)	Estimated ADT
1	1	+	66 45	11,000	66 45	6,300
2	1	+	80 55	21,000	80 55	11,000
3	2	+	59 40	9,000	59 40	4,400
4	2	T	66 45	14,200	66 45	1,100
5	2	+	80 55	9,400	66 45	2,500
6	1	+	66 45	11,000	66 45	2,400

Note-- Sites 1, 2, and 6 are each in a different district. Sites 3-5 are in the same district.

TABLE 2 Summary of Accident Data

SITE	REAR END ACCIDENTS				ANGLE ACCIDENTS				TOTAL			
	BEFORE	AFTER	DIFFERENCE NO.	%	BEFORE	AFTER	DIFFERENCE NO.	%	BEFORE	AFTER	DIFFERENCE NO.	%
1	4	4	0	0	13	8	-5	-38	19	20	1	5
2	2	7	5	250	1	5	4	400	3	15	12	400
3	4	4	0	0	8	3	-5	-63	13	7	-6	-46
4	6	6	0	0	4	1	-3	-75	12	9	-3	-25
5	0	0	0	0	1	1	0	0	2	2	0	0
6	3	6	3	100	12	15	3	25	15	28	13	87

Sites 1, 2, and 6 have one strobe light per approach, whereas Sites 3 through 5 have two per approach. Both sites that had an increase in rear-end and angle accidents had one strobe light per approach. For total accidents, two sites with one strobe light had an increase of more than 80 percent whereas two sites with two lights per approach had a decrease of at least 25 percent.

Although the sample size is too small to conclude definitively, the use of two strobe lights per intersection appears to be more effective than one strobe light per approach. It seems logical that if two strobe lights reduced accidents, then one strobe would also reduce accidents, possibly to a lesser degree. Because accidents tended to increase at sites with one strobe light, it appears that factors other than number of strobe lights may be influencing the accident experience. The study sites were further examined to determine what factors other than the strobe lights may have contributed to the accident experience.

Sites 1, 3, and 5 are in rural areas with no distinguishing features. Site 2 is in an industrial area with a high volume of trucks. The side street that is a primary arterial is being widened from two to four lanes. Subsequently, the intersection is being rebuilt to include dual left-turn lanes from mainline in one direction and a sweeping right turn lane in the opposing direction. The additional capacity should help to reduce some of the accidents. Site 4 was once the first signal inbound near a town. Around the time the strobe light was installed, a new signal was installed about 670 m (2,200 ft) in advance of Site 4; therefore, it is no longer the first signal. Also, a right turn lane was added to the mainline. It is likely that these changes influenced the lower accident frequency at Site 4. Site 6 has one leg of the side street for access to a shopping mall with heavy traffic, and the opposing side street approach has light traffic. In May 1994, two traffic signal changes were made to improve operations and safety at the intersection: the exclusive/permissive left-turn signal phasing on the mainline was replaced with an exclusive left-turn phase, and split phases replaced a shared phase for the two side street approaches. Such factors that led to the improvements likely contributed to the accident experience. Also, it is unclear whether there is a benefit for installing two strobes per approach compared with one per approach.

Limitations of the Analysis

Strobe lights flash only when the red signals in which they are housed are on. Ideally, there should have been some means to ensure that the accidents under review involved a vehicle traveling on an approach when the strobe light was flashing. Unfortunately, there was no reliable item on the accident report form to provide this information. The item, "driver action," which includes "disregard for the stop-go signal/ran the red light," is potentially useful. However, the majority of accidents under review had "driver inattention," a catchall description with little value, as the driver action. Although a copy of the actual accident reports completed by the police may have been helpful in determining driver action, the reports for most of the accidents were more than 5 years old and not readily available. An alternative measure of effectiveness, field observations of red signal violators and driver reaction as they approach the red signal, was not pursued because of resource and time constraints.

The strobe lights were installed at locations with potential safety problems. These sites may have a propensity for higher-than-normal accidents. The strobe light sites were not selected randomly

but because of their accident history or potential for accidents. Statistical analysis of the accidents was not reported because a much larger sample size would be needed to obtain useful results.

Other Issues

A western district requested some guidelines on when to remove strobe lights. There was some concern about liability in the event of an accident after removal. In the author's opinion, the lack of evidence that strobe lights are effective in reducing accidents on the basis of the accident analysis can be used as justification for the removal of strobe lights.

On the basis of comments from some Department of Traffic Engineering (DTE) staff, in some areas, motorists and VDOT personnel perceive strobe lights as effective in improving safety at an intersection. For example, DTE staff from one district commented that the strobe lights were especially useful at dawn and dusk and at other times of reduced visibility. Clearly, the effectiveness of the strobe lights has not been demonstrated in this study. If other bona fide measures of effectiveness can be identified, then they should be considered.

At the October 1993 meeting of the Traffic Research Advisory Committee of the Virginia Transportation Research Council, the number one research priority was noncompliance with traffic control devices. Driver noncompliance, such as running red traffic signals, is increasingly common. Willful, defiant behavior is not likely to be affected by the presence of a strobe light. This type of behavior may be a contributing factor to the lack of effectiveness of the strobe light.

Alternatives to a Strobe Light

Three of the four applications for the use of strobe lights listed in the introduction involve conditions under which a traffic signal may not be expected, i.e., isolated rural intersections or the first signal after an extended road section without traffic signals. An alternative method in the MUTCD to alert motorists to a traffic signal ahead is to use the signal-ahead warning sign (W3-3). Hazard identification beacons (flashing yellow lights) should supplement the sign to increase its attention-getting value. An alternative to the fourth application of strobe lights, conditions where visual noise is a problem, is the use of a back-plate to increase the signal target value.

One of the four reasons for installing a strobe light given in the VDOT DTE survey was road geometrics that limit sight distance. The use of "prepare to stop when flashing" warning signs is an alternative. One district is testing this alternative. No additional alternatives other than the signal ahead and "prepare to stop when flashing" warning signs come to mind for the two reasons noted in the DTE survey results but not previously addressed: high truck volume and high speeds, and accident experience.

CONCLUSIONS

VDOT DTE Survey

1. VDOT has 22 intersections with strobe lights; this is up from 3 intersections in 1987. Nineteen (86 percent) of these are in the western part of the state and have the Barlo strobe in the red signal over the left through lane.

2. Strobe lights are used primarily for (a) high truck volumes and high speed, (b) accident experience, (c) road geometrics, especially grades (downgrade), horizontal curves, and other features that result in limited sight distance, and (d) isolated intersections where a signal is unexpected.

3. There have been few requests for strobe lights recently. The cost of a red signal head with a Barlo strobe light is about \$765.

Accident Analysis

1. On the basis of the trend analysis of the six study sites, there was no evidence that strobe lights are consistently effective in reducing accidents. It is unclear whether two strobe lights per approach are more effective than one strobe light per approach. The limitations of the analysis were identified in the study.

2. There is no basis for recommending use of strobe lights unless there are other bona fide measures of effectiveness that justify their

installation. The findings can be used as justification for removal of the strobe lights.

ACKNOWLEDGMENTS

This technical assistance effort was funded with state planning research funds through FHWA.

REFERENCES

1. *Accident Countermeasures at High-Speed Signalized Intersections: Phase I—Synthesis of Practice*. Department of Civil Engineering, West Virginia University, Morgantown, 1984.
2. *Manual on Uniform Traffic Control Devices*. FHWA, U.S. Department of Transportation, Washington, D.C., 1988.

Publication of this paper sponsored by Committee on Traffic Control Devices.

High-Volume Pedestrian Crosswalk Time Requirements

MARK R. VIRKLER, SATHISH ELAYADATH, AND GEETHAKRISHNAN SARANATHAN

Existing methods to determine pedestrian crossing times at signalized intersections are described. These approaches have significant shortcomings under high-volume conditions. They can indicate that adequate crossing time is present when a high volume of pedestrians would not be able to clear the intersection in the time provided. Alternative shock wave approaches are developed to provide a more appropriate means of estimating flow characteristics when pedestrian volumes are high. The results can be used to determine crosswalk capacity, to assist in developing signal timing plans, and to determine desirable crosswalk widths and lengths.

A variety of methods have been developed for determining appropriate pedestrian crossing times at signalized intersections. Although many of these methods have useful applications, all have significant shortcomings when estimating the crossing time required under high-volume conditions. Existing methods are described. A shock wave approach is then used to develop a more appropriate means of estimating flow characteristics when pedestrian volumes are high. This approach is then adapted to allow one to estimate parameters required for operation or design.

BACKGROUND

Crossing Time

Many crossing time recommendations have been based on assumed start-up delay and walking speed. The Manual on Uniform Traffic Control Devices [MUTCD (1)], Pignataro (2), and the Signalized Intersection Chapter of the Highway Capacity Manual (HCM) (3) have formulations similar to those in Equation 1. The parameters of each model are indicated in Table 1. A time-space diagram of the model appears in Figure 1.

$$T = D + L/u \quad (1)$$

where

- T = time required for crossing (sec),
- D = initial start-up delay to step off curb and enter crosswalk (sec),
- L = walking distance (m), and
- u = walking speed (m/sec).

M.R. Virkler, Department of Civil Engineering, University of Missouri-Columbia, Columbia, Mo. 65211. S. Elayadath, Southern New Hampshire Planning Commission, 159 Orange Street, Apt. 3W, Manchester, N.H. 03104. G. Saranathan, Public Works Department P.O. Box 90012, Bellevue, Wash. 98009-9012.

If only a small number of pedestrians use the crosswalk during a given phase, this time should be sufficient. However, if the number of people crossing is large, the time D may not be sufficient for everyone to leave the curb. If the platoon uses the assumed walking speed, the crosswalk will not be cleared of pedestrians within the time T .

The 1962 Institute of Traffic Engineers (ITE) School Crossing Guidelines (4) consider platoon size. The crossing time can be described as

$$T = D + L/u + 2[(N/5) - 1] \quad (2)$$

where N is the number of pedestrians crossing during an interval. It is assumed that the students walk in rows, five abreast, with a 2-sec headway between rows. Figure 2 shows a one-way platoon flow to correspond to this equation.

Virkler and Guell (5) recommended an equation for one-directional flow that also considers platoon size. The equation takes the following form:

$$T = D + L/u + x(N/W) \quad (3)$$

where

- x = average headway (sec/pedestrian/m of crosswalk width) and
- W = crosswalk width (m).

The first term, D , is perception/reaction time. The third term equals the time required for the platoon to pass a point. Figure 2 also can be used to represent this equation. Although the above two formulations consider platoon size, they do not address the problem of two opposite-direction platoons meeting in a crosswalk.

Platoon Flow Rate

The Interim Materials on Highway Capacity (6) provided a procedure to estimate crosswalk level of service by converting the pedestrian flow rate to a "platoon" flow rate. The platoon flow rate was calculated as

$$q_{\text{platoon}} = q[C/(G - 3)] \quad (4)$$

where

- q_{platoon} = platoon flow rate (pedestrians/min),
- q = actual pedestrian flow rate (pedestrians/min),
- C = cycle length (sec), and
- $G - 3$ = green time minus 3 sec of start-up delay (sec).

The platoon flow rate assumes that, when pedestrians are in the crosswalk, a uniform rate of flow exists during the green phase

TABLE 1 Crossing-Time Parameters of Three Models

Method	Parameters	
	Initial Start-up Delay (sec)	Walking Speed (m/sec)
MUTCD (1)	4 to 7	1.22
Pignataro (2)	5 or more	1.07 to 1.22
HCM Ch. 9 (3)	7	1.22

(minus 3 sec for start-up delay). For instance, consider a crosswalk serving 30 pedestrians per minute with a 27-sec green indication (for vehicles and pedestrians) and a 60-sec cycle length. The platoon flow rate would be

$$q_{\text{platoon}} = 30[60/(27-3)] = 30[60/24] = 75 \text{ pedestrians/min}$$

One advantage of this procedure is that it can be applied to estimate walkway width requirements for two-way pedestrian flow. Unfortunately, an implicit assumption is that a uniform platoon flow rate will exist throughout the crosswalk for all but 3 sec of the green time. For this to be a realistic estimate of the flow rate, the crossing time for the crosswalk would have to be 0. Virkler (7) suggested that this equation would be appropriate for one-way flow if the crossing time were also deducted from the available green time, as shown below:

$$q_{\text{platoon}} = q[C/(G - T - 3)] \quad (5)$$

where T is walking time for one individual to cross in seconds.

For instance, using the previous example with a crosswalk length of 13 m and a walking speed of 1.3 m/sec, the walking time for one individual would be 10 sec, and the flow rate within the platoon would become

$$\begin{aligned} q_{\text{platoon}} &= 30[60/(27 - 10 - 3)] = 30[60/14] \\ &= 129 \text{ pedestrians/min} \end{aligned}$$

Time-Space Concept

The pedestrian chapter of the HCM (3) uses a time-space approach to deal with crosswalk level of service but suffers from a flaw similar to that in the interim materials. The entire area of the crosswalk is assumed to be available to pedestrians during all but 3 sec of the walking phase (on a typical crosswalk with concurrent vehicular

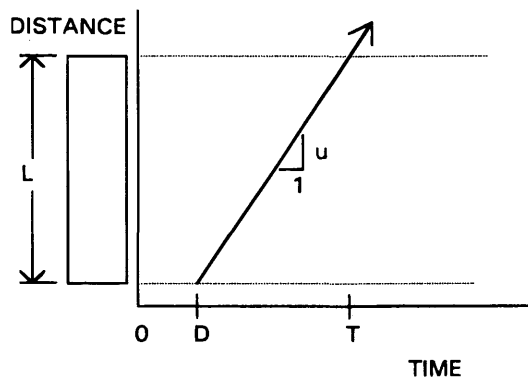


FIGURE 1 Time-space diagram for a single pedestrian.

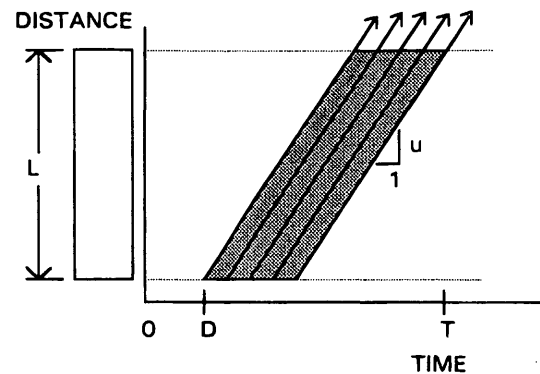


FIGURE 2 Time-space diagram for a one-way platoon.

green, the walking phase equals the vehicular green plus yellow time). For example, the HCM has an example with a cycle length of 80 sec and two walk phase times of 48 and 32 sec. For the latter walk time

Crosswalk width = $W_d = 5$ m,

Crosswalk length = $L_d = 15$ m,

WALK phase time = $G_w = 32$ sec - 3 sec = 29 sec = 0.48 min, and

Time-space = $TS = [(5 \text{ m})(15 \text{ m}')] (0.48 \text{ min}) = 36 \text{ m}^2/\text{min}^2$

The time-space diagram for this approach is shown in Figure 3. If 100 pedestrians (total from both directions) required 10 sec each to cross, then the average space per pedestrian would be

$$\frac{2175 \text{ m}^2 \cdot \text{sec}}{(100 \text{ pedestrians})(10 \text{ sec})} = 2.175 \text{ m}^2/\text{ped}$$

A level of service would then be associated with the average space per pedestrian ($2.175 \text{ m}^2/\text{pedestrian}$). Although this technique has the advantage of dealing with two-directional walking, there are two problems with the approach:

1. The available time-space is overstated and
2. The approach does not ensure that adequate walking time is provided.

Overestimation of Time-Space

As indicated in Figure 3, the entire space of the crosswalk is assumed to be available to pedestrians during the walk phase time. However, if pedestrians are to cross safely, the space in the middle of the street is not available during the beginning of the walk phase (because pedestrians could not yet have reached it) or near the end of the walk phase (if pedestrians are to reach the curb before the walk phase time ends). Figure 4 illustrates that the available time space has been overestimated by 20 percent.

Adequacy of Walking Time

The HCM methodology does not ensure that adequate walking time exists for a platoon of pedestrians to cross the street. In the first

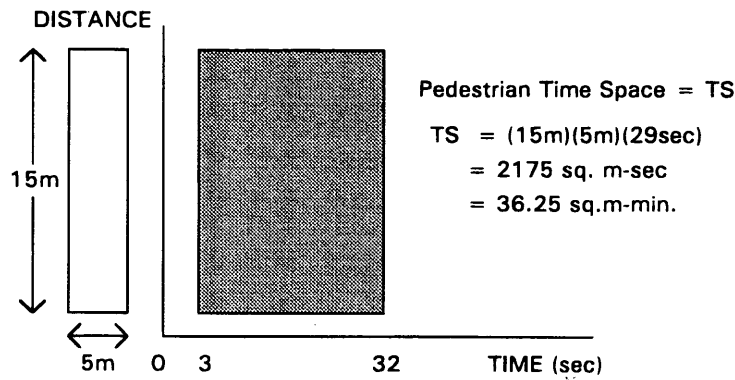


FIGURE 3 Time-space diagram for HCM approach.

example, the pedestrian space available (2.175 m²/pedestrian) would be the same whether the walkway was 5 × 15 m or 1 × 75 m. In the latter case no one could safely cross during the green. A different formulation is necessary to ensure that adequate space and time exist at crosswalks. A proposed method is developed in the next section.

PROBLEM FORMULATION

Equation 1 [$T = D + L/u$] is appropriate when pedestrian flow rates are low. When pedestrian flow rates are high and in one direction only, the Virkler and Guell formulation of Equation 3 [$T = D + L/u + x(N/W)$] appears appropriate. This form, with a 3-sec start-up time and the parameters for LOS B (associated with the flow rate found by Virkler and Guell) would be

$$T = 3 \text{ sec} + L/(1.27 \text{ m/sec}) + (2.61 \text{ sec/pedestrian/m})(N/W) \quad (6)$$

This approach could also be modeled as shown in the shock wave analysis of Figure 5. Figure 5 shows low-density pedestrians arriving on an approach (Flow State A) and forming a high-density queue (Flow State B) while the signal is effectively red (actual red plus start-up delay plus crossing time). When the signal turns effectively green for pedestrians (i.e., when pedestrians can safely leave the curb), a moderate-density platoon moves over the crosswalk (Flow State C). The largest possible platoon for the given red time and cycle length is shown in the figure. The maximum depth of the standing queue is shown as L_q .

The distance traveled by the last pedestrian in the queue would be $L_q + L$. Ignoring the start-up delay, the time to clear all pedestrians would be the time between when the front of the queue begins to move and when the rear of the queue begins to move (t_0) plus the time (t_1) for the last pedestrian to travel $L_q + L$. The required effective green time, derived from shock wave theory (8) would therefore be

$$G_{\text{req}} = t_0 + t_1 \quad (7)$$

$$G_{\text{req}} = R \cdot \left(\frac{\omega_{AB}}{\omega_{BC} - \omega_{AB}} \right) + \frac{[(k_A)(N/W)] + L}{U_c} \quad (8)$$

where

- G_{req} = required effective green time (sec),
- R = effective red time (sec),
- $\omega_{AB} = -q_A/(k_B - k_A)$,
- $\omega_{BC} = -q_C/(k_B - k_C)$,
- q_A = flow rate of pedestrians approaching the queue (pedestrians/min),
- q_C = flow rate of the pedestrians leaving the queue (pedestrians/min),
- k_B = density of platooned pedestrians (pedestrians/m²),
- k_A = density of arriving pedestrians (pedestrians/m²).

With high-volume two-way flow a more intricate approach is necessary. The assumptions are as follows:

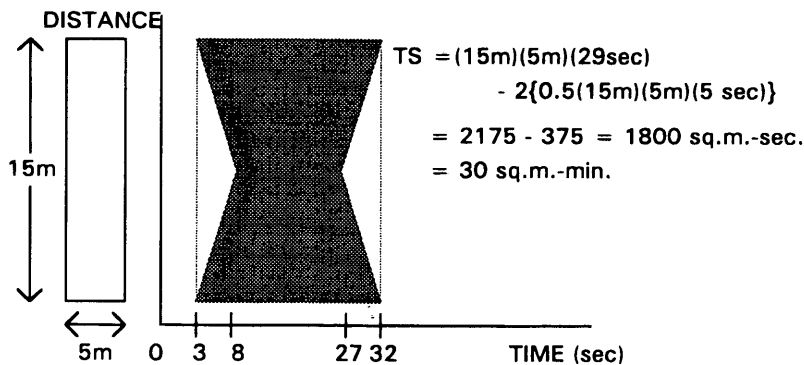


FIGURE 4 Time-space available considering walking speed.

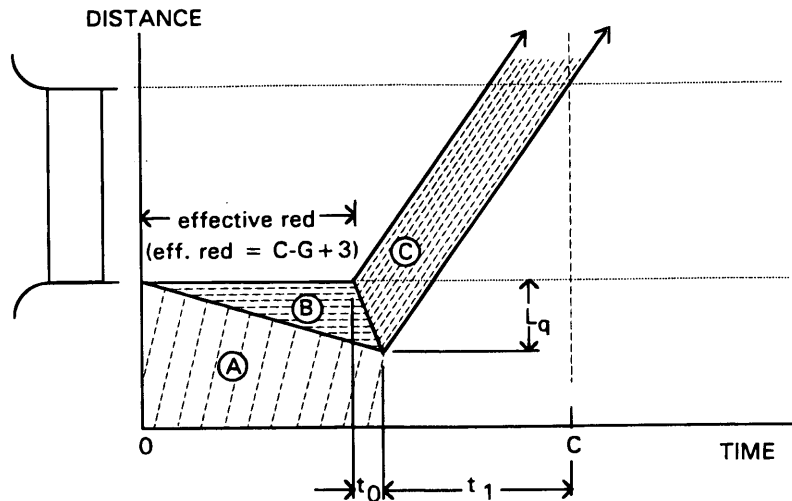


FIGURE 5 Time-space diagram for largest one-way platoon.

1. Before the flows meet, each flow occupies the full walkway width.
2. Until flow from the opposite direction is encountered, pedestrian walk speed is u_C and density is k_C . When the flows meet, the density increases to k_D and the speed reduces to u_D . The low speed of u_D will continue after the flows separate.
3. When the flows meet, each opposing flow will occupy one-half of the walkway width.

The speed and density assumptions are based on the work of Virkler and Guell (5) and the authors' experience. The assumptions are illustrated in Figure 6, where the higher flow rate is moving upward. The authors' experience suggests that Flow State C would

be in LOS B (with $u_C = 1.27$ m/sec and $k_C = 0.269$ pedestrians/m²). Flow state D would be at capacity ($u_D = 0.762$ m/sec and $k_D = 1.794$ pedestrians/m²).

One might expect that the assumption that the low speed of u_D will continue after the flows separate is too conservative. On the other hand it is likely that pedestrians will anticipate downstream high-density conditions by reducing their speed while their own density is still low. Therefore the assumed low-density speed (u_C) may be too high (or unconservative).

Following the assumptions of Figure 6, the total time required can be derived as

$$G_{req} = t_0 + t_1 + t_2 \tag{9}$$

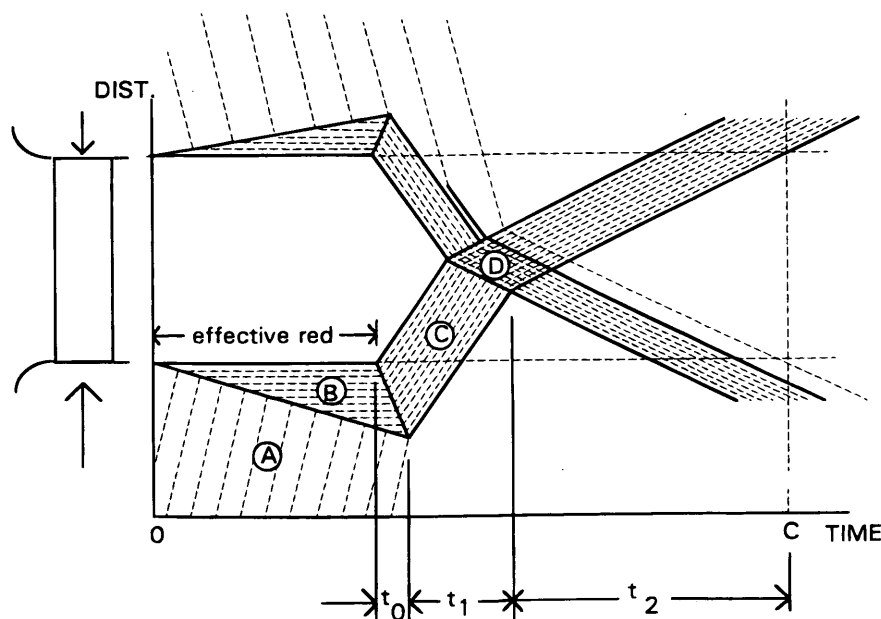


FIGURE 6 Time-space diagram for two-way platoons.

where

$$t_0 = R \cdot \left(\frac{\omega_{AB}}{\omega_{BC} - \omega_{AB}} \right) \tag{10}$$

$$t_1 = \frac{L_q + \frac{L}{2} - \left[u_D \cdot \frac{L_q + u_C \cdot t_0}{u_C + u_D} \right]}{u_C} \tag{11}$$

$$t_2 = \frac{(L/2) + u_D \cdot \left[\frac{L_q + u_C \cdot t_0}{u_C + u_D} \right]}{u_D} \tag{12}$$

However, if the opposing stream passes the last pedestrian before he or she begins to move, the required green time would be

$$G_{req} = t_0 + (L + L_q)/u_D \tag{13}$$

APPLICATIONS

This shock wave approach could be used to

1. Determine the capacity of a crosswalk,
2. Assist in developing a signal timing plan adequate for pedestrians, and
3. Determine a desirable crosswalk width or length,

Figures 7 through 9 provide a broad range of required crossing times for crosswalks while varying the demand, cycle length, and crosswalk length. The crosswalk LOS predicted by the HCM is shown in the cell, below the crossing time. The first letter represents the LOS and the second letter represents the surge LOS. The surge occurs when "the two lead platoons from opposite corners . . . are simultaneously in the crosswalk" (3).

In Figures 7 through 9 several cells (which are shaded) have crossing times greater than the crossing time available (i.e., the green time is not sufficient for demand. Note that none of the cells with inadequate crossing times are identified as being over capacity by the HCM. Many are reported to operate at the relatively high quality LOS B or C, even though pedestrians would not have sufficient time to clear the crosswalk before the onset of red. This occurs because the HCM does not consider whether crossing time is adequate. LOS is based solely on the average space available per pedestrian.

OTHER CONSIDERATIONS

The HCM considers the effects of turning vehicles by reducing the time-space available to pedestrians by the time-space used by each turning vehicle. A similar treatment for crossing time would require that the crossing time be increased by the number of seconds that each turning vehicle would delay the major pedestrian platoon. An alternative view would be that the vehicular green time for turning vehicles should provide for the number of seconds that the crosswalk space is not available to the turning vehicles because of the presence of pedestrians.

The HCM also provides an LOS measure for the corner through a similar time-space analysis. The time-space (in square meters per second) available on the corner is compared with the time-space demand required by queued pedestrians, crosswalk users passing through the corner area, and other pedestrians using the same space but not using a crosswalk. Because the shock wave method developed earlier can find the space occupied by queued pedestrians, it appears likely that a shock wave approach could be used to analyze corner operations. Shock wave analysis could determine the adequacy of the corner throughout the signal cycle. Time-space analysis only examines average conditions during the cycle. Critical situations may exist that could not be identified by the time-space approach.

Length	REQUIRED CROSSING TIME (sec) & AVERAGE LOS/SURGE LOS							
	One-way Flow in Major Direction (ped/hr)							
	250	500	750	1000	1250	1500	1750	2000
8.5m (28')	11.6 A/B	14.1 B/B	16.7 B/C	19.25 B/C	21.8 B/D	24.3 C/D	26.7 C/D	29.2 C/E
12.2m (40')	15.4 A/A	18.0 B/B	20.6 B/B	23.1 B/C	25.6 B/C	28.1 C/D	30.6 C/D	33.0 C/D
15.8m (52')	19.3 A/A	21.9 B/B	24.4 B/B	27.0 B/B	29.5 B/C	32.0 C/C	34.5 C/D	36.9 C/D
19.5m (64')	23.1 A/A	25.7 B/B	28.2 B/B	30.8 B/B	33.3 B/C	35.8 C/C	38.3 C/C	40.7 C/D
23.2m (76')	26.9 A/A	29.5 B/B	32.1 B/B	34.6 B/B	37.1 B/B	39.6 C/C	42.1 C/C	44.5 C/C
26.8m (88')	30.8 A/A	33.3 B/B	35.9 B/B	38.5 B/B	41.0 B/B	43.5 C/C	45.9 C/C	48.4 C/C

ASSUMPTIONS: Cycle Length = 40 sec, Effective Green Time = 20 sec, 67/33 directional split, no turning vehicles, Crosswalk Width = 3.0m (10.0')
 INADEQUATE CROSSING TIME INDICATED BY SHADING

FIGURE 7 Required crossing time and LOS with 40-sec cycle.

Length	REQUIRED CROSSING TIME (sec) & AVERAGE LOS/SURGE LOS							
	One-way Flow in Major Direction (ped/hr)							
	250	500	750	1000	1250	1500	1750	2000
8.5m (28')	12.9 A/B	16.7 B/C	20.6 B/C	24.4 B/D	28.2 B/D	31.7 C/E	35.1 C/E	38.5 C/E
12.2m (40')	16.7 A/B	20.6 B/B	24.4 B/C	28.2 B/C	32.0 B/D	35.8 C/D	39.5 C/E	43.1 C/E
15.8m (52')	20.6 A/B	24.5 B/B	28.3 B/B	32.1 B/C	35.9 B/C	39.7 C/D	43.3 C/D	47.0 C/D
19.5m (64')	24.4 A/A	28.3 B/B	32.1 B/B	35.9 B/C	39.7 B/C	43.5 C/D	47.1 C/D	50.8 C/D
23.2m (76')	28.2 A/A	32.1 B/B	35.9 B/B	39.8 B/C	43.6 B/C	47.3 C/C	51.0 C/D	54.6 C/D
26.8m (88')	32.0 A/A	35.9 B/B	39.8 B/B	43.6 B/B	47.4 B/C	51.1 C/C	54.8 C/C	58.5 C/D

ASSUMPTIONS: cycle length = 60 sec, effective green time = 30 sec,
67/33 directional split, no turning vehicles, crosswalk width = 3.0m (10.0')
INADEQUATE CROSSING TIME INDICATED BY SHADING

FIGURE 8 Required crossing time and LOS with 60-sec cycle.

RECOMMENDATIONS

It has been shown above that when a large number of pedestrians cross an intersection the required crossing time is greater than that currently required by the methods commonly used. The platoon size to consider as large and the walking time to provide are addressed next.

Determining When Platoon Is Large

Four alternative guidelines are discussed below, as they relate to the present, provided by Chapter 9 of the HCM.

1. *A Large One-Way Platoon Can Be Found by the ITE School Crossing Protection Philosophy*—Chapter 9 of the HCM (3) allows 7 sec for pedestrians to leave the curb. The ITE School Crossing Protection formulation (4) assumes that a 3 sec start-up delay is required before students move in rows of five, with a 2-sec headway between rows (i.e., the rows enter the intersection at 3,5,7, and 9 sec, and so forth after the signal turns green). Because the fourth row would enter the intersection after the HCM's initial 7-sec period, a large platoon can be defined as 16 pedestrians.

2. *A Large One-Way Platoon Can Be Found by the Virkler and Guell Formulation*—Virkler and Guell found that a one-way platoon requires 2.61 sec/(pedestrians/m) to pass a point. With a 3-sec start-up delay, the HCM allows 4 sec for a platoon to leave the curb. In 4 sec the volume would be 4 sec/[2.61 sec/(pedestrian/m)] or 1.53 pedestrian/m. For walkway widths of 3, 4, and 5 m, the volumes that could leave the curb would be 4.6, 6.1, and 7.6 pedestrians, respectively. A large one-way platoon might be defined as 7 or more pedestrians.

3. *A Large Two-Way Platoon Can Be Found by the Virkler and Guell Formulation*—With two-way flows, the two platoons must pass each other on the crosswalk. Using the same platoon headway

of 2.61 sec/(pedestrian/m) to pass a point, a large two-way volume can be defined as 7 or more pedestrians (total for both directions) when the walkway is 4 m wide.

4. *A Large Two-Way Platoon Can Be Found by Equation 9*—One could use Equation 9 (required green time for two-way flow) to determine when the needed green time exceeded that provided by Chapter 9 of the HCM. Because of the reduced walking speed after the platoons meet, it is likely that a large platoon would be somewhat less than seven pedestrians. The exact number would depend on the crosswalk length and width.

Equation 9 has not been tested with field data. The authors therefore support alternative Guideline 3 because it appears rational and incorporates two-way flow. Recognizing that the pedestrian volume at which Chapter 9 of the HCM crossing time would be exceeded depends on the assumed walking speed, crosswalk length, and crosswalk width, the authors recommend that seven pedestrians crossing during a phase be considered as a large platoon. The hourly demand that would be expected to have a design volume (e.g., perhaps the 85th percentile volume) per cycle of 7 pedestrians would depend on the cycle length and peaking characteristics but might be roughly estimated as 300 pedestrians per hour.

Recommended Crossing Time

Three alternative guidelines for determining adequate crossing times are discussed.

Provide Crossing Time for Large One-Way Platoon

Virkler and Guell found that a one-way platoon requires 2.61 sec/(pedestrian/m) to pass a point. With the conservative HCM walking speed of 1.22 m/sec rather than 1.27 m/sec, Equation 6 can be modified to become

Length	REQUIRED CROSSING TIME (sec) & AVERAGE LOS/SURGE LOS							
	One-way Flow in Major Direction (ped/hr)							
	250	500	750	1000	1250	1500	1750	2000
8.5m(28')	14.2 A/B	19.3 B/C	24.5 B/D	29.3 B/D	33.9 B/E	38.5 C/E	43.1 C/E	47.7 C/E
12.2m(40')	18.0 A/B	23.2 B/C	28.3 B/C	33.4 B/D	38.4 B/D	43.3 C/E	47.9 C/E	52.5 C/E
15.8m(52')	21.9 A/B	27.0 B/B	32.2 B/C	37.3 B/C	42.3 B/D	47.2 C/D	52.0 C/E	56.7 C/E
19.5m(64')	25.7 A/B	30.8 B/B	36.0 B/C	41.1 B/C	46.1 B/D	51.1 C/D	56.0 C/D	60.9 C/E
23.2m(76')	29.5 A/B	34.7 B/B	39.8 B/B	44.9 B/C	50.0 B/C	54.9 C/D	59.9 C/D	64.7 C/D
26.8m(88')	33.4 A/A	38.5 B/B	43.7 B/B	48.8 B/C	53.8 B/C	58.8 C/C	63.7 C/D	68.6 C/D

ASSUMPTIONS: cycle length = 80 sec, effective green time = 40 sec, 67/33 directional split, no turning vehicles, crosswalk width = 3.0m (10.0')
 INADEQUATE CROSSING TIME INDICATED BY SHADING

FIGURE 9 Required crossing time and LOS with 80-sec cycle.

$$T = 3 \text{ sec} + L/(1.22 \text{ m/sec}) + (2.61 \text{ sec/pedestrian/m}) (N_{1\text{-way}}/W) \quad (14)$$

where

T = time required for crossing (sec),

L = walking distance (m),

$N_{1\text{-way}}$ = larger one-way pedestrian volume during a phase, and

W = crosswalk width (m).

Because of the slightly lower walking speed, this equation is more conservative than Equation 6. The form of the equation has been derived from field data on one-way flow (5).

Provide Crossing Time for Two-Way Platoons with Constant Headways

Equation 14 would be extended to recognize that the larger of the two one-way volumes using the crosswalk would require more time to cross the intersection if an opposite direction flow is using the same crosswalk. The same platoon headway of 2.61 sec/pedestrian/m to pass a point is used, but the volume to pass the point includes both the larger one-way flow and the smaller, opposite-direction, one-way flow.

$$T = 3 \text{ sec} + L/(1.22 \text{ m/sec}) + (2.61 \text{ sec/pedestrian/m})(N_{2\text{-way}}/W) \quad (15)$$

where

T = time required for crossing (sec),

L = walking distance (m),

$N_{2\text{-way}}$ = two-way pedestrian volume during a phase,

W = crosswalk width (m).

The point on the crosswalk that both platoons must pass could be imagined as a doorway or bottleneck. The same number of seconds would be required to allow N people through the doorway whether the directional split was 50:50, 60:40, or 100:0. Because two-way

pedestrians would be walking under higher-density conditions over a significant length of the crosswalk, rather than just at a point, the assumed walking speed is probably high, making the crossing time unconservative (too short). However this crossing time is more conservative than that presently provided.

Provide Crossing Time Called for in Equation 9

The authors view Equation 9 as a rational interpretation of two-way flow conditions on the basis of the shock wave theory and personal observation. It would provide the most conservative (longest) crossing times under two-way flow conditions.

Because Equation 9 has not been tested with field data, the authors do not recommend it for implementation. The speed used in Equation 15 is accepted in current practice, and the headway was derived from field data, although that headway was limited to one-way flow. Under high-volume two-way flow conditions, Equation 15 is probably somewhat unconservative, but it is more conservative than Equation 14 and would be a significant improvement on current practice. For these reasons, Equation 15 is recommended for use where high-volume conditions are present (i.e., seven or more pedestrians in a phase).

CONCLUSIONS

Adequate methods exist to determine low-volume pedestrian crossing times. When high pedestrian volumes are present, the existing methods are inadequate to ensure safe operation. A shock wave approach, as developed earlier, can be used to ensure that adequate crossing time is present for large one-way or two-way platoon flows. The authors recommend that a shockwave approach (i.e., Equation 15) be used in the procedure from the HCM chapter on pedestrians as a check on whether adequate crossing time is present. Without such a check, an analysis could indicate a high-quality LOS when inadequate crossing time could yield unsafe conditions.

SUGGESTIONS FOR FURTHER RESEARCH

The approaches developed earlier need to be tested by field data. A field study could refine the assumptions used for start-up delay, walking speeds, pedestrian densities, queue depth, and crosswalk widths used. Such a study could also examine the effects of turning vehicles on individual pedestrians and on platoon operations. For example, do all turning vehicles conflict with platoons, or does the time of the vehicle movement within the green phase alter the effect?

Examination of corner operations could assist in the development of an alternative means to examine corner operations. A study could examine whether the various flows that occur on a corner follow predictable patterns that could be modeled by shock wave analysis, simulation, or some other method.

REFERENCES

1. *Manual on Uniform Traffic Control Devices for Streets and Highways*. FHWA. U.S. Department of Transportation, Washington, D.C., 1988.
2. Pignataro, L. J. *Traffic Engineering: Theory and Practice*. Prentice Hall, Inc., Englewood Cliffs, N.J., 1973.
3. *Special Report 209: Highway Capacity Manual*. TRB, National Research Council, Washington, D.C., 1985.
4. A Program for School Crossing Protection—A Recommended Practice of the Institute of Traffic Engineers, *Traffic Engineering*, Oct. 1962, pp. 51–52.
5. Virkler, M. R. and D. L. Guell. Pedestrian Crossing Time Requirements at Intersections. In *Transportation Research Record 959*, TRB, National Research Council, Washington, D.C., 1984, pp. 47–51.
6. *Transportation Research Circular 212: Development of an Improved Highway Capacity Manual. Interim Materials on Highway Capacity*. TRB National Research Council, Washington, D.C., June 1980, pp. 3–147.
7. Virkler, M. R. Pedestrian Flows at Signalized Intersections. In *Transportation Research Record 847*, TRB, National Research Council, Washington D.C., 1982, pp. 72–77.
8. May, A. D. *Traffic Flow Fundamentals*. Prentice Hall, Englewood Cliffs, N.J., 1990.

Publication of this paper sponsored by Committee on Traffic Control Devices.

Empirical Analysis of Traffic Characteristics at Two-Way Stop-Controlled Intersections in Alaska

JIAN JOHN LU AND B. KENT LALL

In the United States, the current capacity estimation procedure of two-way stop-controlled intersections was based on the German guidelines. Professionals in the transportation field have called for a modification of this procedure or for development of new procedures verified by U.S. field data. A research study sponsored by Region 10 of the U.S. Department of Transportation University Transportation Center was undertaken to study traffic characteristics at two-way stop-controlled intersections, including delay, capacity, and gap acceptance characteristics. Field data were collected from six test sites in Fairbanks, Alaska. For the analysis of delay and capacity characteristics, about 34 hr of traffic data were recorded in 17 videotapes. Data average intervals of 5- and 15-min were used to reduce field data by using a specialized computer program, called Traffic Data Input Program. The main purpose for using this program was to obtain summarized traffic data from the videotapes with certain average intervals (5 and 10 min), such as service delay, queue delay, major traffic volume, minor traffic volume, movement distribution, and so on. For the gap acceptance data, observers reviewed field pictures shown on a TV set and manually collected the accepted gap data. Researchers used empirical methods to develop regression models that characterize the statistical relationships between service delay and conflicting volume, minor street capacity and conflicting volume, and total delay and minor and conflicting volumes. Researchers used linear, negative exponential, and nonlinear two-variable functions, respectively, to fit these models. Reasonably good fitness of these models resulted and modeling results showed that the major street speed limit did not significantly affect these models. Concerning driver's gap acceptance behavior, the field data were collected to quantify the relationship between service delay and critical gap. Researchers in this field have assumed that minor-street drivers tend to accept smaller gaps as they wait a longer time at the stop line or in queue. Results obtained from this study verified the assumption and researchers obtained a quantitative model to quantify the relationship.

Chapter 10 of the 1985 Highway Capacity Manual (HCM) (1) provides the procedure for capacity analysis of two-way stop-controlled (TWSC) intersections. This procedure is based on the distribution of gaps in the major street traffic stream and drivers' judgment in selecting gaps through which to execute their desired maneuvers. In recent years, issues regarding the capacity analysis procedure have been raised to address the inadequacy of the present procedures. The current method is based on the German guideline which was validated with a limited U.S. data base. One of the major limitations is a methodological problem related to the use of the critical gap. As presented in the compendium of papers (2) presented at the 1988 International Workshop, Intersection without Traffic Signals, the methodology used in the 1985 HCM to estimate the

critical gap usually results in an overestimation of this parameter. The 1985 HCM assumes that the critical gap remains constant without considering the impact of delay or waiting time. Preliminary studies (3-5) have shown that the critical gap is not constant because drivers tend to accept smaller gaps as they wait in queue or at the stop line for longer time.

To assess the current HCM and develop new procedures for capacity analysis of TWSC intersections, a work program was developed by the Unsignalized Intersection Subcommittee of TRB. A Transportation Research circular (6) was published by the subcommittee to provide guidelines for the standard data collection technique for unsignalized intersection capacity/delay characteristics. Under this program, research studies have been initiated to develop a national data base and new capacity analysis procedures. An NCHRP project entitled New Procedures for Capacity and Level of Service Analysis at Unsignalized Intersections was conducted by the University of Idaho. According to 1993 NCHRP statements (7), the major objectives of this NCHRP project were to examine analysis methods, conduct validation studies, recommend revised computational methodologies, and calibrate the recommended procedures that are needed to replace the outdated procedures in Chapter 10 of the 1985 HCM. Another research study entitled Study of Sign Controlled Intersections and Uniform Data Collection and sponsored by Region 10 of University Transportation Center (Transportation Northwest Center), was conducted by the University of Alaska Fairbanks and Portland State University during 1993 and 1994. This paper summarizes some of the research efforts in the study with the activities focused on the following:

Traffic data at six TWSC intersections were collected in Fairbanks, Alaska, and 34-hr traffic data were recorded by video cameras. The recorded traffic data were reduced from videotapes by a specialized computer program, Traffic Data Input Program (TDIP) (8), to generate major and minor street volumes, conflicting volumes, minor queue and service delays, turning movements, gaps, headway distribution, and other characteristics. Empirical methods were used to analyze the interrelationships between conflicting volume, delay, and capacity. The main purpose to develop such models was to seek a simplified method to estimate minor street capacity at TWSC intersections. Drivers' acceptable gap data were collected from these intersections. These gap data were analyzed to generate the statistical relationship between intersection service time (delay) and the critical gap.

The main objective of this effort was to collect traffic data at TWSC intersections under Alaska's environment. These data may be added to the data base of the Pacific Northwest region of the United States and to a national traffic data base for developing TWSC intersection capacity estimation models. Because Alaska is a special state, with larger areas and relatively less traffic compared with other

J. J. Lu, Transportation Research Center, University of Alaska Fairbanks, Fairbanks, Alaska 99775. B. Kent Lall, Department of Civil Engineering, Portland State University, Portland, Oreg. 97207.

states, the data from Alaska may have certain meanings to the data bases used for the development of capacity estimation models.

FIELD DATA COLLECTION AND REDUCTION

To study traffic delay, capacity, and gap acceptance characteristics at TWSC intersections, it was necessary to obtain field data at intersections that typically represented most TWSC intersections. The selection of suitable sites involved considerations of several factors, such as geometric conditions, sight distance, speed limit, traffic volume, traffic directional distribution, and randomness of approaching traffic. In this study, six test sites were selected. Table 1 summarizes these test sites.

As suggested in a TRB research circular (6), video cameras were used in the field to record traffic in both major and minor approaches. In addition, time data displayed in the screen of the video cameras were also recorded.

To obtain delay, volume, and gap acceptance data, time data at which each vehicle entered the end of the queue, reached stop line, and entered the intersection were necessary. Time data were obtained from videotapes that recorded time information. For the reduction of delay, capacity, and volume data, the computer program TDIP was used. This program was developed by the University of Idaho to collect traffic volume, delay, movement, and gap (headway) data. In this effort, data collection was performed during the day on normal weekdays, including rush-hour and nonrush-hour traffic. Through field data collection, approximately 34-hr traffic data were collected from Test Sites 1 through 6 for the analysis of delay, capacity, through volume, and gap acceptance characteristics. Statistical traffic data collected from Test Sites 1 through 6 and generated by TDIP were traffic volume on major and minor approaches, queue delay, service delay, total delay, and traffic movement distribution. These data were based on both 5- and 10-min averages and may be contributed to a data base for development of a capacity estimation procedure of TWSC intersections.

DELAY AND CAPACITY MODELS

Empirical methods for estimating minor street capacity at TWSC intersections have been attempted in previous studies (3, 9-12).

Basically, in these studies, it was assumed that the minor street capacity was a function of the traffic volume and the speed on the major street. The function was estimated by statistical regression analysis with a linear function format or exponential function format. Although the models obtained in these studies were not the final ones, they gave better understanding of the statistical relationships between delay, capacity, and volume at the TWSC intersections. Results from these studies indicated that the empirical model approach might provide an alternative to the gap acceptance method currently used in the 1985 HCM.

The research effort summarized in this paper used the same approach to develop three statistical models for minor street service delay, minor street capacity, and minor street total delay, respectively. In the first model, it was proposed that the minor street service delay was the function of the subject conflicting volume. Raw data indicated that this relationship could be a first-order function. In the second model, minor street capacity data were converted from service delay. Then an exponential function was used to fit the relationship between minor street capacity and conflicting volume. In the third model, the total delay in the minor street approach was fitted by a nonlinear multivariable regression model with the conflicting volume and subject minor street volume as the independent variables. Traffic data were based on 5- and 15-min averages. Data generated through TDIP included major street traffic volume, subject minor street traffic volume, subject minor street queue delay, and subject minor street service delay with a total 408 of data points obtained for each variable if a 5-min average was used and 136 data points for each variable if a 15-min average was used. Besides, the major street speed limit might also affect a driver's judgment to enter the intersection from the stop line. In this case, traffic data were divided into two groups, one with a major street speed limit of 56 kph (35 mph) (Test Sites 1 through 3), and the other with 88 kph (55 mph) (Test Sites 4 through 6). For each model, four equations were obtained: that is, the combinations of two speed limits and two intervals of data average.

Estimation of Capacity from Service Delay

The capacity of a minor approach can be obtained from the corresponding service delay by the following equation:

TABLE 1 Summary of Test Site Conditions at Fairbanks

Test Sites	Major Street	Minor Street	Development Along Minor Street	Major Street Speed Limit	Sight Condition	Minor Approach Grade
1	3rd Ave.	Eagle Ave.	Resident	56 km/hr.	Very Good	Level
2	University Ave.	Davis Rd.	Resident	56 km/hr.	Fair	Level
3	Gaffney Rd.	604th St.	Military Base	56 km/hr.	Very Good	Level
4	Richardson Hwy.	Old Richardson Hwy.	Industry	88 km/hr.	Good	Level
5	Steese Exp.	Farmers loop Rd. (W.B.)	Resident	88 km/hr.	Very Good	Level
6	Steese Exp.	Farmers Loop Rd. (E.B.)	Resident	88 km/hr.	Very Good	Level

Note: 1 km = 0.6 mi.

$$\text{Capacity} = \frac{3600}{\text{Service Delay}} \tag{1}$$

where the unit of capacity is vehicle per hour and the unit of service delay is a second. The calculation of capacity from service delay using Equation 1 may not be used in a practical case. According to the definition, the minor street capacity is the maximum number of vehicles that cross the stop line and enter the intersection from the subject minor street approach. Practically, this capacity can be calculated by Equation 2:

$$\text{Capacity} = \frac{3600}{T} \tag{2}$$

where T is the average interval (seconds) of two successive vehicles entering the intersection from the subject minor street approach and T is not equal to service delay. Assume at time t_1 , the first vehicle begins to enter the intersection. Meanwhile, the second vehicle begins to move to approach to stop line if lost time is ignored. At time t_2 , the second vehicle arrives at the stop line. This vehicle has to stop at the stop line and look for an available gap to enter the intersection. The time taken by the second vehicle waiting at the stop line is the service delay. At time t_3 , the second vehicle accepts an available gap and begins to enter the intersection. Service delay is the interval between t_2 and t_3 or

$$\text{Service Delay} = t_3 - t_2$$

and

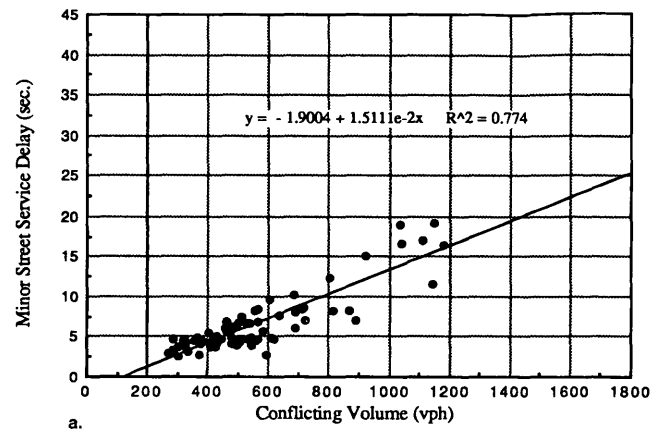
$$T = t_3 - t_1 = t_3 - t_2 + t_2 - t_1 = \text{Service Delay} + \Delta \tag{3}$$

where $\Delta = t_2 - t_1$ and Δ should be greater than 0. Generally, Δ is not affected by traffic on the major street and is dependent only on driver's behavior and vehicle's acceleration characteristic. In fact, T can be considered the follow-up gap of the subject minor street approach. Statistically, Δ can be estimated from field observations. By reviewing videotapes, an average Δ value (4.1 sec) was obtained. Capacity, therefore, can be calculated by Equation 4:

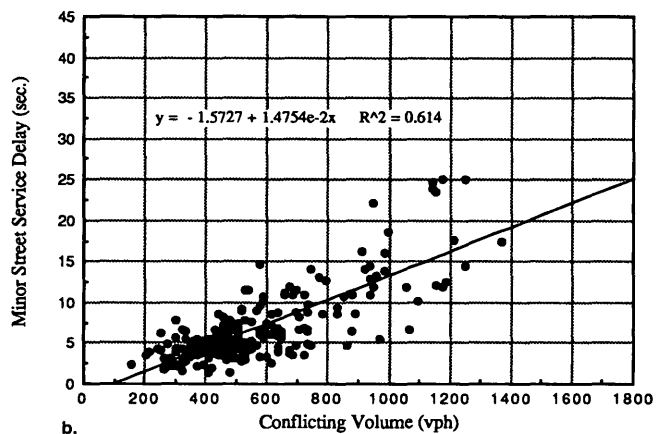
$$\text{Capacity} = \frac{3600}{\text{Service Delay} + 4.1} \tag{4}$$

Service Delay versus Conflicting Volume

Service delay or service time is defined as the time between the arrival of minor approaching traffic at the stop line and the departure from the stop line. The major factor that contributes to service delay is the conflicting volume or major traffic volume because what a driver needs is an acceptable gap between two successive vehicles in the conflicting traffic stream. Figures 1 and 2 present the relationships between service delay and conflicting volume for the test sites with major street speed limits of 56 kph (35 mph) and 88 kph (55 mph), respectively. Parts *a* and *b* of each figure represent the relationships with 5- and 10-minute averages, respectively. Statistical regression models and correlation coefficients are shown in the corresponding figures from which it can be seen that these models have relatively good fitness, meaning service delay can be



Note: 1 km = 0.6 mi.



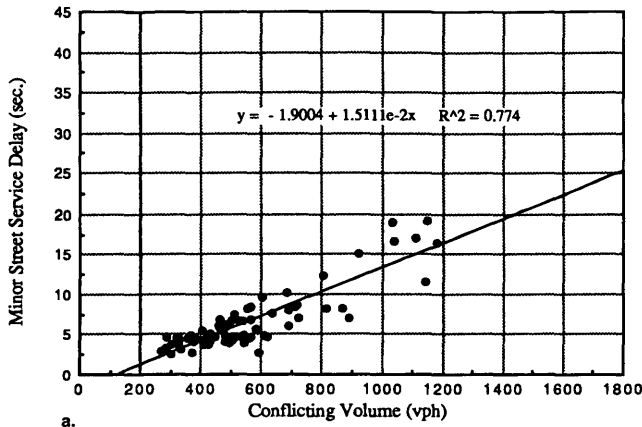
Note: 1 km = 0.6 mi.

FIGURE 1 Relationship between minor street service delay and conflicting volume. Major street speed limit: (a) 56 kph; average interval, 15 min; (b) 88 kph; average interval, 15 min.

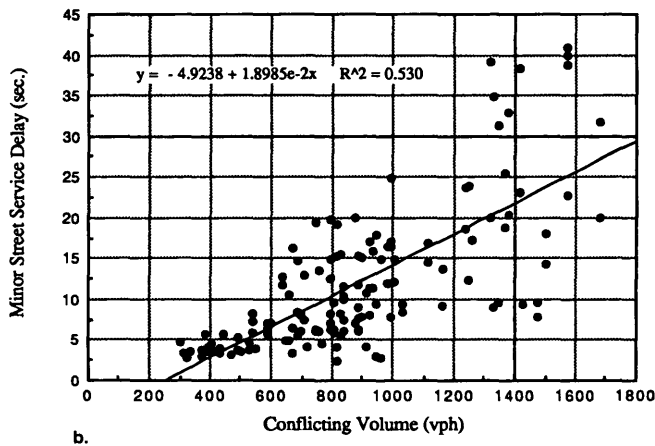
adequately estimated directly from the conflicting volume. Figure 3 shows the statistical relationship between service delay and conflicting volume for different major street speed limits and time averages. On the basis of this figure, two conclusions can be made. First, the factor of data average interval does not significantly affect the statistical models if enough data points were obtained. Second, the minor approach service delay is slightly more sensitive to a higher speed limit in the major street when the conflicting traffic is heavier. However, the impact of speed limit on minor street service delay is not significant. It should be stated that these statistical equations cannot be used for the case that the conflicting volume is very low (≤ 200 vehicles per hour) because the models were developed on the basis of the conflicting volume that was heavier than 200 vehicles per hour.

Minor Street Capacity versus Conflicting Volume

Minor street capacity at TWSC intersections can be calculated by Equation 4 if service delay data are available. On the basis of field data, the relationships between subject minor street capacity and



Note: 1 km = 0.6 mi.



Note: 1 km = 0.6 mi.

FIGURE 2 Relationship between minor street service delay and subject conflicting volume. Major street speed limit: (a) 88 kph, average interval, 15 min; (b) 88 kph; average interval, 5 min.

conflicting volume were obtained and shown in Figure 4 with a major street speed limit of 56 kph (35 mph) and Figure 5 with a major street speed limit of 88 kph (55 mph). Parts *a* and *b* of these figures represent the results with 5- and 10-min averages, respectively. According to the data points shown in these figures, an exponential functional form was used to fit these curves. Statistical capacity estimation models are listed as follows:

Speed limit, 56 kph (35 mph), 15-min average:

$$\text{Capacity} = 683.76 e^{-0.0011744 V_c} \quad R^2 = 0.774 \quad (5)$$

Speed limit, 56 kph (35 mph), 5-min average:

$$\text{Capacity} = 665.27 e^{-0.0011196 V_c} \quad R^2 = 0.602 \quad (6)$$

Speed limit, 88 kph (55 mph), 15-min average:

$$\text{Capacity} = 675.13 e^{-0.0011519 V_c} \quad R^2 = 0.689 \quad (7)$$

Speed limit, 88 kph (55 mph), 5-min average:

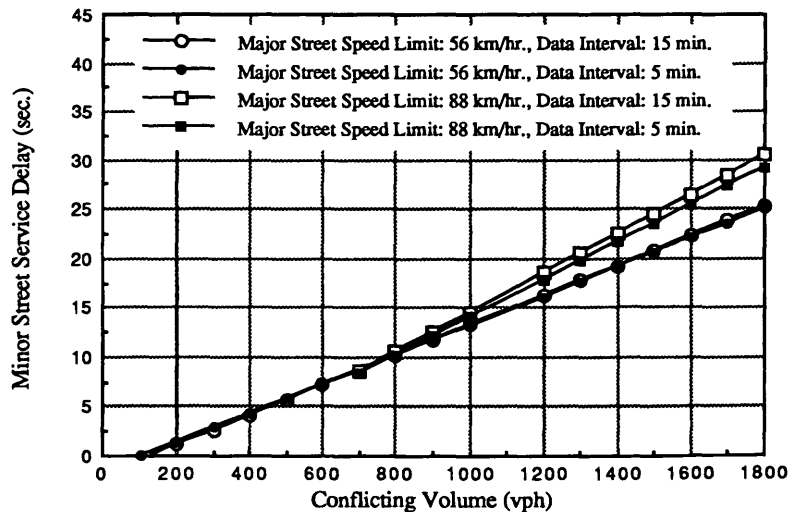
$$\text{Capacity} = 661.69 e^{-0.0010795 V_c} \quad R^2 = 0.565 \quad (8)$$

where V_c is the conflicting volume.

These functions in Equations 5 through 8 are drawn together in Figure 6 to show the differences between these functions. From Figure 6, it can be concluded that (a) the factor of major street speed limit is not an important one to affect the subject minor street capacity, and (b) the data average interval does not show a significant impact on the modeling results. By averaging the models with 5- and 15-min data averages, the following capacity models can be obtained.

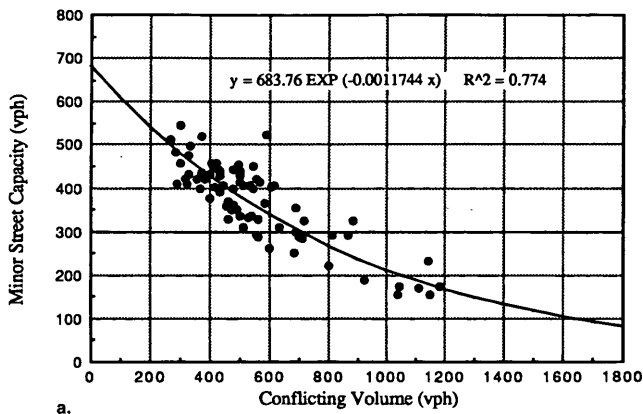
Speed limit, 56 kph (35 mph):

$$\text{Capacity} = 674.52 e^{-0.001147 V_c} \quad (9)$$

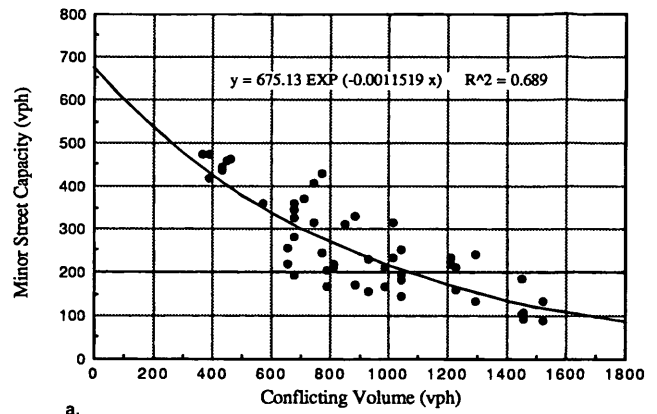


Note: 1 km = 0.6 mi.

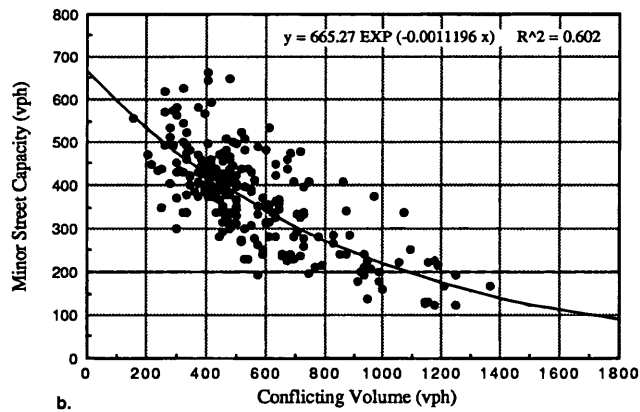
FIGURE 3 Statistical relationship between minor street delay and conflicting volume.



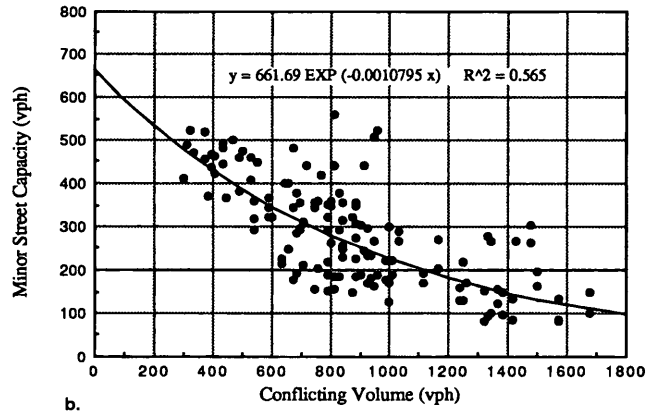
Note: 1 km = 0.6 mi.



Note: 1 km = 0.6 mi.



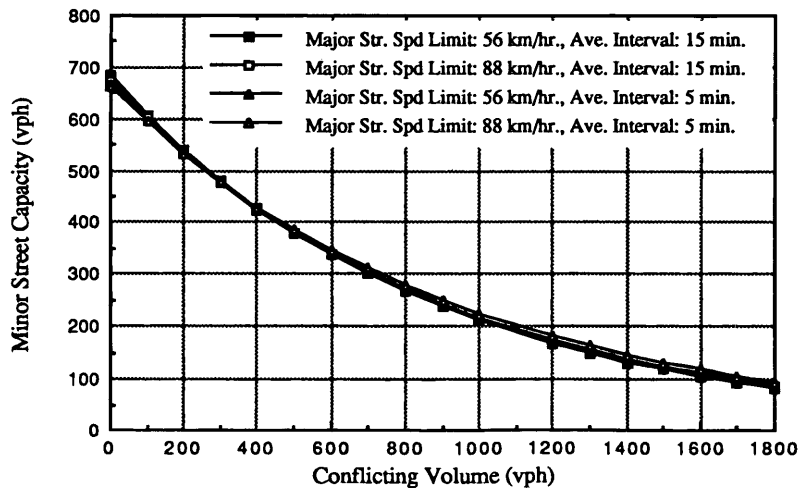
Note: 1 km = 0.6 mi.



Note: 1 km = 0.6 mi.

FIGURE 4 Relationship between minor street capacity and conflicting volume. Major street speed limit: (a) 56 kph; data interval, 15 min; (b) 56 kph; data interval, 5 min.

FIGURE 5 Relationship between minor street capacity and conflicting volume. Major street speed limit (a) 88 kph; data interval, 15 min; (b) 88 kph; data interval, 5 min.



Note: 1 km = 0.6 mi.

FIGURE 6 Statistical relationship between minor street capacity and conflicting volume.

Speed limit, 88 kph (55 mph):

$$\text{Capacity} = 668.41e^{-0.0011157 V_c} \quad (10)$$

Total Delay versus Subject Minor and Conflicting Volumes

The total delay at the subject minor street approach consists of service delay and queue delay. The queue delay, or queue time, is defined as the time spent waiting in queue until arriving at the stop line. The queue delay is not only the function of the conflicting volume, but also the function of the subject minor street approaching traffic volume. In this case, the total delay can be considered the function of both conflicting volume and minor volume. The following equational form was tried in the effort:

$$D_i = a + b V_{mi} + ce^{dV_c} \quad (11)$$

where

D_i = the subject minor street total delay (sec);

V_c and V_{mi} = conflicting volume and minor traffic volume, respectively; and

a , b , c , and d = coefficients to be estimated.

As stated previously, major street speed limit did not significantly affect the minor street capacity or service delay. The data base used to develop the model represented by Equation 11, therefore, included data with both major street speed limits of 56 kph (35 mph) and 88 kph (55 mph). Statistical analysis was conducted to obtain the coefficients shown in Equation 11. Table 2 shows the modeling results for both average intervals of 5 and 15 min. The regression parameters b , c , and d are positive, meaning that as traffic volumes in subject conflicting approach or subject minor street approach increases, or both, the total delay in the subject minor approach

increases. This represents the real situation because as more minor street traffic approaches the intersection, more vehicles wait in the queue line, resulting in a longer queue delay. If all data with both 5- and 15-min averages are combined together, a final model can be obtained as shown in Equation 12.

$$D_i = -3.411 + 0.022 V_{mi} + 5.634 e^{0.00125 V_c} \quad (12)$$

The corresponding statistics are shown in Table 2.

IMPACT OF SERVICE DELAY ON GAP ACCEPTANCE BEHAVIOR

Traffic gap acceptance characteristics have been used to calculate the capacity of unsignalized intersections, decide the warrants for stop signs, analyze the capacity of weaving and merging areas, select parameters for ramp metering, and solve other design problems. The availability of quantitative data for gap acceptance characteristics, therefore, is very important for these applications. One of the main tasks studied in this research effort was to verify whether a driver waiting at the stop line would take a smaller gap if he or she had waited a longer time at stop line. The statistical relationship, which characterizes this behavior, was quantified in this task.

The 1985 HCM uses constant critical gaps to estimate minor street capacity with the assumption that the critical gaps do not change over time. In recent years, suggestions have been made to state that the critical gaps are not constant and that drivers waiting at the stop line tend to accept smaller gaps as they wait a longer time at the stop line or in queue. Efforts were made in this study to quantify the variability in the critical gap related to the minor street approach service delay. Gap data used for this task were collected from Test Sites 1 through 6. Vehicles approaching the stop line from the subject minor

TABLE 2 Multiple Regression Analysis for Total Delay Model

	Coefficient	Std. Err Estimate	t Statistic	Prob>t	R ²
Part a Data Average Interval: 15 Min.	a = -1.403	2.152	-0.652	0.516	0.560
	b = 0.025	0.014	1.752	0.082	
	c = 3.309	0.269	12.306	0.000	
Part b Data Average Interval: 5 Min.	a = -3.697	1.590	-2.324	0.021	0.333
	b = 0.022	0.006	3.651	0.000	
	c = 5.833	0.429	13.602	0.000	
Part c Modeling Results with All Data	a = -3.411	1.308	-2.609	0.009	0.365
	b = 0.022	0.005	3.957	0.000	
	c = 5.634	0.334	16.878	0.000	

street at each site were monitored to get their service delay and accepted gap data. These gap data were divided into three groups according to the corresponding service delay (Group 1, Service delay = 1 to 10 secs; Group 2, Service delay = 11 to 20 sec; and Group 3, Service delay \geq 21 sec) without consideration of traffic movement. In each group, a critical gap was calculated. The cumulative distribution (percent acceptance) curves of accepted gaps in each service delay group was fitted by a logit equation and is shown in Figure 7 with the resulting critical gaps shown as follows:

- Group 1: Critical gap = 8.39 sec,
- Group 2: Critical gap = 8.21 sec, and
- Group 3: Critical gap = 7.84 sec.

Statistically, it was found that as service delay increased, the corresponding critical gap decreased or the drivers waiting at the stop line

seemed to accept smaller gaps. This conclusion verifies the assumption mentioned previously. To quantify the relationship between the critical gap and service delay, a second-order polynomial equation was used with the following definition of a new variable, g :

- $g = 1$ (if service delay belongs to Group 1),
- $g = 2$ (if service delay belongs to Group 2), and
- $g = 3$ (if service delay belongs to Group 3).

Then, the critical gap was mathematically fitted by the following equation:

$$\text{Critical gap} = 8.38 + 0.105g - 0.095g^2 \tag{13}$$

This equation is graphically shown in Figure 8. This curve does not assume that as service delay continuously increases the corre-

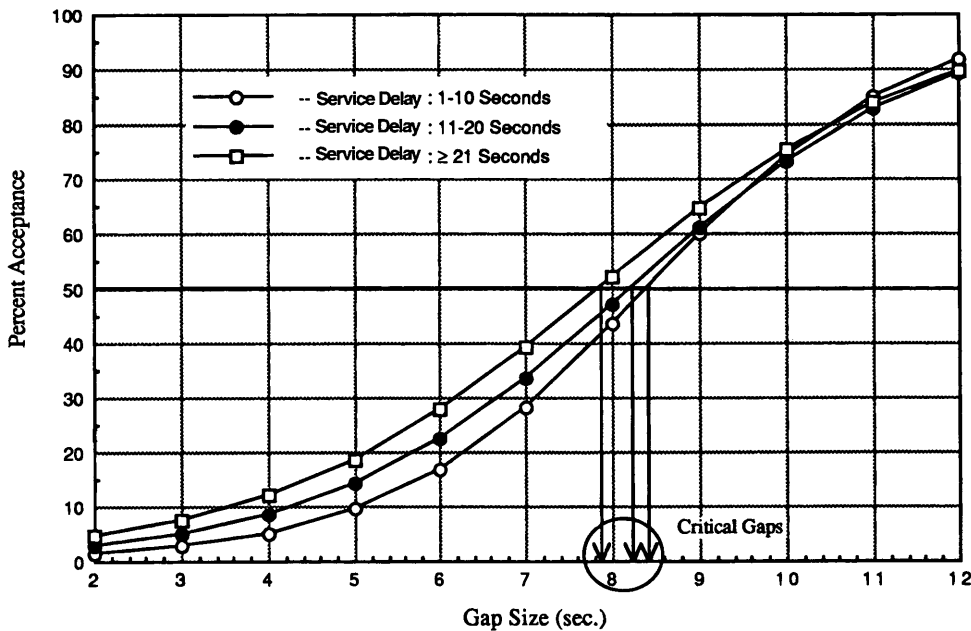


FIGURE 7 Impact of service delay on driver's gap acceptance behavior.

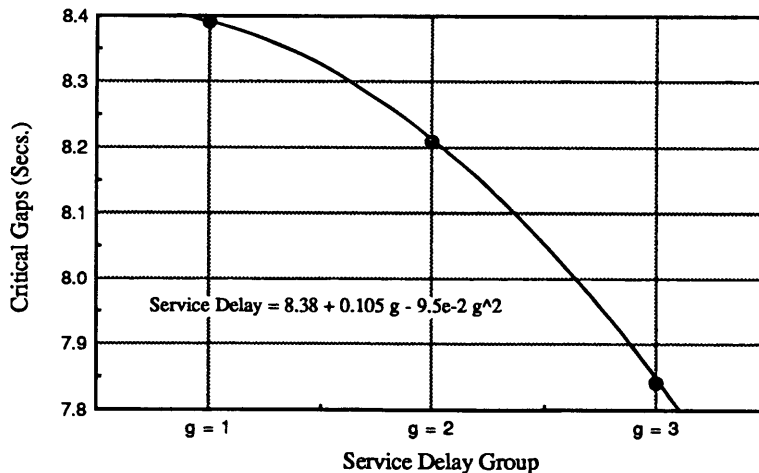


FIGURE 8 Statistical relationship between critical gap and service delay.

sponding critical gap would unrestrictedly decrease. A certain limitation should be reached. The detailed behavior is yet to be studied.

CONCLUSIONS

The following conclusions can be made:

1. Empirical methods have been proven to be an alternative for the estimation of minor street capacity at TWSC intersections. On the basis of empirical methods, a procedure to estimate minor street capacity at TWSC intersections can be developed.

2. Service delay is mainly caused by the conflicting traffic or major street traffic. A linear equation high correlation was obtained to represent this relationship.

3. Minor street capacity can be directly estimated from the conflicting traffic volume or major street traffic volume with an exponential equational form. The models developed in this effort showed good correlation between capacity and conflicting volume. As discussed previously, the minor street capacity is not inversely proportional to service delay, but the follow-up gap of the subject minor street traffic. The follow-up gap consists of service delay and a time interval Δ defined previously. The time interval Δ is dependent on driver's behavior and vehicle acceleration characteristics. Estimation of Δ was made in this effort. However, further study of this variable is recommended because it appears that no studies have been conducted to evaluate this variable, which definitely affects the capacity in the subject approach.

4. Total delay depends on not only the conflicting traffic volume or major street traffic volume but also the subject minor street traffic volume. As more vehicles approach the intersection, the corresponding total delay will increase because more vehicles may enter the queue line in the subject minor street approach. A nonlinear multivariable model was used in this effort to describe this relationship. Reasonably good fitness of the model was obtained.

5. It appeared from this study that the factor of major street speed limit did not significantly affect service delay and capacity estimation models, and modeling results did not show a significant difference between 5- and 15-min averages.

6. It was proven that drivers tended to accept smaller gaps in the subject traffic stream as service delay increased. To develop better-capacity estimation procedure, this behavior should be taken into consideration.

REFERENCES

1. Special Report 209: Highway Capacity Manual, Chapter 10, TRB, National Research Council, Washington, D.C., 1985.
2. W. Brilon (ed.), *Intersections Without Traffic Signals*, Springer-Verlag, New York, 1988.
3. Kyte, M., C. Clemow, N. Mahfood, B. K. Lall, and C. J. Khisty. Capacity and Delay Characteristics of Two-Way Stop-Controlled Intersections. In *Transportation Research Record 1320*, TRB, National Research Council, Washington, D.C., 1991, pp. 160-167.
4. Kittelson, W. K., and M. A. Vandehey. Delay Effects on Driver Gap Acceptance Characteristics at Two-Way Stop-Controlled Intersections. In *Transportation Research Record 1320*, TRB, National Research Council, Washington, D.C., 1991, pp. 154-159.
5. Brilon, W., M. Grossmann, and B. Stuwe. Toward a New German Guideline for Capacity of Unsignalized Intersections. In *Transportation Research Record 1320*, TRB, National Research Council, Washington, D.C., 1991, pp. 168-174.
6. *Transportation Research Circular 373: Interim Materials on Unsignalized Intersection Capacity*, TRB, National Research Council, Washington, D.C., 1991.
7. *Briefs of Research Problem Statements Considered by the AASHTO Standing Committee on Research for the 1993 Program of the NCHRP*. TRB, National Research Council, Washington, D.C., Oct. 1991.
8. Boesen, A., M. Kyte, and B. Rindlisbacher. *Traffic Data Input Program (TDIP), Program Documentation and User's Manual Version 3.0*. University of Idaho, Moscow, March 1991.
9. Kyte, M., B. K. Lall, and N. Mahfood. Empirical Method to Estimate the Capacity and Delay of the Minor Street Approach of a Two-Way Stop-Controlled Intersection. In *Transportation Research Record 1365*, TRB, National Research Council, Washington, D.C., 1992, pp. 1-11.
10. Kimber, R. M., and R. D. Coombe. *The Traffic Capacity of Major/Minor Priority Junctions*. TRRL Supplementary Report 582. U.K. Transport and Road Research Laboratory, Crowthorne, Berkshire, England, 1980.
11. Kimber, R. M. Gap-Acceptance and Empiricism in Capacity Prediction. *Transportation Science*, Vol. 23, No. 2, May 1989, pp. 100-111.
12. Semmens, M. C. *The Capacity of Major/Minor Priority Junctions on High Speed Roads*. Working Paper TMN 157. U.K. Transport and Road Research Laboratory, Crowthorne, Berkshire, England, Oct. 1987.

The contents of this paper reflect the views of the authors, who are responsible for the facts and the data presented herein. The contents do not necessarily reflect the official views or policies of FHWA. This paper does not constitute a standard, specification, or regulation.

Publication of this paper sponsored by Committee on Traffic Control Devices.

Evaluation of Proposed Minimum Retroreflectivity Requirements for Traffic Signs

CLETUS R. MERCIER, CHARLES GOODSPEED, CAROLE J. SIMMONS,
AND JEFFREY F. PANIATI

An FHWA study was recently completed as part of its retroreflectivity research program; the goal was to determine minimum retroreflectivity requirements for traffic signs. Results were summarized in tables providing recommended minimum R_s values for warning, regulatory, and guide signs, with the tables designed to provide a framework of minimum retroreflectivity requirements for field implementation. However, the level of accommodation could only be estimated in the range of 75 to 85 percent. The study measured luminance threshold for traffic signs. Subjects in a darkened laboratory viewed a series of scaled traffic signs. Simulated viewing distance was the "minimum required visibility distance," that is, the minimum distance that would allow a driver sufficient time to respond safely to the sign. Sign luminance was increased in steps until the subject was able to correctly recognize it. Data scatter plots showed an increased need for sign luminance with subject age. To specify the percent accommodated for the driving population, laboratory data were extrapolated statistically. For each sign, the mean and variance for the subjects tested were used to generate model data points, and percentiles were determined using U.S. driving population age distribution data. Analysis showed that 85 percent or more of all drivers (98 to 100 percent for most signs) would be accommodated by the level of retroreflectivity recommended for nearly all signs tested. Results indicate that minimum retroreflectivity table values are fairly conservative, allowing a margin for safety.

This paper is based on a study completed as part of the FHWA retroreflectivity research program. The program has two primary goals: (a) to define minimum nighttime visibility requirements for traffic control devices, and (b) to develop measurement devices and computer management tools necessary to effectively implement these requirements.

Two separate studies were directed toward the first goal. The first of these was the development of a computer model designed to define minimum retroreflective values for in-service traffic signs. The second study, described in this paper, is an evaluation of the proposed values.

Current national guidelines relating to traffic sign nighttime visibility are limited to the stipulation in the Manual on Uniform Traffic Control Devices for Streets and Highways (1) that all warning and regulatory signs be illuminated or reflectorized to show the same color and shape by day or night. No objective measures are stated that can be used to determine end-of-sign service life, when it needs replacement.

C. R. Mercier, Department of Engineering, Iowa State University, Ames, Iowa 50011. C. Goodspeed, SAIC, 6300 Georgetown Pike, McLean, Va. 22101-2296. C. J. Simmons and J. F. Paniati, Turner-Fairbank Highway Research Center, 6300 Georgetown Pike, McLean, Va. 22101-2296.

SUPPLY AND DEMAND

Visibility of retroreflective traffic signs can be examined on the basis of supply and demand. Retroreflective materials included in sign manufacture combine with light received from vehicle headlights to "supply" a given level of luminance, reflected back to the driver. This provides a "lighted" sign, which is easier for vehicle drivers to see and read at night.

The demand side is associated with driver needs to gain access to information provided by the sign at a particular distance to take timely and proper action. When sign luminance falls below that demanded by the driver because of inadequate retroreflectance, the sign should be replaced. The study goal was to define a "threshold" level of sign retroreflectivity, when supply satisfies demand. One of the main problems is that demand varies according to the vision characteristics of the driver. Part of the driving population, aware of their nighttime visibility problems, compensate by either avoidance of nighttime driving, by driving only on familiar streets at night, or by driving at slower speeds to have enough time to react to traffic sign messages and to unexpected situations.

The challenge of determining threshold levels that are suitable for a high percentage (for example, 90 percent) of the driving population remains a policy decision because it is not economically feasible to select threshold levels that will serve all drivers. This study will help in the decision-making process by providing minimum retroreflective values needed to accommodate varying percentages of the driving population. If the threshold is not high enough to serve the selected population, then minimum retroreflectivity values must be changed.

However, the wide range of visual, cognitive, and psychomotor capabilities among drivers complicates the problem of determining the percentage of driving population served. Also, there is substantial complexity in relationships among driver, vehicle, signs, and the roadway.

COMPUTER MODEL

A 1993 FHWA study by Paniati and Mace (2) addressed the first of the two goals described earlier. The research developed minimum retroreflectivity requirements for warning, regulatory, and guide signs. Researchers utilized a mathematical model to study the complex relationships between the driver, the vehicle, the signs, and the roadway. The model produced is called Computer Analysis of the Retroreflectance of Traffic Signs (CARTS). The model's theoretic-

cal construct is based on two validated theoretical models and one submodel developed expressly for CARTS.

The fundamental basis for CARTS is the concept of minimum required visibility distance (MRVD). The MRVD is the shortest distance at which a sign must be visible to enable a driver to respond safely and appropriately. MRVD includes the distance required for a driver to detect the presence of a sign, recognize the message, decide on a proper action (if necessary), and make the appropriate maneuver (if necessary) before the sign moves out of the driver's vision. For a selected sign, CARTS calculates the required MRVD, determines the luminance required at the MRVD, and then converts this luminance to a minimum required retroreflectivity value. The model allows the user to vary numerous parameters, including the type, size, and location of the sign; the headlamp design and driver position; the driver age and visual characteristics; the roadway design; and the traffic volume. Details of the CARTS model are provided in the Minimum Visibility Requirements for Traffic Signs project report.

Paniati and Mace (2) used the CARTS model in their research to identify the critical variables affecting sign retroreflectivity and to provide insight into the levels of retroreflectivity that are required for meeting driver needs. The result of this work was a set of minimum retroreflectivity requirement tables (see Table 1). The tables

were designed to provide a framework for field implementation of research results. Paniati and Mace estimated that values provided in the tables would accommodate at least 75 to 85 percent of all drivers, but for various reasons (described in the project report) they were unable to provide a more definitive estimate. This paper describes a second research project, conducted to more fully study the levels of driver accommodation.

STUDY PROBLEM

Resulting minimum retroreflectivity values derived from CARTS seem consistent with experimental values derived from other studies but need to be specifically validated in the context of their intended use. The validation problem was further complicated by the variability of driver nighttime vision exacerbated by accelerated deterioration of contrast sensitivity loss experienced by some older drivers. A lack of significant correlation between age and contrast sensitivity loss provides another variable important in the validation study. This lack of correlation provided the rationale for two elements of this study. It was hypothesized that age-related deterioration in vision contrast sensitivity is the proximate cause for nighttime visibility problems experienced by some older drivers. This

TABLE 1 Summary of Minimum Retroreflectivity Guidelines for Signs Covered in the Study (2)

Legend Color: Black		Background Color: Yellow or Orange					
Sign Size		>=48 in ¹		36 in ¹		<= 30 in ¹	
Legend	Material Type	Minimum retroreflectivity values ²					
Bold Symbol	All	15		20		25	
	I	20		30		45	
	II	25		40		60	
	III	30		50		80	
Fine Symbol and Word	IV, VII	40		70		120	
Legend Color: White		Background Color: Red					
Traffic Speed		45 mph or greater			40 mph or less		
Sign Size		>= 48 in		36 in		<= 30 in	
		W ²	R ²	W ²	R ²	W ²	R ²
All Signs		50	10	60	12	70	14
		30	6	35	7	40	8
Legend Color: Black and/or Black and Red		Background Color: White					
Traffic Speed		45 mph or greater			40 mph or less		
Sign Size		>= 48 in		30-36 in		<= 24 in	
Material							
Grnd Mntd	I	20	35	50	15	20	35
	II	25	45	70	20	30	55
	III	30	60	90	25	45	75
	IV, VII	40	80	120	35	60	100
Over-head Mntd	I				40	50	100
	II				50	75	135
	III				65	115	185
	IV, VII				90	150	250
Legend Color: White		Background: Green					
Traffic Speed		45 mph or greater			40 mph or less		
Color		White ²		Green ²		White ²	
Grnd Mntd		35		7		25	
Ov'hd Mntd		110		22		80	

¹ 1 in = 25.4 mm

² Shown below are minimum reflectivity values for the material and color indicated, in cd/lux/m².

1 mph (mile per hour) = 1.6 kph (kilometers per hour)

translates to a need for higher retroreflectivity values to be able to read traffic sign messages.

Therefore, the population of participants recruited was weighted to include a significant number of drivers aged 65 and older—ages at which a higher incidence of vision with diminished contrast sensitivity would be expected. Second, data were collected on high and low luminance vision contrast sensitivity for all subjects for later analysis.

The experimental design includes a simulation designed to approximate CARTS reference conditions described earlier, used to generate traffic sign minimum retroreflectivity requirements incorporated in the tables. Analysis of data collected from this study was directed toward the evaluation of these minimum retroreflectivity values.

RESEARCH METHODOLOGY

A luminance threshold experiment was conducted in which subjects in a darkened laboratory viewed a series of signs at corresponding MRVDs. Test conditions simulated CARTS reference conditions. Luminance provided for each sign was increased in steps until the subject was able to correctly read or recognize the sign. The luminance level when the subject correctly recognized the sign was recorded as the "threshold" value.

Sign luminance was controlled by varying the illuminance level on the sign. The light source used to illuminate the signs was placed at a 45 degree angle from perpendicular, such that sign luminance in the direction of the subjects did not utilize the retroreflective properties of the signing material. To compare the experimental data with the candidate guideline values in the Minimum Retro-

reflectivity Requirements for Traffic Signs report, guideline R_a values were converted to luminances using the CARTS model. A detailed account of the experimental methods and results follows.

Experimental Setup

The experiment was conducted in the Photometric and Visibility Laboratory at the Turner-Fairbank Highway Research Center. The main part of the laboratory consists of a single, windowless room, measuring 4.3 m (14 ft) by 36.6 m (120 ft) in length. All interior surfaces (walls, ceiling, and floor) are black to minimize light reflection and allow better control of light levels. The laboratory was darkened to a level of approximately .01 cd/m², to simulate a nighttime rural highway environment.

A total of 25 signs were selected as representative of the regulatory, warning, and guide signs included in the candidate guideline tables. These comprised thirteen yellow diamond warning signs (nine with symbol legends, four with word legends), three white-on-red regulatory signs and two white-on-green guide signs. Five of the signs were fabricated and tested in two different sizes to evaluate the effect of sign size on required retroreflectivity.

Signs were tested at distances corresponding to the MRVDs for two speeds: 88 kph (55 mph) and 48 kph (30 mph). Because a maximum sight distance of less than 36.6 m (120 ft) was available in the laboratory, it was not possible to model driving conditions at full scale. Instead, signs were scaled using available laboratory distance and the calculated MRVD for each sign tested. For example, if a sign's MRVD was 62.2 m (204 ft), the sign was fabricated at 0.5 scale and shown at 31.1 m (102 ft). (In most cases, signs were scaled at half size.) Tables 2 and 3 provide a complete listing of

TABLE 2 Description of Stimuli Tested in Phase 1

SIGN	MUTCD Code	Actual Size (m)	Scaled Size (m)	MRVD @ 48 km/h (m)*	MRVD @ 88 km/h (m)*
Right Curve	W1-2R	.762	.381	50.3	61.3
Right Intersection	W2-2	.762 .914	.381 .457	50.3 50.6	61.3 61.9
Narrow Bridge	W5-2	.762	.381	50.3	61.3
Right Lane Ends	W2-2	.762 .914	.381 .457	50.3 50.6	61.3 61.9
Bicycle Crossing	W11-1	.762	.381 .457	50.3 50.6	61.3 61.9
Pedestrian Crossing	W11-2	.762	.381	50.3	61.3
Do Not Pass	R4-1	.61	.305	49.7	61
Keep Right	R4-7	.61 .762	.318 .356	56.4	61
No Right Turn	R3-1	.61	.305	50.6	61 73.2
One Way	R6-1	.914	.457	50.6	61.9
Stop	R1-1	.914	.152 .33	70.4	185.3
Do Not Enter	R5-1	.762	.127 .254	46.6	185.3
Coming (destination)	D2-1	1.27	.229	51.5	62.8
Creston/Gravity (destination)	D2-2	1.524	.762	52.4	63.4

1 m = 3.28 feet

TABLE 3 Description of Stimuli Tested in Phase 2

SIGN	MUTCD Code	Actual Size (m)	Scaled Size (m)	MRVD @ 48 km/h (m)*	MRVD @ 88 km/h (m)*
Merge	W4-1	.762	.381	n/a	61.3
Deer Crossing	W11-3	.762	.381	n/a	61.3
Slippery When Wet	W8-5	.762	.381	n/a	61.3
No Passing	W14-3	1.22	.283	n/a	133.8
Narrow Bridge	W5-2	.914	.457	n/a	62.5
Flagger	W20-7a	.914	.457	n/a	61.9
Worker	W21-1a	.914	.457	n/a	61.9
Road Work 1 Mile	W21-4	.914	.457	n/a	61.9
Stop	R1-1	.762	.127	70.4	185.3
Yield	R1-2	.762	.127	70.4	185.3
Do Not Enter	R5-1	.762	.127	70.4	185.3
Speed Limit 50	R2-1	.61	.259	n/a	73.2
Reduced Speed Ahead	R2-5a	.61	.311	n/a	61
Route 40	M1-4	.61	.311	n/a	61

1 m = 3.28 feet

scaled sign sizes and viewing distances for Phases 1 and 2, respectively.

For ease of presentation, signs to be displayed were mounted on a rotating wheel approximately 2 m (6 ft) in diameter. Five signs could be placed on the wheel at one time, although one at a time would be visible.

Signs were illuminated by a Standard Illuminant A light source, positioned at a distance of 2.6 m (8.5 ft) from the sign, with an entrance angle of 45 degrees (see Figure 1). It was not possible to vary the light source intensity directly without causing color shifts. Instead, the desired illumination levels were achieved with the aid of a neutral density filter wheel with 20 neutral density settings ranging from 0.02 to 3.0. The filter settings were calibrated with an LMT 1009 luminance meter. Sign panel luminance was also measured with the light source unfiltered, for each of the sign background colors used. Exposure time for each trial was controlled by a shutter on the light source. Type 1 engineering grade sheeting was used for all signs.

The study was conducted in two phases. In Phase 1, a total of 14 different signs were tested at various size/speed combinations, for a total of 34 trials. In Phase 2, a total of 14 different signs were tested (17 trials). Three signs from Phase 1 were repeated in Phase 2 (Narrow Bridge, Stop, Do Not Enter), but only two trials were exactly replicated in the two phases [Do Not Enter, .76-m (30-in.) size, at 88 and 48 kph].

Subjects

Subjects were recruited from a list of drivers who regularly take part in various FHWA human factor studies and were paid for their participation. An attempt was made to balance each age group by gender. Subjects were required to hold a current valid driver's license. Subject age distributions for both phases of the study are shown in Table 4. All subjects were tested for static visual acuity using a

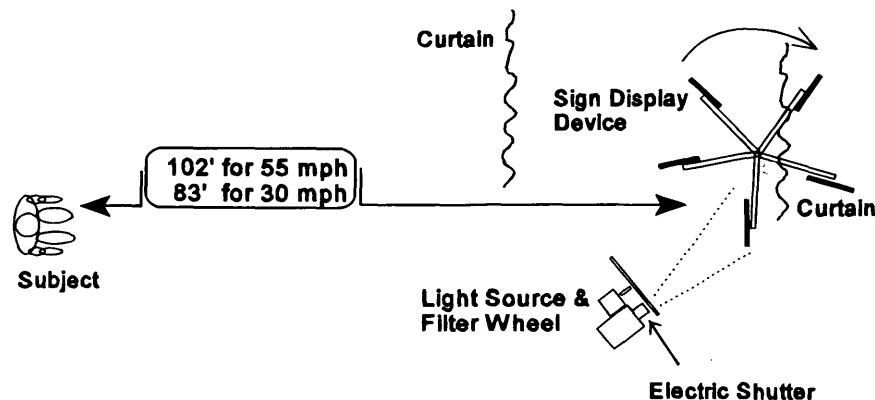


FIGURE 1 Experimental set-up.

TABLE 4 Age and Visual Acuity Data for Subjects

Ages	# of Subjects		Mean Age (S.D.)		Mean Visual Acuity (S.D.)	
	Phase I	Phase II	Phase I	Phase II	Phase I	Phase II
16-34	10	10	28 (3.6)	32.9 (7.4)	19.8/40 (3.4)	21.2/40 (3.9)
35-44	10	*	39 (2.7)	*	19.9/40 (2.9)	*
45-54	10	10	49 (3.1)	50.0 (3.0)	20.7/40 (1.9)	20.0/40 (1.9)
55-64	10	10	59 (2.8)	59.0 (2.7)	21.8/40 (1.9)	22.3/40 (3.2)
65-74	13	7	71 (3.5)	70.1 (3.2)	27.0/40 (5.6)	25.9/40 (4.3)
75+	10	8	8 (2.8)	77.0 (2.2)	25.9/40 (7.0)	24.6/40 (5.4)

For Phase II, there were a total of 10 subjects in the age range of 16-44.

Bosch and Lomb Orthorater and were required to have a minimum of 20/40 (Table 3). All subjects were tested for contrast sensitivity using the Vistech 6500 (3) test chart at high luminance (20 cd/m²) (Figure 2). In addition, subjects in Phase 2 of the study were tested for color vision with American Optics Pseudo-isochromatic Color Plates, and their low luminance contrast sensitivity (1.85 cd/m²) was measured at the end of the experiment while their eyes were still dark adapted.

Experimental Procedure

Subjects were seated in the darkened laboratory for 5 min to allow their eyes to dark adapt, while being instructed on the experimental task. After the adaptation period, the sign visibility data collection portion of the study commenced.

Subjects were first shown all the signs at one viewing distance, then moved to view the signs at the second distance. Half of the subjects viewed the signs from a distance of 88 kph first and half viewed the signs from a distance of 48 kph first. To minimize possible learning effects, signs were arranged so that similar signs were

not shown consecutively. The sets of signs that were placed on the rotating wheel were shown in an order that was counterbalanced across subjects.

For each trial, a single sign was displayed for a 1-sec interval, and subjects were asked if they could see and describe the sign message. If the subject failed to respond correctly, the wheel was rotated to display the next sign in the set at the same illuminance. If the subject correctly identified the sign message, the filter setting was recorded and the sign was removed from the sequence. When all signs had been presented at a given illuminance level and the correctly identified signs had been removed, the illuminance level was increased by one step of the filter wheel, and the remaining signs were presented to the subject. This procedure was repeated until all of the signs in the group were correctly identified or the maximum luminance level was reached.

RESULTS AND DISCUSSION

The first step in the data analysis was the generation of scatter plots for each sign, plotting subject age (x-axis) versus required lumi-

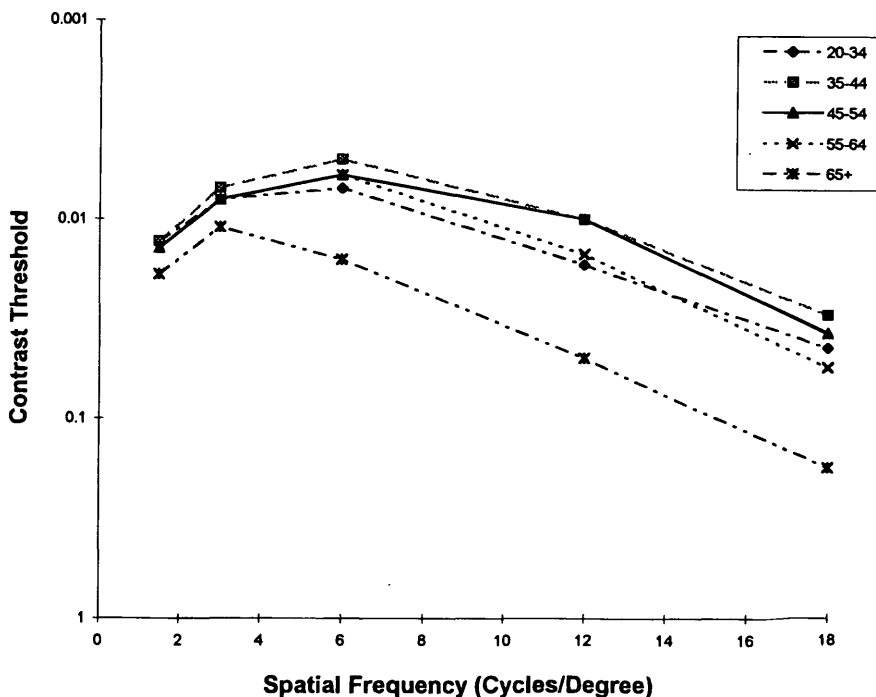


FIGURE 2 Contrast sensitivity test results for Phase I subjects (means for each group).

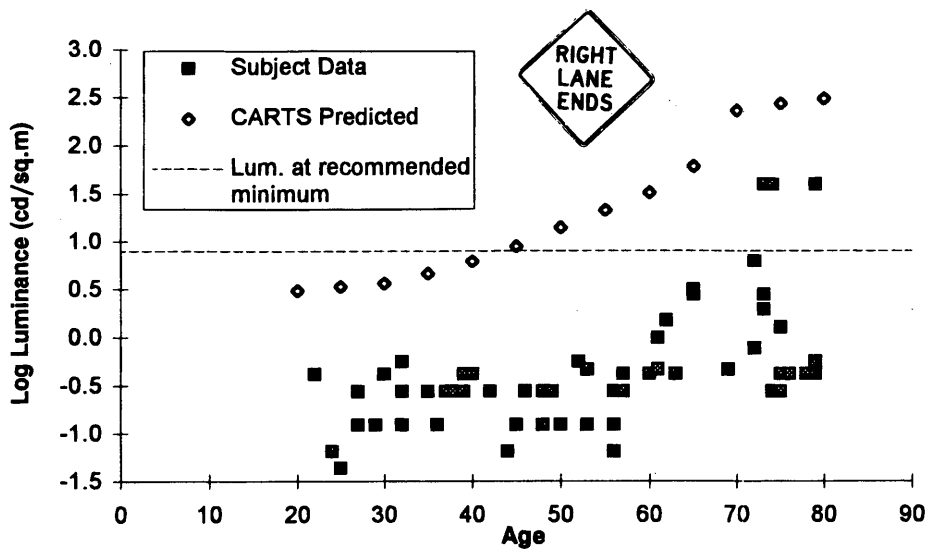


FIGURE 3 Luminance required to identify Right Lane Ends warning sign as a function of subject age (four subjects unable to read at highest luminance). Speed = 55 mph, sign width = 36 in.

nance (y-axis) for each sign tested. The full set of scatter plots are provided in the project report, but three representative plots are presented here to illustrate some of the typical features. The square data points represent the threshold luminance value for each subject.

Data for the text warning sign "right lane ends" (0.914 m, 48 kph) are shown in Figure 3. In general, older subjects required higher luminances than did the younger subjects to recognize the sign, and data variability tended to increase with age. These patterns were typical of the text warning signs tested.

Figure 4 shows data for the right turn arrow (0.72 m, 88 kph), which is typical of the bold symbol signs. Results were different from the text signs in that even older subjects were able to recognize the sign at low luminances.

Figure 5 is the scatter plot for a bicycle symbol (0.914 m, 88 kph) warning sign. This is categorized as a "fine symbol" sign and grouped with text warning signs in the Paniati and Mace tables. The

plot for this sign is similar to that of text signs in that older subjects tended to require more light than did the younger subjects to recognize it. There were a number of cases in which a subject failed to correctly identify a sign even when it was shown at the highest luminance level. The number of subjects unable to read or recognize the sign is indicated on each of the scatter plots. Table 5 lists six different signs that were not recognized at the highest luminance level by five or more subjects. As can be seen, with the exception of the No Passing Zone sign, almost all of the subjects were in the 65+ age group. This points to a problem with the design of these signs that cannot be remedied by additional sign brightness. Instead, these signs need to be either redesigned or made larger to enable older drivers to resolve the level of detail needed for recognition.

Each scatter plot indicates values predicted by the CARTS model by the diamond-shaped data points. The CARTS model used was a recently modified version (July 1994) that correctly accounts for

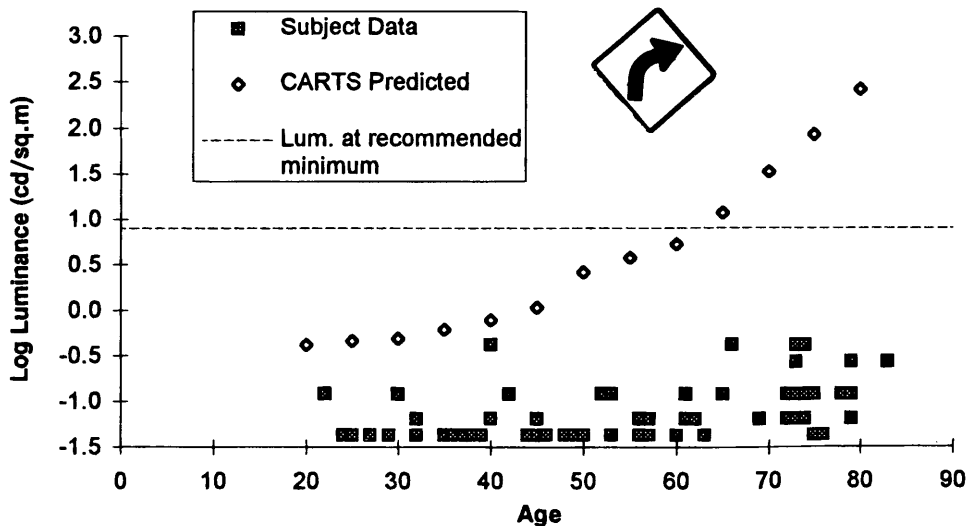


FIGURE 4 Luminance required to identify Curve symbol warning sign as a function of subject age. Speed = 55 mph, sign width = 30 in.

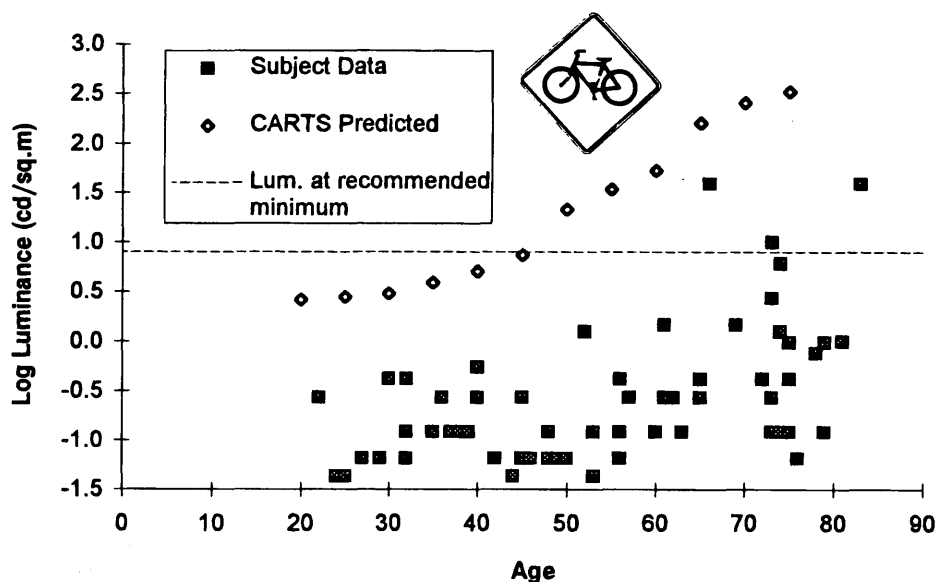


FIGURE 5 Luminance required to identify Bicycle symbol warning sign as a function of age. Speed = 55 mph, sign width = 30 in.

effects of two headlights on observation angle. All signs were assumed to follow MUTCD-specified heights and offsets. All signs were assumed to be right-mounted, with the exception of the No Passing Zone (left-mounted) and Keep Right (median placement) signs.

In most cases the experimental data fall well below the CARTS predicted values. More importantly, each plot also contains a horizontal line indicating the luminance value supplied by the candidate minimum R_a recommended by Paniati and Mace. For each plot, almost all the subject data fall below this line, indicating that most subjects tested would be accommodated by the minimum R_a values.

Although the scatter plots offer qualitative evidence that most test subjects would be accommodated by the candidate guidelines, a second level of analysis was necessary to estimate percent accommodated for the driving population at large. Table 6 indicates the age distribution of the test sample versus the U.S. driving popula-

tion (4). The test sample was not reflective of the whole driver population because older drivers were purposely oversampled for the study.

To develop an unbiased estimate, hypothetical data for each age group were generated by randomly sampling data from a normal distribution having the same mean and standard deviation as the corresponding subject age group. A total of 100 hypothetical data points were generated, with the same age distribution as that of the whole driving public. This resulted in 39 hypothetical threshold luminance values generated for the age group 16 to 34, 22 values for the 35 to 44 age group, 14 for the 45 to 54 age group, 11 for the 55 to 64 age group, and 14 for the 65 and older age group. For cases where an age group included some percentage of subjects who could not recognize the sign at maximum luminance, the number of data points generated for that age group was reduced proportionately.

TABLE 5 Stimuli That Five or More Subjects Were Unable to Recognize Even At Highest Luminance Level Tested

Sign	Size Width-m	Speed mph	Number of Subjects Tested Unable to Recognize Sign	Number of Older Subjects Unable to Recognize Sign
Narrow Bridge	.76	88	5	5
Right Lane Ends	.76	88	5	5
Do Not Enter (Phase 1)	.76	88	16	12
Corning 12 (D2-1)	1.27	88	8	8
No Passing Zone	1.22	88	22	11
Yield	.76	88	6	5
Yield	.76	48	6	6
Do Not Enter (Phase 2)	.76	88	12	8
Do Not Enter (Phase 2)	.76	48	5	4

TABLE 6 Age Distribution of Test Samples and U.S. Driving Population

Age Group	Percent of Test Sample (#/subjects)		Percent of U.S. Driving Population
	Phase I	Phase II	
16-34	15.9 (10)	22.2 (10)	39
35-44	15.9 (10)		22
45-54	15.9 (10)	22.2 (10)	14
55-64	15.9 (10)	22.2 (10)	11
65+	36.4 (10)	33.4 (15)	14
Totals	100.0 (63)	100.0 (45)	100

N for Phase I was 63 and for Phase II was 45.

This same procedure was used for each sign tested. To determine percent accommodated by candidate guideline values, the recommended R_a for a given sign was converted to a luminance value using the CARTS model. Tables 7 and 8 show the percent accommodated, that is, the percent of hypothetical data points falling below the candidate guideline luminance. As can be seen, the recommended R_a values would accommodate at least 85 percent of all drivers for all but two signs: the No Passing Zone pennant (63 percent accommodated) and the Narrow Bridge sign (65 to 67 percent at 88 kph).

The problem that subjects had with the No Passing Zone pennant was likely related to lack of familiarity. Study subjects were from Northern Virginia and do most of their driving in suburban areas where the pennant is not used. Even so, given the problems with this sign and the fact that it is left-mounted (thus receiving less light from vehicle headlamps), consideration should be given to increasing the required R_a for this sign.

It is more difficult to account for the lower percentages accommodated for the Narrow Bridge sign (at 88 kph). Values were only 65 percent accommodated for the 30-in. sign and 67 percent for the 36 in. sign. This was lower than the three-line text sign Right Lane

Ends (which accommodated 90 and 92 percent for the corresponding sizes at 88 kph). Perhaps the difference was because of the word length or lack of familiarity with the sign message.

A third level of analysis was completed in which the experimental data were used to calculate the retroreflectance that would be required to accommodate three levels (67, 85, and 95 percent) of the driving population. Tables 9 and 10 contain these data. Those signs requiring more light than the recommended retroreflectance values supply are highlighted. At the 67 percent accommodated level, only one sign (Narrow Bridge, 30 in., 55 mph) requires a higher R_a than the recommended value. At the 85 percent level, only two signs would require a higher R_a than was recommended (Narrow Bridge and Deer warning signs). Finally, for 95 percent accommodation, the number of signs requiring more retroreflectance than the recommended R_a increases to 9. In addition, there were four signs for which the 95 percentile level could not be accommodated.

A subset of the preceding data was used to examine the effects of sign size and traffic speed on required retroreflectivity. These were two of the critical variables used by Paniati and Mace in constructing the framework for their minimum retroreflectivity requirement

TABLE 7 Percent Accommodated: Black-on-Yellow and Black-on-Orange Warning Signs

Sign	Sign Type		Speed/Sign Size				
			55 mph (88kph)			30 mph (48 kph)	
	Text	Symbol	1.2 m (48 in)	.92 m (36 in)	.77 m (30 in)	.92 m (36 in)	.77 m (30 in)
Right Lane Ends	x			92	90	92	93
Narrow Bridge	x			67	65		95
No Passing Zone	x		63				
Merge		x			100		
Right Curve		x			100		100
Right Intersection		x		100	100	100	100
Pedestrian Crossing		x			99		100
Bicycle Crossing		x		97	97	99	99
Deer Crossing		x			100		
Slippery When Wet		x			99		
Road Work 1 Mile	x			85			
Worker		x		91			
Flagger		x		100			

TABLE 8 Percent Accommodated for White-on-Red Regulatory Signs, Black- or Black-on-Red-on-White Regulatory and Guide Signs, and White-on-Green Signs

Sign	Speed/Sign Size			
	55 mph (88 kph)		30 mph (48 kph)	
	.92 m (36 in)	.77 m (30 in)	.92 m (36 in)	.77 m (30 in)
Yield		94		95
Do Not Enter		90		92
Stop	98	98	99	100
	.92 m (36 in)	.61 m (24 in)	.92 m (36 in)	.61 m (24 in)
One Way	94		95	
Speed Limit 50		88		
Keep Right		99		
Route Marker		99		
Reduced Speed Ahead		89		
Do Not Pass		92		
No Right Turn		95		
Corning (D2-1)		97		97
Gravity/Creston (D2-2)		91		97

TABLE 9 R_s Required To Accommodate 67, 85, and 95 Percent of Drivers for Black-on-Yellow or Black-on-Orange Signs

Sign	Size (m)	Speed (km/h)	Minimum R_s (Paniati and Mace)	R_s to Accommodate		
				67%	85%	95%
Right Lane Ends	.914	88	30	2	2	66
	.914	48	30	2	3	65
	.762	88	45	9	24	100
	.762	48	45	3	7	90
Narrow Bridge	.914	88	30	30	71	92
	.762	88	45	48	70	108
	.762	48	45	4	7	55
No Passing Zone	1.22	88	20	24	*	*
Merge	.762	88	45	<1	1.5	5.5
Right Curve	.762	88	25	<1	<1	1
	.762	48	25	<1	<1	<1
Right Intersection	.914	88	20	<1	<1	<1
	.914	48	25	<1	<1	<1
	.762	88	25	<1	<1	<1
	.762	48	25	<1	<1	<1
Pedestrian Crossing	.762	88	45	<1	<1	<1
	.762	48	45	<1	<1	2
Bicycle Crossing	.914	88	30	<1	<1	10
	.914	48	30	<1	1	8
	.762	88	30	<1	2	25
	.762	48	45	<1	2	17
Deer Crossing	.762	88	45	6	7	20
Slippery When Wet	.762	88	45	<1	2	2
Road Work 1 Mile	.914	88	30	4	27	94
Worker	.914	88	30	1	3	53
Flagger	.914	88	30	<1	<1	<1

* Indicated percentage level cannot be accommodated.

Shaded cells indicate values exceeding recommended minimums.

TABLE 10 R_a Required To Accommodate 67, 85, and 95 Percent of Drivers for Regulatory and Guide Signs

Sign	Size (m)	Speed (km/h)	Minimum R_a (Paniati and Mace)	R_a to Accommodate		
				67%	85%	95%
White-on-Red Regulatory						
Yield	.762	88	70	<1	2	*
	.762	48	40	<1	<1	*
Do Not Enter	.762	88	70	12	38	*
	.762	48	40	2	10	55
Stop	.914	88	60	2	7	34
	.914	48	35	<1	<1	8
	.762	88	70	6	10	26
	.762	48	20	<1	<1	<1
Black or Black-and-Red-On-White Regulatory and Guide:						
One Way	.914	88	35	2	11	43
	.914	48	20	1	5	19
Keep Right	.61	88	50	<1	<1	14
	.61	48	35	<1	<1	3
Route Marker	.61	88	50	<1	2	11
Reduced Speed Ahead	.61	88	50	11	21	*
Do Not Pass	.61	88	50	5	13	124
	.61	48	50	2	6	43
Speed Limit 50	.61	88	50	<1	9	98
No Right Turn	.61	88	50	3	4	49
	.61	48	35	<1	1	54
White-on-Green Guide Signs						
Coming 12 (Destination)	1.27	88	35	2	7	25
	1.27	48	25	<1	1	16
Gravity/Creston (Destination)	1.52	88	35	2	21	51
	1.52	48	25	<1	2	18

* Indicated percentage level cannot be accommodated.

Shaded cells indicate values exceeding recommended minimums.

tables. Because only five signs were tested at two different sizes, no definitive conclusions could be drawn about the effect of sign size. However, as indicated in Table 11, there was a fairly consistent decrease in the required retroreflectivity values for the larger signs. This is particularly apparent for signs with text (Narrow Bridge, Right Lane Ends) and fine symbol (Bicycle) messages.

The effects of speed are also evident in the results, although less consistent than for sign size. In the minimum retroreflectivity tables developed by Paniati and Mace, speed is included as a critical variable for all sign types except for warning signs. Because warning

signs involve little reading time and are placed well in advance of the hazard, speed has only a small effect on the MRVD for these signs and thus was not expected to affect the required retroreflectivity. The results for warning signs, indicated in Table 12, generally support this conclusion, with the exception of the Narrow Bridge sign. For the regulatory and guide signs, longer MRVDs are required at higher speeds; therefore, speed was expected to affect the required retroreflectivity. This is generally confirmed by data in Table 12. Study results (Table 12) can be compared with results of the Paniati and Mace study (see Table 1).

TABLE 11 Effect of Sign Size on Required Retroreflectivity

Sign (speed)	Required R_a for 95 % Accommodation	
	.762 m Width	.914 m Width
Right Intersection (88 km/h)	<1	<1
Narrow Bridge (88 km/h)	108	92
Right Lane Ends (88 km/h)	100	68
Right Lane Ends (48 km/h)	90	65
Bicycle Crossing (88 km/h)	25	10
Bicycle Crossing (48 km/h)	17	8
Stop (88 km/h)	26	34
Stop (48 km/h)	<1	8

TABLE 12 Effect of Speed on Required Retroreflectivity for Warning Signs and on Regulatory and Guide Signs

Sign (size)	Required R_a for 95% Accommodation	
	48 km/h	88 km/h
Right Curve (.762 m)	<1	1
Right Intersection (.762 m)	<1	<1
Right Intersection (.914 m)	<1	<1
Narrow Bridge (.762 m)	55	108
Right Lane Ends (.762 m)	90	100
Right Lane Ends (.914 m)	65	68
Bicycle Crossing (.762 m)	17	25
Bicycle Crossing (.914 m)	8	10
Pedestrian Crossing (.762 m)	2	<1
Do Not Pass (.61 m)	43	124
Keep Right (.61 m)	3	14
No Right Turn (.61 m)	64	49
One Way (.914 m)	19	43
Stop (.762 m)	<1	26
Stop (.914 m)	8	34
Do Not Enter (.76 m)	46	N/A
Coming - D2-1 (1.27 m)	19	25
Gravity/Creston - D2-2 (1.52 m)	18	51

CONCLUSIONS AND RECOMMENDATIONS

Analyses of the experimental data indicate that candidate minimum R_a values from the Paniati and Mace report are sufficient to accommodate a high percentage of drivers for all but a few of the signs tested. The project report did not recommend a percentile value, although the authors were confident that the recommended tabular values would provide a "reasonable level of driver accommodation for most driving situations." In view of the analysis provided in this paper, it appears that the percent of drivers accommodated by the recommended retroreflectivity values is comfortably above the 85th percentile level. The recommended retroreflectivity values also exceed the values suggested by Sivak and Olson (5) or Jenkins and Gennouai (6).

For the bold symbol signs tested, legibility thresholds were well below the recommended minimum values. Lower minimums are not recommended, however, because even though the signs are legible at dim levels, they would not be sufficiently conspicuous. (In fact, the candidate minimum R_a values for these signs were based on conspicuity requirements rather than on legibility requirements.)

Additional research is needed on the effect of sign size on minimum retroreflectivity requirements. For the limited number of signs tested at two sizes in this study, there seems to be a fairly consistent improvement in threshold values for the larger signs. Future research should examine a wider range of signs and sizes.

Finally, as already noted, certain signs did not perform as well as most, especially for older subjects. Additional research is recommended to determine the nature of the problems with these signs (and others like them). This research should evaluate whether

changes in sign design or in recommended sign size, or both, would produce the needed improvement.

ACKNOWLEDGMENTS

Funding support for this study was provided by FHWA's Office of Research and Development under an Intergovernmental Personnel Act contract with Iowa State University. The study was performed at the Turner-Fairbank Highway Research Center in McLean, Virginia.

REFERENCES

1. *Manual on Uniform Traffic Control Devices*. U.S. Department of Transportation, Washington, D.C., 1988.
2. Paniati, J. F., and D. J. Mace. *Minimum Retroreflectivity Requirements for Traffic Signs*. FHWA Report FHWA-RD-93-077, 1993.
3. *Vistech Application Manual*. Vistech Consultants, Inc., Dayton, Ohio, 1987.
4. *Highway Statistics*. U.S. Department of Transportation, Washington, D.C., 1991.
5. Sivak, M., and P. L. Olson. *Optimal and Replacement Luminance of Traffic Signs: A Review of Applied Legibility Research*. Final Report UMTRI 1-37. The University of Michigan Transportation Research Institute, Ann Arbor, 1983.
6. Jenkins, S. E., and F. R. Gennouai. Terminal Value of Road Signs. *CIE Proc.*, Vol. 22, 1991.

Publication of this paper sponsored by Committee on Traffic Control Devices.

Detectability of Pavement Markings Under Stationary and Dynamic Conditions as a Function of Retroreflective Brightness

GREGORY F. JACOBS, THOMAS P. HEDBLUM, T. IAN BRADSHAW, NEIL A. HODSON,
AND ROBERT L. AUSTIN

With the availability of pavement marking systems having varying reflective performance, the brightness a road surface marking must have to provide safe and effective guidance has remained undefined. This work studied minimum reflective brightness needed for a pavement marking to be visible to a driver as a function of distance of the marking from a vehicle. Six pavement marking products having a wide range of retroreflective brightness performance were viewed as isolated center skip lines from stationary vehicles at distances from 30 to 250 m in a dark rural setting. Product detectability for each viewer/marking combination was determined. Also, seven pavement marking products were viewed from moving vehicles with a driver approach speed of 24 kph. Detection distances for each driver/marking combination were determined. Retroreflective brightness of the products as a function of distance was measured at geometries corresponding to the vehicle-driver distances of the experiment. Detectability of pavement markings depends on the viewing conditions. A correlation could be seen between detectability of pavement markings and product brightness and viewing distance. The nature of this correlation was different when the experiment was changed from a stationary viewing to one with a moving vehicle with shorter detectability distances for the same marking in a moving vehicle.

There has long been interest in the description of the minimum brightness requirements for retroreflective pavement markings (1-3). Recently that interest has been renewed (4,5). It has been shown that photometric measurements of pavement marking brightness made under geometric conditions approximating those of driver visual observations at a range of viewing distances correlate well with driver visual perception (5,6).

With the availability of pavement marking systems having varying reflective performance, the retroreflective brightness needed for a road surface marking to provide safe and effective guidance has remained undefined. A better understanding of the minimum reflective brightness for a pavement marking to be visible to a driver as a function of distance of the marking from a vehicle was needed. The approach in this work involved the determination of pavement marking detectability as a function of distance and the coefficient of retroreflected luminance at the distances of detection.

EXPERIMENTAL APPROACHES

Two different viewing experiments were conducted to assess minimum brightness for pavement marking detectability. In the first

experiment, drivers viewed different pavement markings at a fixed set of distances from a stationary vehicle. In the second study, drivers approached pavement markings in a moving vehicle and the marking detectability distance was noted.

Night viewings were held on two consecutive nights in the summer of 1993. A test roadway with black asphalt pavement in a dark rural setting was used. Tests began after dark at about 10:00 p.m. The sky was dark, overcast, and moonless. Samples were illuminated with standard low-beam headlamps. The vehicle type used in the viewings was a 1993 Ford Taurus 4-door sedan.

Retroreflective properties of the marking materials were characterized before the viewing experiments to ensure that the selection of test samples represented a wide range of retroreflective performance. The reflective brightness of the materials at each detection distance was calculated from the photometric data.

Photometric Measurements

Retroreflectivity of the test pavement markings was measured in a laboratory photometric range similarly to ASTM D 4061-89 using actual optical geometries calculated to correspond to the night viewing conditions as described by Hedblom et al. (5). For this experiment the measurement was simplified by using a two-dimensional geometry. The presentation and orientation angles were set at 0 and -180 degrees, respectively, and the headlamp illumination, marking, and driver eye position were all in the same plane.

Measurement geometries were calculated for drivers in a 1993 Ford Taurus for distances from 30.5 to 167.6 m from vehicle to center line target for both left and right headlights. Table 1 shows the geometries at which the coefficient of retroreflected luminance, R_L , was measured.

Brightness was measured at each geometry for seven pavement marking products used in the night viewing experiments. These measurements are presented graphically as a function of distance in Figure 1 for the driver-left headlight-two-dimensional geometry.

Night Viewings

A set of 23 driver viewers and a 1993 Ford Taurus 4-door sedan were assembled for the stationary viewings. Three automobiles (all 1993 Ford Taurus sedans) and 19 observers were used for the dynamic viewings (moving vehicle). All vehicle headlights were aligned before the viewing.

TABLE 1 Simplified Two-Dimensional Geometries as a Function of Distance for Left and Right Headlights

Distance (m)	Angles in Degrees for:			
	Left Headlight		Right Headlight	
	Entrance	Observation	Entrance	Observation
30.5	88.6	0.95	88.6	2
45.7	89.1	0.67	89.1	1.86
50.0	89.2	0.63	89.2	1.72
61.0	89.3	0.52	89.3	1.37
76.2	89.5	0.42	89.5	1.08
79.9	89.5	0.4	89.5	1.04
91.4	89.6	0.35	89.6	0.9
106.7	89.6	0.31	89.6	0.76
121.9	89.7	0.27	89.7	0.67
137.2	89.7	0.24	89.7	0.59
152.4	89.7	0.21	89.7	0.53
167.6	89.8	0.2	89.8	0.48

All viewers held valid driver's licenses from the state of Minnesota or Wisconsin and most had "good" vision. Four of the 23 viewers were women. Six were 50 to 60 years old and eight were under 30. Eight of the observers wore corrective lenses. Visual acuity of the test subjects was measured on an orthorater using the Snellen test. Comparison of the test subject data with the general population (7) is presented in Table 2.

Stationary Experiment

Pavement marking samples 0.1 m wide by 3.0 m long were prepared for viewing. Each sample of pavement marking was applied to alu-

minum panels 0.2 cm thick of the same dimension with the leading edge of the aluminum panel masked with black colored matte finished tape. The samples were viewed on top of a viewing table 0.3 m wide by 3.2 m long with a matte black surface finish. The table stood 3.8 cm above the road surface. The function of the table was to keep the samples optically flat and level.

The samples were viewed at distances of 30, 50, 80, 120, 160, 200, and 250 m from the front of the vehicle to the leading edge of the marking. Markings were presented as isolated centerlines 3.7 m from the right edge of the road. Markings were viewed from the driver position of a stationary vehicle parked centered in the lane between the centerline and edge of the road. All other markings on the road surface were obliterated for the course of the experiment.

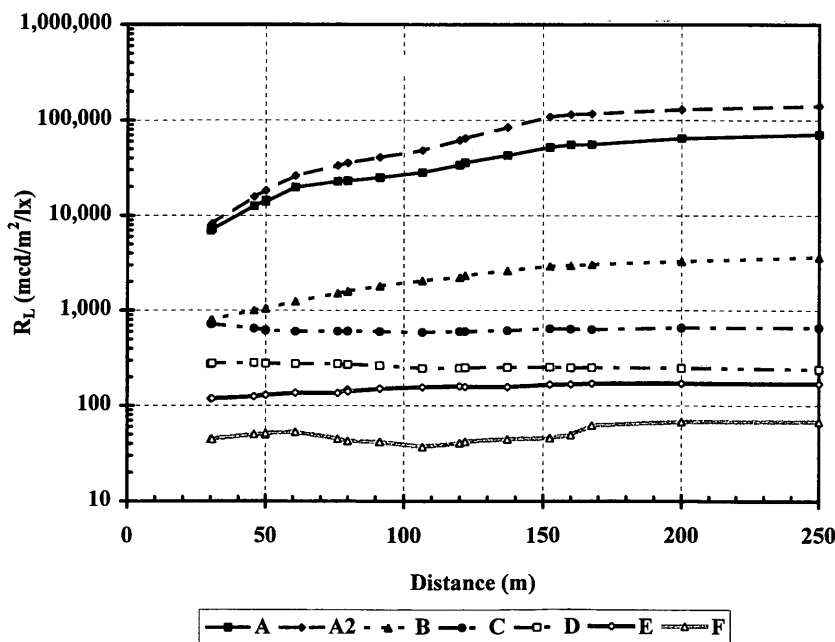


FIGURE 1 Coefficient of retroreflected luminance, R_L , with distance for seven marking products measured for distances of 30 to 250 m using a two-dimensional left headlight geometry.

TABLE 2 Comparison of Viewers to Standard Population

Best Binocular Visual Acuity with Corrected Lenses

	% of Population below Visual Acuity			
	20/20	20/25	20/30	20/40
	Experiment	37.5	18.8	6.3
U.S. 1977 (7)	26.8	12.9	6.9	3.5

Six distinctly different white preformed pavement marking products (A, B, C, D, E, and F) were tested representing a wide range of retroreflective characteristics as indicated in Figure 1. The materials included experimental products designed for this work having higher and lower retroreflectivities than those normally commercially available to extend the range of the experiment.

Samples were viewed one at a time at each distance. A replicate of at least one of the six samples was included at each distance. A blank of either no sample present or one that had not been visible to any of the viewers at a shorter distance was presented at each distance. Each distance had its own randomized sample presentation order.

Individual samples were installed on the top of the viewing table and covered with a black cloth. The viewers then turned on the vehicle headlights (low beam) and the test sample was exposed for 2 sec. The sample was then covered and the headlights extinguished. After viewing the test area for 2 sec, each subject was asked to write down whether a sample was visible or not visible. For each product at each distance the number of positive sightings of samples and the number of presentations were counted. Table 3 shows the percent of positive sightings of samples for each product at each distance. Figure 2 shows the same data in graphic form for each product at each distance.

TABLE 3 Percentage of Positive Sightings of Pavement Marking Products with Distance Viewed under Stationary Conditions

distance (m)	Product						
	A	B	C	D	E	F	G
30	100	100	100	100	98	96	0
50	100	100	97	91	91	87	4
80	100	91	96	83	54	13	13
120	92	96	33	22	20	13	0
160	87	39	2	0	4	0	8
200	91	30	0	0	0	0	0
250	52	0	0	0	0	0	0

Dynamic Experiment

As in the stationary viewing experiment, pavement marking samples 0.1 m wide by 3.0 m long were prepared for viewing and mounted on top of a viewing table (described earlier) for each viewing run for each sample.

Pavement markings were viewed one at a time as isolated center skip lines by subjects driving a Ford Taurus sedan traveling along a straight section of test road. Samples were placed at center line locations randomly within a 70-m section of the test roadway. Ambient conditions were dark overcast, moonless sky, rural setting with black asphalt pavement as described above.

Seven different pavement marking samples were viewed in the dynamic experiment. Photometric data for the seven samples as a function of distance are indicated in Figure 1. A blank in which no sample was present on the viewing table was also included.

The drivers approached the marking at a speed of 24 kph with low beam headlights illuminated. When drivers decided that they had detected the pavement marking, a passenger in the vehicle was

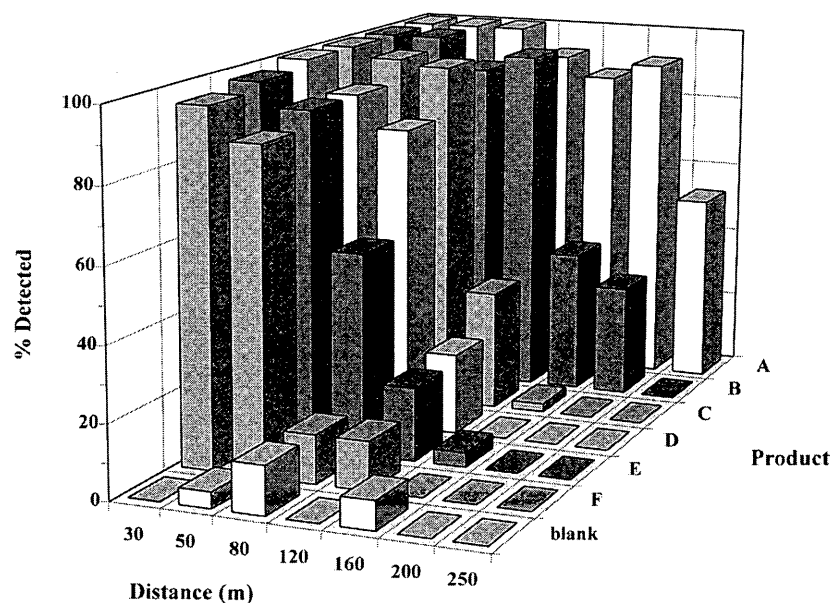


FIGURE 2 Percentage of positive sightings of pavement marking products with distance viewed under stationary conditions.

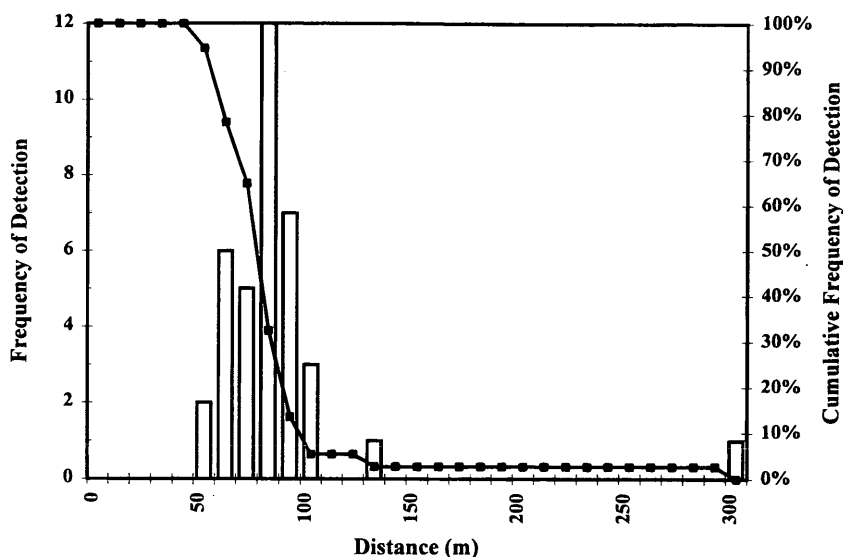


FIGURE 3 Detection distances of Product C under dynamic conditions.

informed and a reflectorized bean bag was immediately dropped from the moving vehicle. Workers along the side of the test roadway retrieved the bean bag and measured the distance from the car to the marking at the time of detection. Detection distances for Product C are shown in histogram form in Figure 3. Table 4 shows detection distance distributions for all seven products.

RESULTS AND DISCUSSION

Age, gender, and the use of corrective lenses by the observers had no distinguishably consistent effect within the sample of observers used in this study. The vision of the test subjects was not different from that estimated for an average population of drivers in the United States (see Table 2). In the dynamic experiment, any effects caused by the three different test vehicles were not distinguishable from the observer variability.

Measurement

From the photometric measurements made at geometries corresponding to distances from 30 to 167 m, reflectivities for intermediate distances were interpolated. Reflectivities at shorter and longer distances were approximated by graphic extrapolation of the available data set. A graph of the extrapolated R_L data is shown in Figure 4.

Stationary Experiment

The distribution of marking detectability as a function of viewer/target distance and product retroreflective brightness was examined. Figure 2 presents the percent of positive sightings of each product at each distance. Figure 5 shows the coefficient of retroreflected luminance, R_L (mcd/m²/lx) for each product at each distance measured using a left-headlight, two-dimensional geometry. A comparison of Figures 2 and 5 shows that although R_L is maintained, and in some cases actually increased with viewing distance, the detectability of a given marking material diminished at greater distances.

TABLE 4 Experimental Detection Distances in Meters of Pavement Markings Products Viewed Under Dynamic Conditions at 24 kph

Product						
A2	A	B	C	D	E	F
99.1	67.1	44.2	45.7	33.5	33.5	12.2
146.3	111.3	83.8	45.7	44.2	44.2	13.7
149.4	114.3	89.9	51.8	53.3	53.3	18.3
163.1	115.8	91.4	53.3	53.3	53.3	19.8
184.4	118.9	100.6	54.9	54.9	54.9	27.4
184.4	118.9	100.6	57.9	54.9	54.9	30.5
211.8	121.9	103.6	57.9	56.4	56.4	30.5
221.0	125.0	105.2	57.9	61.0	61.0	32.0
225.6	134.1	108.2	62.5	65.5	65.5	33.5
246.9	143.3	121.9	64.0	67.1	67.1	44.2
248.4	146.3	125.0	64.0	67.1	67.1	50.3
262.1	147.8	128.0	68.6	70.1	70.1	51.8
285.0	149.4	128.0	68.6	70.1	70.1	53.3
286.5	152.4	131.1	70.1	71.6	71.6	56.4
298.7	152.4	134.1	71.6	82.3	82.3	59.4
420.6	153.9	134.1	71.6	88.4	88.4	64.0
423.7	158.5	140.2	71.6	93.0	93.0	64.0
975.4	173.7	144.8	71.6	99.1	99.1	64.0
		149.4	71.6	99.1	99.1	
			76.2			
			76.2			
			76.2			
			76.2			
			76.2			
			77.7			
			80.8			
			82.3			
			83.8			
			85.3			
			85.3			
			88.4			
			88.4			
			94.5			
			94.5			
			96.0			
			125.0			
			298.7			

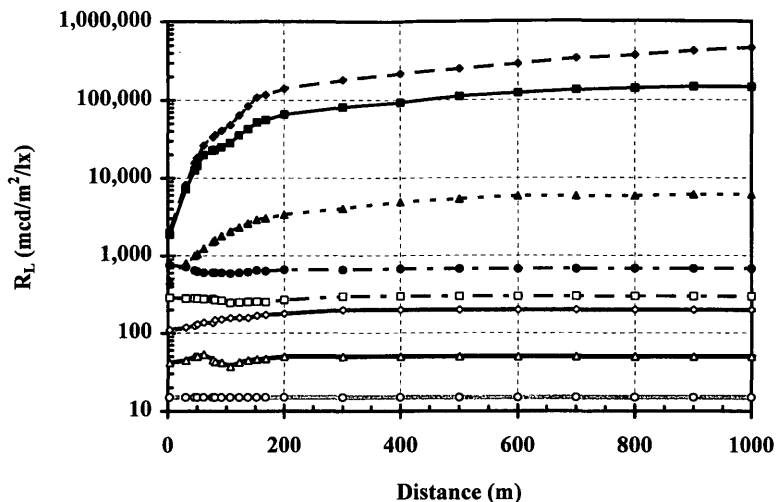


FIGURE 4 Coefficient of retroreflected luminance, R_L , with distance for seven marking products extrapolated to 1,000 m.

Figure 6 shows (a) a three-dimensional contour plot of the percent of positive sightings mapped onto brightness R_L and distance and (b) a projection contour viewing the surface from directly above the brightness-distance plane. The contours on the surface represent 5th percentile intervals of marking detectability. For example, the contour line corresponding to the 75th percentile means that at the set of brightnesses and distances along this curve, 75 percent of the observers could see the marking and 25 percent of them could not see the marking. As brightness of a marking is increased, its detectability improves. For a marking of given luminance, detectability improves at shorter distances.

Relations presented in a CIE publication (8) predicted the visibility distance of road markings having a given coefficient of retroreflected luminance. The measurement geometry of R_L is unclear from the text. For the work presented here, R_L was measured in the laboratory at geometries corresponding to the actual viewing conditions of the experiment.

Figure 7 presents the 5th, 25th, 50th, 75th, and 95th percentiles of marking detectability interpolated from the data of the stationary experiment in a 2-dimensional graph of visibility distance versus R_L . This graph is similar in format to that of Figure 2.2 of the CIE publication (9). Included in Figure 7 are data taken from the curve in the CIE publication for comparison with the data in this paper. The CIE curve covers a much narrower range of R_L values. It falls close to the 75th and 50th percentile detectability curves for the stationary experiment and has similar curvature to the percentile contours obtained from this work.

Dynamic Experiment

The distribution of marking detectability as a function of viewer/target distance and product retroreflected brightness was examined. Figure 8 is an example of a plot of product brightness with distance

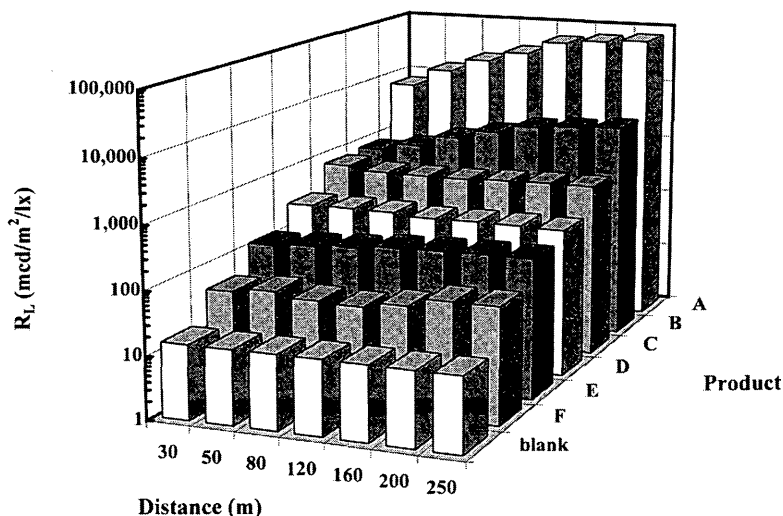


FIGURE 5 Coefficient of retroreflected luminance, R_L , for each product and distance in the stationary viewing experiment.

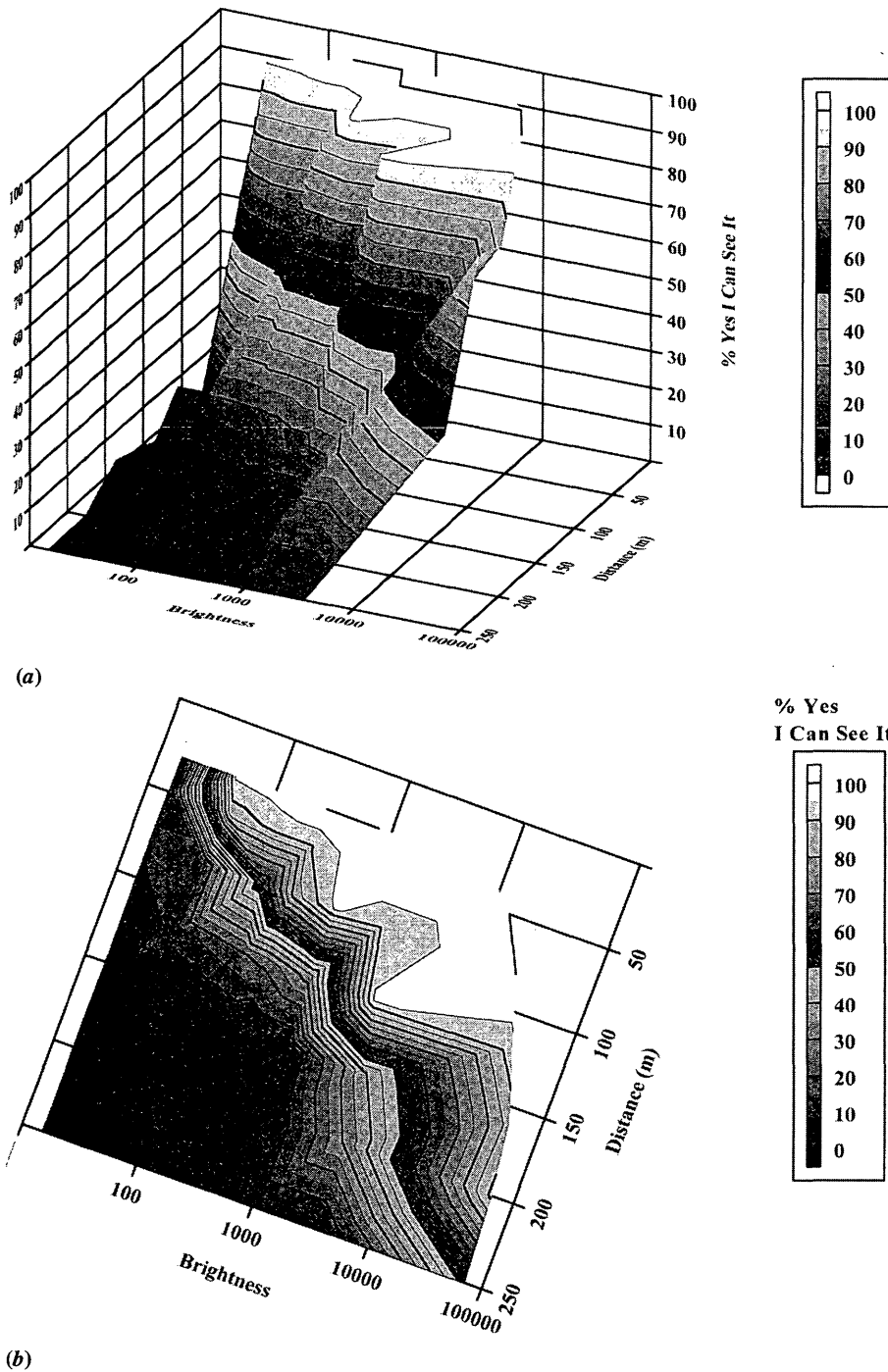


FIGURE 6 (a) Three-dimensional contour of the percentage of positive sightings of pavement marking products viewed under stationary conditions mapped onto coefficient of retroreflected luminance, R_L , and distance; (b) two-dimension projection of the same contour viewed from directly above the R_L distance plane.

for each observer's detection of Product C. The points on the graph correspond to each detection of C by the various observers at different distances and the brightness of the marking at each set of viewing conditions. This can be obtained through comparison of the histogram for Product C in Figure 3 and the extrapolated R_L values from Figure 4.

Figure 9 shows the cumulative frequency of detection with distance from 0 to 250 m for each product in the dynamic experiment.

These data were used to calculate the 5th, 25th, 50th, 75th, and 95th percentiles of marking detectability with distance and brightness for the dynamic data. These curves are presented in a plot of visibility distance versus coefficient of retroreflected luminance in Figure 10.

Comparison of Figures 7 and 10 shows that the detectability contours for the dynamic experiment are shifted to shorter-visibility distances than for the stationary experiment. Also this shift is not linear. The shift for the less-bright samples appears to be about

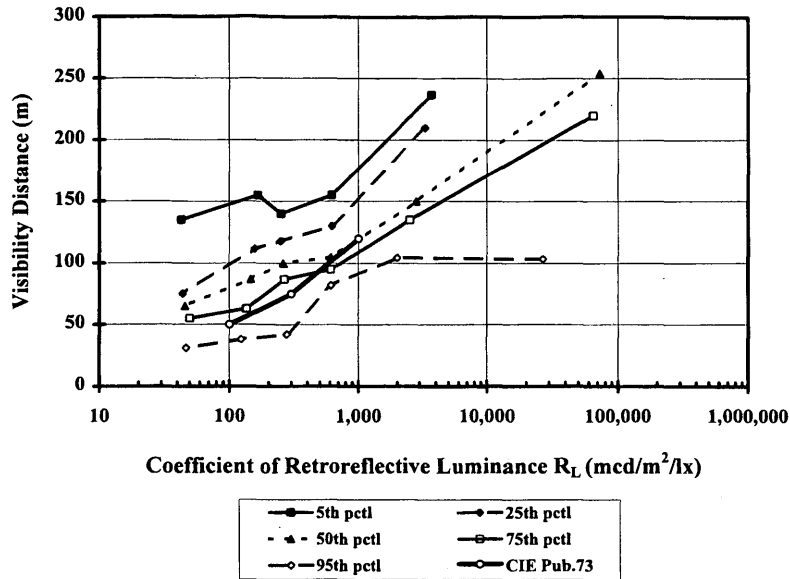


FIGURE 7 Marking visibility distance (5th, 25th, 50th, 75th, and 95th) percentiles with R_L under stationary viewing conditions.

20 m for the moving vehicle experiment relative to the stationary experiment. For brighter materials, for example, in the 10,000 to 100,000 $mcd/m^2/lx$ range, the shift could be as much as 100 m or more.

The curvature of the contours of detectability appears to be different for stationary compared with dynamic conditions. There was a stronger increase in detection distance with increased brightness for the stationary experiment than for the dynamic experiment. From this limited data set, there appears to be a decrease in visibility distance on the order of 40 percent changing from a stationary vehicle to one moving at about 24 kph.

Assuming a vehicle traveling speed of 24 kph with an estimated delay time of about 1 sec for driver reaction time, statement by dri-

ver to passenger and dropping of the reflective bean bag marker by the passenger, and falling to the ground and an inertial roll of the marker of less than about 1.5 m, a lag distance based solely on mechanical aspects of the experiment would be 11 m or less. The shift in detectability distance seems to be more complex than simple physical delay. In both the stationary and dynamic experiments, the observers were well trained to know approximately when and where to look to detect a marking. The complexity of the driving task at speeds as slow as 24 kph may be a contributor to this shift.

Figure 10 also includes the curve for the predicted visibility with distance from a CIE publication (9). The CIE prediction appears to cross more of the detectability contours for the dynamic experiment than for the stationary experiment. The CIE data are not consistent

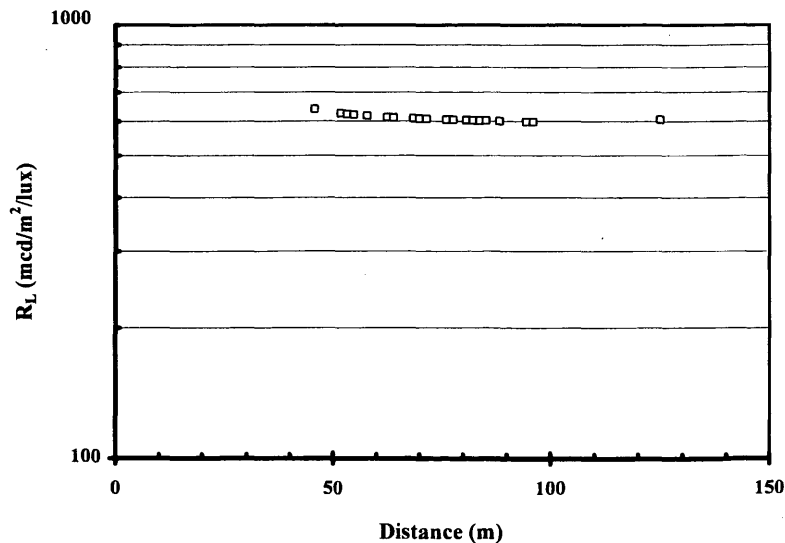


FIGURE 8 Product brightness with distance for each observer's detection of product C.

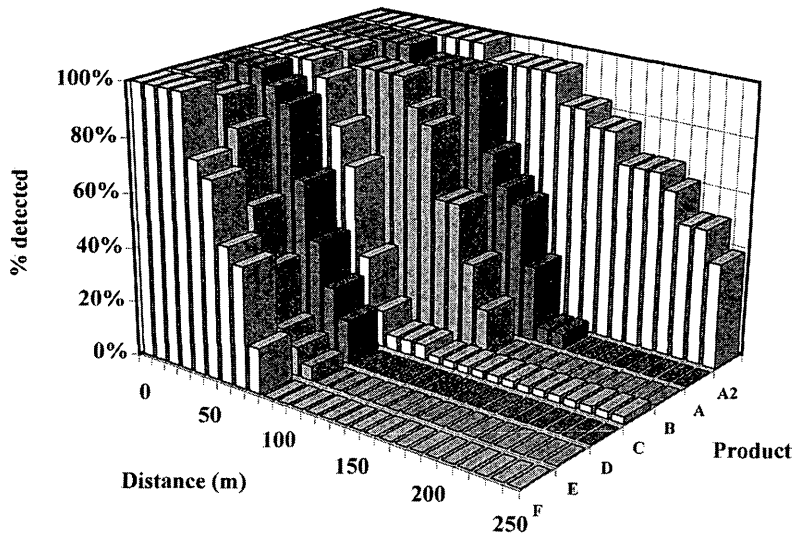


FIGURE 9 Cumulative frequency of detection for each product from 0 to 250 m for the dynamic viewing experiment.

with the dynamic portion of this work. This could be partially because of the difference in reflectivity measurement geometry. Perhaps, more importantly, it could be the result of the differences in detectability that occur when the observers are driving a moving vehicle.

Recent work in the area of pavement marking detection distances has also been done by Zwahlen and Schnell (4). Their work used a range of commercially available markings with different brightness performance. They did not have data available at the time for the coefficient of retroreflected luminance at geometries corresponding to their viewing conditions. Photometric measurements have been made for one of the products they used, and the data points for 5th, 25th, 50th, 75th, and 95th percentiles are included on the graph of visibility distance with coefficient of retroreflected luminance in Figure 10. With

the appropriate measures of R_L now available, it can be seen that their moving vehicle experiment at a similar speed agrees well with this work in describing effects of marking brightness on detection distance.

CONCLUSIONS

Measurement of the brightness of retroreflective markings at geometries corresponding to actual driver viewing conditions has provided a better understanding of minimum brightness requirements for detectability of pavement markings. As expected, brighter markings were detectable at greater distances from observer to marking in both stationary and dynamic viewing experiments.

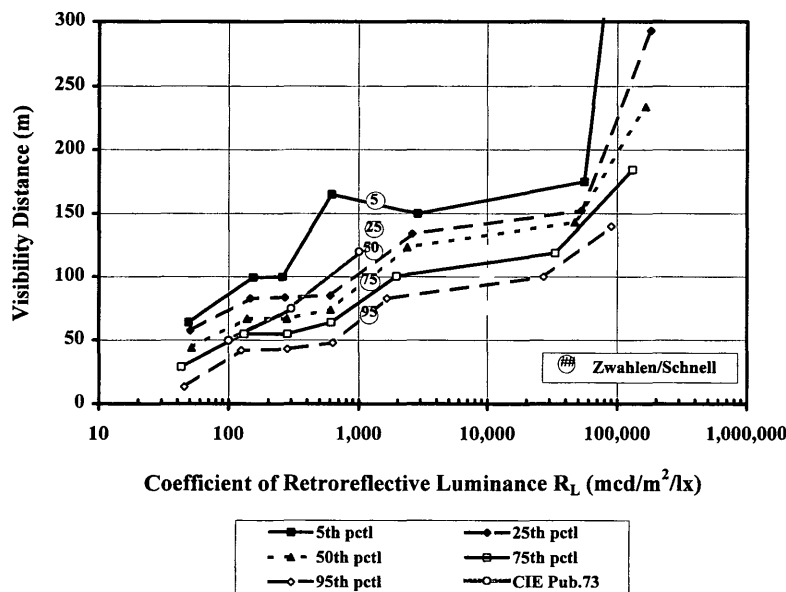


FIGURE 10 Percentiles of marking visibility distance (5th, 25th, 50th, 75th, and 95th) with R_L under dynamic viewing conditions.

Detectability of pavement markings depends on the viewing conditions. A correlation could be seen between detectability of pavement markings and product brightness and viewing distance. The nature of this correlation was different when the experiment was changed from a stationary viewing to viewing the same set of products from a moving vehicle. Both the detectability distances and the dependence of detectability on distance and brightness changed with the added complication of vehicle movement. A speed of as little as 24 kph was sufficient to significantly shift marking detectability to shorter distances.

Marking detectability also depends strongly on the viewers themselves. For example, the visibility distance for a marking with a value of R_L of about 120 mcd/m²/lx at 30 m ranged from less than 30 m to more than 160 m for the stationary experiment and from 20 to 95 m for the dynamic experiment. These ranges were obtained using trained viewers who knew approximately when and where to observe a specific type of object.

Minimum brightness requirements for detectability of pavement markings in actual road use are subject to the safety needs of the driving environment in question. Many factors, including vehicle speed, the background surround and contrast, and the consequences of not being able to detect a road surface marking need to be considered when defining such limits for a particular driving scenario. More effort will be required to fully understand these effects on marking detectability to define meaningful minimum brightness levels.

REFERENCES

1. Ethen, J. L., and H. L. Woltman. Minimum Retroreflectance for Night-time Visibility of Pavement Markings. In *Transportation Research Record 1093*, TRB, National Research Council, Washington, D.C., 1986, pp. 43-47.
2. Serres, A.-M. The Visibility of Highway Markings (in French) *Lux*, Vol. 112, April 1981.
3. Graham, G. R., and L. E. King. Retroreflectivity Requirements for Pavement Markings. In *Transportation Research Record 1316*, TRB, National Research Council, Washington, D.C., 1991, pp. 18-23.
4. Zwahlen, H. T., and T. Schnell. Visibility of New Pavement Markings at Night Under Low Beam Illumination. Presented at 73rd Annual Meeting of the Transportation Research Board, Washington, D.C., Jan. 1994.
5. Hedblom, T. P., T. I. Bradshaw, D. C. May, G. F. Jacobs, T. J. Szczech, N. A. Hodson, and R. L. Austin. Correlation of the Nighttime Visibility of Pavement Marking Tapes with Photometric Measurement. In *Transportation Research Record 1409*, TRB, National Research Council, Washington, D.C., 1994, pp. 69-75.
6. Harrington, T. L., and M. D. Johnson. An Improved Instrument for Measurement of Pavement Marking Reflective Performance. In *Bulletin 336*, HRB, National Research Council, Washington, D.C., 1962.
7. *Monocular Visual Acuity of Persons 4-74 Years in the United States, 1971-1972. Publication 201, Series II. U.S. Department of Health, Education, and Welfare, 1977.*
8. *Visual Aspects of Road Markings.* Joint technical report of CIE/PIARC. CIE Publication 73. Central Bureau of the CIE. Vienna, Austria, 1988.

Publication of this paper sponsored by Committee on Visibility.

Visibility of New Yellow Center Stripes as a Function of Obliteration

HELMUT T. ZWAHLEN, TORU HAGIWARA, AND THOMAS SCHNELL

Temporary center stripe pavement markings in newly resurfaced zones were selected to study driver visibility as a function of the degree of pavement marking obliteration. The Manual on Uniform Traffic Control Devices (MUTCD) specifies 0.1-m-wide retroreflective single dashed yellow stripes with a gap/stripe ratio of 10.98/1.22 m as minimum temporary center stripes in resurfaced zones. The study also investigated the begin and end detection distances of double-dashed (10.98/1.22m) 0.05-m-wide yellow retroreflective center stripes. Such thin double stripes could be used (same amount of material) to actually indicate to a driver whether the traveled section of the newly resurfaced road is a passing or no-passing section by using the double-dashed pattern as a coding mechanism. The center stripe pavement marking treatments were randomly obliterated by removing 0, 50, and 75 percent of the retroreflective material from the stripes. Overall, it is possible to conclude that severe obliteration reduces the begin and end detection distance to a considerable degree. However, using four times less material and the shortest specified stripe length (10.98/1.22 m) reduces, for example, the 85th percentile begin and end detection distances from about 53 to 30 m. Therefore, from a begin or end detection distance point of view, if the nonobliterated center-line pavement marking treatment provides barely adequate visibility performance it may not be possible to tolerate much obliteration at all (more than 5 to 10 percent before the visibility performance of the overall system (driver-vehicle-center stripe system) falls below the acceptable minimum safety level.

Several investigators (1,2) investigated the effects of roadway delineation visibility on driver steering performance in terms of lateral lane position standard deviation. The data for their model were collected in both an interactive driving simulator and an instrumented vehicle on the open highway. The collected experimental data were evaluated using a regression analysis to determine the functional relationship between a driver's steering performance and a number of delineation visibility factors including road-marking size and spacing, contrast with respect to the road surface, atmospheric scattering characteristics as a result of fog, snow, and ice, and the visibility range caused by headlight characteristics. The model uses Blackwell's threshold contrast data to evaluate the visibility of the markings. Allen also investigated the effects of delineation contrast on a driver's lateral lane position maintenance performance.

Harkey et al. (3) investigated the effect of various pavement-marking configurations on driver performance in work zones. The researchers used the following 0.1-m-wide white pavement-marking pattern types:

1. 0.6-m stripes with 11.58-m gaps,
2. 1.22-m stripes with 10.98-m gaps, and
3. 3-m stripes with 9.14-m gaps, including edge lines.

H. T. Zwahlen and T. Schnell, Human Factors and Ergonomics Laboratory, Department of Industrial and Systems Engineering, Ohio University, Athens, Ohio 45701-2979. T. Hagiwara, Traffic Engineering Laboratory, Department of Civil Engineering, Hokkaido University, Sapporo, Japan.

The first two configurations are commonly used for temporary pavement markings in work zones. These two configurations usually do not include edge lines when applied in pavement resurfacing work zones. The third configuration is the standard dashed pattern as specified in the Manual on Uniform Traffic Control Devices (MUTCD) (4). Because it is a permanent center line configuration, edge lines are present most of the time. It is highly questionable to introduce edge lines in a study dealing with nonpermanent markings, especially because the right edge line is considerably more conspicuous and therefore likely to mask the effect of the dashed center line because of the vehicle headlamp geometry (hot spot is 2 degrees to the right and 2 degrees down). The following performance measures were used as independent variables: lateral placement of the vehicle in the roadway; average vehicle speed within the test segment; average number of edge line and lane line encroachments per run; and number of erratic maneuvers. Harkey et al. (3) selected a 6.4-km-long experimental site with relatively mild horizontal and vertical curvature. Three sections with the previously described pavement-marking patterns were installed in the newly paved test site. It seems to be a questionable approach to investigate the effect of different pavement-marking patterns by installing them in subsequent sections of a highway. The observed effects might be influenced by the different road geometry and other environmental structures in the three sections. Harkey et al. (3) found that there were significant differences in the average running speeds between the Type 1 and the Type 3 patterns. In general, the speeds decreased as the marking length decreased. There was no significant difference between the two temporary pavement markings Types 1 and 2 with respect to lateral placement of the vehicle. There was a significant difference with respect to lateral placement of the vehicle between the two temporary markings (Types 1 and 2) and the full markings (Type 3). In their paper, Harkey et al. present a number of bar graphs that show graphically fairly large effects among the three patterns. However, the scale of the speed graph, the lateral position graph, and the lateral position variance graph is misleading because it does not start at 0. Primarily on the basis of the number of encroachments, the researchers conclude that it would be favorable to install the full (Type 3) pattern rather than the temporary Type 1 or Type 2 pattern in a temporary work zone. However, it appears that the observed average number of encroachments of 0.689 per 36 observed vehicles for the full pattern (Type 3) is hardly sufficient for a sound statistical analysis.

King and Graham (5) conducted a field experiment and a laboratory experiment to assess the retroreflectivity requirements of pavement markings. The field experiments consisted of objective retroreflectivity and luminance measurements (for one geometry only) to which the subjective responses of 59 observers were related. In the laboratory experiment only the luminances were measured and related to the subject responses. The field experiment

was conducted on an observation route of approximately 32 km, which included 20 test locations. For safety reasons the researchers decided to take the luminance and retroreflectivity measurements from the road shoulder. A small study, conducted in a dark parking lot, was used to relate the field data to the correct geometric conditions that would exist if the measurements were taken from the center of the lane. Conducting retroreflectivity measurements (for a selected geometry only) from the road shoulder seems to be a questionable approach. The subjects were to judge the adequacy of the presented pavement markings as follows:

- Less than adequate,
- Adequate, and
- More than adequate.

From the field study, King and Graham (5) found that all pavement markings having a coefficient of retroreflection greater than 93 mcd/m²/lx (at a selected single geometry) were judged as being adequate or more than adequate by over 90 percent of the observers. A regression analysis of the average subjective ratings revealed a logarithmic relationship with the measured coefficient of retroreflection. The subsequent laboratory experiment was used to evaluate simulated roadway markings of varied luminance. The experimental setup included a dark tunnel constructed of heavy cloth and a platform 0.91 by 1.82 m installed 0.76 m above the floor. The pavement markings were installed on the platform. Gray and black background colors were used to simulate Portland cement and asphalt road surfaces. A booth with a viewport was used to observe pavement-marking samples 1.82 m long and 2.54 cm wide (3M 5730 white and 3M 5731 yellow). King and Graham found that pavement-marking samples with a luminance greater than 0.38 cd/m² were judged as being adequate or more than adequate by over 90 percent of the observers. A logarithmic relationship between subject ratings and luminance, similar to the one found in the field experiment, was obtained.

Zwahlen and Schnell (6) investigated the visibility of new pavement markings at night under low-beam illumination in terms of pavement marking begin and end detection distance. Three independent experiments were conducted as part of this study. The objective of Study 1 was to obtain exploratory pavement marking visibility field data for detecting the begin and end of continuous pavement marking lines as a function of line width, retroreflective material, and lateral position of the line. The results of Study 1 indicate that the width of the lines does not appear to significantly increase the average detection distance. It was further found that the average begin and end detection distance for a white continuous pavement marking tape line was slightly but statistically not significantly longer (at $\alpha = 0.05$) than the average begin and end detection distance for a continuous white painted pavement marking line. The average begin and end detection distances for pavement marking lines located to the right of the car are slightly but statistically not significantly longer (at $\alpha = 0.05$) than the average begin and end detection distances for pavement marking lines located to the left of the car. Study 2 was conducted with the objective of obtaining some exploratory pavement marking nighttime visibility data under low-beam conditions in terms of detection distances of the onset of a left or right curve. Regular white continuous edge lines 0.05, 0.1, and 0.2 m wide were used as a stimulus. The results of Study 2 indicate that the width of the edge lines appears to slightly increase the average detection distance. Further, right curves were much more easily detected than left curves. Study 3 had the objective of obtaining

the nighttime average detection distances under low-beam illumination conditions for the begin and the end of different new yellow taped center-stripe configurations having different widths (0.05, 0.1 and 0.2 m). The center stripe configurations were as follows:

- Double solid,
- Single solid with dashed line having a gap/stripe ratio of 9.15/3 m,
- Dashed line having a gap/stripe ratio of 9.15/3 m, and
- Dashed line having a gap/stripe ratio of 10.98/1.22 m.

The results of Study 3 indicate that the width of the lines appears to increase the detection distances only slightly.

Except for the data provided by Zwahlen and Schnell (6) there appears to be little pavement marking visibility data available in terms of begin and end detection distances. Further, the literature does not seem to provide any information about the effect of pavement marking obliteration on visibility. Such data, however, would be particularly important to quantify the effect of obliteration on the visibility of pavement markings. Further, having begin and end detection distance data available might provide a basis for specifying a minimum distance, below which no temporary pavement markings need to be applied during the period after the permanent pavement markings of a short section of a road have been totally covered or removed by some maintenance activity until permanent markings are installed again.

OBJECTIVES

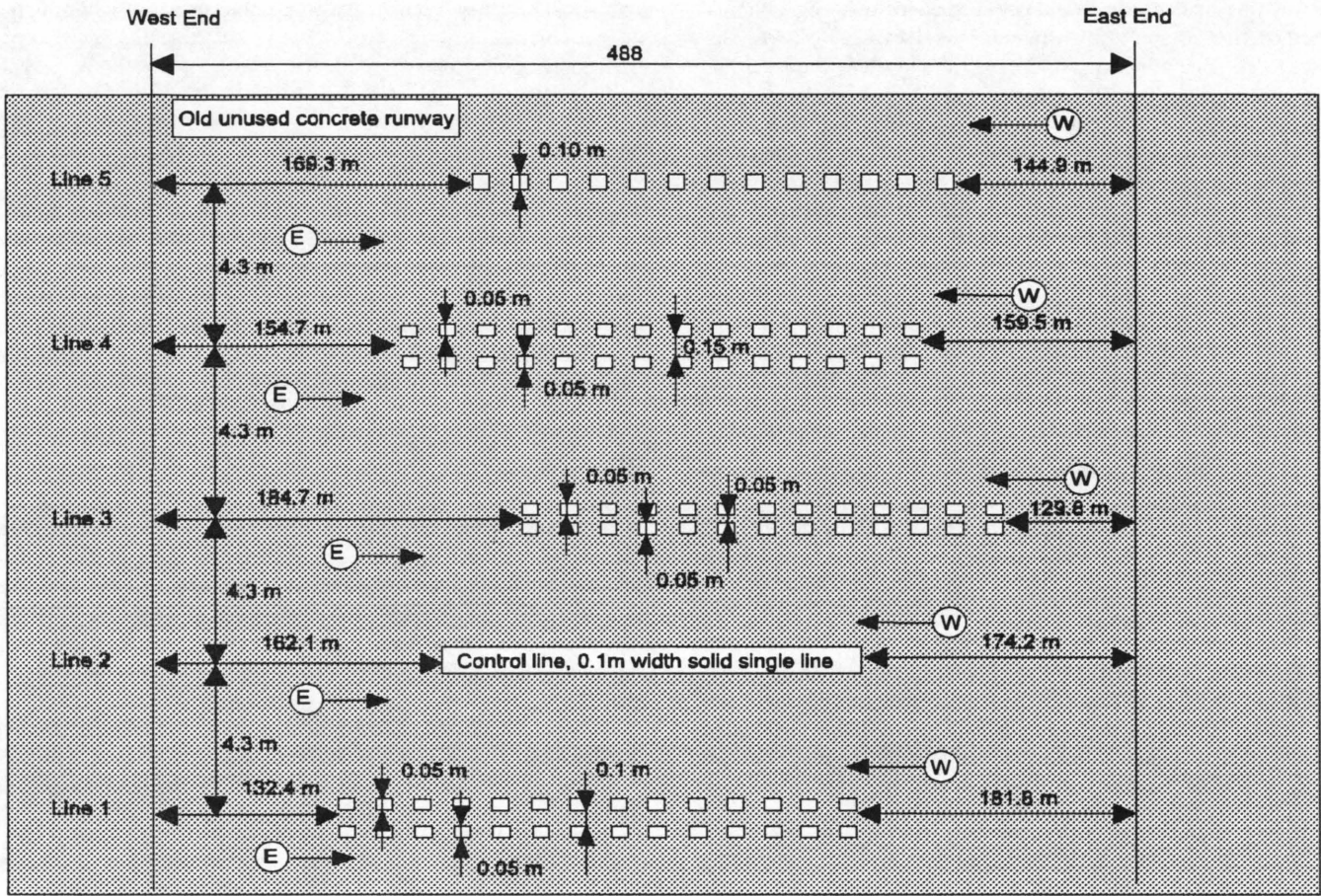
On the basis of previously mentioned needs to quantify the effect of obliteration on the visibility of new yellow center stripes, the objectives of this study were as follows:

- To determine the visibility distances under automobile low-beam illumination at night for new yellow temporary center stripes of finite length as a function of the degree of obliteration (0, 50, and 175 percent of the retroreflective material randomly removed from the new yellow center stripes) in terms of detecting the begin and end of the center stripes;
- To provide these visibility distances in terms of psychometric curves in addition to the average and standard deviation values; and
- As a secondary objective, to investigate the obliteration effect on visibility not only for 0.1-m-wide yellow center stripes with a gap/stripe ratio of 10.98/1.22 m but also for 0.05-m-wide double dashed (coded) center stripes with a gap/stripe ratio of 10.98/1.22 m. If such double dashed 0.05-m-wide coded center-stripe pavement markings would provide the same or better robustness to obliteration and the same or better begin and end detection distances as the single dashed 0.1-m-wide center-stripe pavement markings, it would seem that for the same area of retroreflective material, the coded center stripes could also convey passing/no-passing information in temporary resurfacing zones.

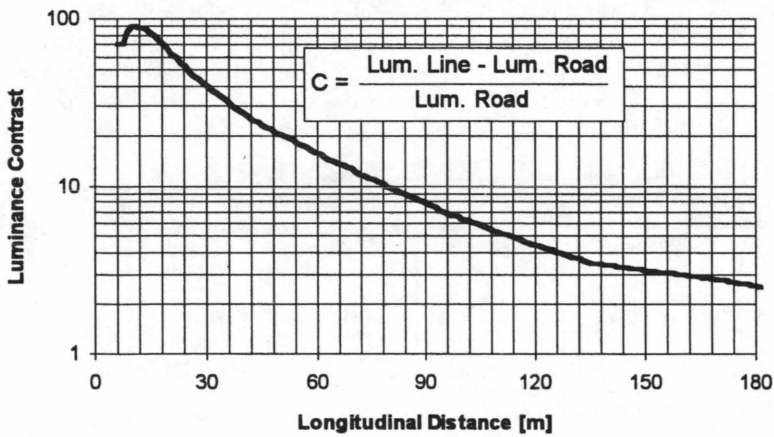
METHOD

Experimental Site

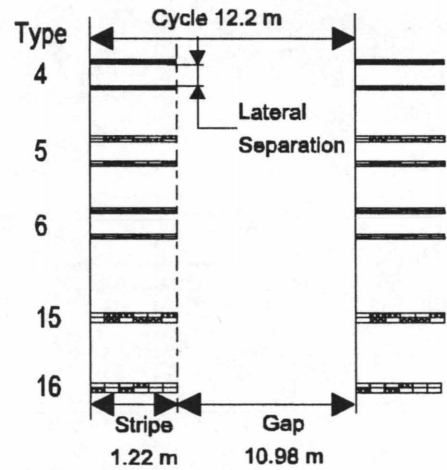
The experiment was conducted on old unused Ohio University airport runway (see Figure 1a), which is about 23 m wide and 500 m



a).



b).



c).

FIGURE 1 Detection of the begin and end of new yellow center stripes having 0, 50, and 75 percent obliteration: (a) experimental treatment layout; (b) approximate computed luminance contrast between centerline and concrete runway as a function of distance ahead of the car; (c) centerline types.

long, running east to west, located on the outskirts of the city of Athens, Ohio. A two-lane state highway with moderate traffic runs parallel about 61 m away from the edge of the runway. The concrete runway was relatively white and provided under low-beam illumination the following approximate luminance values as a function of distance to the front of the car: 0.03 cd/m² at 6 m, 0.05 cd/m² at 20 m, and 0.027 cd/m² at 40 m. Beyond 40 m, the runway luminance asymptotically approached 0.01 cd/m² (as a result of ambient illumination). Figure 1b shows the luminance contrast between the center line treatments and the concrete runway. During the course of the experiment, the experimental car was driven in both the eastbound and westbound directions. The eastbound direction provided a somewhat darker night horizon background with only a few luminaries in the left part of the driver's visual field, whereas the westbound direction provided a relatively bright night horizon background with a number of luminaries from a nearby shopping mall parking area directly ahead of the driver. The layout of the center stripe treatments on the old Ohio University airport runway is illustrated in Figure 1a. The vehicles were driven at about 8 to 16 kph in the lane assigned by the experimental design protocol such that the current center-stripe treatment was always located about 1.8 m to the left of the longitudinal car axis. All center stripes were 3M 5161 yellow pavement marking tape.

Subjects

A total of nine young healthy women college students with an average age of 21.77 years and 27 young healthy men college students with an average age of 21.24 years participated in the experiment. The 36 subjects were distributed over three groups (see also experimental order in Table 1) as follows:

- Group 1 (average age 21.6 years) contained two subjects who were women (average age 23 years) and ten subjects who were men (average age 21.44 years),
- Group 2 (average age 20.8 years) contained four subjects who were women (average age 21 years) and eight subjects who were men (average age 20.75 years); and
- Group 3 (average age 21.5 years) contained three subjects who were women (average age 21.33 years) and nine subjects who were men (average age 21.55 years).

The subjects had an average driving experience of 4.52 years and all of them possessed a valid U.S. driver's license. All subjects were

tested on a Bausch and Lomb vision tester and showed visual acuities ranging from 20/17 to 20/22 (average 20/19.6). Out of the 36 subjects 2 wore corrective contact lenses and 12 wore corrective glasses. The contrast sensitivity of all subjects was tested using the Vistec contrast sensitivity chart, Type C. All subjects showed a normal contrast sensitivity.

Experimental Vehicles

Group 1 used a 1994 Ford Probe with a line-of-sight windshield transmission of about 0.7, Group 2 used a 1979 Chevrolet Chevette with H6054 headlamps and a line-of-sight windshield transmission of about 0.7, and Group 3 used a 1990 Eagle Summit DL with a line-of-sight windshield transmission of about 0.7 as experimental vehicle. The average eye height of the drivers in group 1 was 1.07 m; in Group 2, 1.08 m; and in Group 3, 1.08 m.

Experimental Design

A randomized block design was used for the experiment. The dependent variables in this study were the average detection distances of the begin and end of the center stripe treatments. The major independent variables were the degree of obliteration and the approach direction (east/west). The following center stripe types were installed:

- Type 4, a double-dashed, 0.05-m-wide line with 0 percent obliteration,
- Type 5, a double-dashed, 0.05-m-wide line with 50 percent obliteration,
- Type 6, a double-dashed, 0.05-m-wide line with 75 percent obliteration,
- Type 15, a single-dashed, 0.1-m-wide line with 50 percent obliteration, and
- Type 16, a single-dashed, 0.1-m-wide line with 75 percent obliteration, (see Figure 1c).

Table 1 lists the various line types and line numbers that were used in the experimental design. The line type determined what degree of obliteration was present, whereas the line number determined whether a center stripe treatment consisted of a single dashed pattern or a double dashed pattern with a defined lateral separation

TABLE 1 Experimental Configuration and Results: Experimental Order and Center Stripe Configuration

Group Number	Line Number					Order of Group Subjected to Experiment
	Line 5	Line 4	Line 3	Line 2	Line 1	
1	Type 4 LS=0.2m	Type 4 LS=0.15m	Type 4 LS=0.05m	Single solid control line 0.1m wide	Type 4 LS=0.1m	3
2	Type 15	Type 5 LS=0.15m	Type 5 LS=0.05m	Single solid control line 0.1m wide	Type 5 LS=0.1m	2
3	Type 16	Type 6 LS=0.15m	Type 6 LS=0.05m	Single solid control line 0.1m wide	Type 6 LS=0.1m	1

(LS = Lateral Separation between Double Lines)

distance between the center stripes of finite length. It should be noted further that a new 0.1-m-wide single solid center line of finite length was used as baseline comparison between the groups. Although it would have been desirable to use a worn single solid control line with a coefficient of retroreflection of about 100 mcd/m² to approximate typical visibility conditions for the control measurements, there was no feasible method available to degrade the new control line material to some specified "used" condition.

The experimental order was determined on the basis of the degree of obliteration. From Figure 1c it can be seen that varying obliteration was obtained by randomly adding retroreflective material in a 2 by 6 matrix within each stripe. For the 75 percent obliteration situation, 3 out of the 12 matrix cells were equipped with retroreflective material; for the 50 percent obliteration situation, 6 out of the 12 matrix cells were equipped with retroreflective material; and all cells were equipped for the 0 percent obliteration situation. This method of representing various degrees of obliteration imposed the experimental order 75 percent obliteration, 50 percent obliteration, and 0 percent obliteration.

Each subject was tested under only one obliteration condition and under the conditions shown in Table 2 using three replications. The presentation order within each group was completely randomized by approach direction (east/west) and by line number (Line 1 to Line 5). Therefore, the total number of observations within each group was 360 (12 subjects with 3 replications each, 5 line numbers, east/west approach, begin/end) each for the begin detection distances and for the end detection distances.

Experimental Procedure

First the subject was given the proper instructions and then asked to adjust the driver's seat, mirror, and so on. After performing a number of familiarization runs, the subjects started the first run. For each run, the subject was instructed to line up the experimental vehicle

in the one driving lane (visible black joints of concrete plates) that was assigned by the experimental design. The subject was then told to accelerate the experimental vehicle to about 8 to 16 kph and to hold this speed as well as the lateral position as constant as possible. As soon as the subject reported seeing the begin of the corresponding center-stripe treatment a sand bag was dropped onto the runway by the experimenter in the passenger seat. A number of assistant experimenters recorded the distance of the sandbag relative to the beginning of the center stripe. The same method was applied for the detection of the end of the finite-length center-stripe treatment. The distances were measured to the nearest 2.54 cm by the assistant experimenters. As soon as the run was completed, the subject was instructed to drive the car to the next starting position, which was given by the experimental design protocol. Each subject performed three replications. One subject always performed ten runs (five eastbound, five westbound) within which the line number was completely randomized. The detection distances were not adjusted for the experimenter's reaction time to drop the sandbag, or for the drop time; therefore, all the actual detection distances may be about 10 ft longer.

RESULTS

Some subjects could sometimes detect the begin, especially of the 0.1-m-wide single solid control line, already from the starting position, because the runway did not provide enough approach run length for these conditions. This experimental artifact may have artificially reduced the begin detection distances for some conditions to some degree. However, because the artificial reduction is likely to be relatively small as a result of the small retroreflective area of the selected treatments, and to provide a complete account of the experimental results, the begin distances are presented nevertheless.

An analysis of variance (ANOVA) was conducted, and it was found that the factor line type (degree of obliteration) and the factor

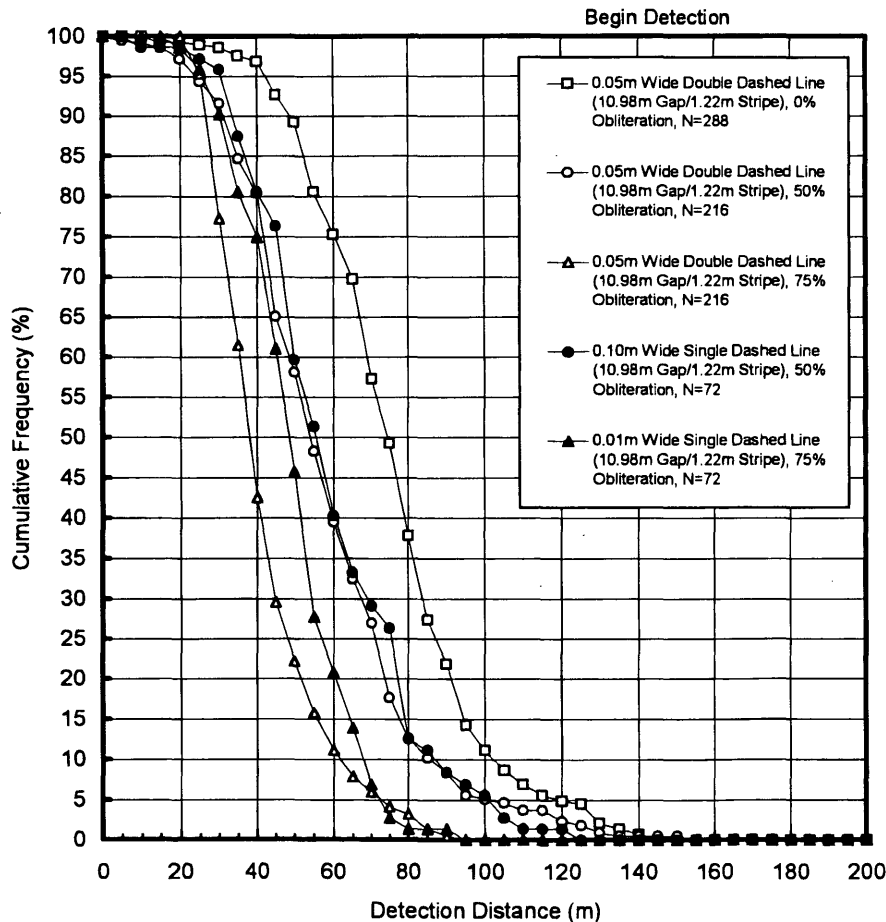
TABLE 2 Begin and End Detection Distances as a Function of Obliteration, Approach Direction, Center Stripe Type, and Gap space

Lat separ.		0%, Obliteration			50%, Obliteration			75%, Obliteration		
		Avg.	SD.	N	Avg.	SD.	N	Avg.	SD.	N
0.05m Lateral Separation, 0.05 m width, Double Dashed Line(10.98/1.22)										
Begin	East	89.0	15.2	36	71.8	31.4	36	46.7	15.8	36
	West	62.7	14.3	36	50.4	16.2	36	45.0	11.7	36
End	East	94.6	18.8	36	74.7	29.3	36	60.9	22.3	36
	West	79.2	26.3	36	66.8	34.3	36	51.7	19.9	36
0.10m Lateral Separation, 0.05 m width, Double Dashed Line(10.98/1.22)										
Begin	East	73.9	13.6	36	61.2	14.1	36	37.6	6.3	36
	West	103.5	26.5	36	79.1	22.6	36	66.7	13.1	36
End	East	78.4	19.0	36	70.8	32.2	36	50.3	26.0	36
	West	86.4	20.1	36	78.2	32.2	36	80.2	27.9	36
0.15m Lateral Separation, 0.05m width, Double Dashed Line(10.98/1.22)										
Begin	East	70.7	24.7	36	56.2	23.9	36	42.4	8.6	36
	West	69.3	18.5	36	51.7	22.2	36	39.5	6.4	36
End	East	79.6	19.1	36	77.2	30.8	36	61.9	28.7	36
	West	82.6	16.7	36	73.0	43.7	36	61.3	25.0	36
0.10m width, Single Dashed Line(10.98/1.22)										
Begin	East	Data not Measured			67.7	24.2	12	55.2	15.4	12
	West				59.8	18.3	12	52.3	13.3	12
End	East				63.3	31.3	12	63.0	33.6	12
	West				62.3	29.1	12	54.1	19.8	12

(All Average and Standard Deviation Detection Distance Values in Meters)

begin and end detection distance were statistically significant. By comparing Figures 2 and 3 it can be seen that the begin of the center stripes was detected very slightly farther than the end of the center stripes. However, the begin detection distances may have been somewhat reduced because of limited available approach run length. The ANOVA further indicated that the approach direction was insignificant, despite the somewhat different background conditions. The interaction effect between the factor line type (degree of obliteration) and the factor begin and end was found to be statistically highly significant. The interaction effect between the factor line type (degree of obliteration) and the factor approach direction was found to be statistically significant, probably because of the high significance of the factor line type. A Scheffe post hoc test generally indicated that the higher the degree of obliteration the shorter the detection distances. Note that the single solid 0.1-m-wide control line data for the begin detection distance was omitted in Figure 3 because of the limited available approach run length.

Figure 2 shows cumulative frequency as a function of the begin detection distance for the experimental center-stripe treatments on a concrete road surface under low-beam illumination conditions at night. The two center-stripe treatments with the highest degree of obliteration of 75 percent (Type 6 and Type 16), clearly provide the shortest begin detection distances. The double-dashed center stripes (Type 6, curve marked with empty triangles) and the single dashed (Type 16, curve marked with filled triangles) show almost the same begin detection distance for a probability of detection greater than 95 percent and smaller than 5 percent. However, in the intermediate probability range it seems that the double dashed 0.05-m-wide center-stripe treatment (Type 6, curve marked with empty triangles) provides somewhat shorter (statistically not significant at $\alpha = 0.05$) begin detection distances than the single dashed 0.1-m-wide center-stripe treatment (Type 16, curve marked with filled triangles). The two center-stripe treatments with 50 percent obliteration (Type 5 and Type 15), provide somewhat longer begin detection distances than



Note: Begin detection distance values may be too short due to limited available approach distance. Both Line type 4 (0.05m wide double solid, 0% obliteration) and the 0.1 m wide single solid control line were omitted in the above figure, because some subjects could detect the begin of those treatments already from the starting position, due to limited available approach run length.

FIGURE 2 Psychometric curves for begin detection distance on a concrete road surface under low-beam illumination at night.

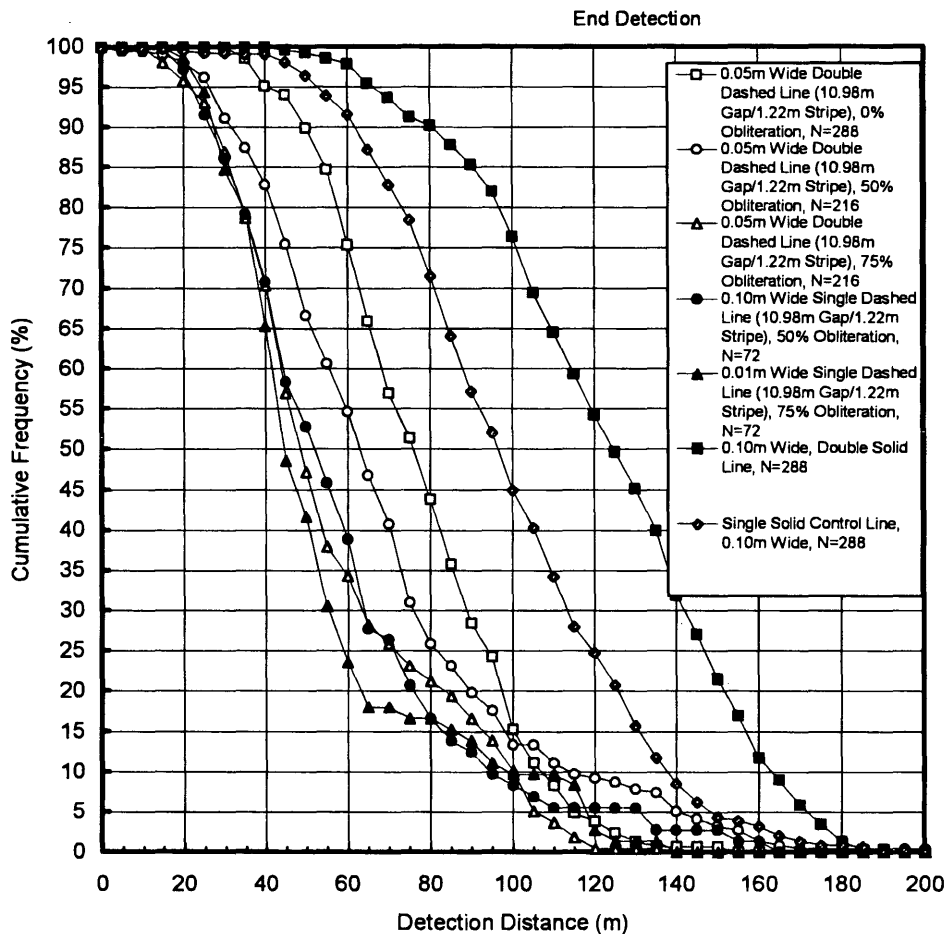


FIGURE 3 Psychometric curves for end detection distance on a concrete road surface under low-beam illumination conditions at night.

the center stripes with 75 percent obliteration. It can be seen from Figure 2 that the double dashed center stripes (Type 5, curve marked with empty disc) and the single dashed center stripes (Type 15, curve marked with filled disc) provide almost identical begin detection distances. The double dashed center stripe with 0 percent obliteration (Type 4, curve marked with empty square) provides, as expected, the longest begin detection distance. On the basis of Figure 2, it seems that obliteration has an effect on begin detection distance in terms of reducing visibility for increased obliteration. It seems that there is no statistically significant difference between the obliterated double dashed, coded center stripes (Types 5 and 6) and their single dashed counterparts (Types 15 and 16) with equivalent area.

Figure 3 shows the psychometric curves as a function of the end detection distance for the experimental center stripe treatments on a concrete road surface under low-beam illumination conditions at night. Strictly for comparison purposes, this figure also includes the end detection distance curve for the 0.1-m-wide yellow single solid control line and the end detection distance curve for a 0.1-m-wide, yellow double solid standard center line. The two center stripe treatments with the highest degree of obliteration of 75 percent (Type 6 and Type 16), clearly provide the shortest end detection distances. The double-dashed center stripes (Type 6, curve marked with empty triangles) and the single dashed (Type 16, curve marked with filled triangles) show almost the same end-detection distance for a prob-

ability of detection greater than 65 percent and smaller than 3 percent. However, in the probability range between 3 and 65 percent, it seems that the double-dashed coded 0.05-m-wide center stripe treatment (Type 6, curve marked with empty triangles) provides somewhat longer (statistically not significant at $\alpha = 0.05$) end detection distances than the single dashed 0.1-m-wide center stripe treatment (Type 16, curve marked with filled triangles). The two center stripe treatments with 50 percent obliteration (Types 5 and 15) provide somewhat longer end detection distances than the center stripes with 75 percent obliteration. It can be seen from Figure 3 that the double-dashed coded center stripes (Type 5, curve marked with empty disc) provides longer end detection distances than the single dashed center stripes (Type 15, curve marked with filled disc). The double dashed center stripe with 0 percent obliteration (Type 4, curve marked with empty square) provides, as expected, the longest end-detection distance among the temporary center stripes. On the basis of Figure 3, it seems that obliteration has an effect on end detection distance in terms of reducing visibility for increased obliteration. There does not seem to be any significant difference between the obliterated double dashed, coded center stripes (Types 5 and 6) and their single dashed counterparts (Types 15 and 16). Therefore, one may conclude that for the same area of retro-reflective material, the coded center stripes provide comparable robustness to obliteration and comparable begin and end detection

distances. Thus, the coded center stripes might be beneficial in temporary resurfacing zones because they could also convey passing/no-passing information in temporary resurfacing zones.

Figure 2 indicates that at the 85th percentile point the 75 percent obliteration treatment provides a begin detection distance of about 28 m, whereas the 0 percent obliteration treatment provides a begin detection distance of about 56 m (twice the distance for four times more material). Similarly, from Figure 3, it can be seen that at the 85th percentile point, the end detection distances are about 30 m for the treatment with 75 percent obliteration and about 56 m for the treatment with 0 percent obliteration. The end detection distance values are close to the begin detection distance values.

Figure 4 indicates a comparison of the average begin/end, east/west detection distances as a function of obliteration for 0.05-m-wide double dashed center stripes with 0.05-, 0.1-, and 0.15-m lateral separation as well as for the single dashed 0.1-m-wide center stripes. From the figure, it can again be seen that the detection distances generally decrease for increasing obliteration.

Figure 5a shows the effect of the retroreflective area for each 12.22-m-long segment of pavement marking on the 85th percentile detection distance, for center stripe Types 4, 5, 6, 15, and 16. Some

subjects have detected some of the lines already at the starting position, which has artificially reduced the begin detection distances to some degree for some conditions. As expected and demonstrated by the ANOVA and the Scheffe post hoc tests, which indicated that line type was highly significant, it was found that a more retroreflective area per 12.22-m-long segment generally results in somewhat longer detection distances for both detection of the begin and the end. Figure 5b shows the effect of retroreflective area for each 12.22-m-long segment of pavement marking on the 50th percentile detection distance for center stripe Types 4, 5, 6, 15, and 16. The 50th percentile begin and end detection distances are on the average about 37 percent longer than the corresponding 85th percentile begin and end detection distances. For the data shown in Figure 5a and b, it can be stated that even though there appears to be an almost linear relationship between the begin/end detection distances and the retroreflective area per 12.22-m segment in the investigated range of 0.0301 m² to 0.123m², there has been enough evidence in related studies (6,7) that further increasing the retroreflective area would not necessarily improve visibility in a linear fashion. In fact, calculations indicated that an increase in the retroreflective area from 0.122 to 2.44 m² for each 12.2-m-long center line segment (20-fold increase) was

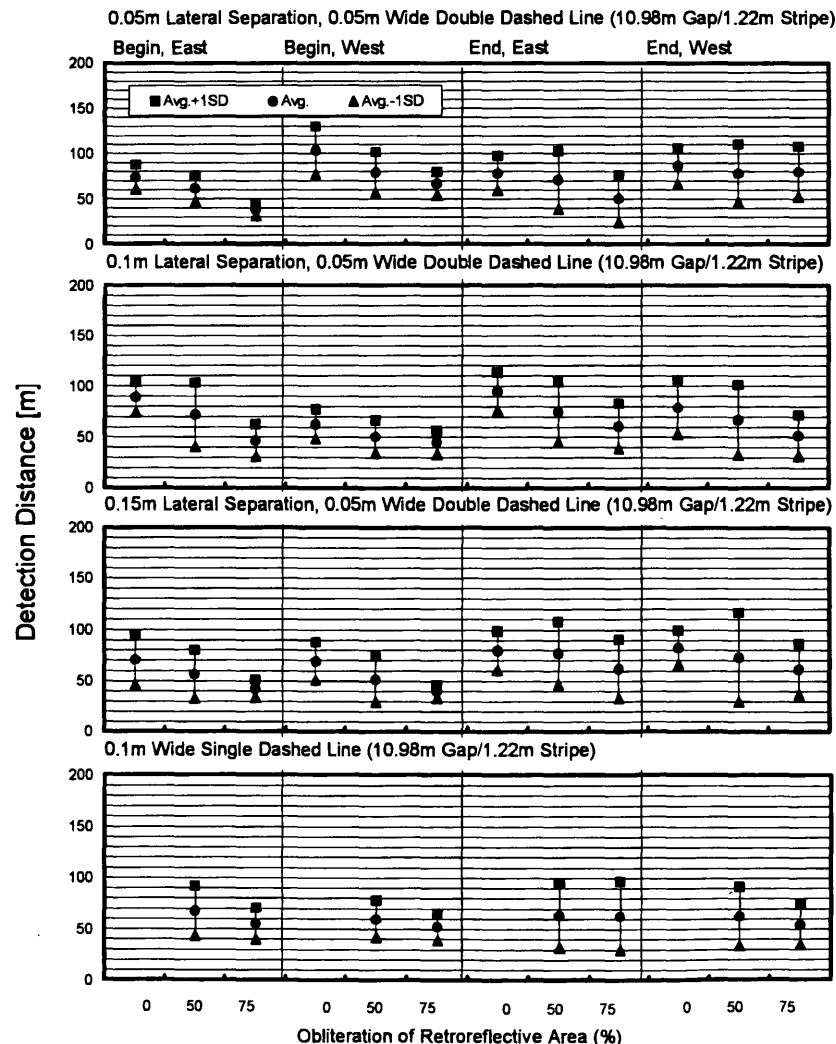
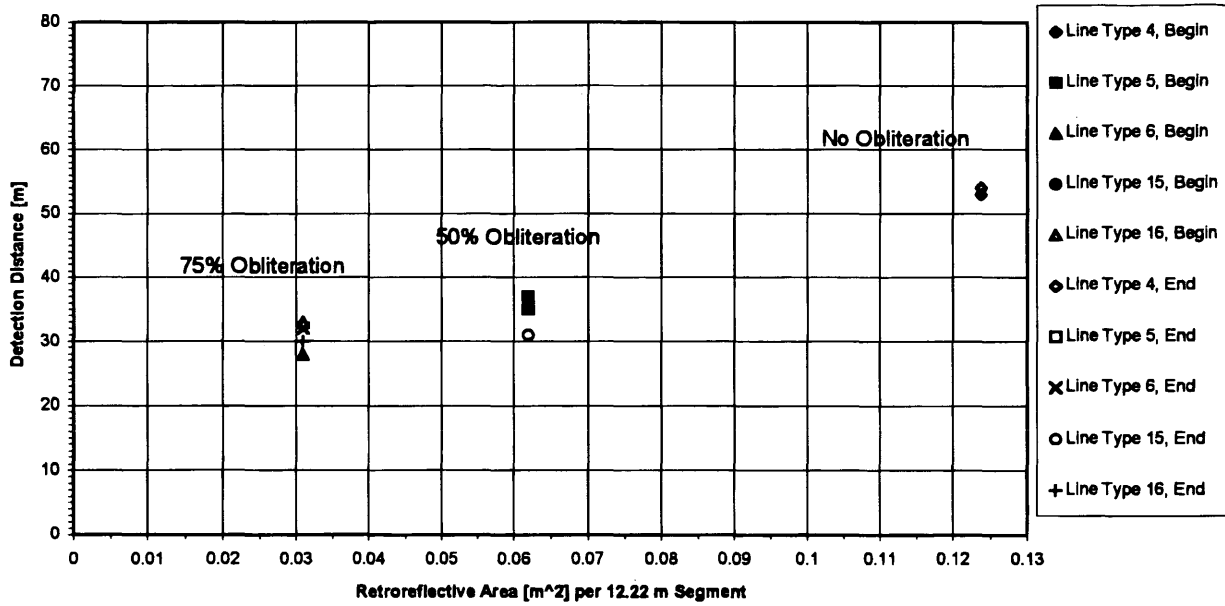
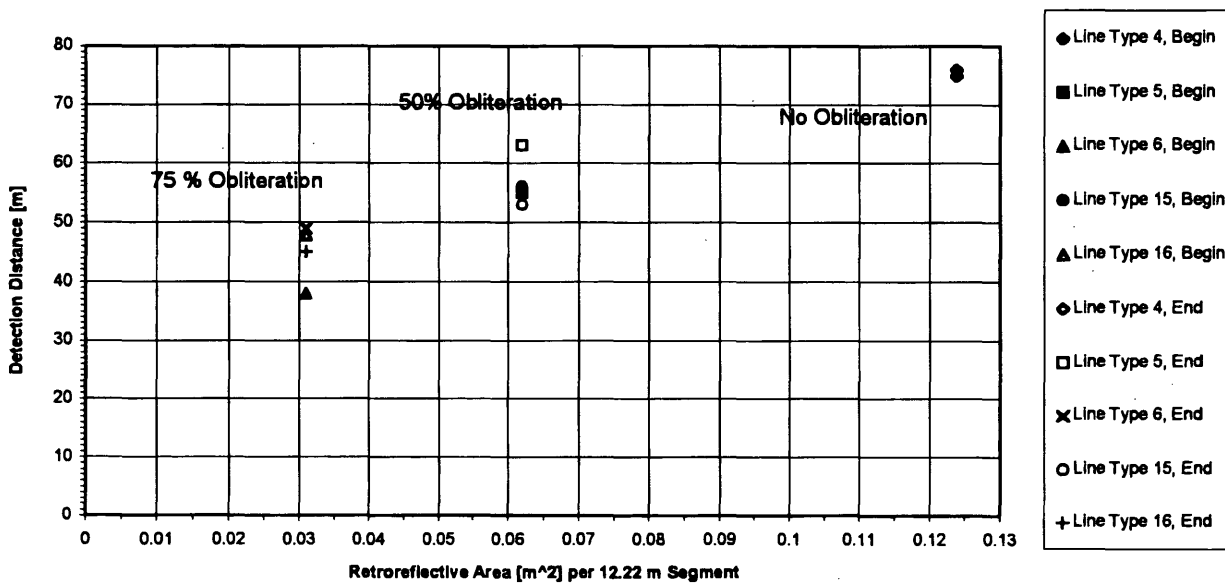


FIGURE 4 Comparison of average begin and end, east/west detection distances as a function of obliteration. Begin detection distance values may be too short because of a limited available approach distance.



a)



b)

FIGURE 5 Detection distances for begin and end on a concrete road surface under low-beam illumination conditions at night as a function of the area of retroreflective material (a) 85th percentile detection distance data; (b) 50th percentile detection distance data. Begin detection distance values may be too short because of a limited available approach distance.

required to increase the average end detection distance from 55 to 90 m, which amounts only to a gain of 65 percent. Therefore, the positive visibility effects of using more retroreflective material may be gradually outdone by the increased cost for the additional material.

DISCUSSION AND CONCLUSIONS

A review of the technical literature about the visibility of center stripes has indicated that, with the exception of the data provided by Zwahlen and Schnell (6), few pavement marking visibility data are

available in terms of begin and end detection distances. Further, the literature does not seem to provide any quantitative information about the effect of pavement marking obliteration on visibility. The study was conducted to overcome this lack of information, which is required to quantify the visibility of obliterated or less-than-full pavement marking treatments. New pavement markings were used in this obliteration study because no feasible method was available to degrade new pavement markings in a uniform manner to some specified "used" condition. The use of the minimum specified dimension center stripes (0.05 m wide) was intended to somewhat counteract the newness of the used pavement marking tapes. This

research also may have some value for the cost-effective installation of enhanced "coded" temporary center stripes in newly resurfaced zones. The current Ohio standard given in the Ohio Manual of Uniform Traffic Control Devices (OMUTCD) (8) and the federal standard given in MUTCD (4) specify 0.1-m-wide single dashed stripes with a gap/stripe ratio of 10.98/1.22 m as temporary center stripes in resurfaced zones, regardless of whether the resurfaced zone happens to be in a no-passing zone. The double dashed 0.05-m-wide "coded" temporary center stripes, which were used in this experiment, have been shown to provide equivalent detection distance performance as the standard OMUTCD/MUTCD single dashed temporary center stripes. However, a driver in a newly resurfaced no-passing zone may be more adequately informed about the passing situation with the double dashed "coded" temporary center stripes using the same amount of retroreflective material. Considering the fact that the thinner double-dashed center stripes can provide additional passing or no-passing information to a motorist in a temporary resurfacing zone without any significant difference in the begin and end detection distances, it may be concluded that the use of temporary double dashed center stripes in resurfaced no-passing zones could improve motorist safety while requiring the exact same amount of material as the presently used single dashed temporary center stripes require. Overall, on the basis of results of this study it is concluded that severe obliteration does reduce the begin and end detection distances to a considerable degree. However, using four times less material and the shortest specified stripe length (10.98/1.22 m) reduces, for example, the 85th percentile begin and end detection distances from about 53 to 30 m (see Figure 5a). Therefore, from a begin and end detection distance point of view, it seems that if the nonobliterated center line pavement marking

treatment already provides barely adequate visibility performance, it is not possible to tolerate much obliteration at all (possibly no more than 5 to 10 percent before the visibility performance of the overall system (driver-vehicle-center line system) falls below the acceptable minimum safety level.

REFERENCES

1. Allen R. W., J. F. O'Hanlon, D. T. McRuer, et al. *Driver Steering Performance Effects of Roadway Delineation and Visibility Conditions*, Paper 229. Systems Technology, Inc., Hawthorne, Calif., 1991.
2. O'Hanlon J. F., R. W. Allen, et al. *Driver's Visibility Requirements for Roadway Delineation*, Vol. 1. Effects of Contrast and Configuration on Driver Performance and Behavior. Report FHWA/RD-77-165. Nov. 1977.
3. Harkey D. L., et al. Effect of Nonpermanent Pavement Markings on Driver Performance. In *Transportation Research Record, 1409*, TRB, National Research Council, Washington, D.C., 1992.
4. *Manual on Uniform Traffic Control Devices for Streets and Highways*, FHWA U.S. Department of Transportation, 1988.
5. King E., and J. R. Graham. Retroreflectivity Requirements for Pavement Markings. In *Transportation Research Record 1316*, TRB, National Research Council, Washington, D.C., 1991.
6. Zwahlen H. T., and T. Schnell. Visibility of New Pavement Markings at Night Under Low-Beam Illumination. Presented at 73rd Annual Meeting of the Transportation Research Board, Washington, D.C., 1994.
7. Zwahlen H. T., and T. Schnell. Effects of Lateral Separation Between Double Center Stripe Pavement Markings on Visibility Under Nighttime Driving Conditions. Presented at 74th Annual Meeting of the Transportation Research Board, Washington, D.C., 1995.
8. *Ohio Manual of Uniform Traffic Control Devices for Streets and Highways*, Division of Operations, Bureau of Traffic, Ohio Department of Transportation, Columbus, 1972.

Publication of this paper sponsored by Committee on Visibility.

Effects of Lateral Separation Between Double Center-Stripe Pavement Markings on Visibility Under Nighttime Driving Conditions

HELMUT T. ZWAHLEN, THOMAS SCHNELL, AND TORU HAGIWARA

Pavement markings on public roads provide driver guidance, convey advisory or warning information to the driver, or both, and are often used as a supplement to other traffic control devices without redirecting the focus of attention from the road. Adequate visibility of pavement markings at night is an important element of driver safety, especially in the absence of public lighting. Increased lateral separation between double center stripes could increase the detection distance because the human visual system would spatially integrate over the lateral space between the parallel lines to form a more visible target that subtends a greater visual angle. Most of the technical literature has shown that there seems to be no available pavement marking visibility data on begin-and-end detection distances. Also, no data are available on the effects of lateral separation between double solid center stripes and the interaction between lateral separation and line width. The current study was conducted to provide a scientific basis for quantifying the effects of lateral separation between double solid center stripes. It is current standard practice in Ohio to implement double solid yellow center stripes (0.1 m wide) with a lateral separation of 0.1 m. On the basis of a field experiment involving 48 subjects, average begin-and-end detection distances were established and psychometric curves were plotted. An ANOVA and Scheffe post hoc test failed to find any significant systematic effect caused by lateral separation between the center lines. On the basis of the findings of this study it is possible to tentatively conclude that an increase in the lateral separation (from 0.05 to 0.2 m) between the double center stripes does not appear to be a useful method to increase driver visibility. In addition, as expected, the amount of retroreflective material (0.05, 0.1, 0.15, or 0.2 m width, double solid versus dashed, gap/stripe ratio of 9.15/3.05 m versus 10.98/1.22 m) has a fairly small effect on the 85th percentile end detection distances, thus indicating a relatively small marginal gain in visibility with a substantially increased retroreflective area. In fact, calculations indicate that an increase in area from 0.122 to 2.44 m² for each 12.2-m-long center line segment (20-fold increase) is required to increase the average end detection distance from 82 to 128 m, which is only an increase of 56 percent.

Except for data provided by Zwahlen and Schnell (1) There seems to be no available pavement marking visibility data on begin-and-end detection distances. Dudek et al. (2) conducted a field study to investigate the effect of temporary pavement markings in newly paved work zones under dry nighttime driving conditions. As independent variables Dudek et al. used the following center stripe types:

- 0.304-m stripes with 11.88-m gaps,
- 0.61-m stripes with 11.58 m gaps, and
- 1.2261-m stripes with 10.97-m gaps.

The dependent variables were

- Vehicle speed,
- Lateral distance of the vehicle from the centerline,
- Lane straddling, and
- Number of erratic maneuvers.

The study was conducted at seven pavement overlay sites in the states of Texas (four sites), Arkansas, Colorado, and Oklahoma (one site each). All newly paved sites had 3.65-m-wide lanes with paved shoulders. No edge lines were installed. A tangent section and one curve were present in each site. A random scheme was used to assign one of the three patterns to one of the three nights during which the traffic was observed. Dudek et al. tested each pattern at exactly the same location at the test site. This approach eliminated effects caused by road geometry differences. In addition to this unobtrusive driver study, Dudek et al. used an in-vehicle response survey to evaluate the three pavement marking patterns. The survey involved 27 paid driver subjects. Dudek et al. found that there were no statistically significant differences between Types 1, 2, and 3 patterns with respect to vehicle speed. Further, there were no statistically significant differences between Types 1, 2, and 3 patterns with regard to lateral vehicle position. No consistent effect was found for the centerline encroachments. The very infrequently observed encroachments were related to passing maneuvers rather than pavement marking effects. Virtually no erratic maneuvers were observed. The in-vehicle observers reported a slight subjective improvement when longer markings were used. At one site the observers even judged the Type 1 pattern to be the most effective. Dudek et al. concluded that the Type 1 and the Type 2 patterns performed as well as the Type 3 pattern that is currently recommended by the Manual on Uniform Traffic Control Devices for Streets and Highways (MUTCD) (4) under the tested conditions. The findings of Dudek et al. (2) were based on fresh black pavement and newly installed retroreflective pavement markings under dry nighttime driving conditions. The researchers pointed out that their results should not be generalized to situations in which the pavement and the markings would not provide as much contrast or to situations involving adverse weather conditions.

Cotrell (5) investigated the effect of wide edge lines on the reduction of run-off-the-road (ROR) accidents. The experiment was set

H. T. Zwahlen and T. Schnell, Human Factors and Ergonomics Laboratory, Department of Industrial and Systems Engineering, Ohio University, Athens, Ohio 45701-2979. T. Hagiwara, Traffic Engineering Laboratory, Department of Civil Engineering, Hokkaido University, Sapporo, Japan.

up on three rural road sections with a total length of 60.7 mi. The experiment consisted of a before-and-after study. Accident data for the before-and-after study were collected over 3 and 2 years, respectively. Cotrell concluded that there is no evidence that wide edge lines significantly affect the incidence of ROR accidents.

Very little can be found in the literature with respect to theoretical pavement marking models that would provide detection distances as a function of factors such as (but not limited to) observer/headlamp/pavement marking geometry, retroreflective material characteristics, human visual performance, headlamp candlepower output, and environmental conditions. There currently exists no pavement marking visibility model to evaluate different pavement marking materials under selected geometrical and environmental conditions within the driving context. The visibility model proposed in CIE Publication 73 (6) has a number of shortcomings. For straight sections, the model proposes a conservative preview time of 5 sec. The threshold contrast function is inaccurate, does not consider driver age, does not consider glare caused by oncoming vehicles, does not consider the contrast sensitivity in the visual periphery, does not consider the probability of detection, does not account for target recognition (accounts for detection only), and most likely uses an inadequate background luminance. In addition, the model considers the farthest visible point of a pavement marking line only. It does not account for the pavement markings visible between this farthest visible point and the point closest to a driver from which the hood of the car obstructs any closer view to the pavement. The pavement marking piece (located at the farthest visible point) is approximated by a rectangle rather than by a trapezoid as it would be seen from the perspective of a driver. The lateral location (edge line, centerline, etc.) of the pavement markings is not considered. The model does not specify how to obtain the candlepower of the headlamps for the given pavement marking location and also does not specify how to obtain the coefficient of retroreflection for the pavement marking material at the given location. The model does not account for the optical characteristics of the various road surfaces. On the basis of these drawbacks, it seems that additional research about pavement marking visibility is essential.

Saito and Garber (7) investigated the effect two different pavement marking patterns have on driver behavior. As the independent variables in their field study they used the following pavement markings:

- Mountain pavement marking (MPM): this type of pavement marking consists of a single broken line (no information about the marking length and color was given in the paper) and two edge lines; and
- MUTCD passing and no passing lines: this included a double solid line, a single solid line with a left broken line, and a single solid line with a right broken line, and always edge lines.

The following dependent variables were considered:

- Traffic volume,
- Vehicle speeds,
- Distance to the leading vehicle (headway maintenance),
- Traffic queues (a platoon of at least two cars with a maximum headway time of 6 sec was considered a queue).

The data were collected with a Leupold and Stevens traffic data recorder. Garber and Saito believed that these dependent variables were justified because the short period of their research did not

allow for a meaningful statistical accident analysis. The researchers conducted the study in a before-and-after manner. The before study investigated the effect of the MPM on the dependent variables. Data for the MUTCD markings were collected in the after study. Garber and Saito found that there was no significant change in the vehicle speed between the before and the after study with the exception of two sites, where the speeds were reduced by 2.57 kph and 3.05 kph respectively. Despite the statistical significance, practically, this change does not indicate a strong speed reduction effect of the MUTCD markings. The speed variance during the after phase was smaller than during the before phase, supporting the hypothesis that the MUTCD markings tend to enhance a smooth flow of traffic. There was no significant change in the queue characteristics with respect to queue speed and queue frequency. The headway distributions did not significantly change. The researchers concluded that on the basis of a lack of difference in driver behavior, the MUTCD pavement-marking pattern should be preferred over any other type of pattern.

Zwahlen and Schnell (1) investigated the visibility of new pavement markings at night under low-beam illumination in terms of pavement marking begin-and-end detection distance. Three independent experiments were conducted as part of this study. The objective of Study 1 was to obtain exploratory pavement markings visibility field data for detecting the beginning and the end of continuous pavement marking lines of finite length as a function of line width, retroreflective material, and lateral position of the line. The results of Study 1 indicate that the width of the lines (from 0.1 to 0.2 m) does not appear to increase the average detection distance.

Study 2 was conducted with the objective of obtaining some exploratory pavement marking nighttime visibility data under low-beam conditions in terms of detection distances of the onset of a left or right curve. Regular white continuous edge lines (0.05, 0.1, and 0.2 m wide), located approximately 1.8 m to the right of the car, were used as a stimulus. The results of Study 2 indicate that the width of the edge lines appears to slightly increase the average detection distance. Further, right curves were much more easily detected than left curves. Study 3 had the objective of obtaining the nighttime average detection distances under low-beam illumination conditions for the beginning and for the end of different new yellow-taped center-stripe configurations having different widths (0.05, 0.1, 0.2 m). The center-stripe configurations were as follows:

- Double solid;
- Single solid with dashed line having a gap/stripe ratio of 9.15/3 m;
- Dashed line having a gap/stripe ratio of 9.15/3 m; and
- Dashed line having a gap/stripe ratio of 10.98/1.22 m.

The results of Study 3 indicate that the width of the lines appears to increase the detection distances only slightly.

Except for the data provided by Zwahlen and Schnell (1) there appears to be no pavement marking visibility data available in terms of begin-and-end detection distances. Further, the literature does not seem to provide any information about the effect of lateral separation between double center-stripe pavement markings on visibility.

OBJECTIVES

On the basis of previously mentioned needs to quantify the effect of lateral separation between new yellow double solid and double

dashed center stripes on driver visibility, the objectives of this study were as follows:

- To determine the visibility distances under automobile low-beam illumination at night for new yellow double solid center stripes as a function of the lateral separation between the double stripes (0.05, 0.1, 0.15, and 0.2 m);
- To provide visibility distances in terms of psychometric curves in addition to the average and standard deviation values;
- A secondary objective was to investigate the effect of retroreflective material area (0.05 versus 0.1 m width of the double center stripes, solid versus gap/stripe ratio 9.15/3.05 m and 10.98/1.22 m) on begin-and-end detection distances.

METHOD

Experimental Site

The experiment was conducted on an old unused Ohio University airport runway (see Figure 1), which is about 23 m wide and 500 m long, running east to west, and is located on the outskirts of the city of Athens, Ohio. A two-lane state highway with moderate traffic runs parallel about 61 m away from the edge of the runway. The concrete runway was relatively white and provided under low-beam illumination the following approximate luminance values as a function of distance to the front of the car: 0.03 cd/m² at 6 m, 0.05 cd/m² at 20 m, 0.027 cd/m² at 40 m. Beyond 40 m, the runway luminance asymptotically approached 0.01 cd/m² (because of ambient illumination). Figure 2b shows the luminance contrast between the centerline treatments and the concrete runway. During the course of the experiment, the experimental car was driven in both the eastbound and westbound directions. The eastbound direction provided a somewhat darker night horizon background with only a few luminaires in the left part of the driver's visual field, whereas the westbound direction provided a relatively bright night horizon background with a number of luminaires from a nearby shopping mall parking area directly ahead of the driver. The layout of the center-stripe treatments on the old Ohio University airport runway is illustrated in Figure 1. The vehicles were driven at about 8 to 16 kph in the lane assigned by the experimental design protocol such that the current center-stripe treatment was always located about 1.8 m to the left of the longitudinal car axis. All center stripes were 3M 5161 yellow pavement marking tape.

Subjects

A total of 10 young healthy women college students with an average age of 26.77 years and 38 young healthy men college students with an average age of 23.1 years participated in the experiment. The 48 subjects were distributed over four groups (see experimental design) as follows:

- Group 1 (average age 26.1 years) contained five women as subjects (average age 30 years) and seven men as subjects (average age 23 years);
- Group 2 (average age 23.6 years) contained two women as subjects (average age 24 years) and ten men as subjects (average age 23.5 years);

- Group 3 (average age 23.9 years) contained one woman as subject (age 20 years) and eleven men as subjects (average age 24.27 years); and
- Group 4 (average age 21.6 years) contained two women as subjects (average age 23 years) and ten men as subjects (average age 21.44 years).

The subjects had an average driving experience of 5.52 years, and all of them possessed a valid U.S. driver's license. All subjects were tested on a Bausch and Lomb vision tester and showed visual acuities ranging from 20/17 to 20/29 (average 20/20.27). Out of the 48 subjects 2 wore corrective contact lenses and 18 wore corrective glasses. The contrast sensitivity of all subjects was tested using the Vistec contrast sensitivity chart, Type C. All subjects showed a normal contrast sensitivity.

Experimental Vehicles

Groups 1 through 3 used a 1981 Volkswagen Rabbit with H6054 headlamps with a line-of-sight windshield transmission of 0.77. Group 4 used a 1994 Ford Probe with a line-of-sight windshield transmission of about 0.7. The average eye height was 1.07 m for the drivers in Group 1, 1.08 m for the drivers in Group 2, 1.08 m for the drivers in Group 3, and 1.07 m for the drivers in Group 4.

Experimental Design

A randomized block design was used for the experiment. The dependent variables in this study were the average detection distances of the beginning and the end of the center-stripe treatments. The major independent variables were the lateral separation between the double center stripes and the approach direction (east/west). The following center-stripe types were installed using 0.05, 0.1, 0.15, and 0.2 m of lateral separation between the lines:

- Type 1, a double solid line that is 0.1 m wide;
- Type 2, a double solid line that is 0.05 m wide;
- Type 3, a double dashed line that is 0.05 m wide and has a gap/stripe ratio of 9.15/3.05 m; and
- Type 4, a double dashed line that is 0.05 m wide and has a gap/stripe ratio of 10.98/1.22 m. (see Figure 1, bottom).

Table 1 lists the different line types and line numbers that were used in the experimental design. The line number determined what lateral separation between the lines was present while the line type determined whether a center stripe consisted of a dashed pattern or a solid line of finite length.

A new 0.1-m-wide single solid center line of finite length was used as base line comparison between the groups. Although it would have been desirable to use a worn single solid control line with a coefficient of retroreflection of about 100 mcd/m² to approximate typical visibility conditions for the control measurements, there was no feasible method available to degrade the new control line material to some specified "used" condition. Each subject was tested under only one line type (Type 1, double solid 0.1-m-wide lines; type 2; double solid 0.05-m-wide lines; Type 3; double-dashed 0.05-m-wide lines with a gap/stripe ratio of 9.15/3.05 m; and Type 4, double-dashed 0.05-m-wide lines with a gap/stripe ratio of 10.98/1.22 m) and under the conditions shown in Table 1 using

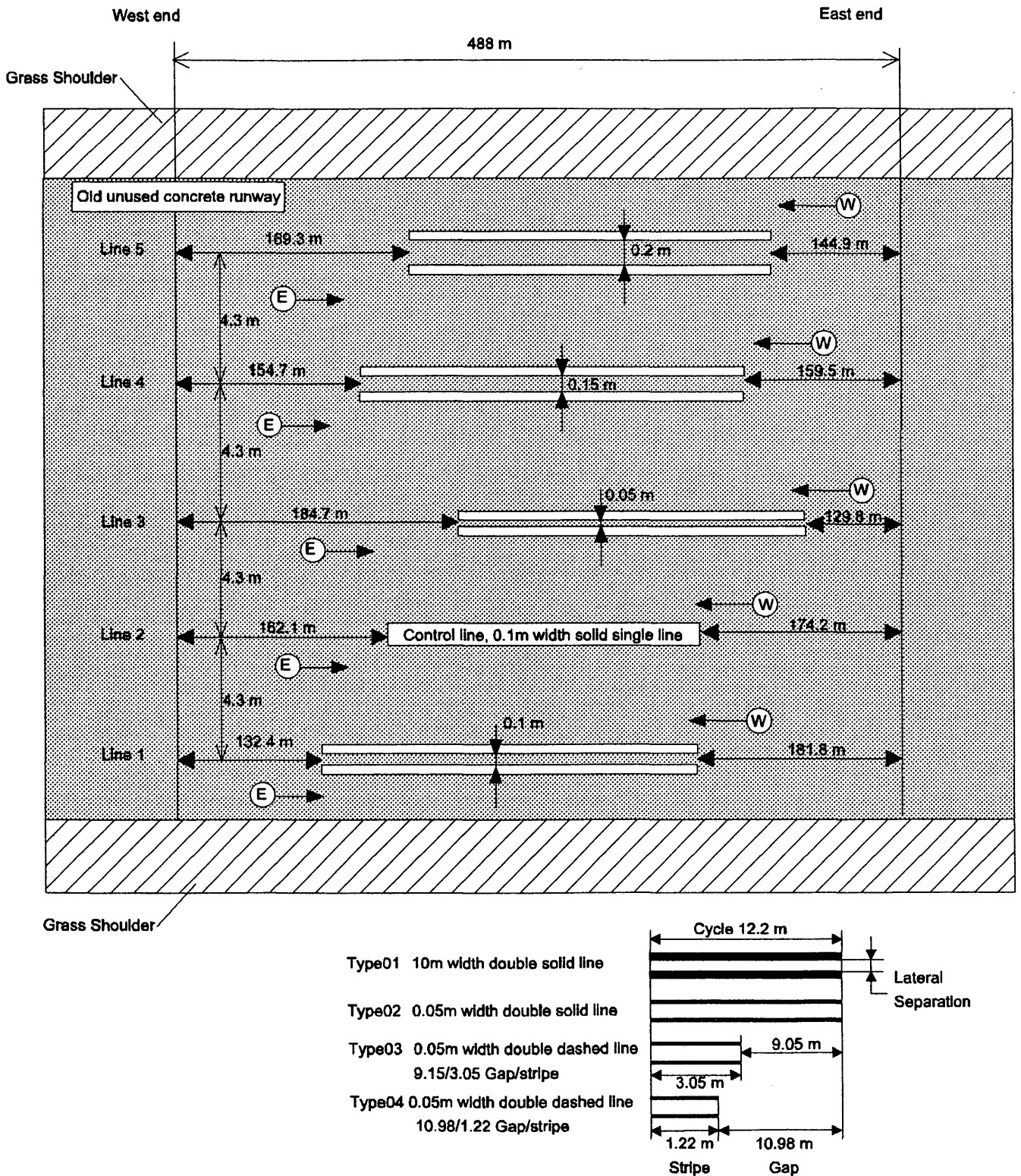
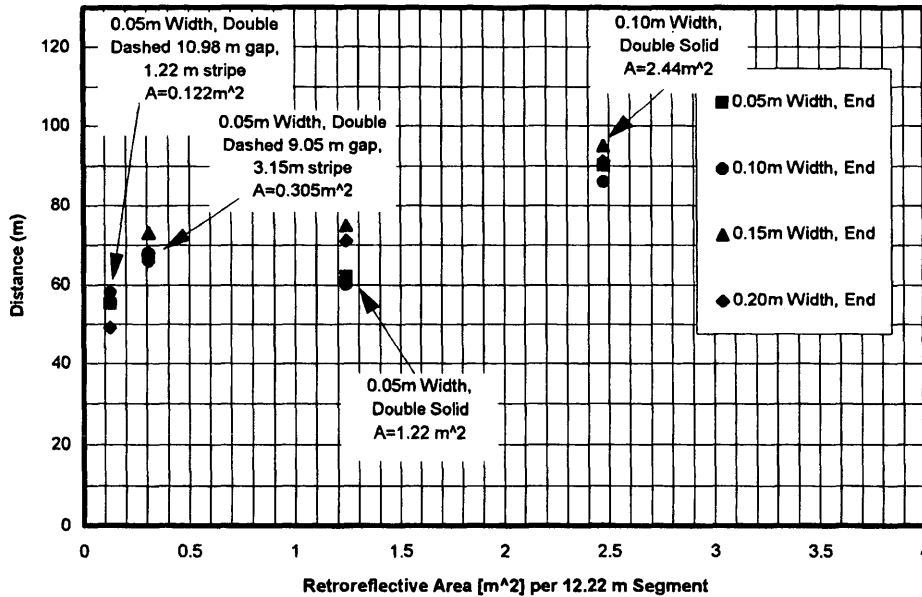
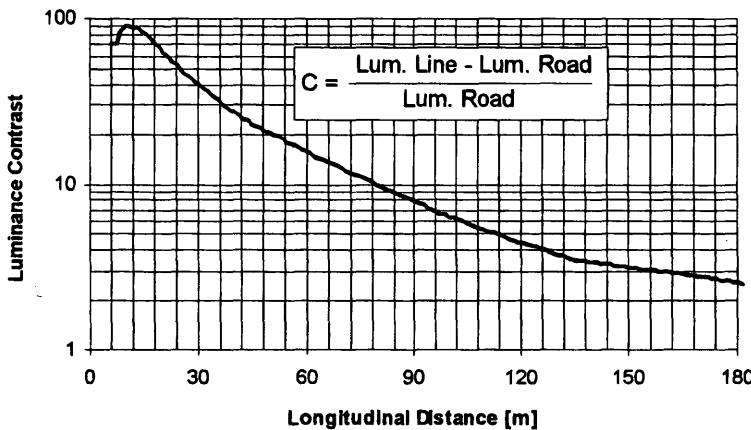


FIGURE 1 Layout for detection of begin and end of new yellow double solid center stripes having 0.05, 0.1, and 0.2 m lateral separation between lines.



a) 85th Percentile Detection Distance for the End of New Yellow Double Solid and Double Dashed Stripes on a Concrete Road Surface under Low Beam Illumination Conditions at Night as A Function of the Area of Retroreflective Material.



b) Approximate Computed Luminance Contrast Between the Center Line Treatments (3M 5161 Yellow, Measured and Extrapolated Ra Matrix) and the Concrete Runway Surface (Ra Matrix measured and Extrapolated) as Function of Distance ahead of the car.

FIGURE 2 Effect of area of retroreflective material on visibility under low-beam illumination and approximate computed luminance contrast ahead of car.

three replications. The presentation order within each group was completely randomized by approach direction (east/west) and by line number (Lines 1 to 5). Therefore, the total number of observations within each group was 360 (12 subjects with three replications each, five line numbers, east/west approach, begin/end) each for the begin detection distances and for the end detection distances.

Experimental Procedure

First the subject was given the proper instructions and then asked to adjust such items as the driver seat and mirror. After performing a

number of familiarization runs, the subjects started the first run. For each run, the subject was instructed to line up the experimental vehicle in the one driving lane (visible black joints of concrete plates) that was assigned by the experimental design. The subject was then told to accelerate the experimental vehicle to about 8-to-16-kph and to hold this speed as well as the lateral position as constant as possible. As soon as the subject reported seeing the beginning of the corresponding center-stripe treatment, a sand bag was dropped onto the runway by the experimenter in the passenger seat. A number of assistant experimenters recorded the distance of the sandbag relative to the beginning of the center stripe. The same method was applied for the detection of the end of the finite-length center-stripe

TABLE 1 Experimental Order and Center Stripe Configuration

Grp No.	Line Number					Order of Group Subjected to Experiment
	Line 5	Line 4	Line 3	Line 2	Line 1	
1	Type 2, Double Solid, 0.05m wide, 0.2m separation	Type 2, Double Solid, 0.05m wide, 0.15m separation	Type 2, Double Solid, 0.05m wide, 0.05m separation	Single solid control line 0.1m wide	Type 2, Double Solid, 0.05m wide, 0.1m separation	3
2	Type 1, Double Solid, 0.1m wide, 0.2m separation	Type 1, Double Solid, 0.1m wide, 0.15m separation	Type 1, Double Solid, 0.1m wide, 0.05m separation	Single solid control line 0.1m wide	Type 1, Double Solid, 0.1m wide, 0.1m separation	4
3	Type 3, Double dashed, 0.05m wide, 0.2m separation, 9.15/3.05m gap/stripe	Type 3, Double dashed, 0.05m wide, 0.15m separation, 9.15/3.05m gap/stripe	Type 3, Double dashed, 0.05m wide, 0.05m separation, 9.15/3.05m gap/stripe	Single solid control line 0.1m wide	Type 3, Double dashed, 0.05m wide, 0.1m separation, 9.15/3.05m gap/stripe	2
4	Type 4, Double dashed, 0.05m wide, 0.2m separation, 10.98/1.22m gap/stripe	Type 4, Double dashed, 0.05m wide, 0.15m separation, 10.98/1.22m gap/stripe	Type 4, Double dashed, 0.05m wide, 0.05m separation, 10.98/1.22m gap/stripe	Single solid control line 0.1m wide	Type 4, Double dashed, 0.05m wide, 0.1m separation, 10.98/1.22m gap/stripe	1

treatment. The distances were measured to the nearest 2.54 cm by the assistant experiments. As soon as the run was completed, the subject was instructed to drive the car to the next starting position, which was given by the experimental design protocol. Each subject performed three replications. One subject always performed ten runs (five eastbound, five westbound) within which the line number was completely randomized. The detection distances were not adjusted for the experiment's reaction time to drop the sandbag, or for the drop time; therefore, all the actual detection distances may be about 10 ft longer.

RESULTS

Some subjects could sometimes detect the beginning, especially of Type 1 double solid, 0.1 m wide and of the single solid control line 0.1 m wide, already from the starting position, because the runway did not provide enough approach run length for these conditions. This experimental artifact has artificially reduced the begin-detection distances for these conditions to some degree. However, to provide a complete account of the experimental results, the begin distances are displayed nevertheless. It is likely that the begin-and-end detection distances would be closer together for a longer approach length. Figure 3 shows the group 1 psychometric curves for new yellow double solid center stripes 0.05 m wide with the lat-

eral separations 0.05, 0.1, 0.15, and 0.2 m, as a function of the begin-and-end detection distance. It can be seen from the figure that the end-detection distances are somewhat longer than the begin-detection distances. Within the begin-detection distances there is an obvious lack of an effect caused by lateral center stripe separation (Line 3 with 0.05 m of lateral separation, Line 1 with 0.1 m lateral separation, Line 4 with 0.15 m lateral separation, and Line 5 with 0.2 m lateral separation). Within the end-detection distance cluster for the Group 1 data indicated in Figure 3 one can observe a slight tendency for the larger lateral separations to provide slightly longer detection distances. Line 5 with the 0.2-m lateral separation seems to provide the longest end-detection distances followed by Line 4 with 0.15 m of lateral separation. Line 3 with the 0.05-m lateral separation seems to provide the shortest end-detection distances for Group 1. The ANOVA, which was conducted for Group 1, confirmed the observations that were made on the basis of Figure 3 because the line number is slightly significant. A Scheffe post hoc test, which was conducted for Group 2, identified, as expected, a significant difference between Line 1 (0.1 m of lateral separation), Line 3 (0.05 m of lateral separation), and Line 4 (0.15 m of lateral separation) and Line 5 (0.2 m lateral separation).

Figure 4 shows the Group 2 psychometric curves for new yellow 0.1-m-wide double solid center stripes with the lateral separations 0.05, 0.1, 0.15, and 0.2 m as a function of the begin-and-end detection distance. The figure indicates that the end-detection distances are

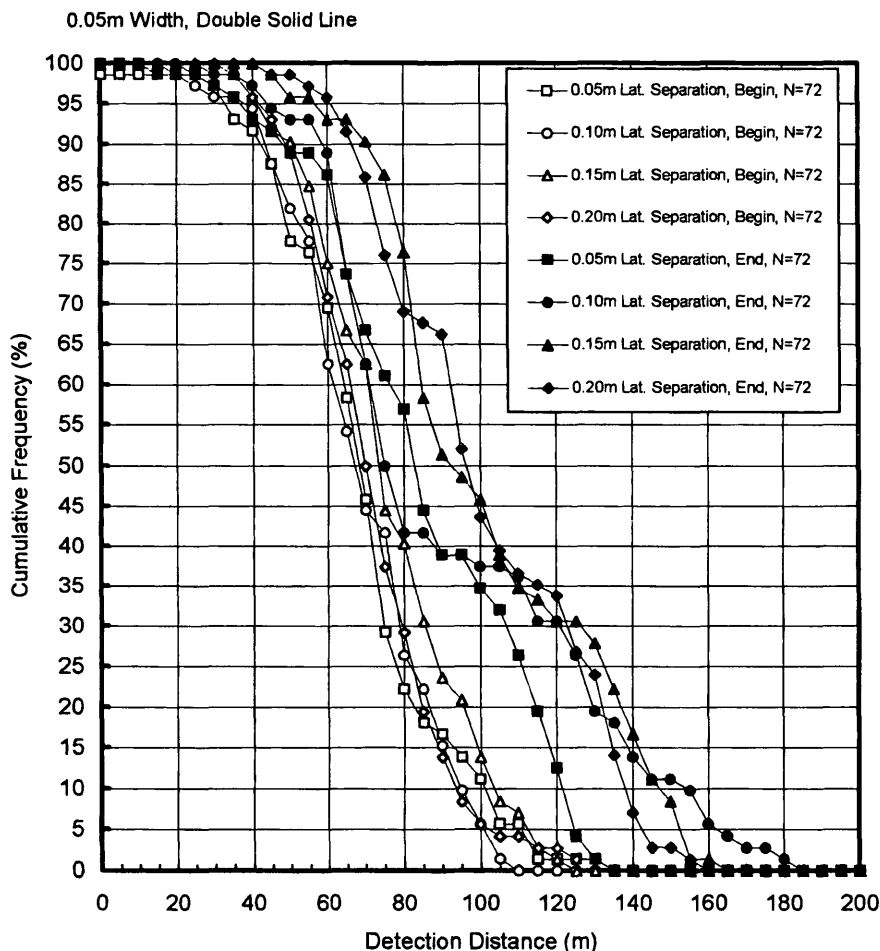


FIGURE 3 Group 1 psychometric curves showing cumulative frequency (percent) for begin and end detection distance of new yellow 0.05-m-wide solid center stripes with lateral separations of 0.05, 0.1, 0.15, and 0.2 m on concrete road surface under low-beam illumination at night as function of detection distance (in meters). Begin detection distance values may be too short because of limited available approach distance.

considerably longer than the begin-detection distances. The analysis of variance (ANOVA) that was conducted for Group 2, confirmed a highly significant difference between the begin-and-end detection distances. Within both the begin-detection distance cluster and the end-detection distance cluster, there is an obvious lack of an effect caused by lateral center stripe separation. The Group 2 ANOVA further indicated that line type (Types 1 to 4) is insignificant, that is, lateral separation does not have a significant effect. A Scheffe post hoc test that was conducted for Group 2, as expected, did not indicate any statistical significance caused by the lateral separation.

Figure 5 shows the Group 3 psychometric curves for new yellow 0.05-m-wide double-dashed center stripes with lateral separations 0.05, 0.1, 0.15, and 0.2 m and a gap/stripe ratio of 9:15/3:05 m as a function of the detection distance. Observations similar to the ones made for Group 2 can be made. However, it can be seen that the difference between begin-and-end detection distance is considerably smaller, probably because of the dashed line treatments. Again, within both the begin-and-end detection distance cluster there is no

significant effect because of lateral separation. The ANOVA, which was conducted for Group 3 indicated that the factor line type (Types 1 through 4) was significant. However, a close investigation of the Group 3 data with a Scheffe post hoc test, revealed that the significance was always against Line 2, which is the single solid control line. Therefore, no statistical significance caused by the lateral separation between the double center stripe pavement markings was indicated by the post hoc test.

Figure 6 shows the Group 3 psychometric curves for new yellow 0.05-m-wide double-dashed center stripes with lateral separations 0.05, 0.1, 0.15, and 0.2 m and a gap/stripe ratio of 10.98/1.22 m as a function of the detection distance. The difference between begin-and-end detection distance is even smaller for this group. It seems that the gap/stripe ratio has an effect on the difference between begin-and-end detection distance. Within both the begin-and-end detection distance cluster there is only a small statistical significance in terms of lateral separation between Lines 4 and 1 (as indicated by the Group 4 Scheffe post hoc test). The ANOVA, which

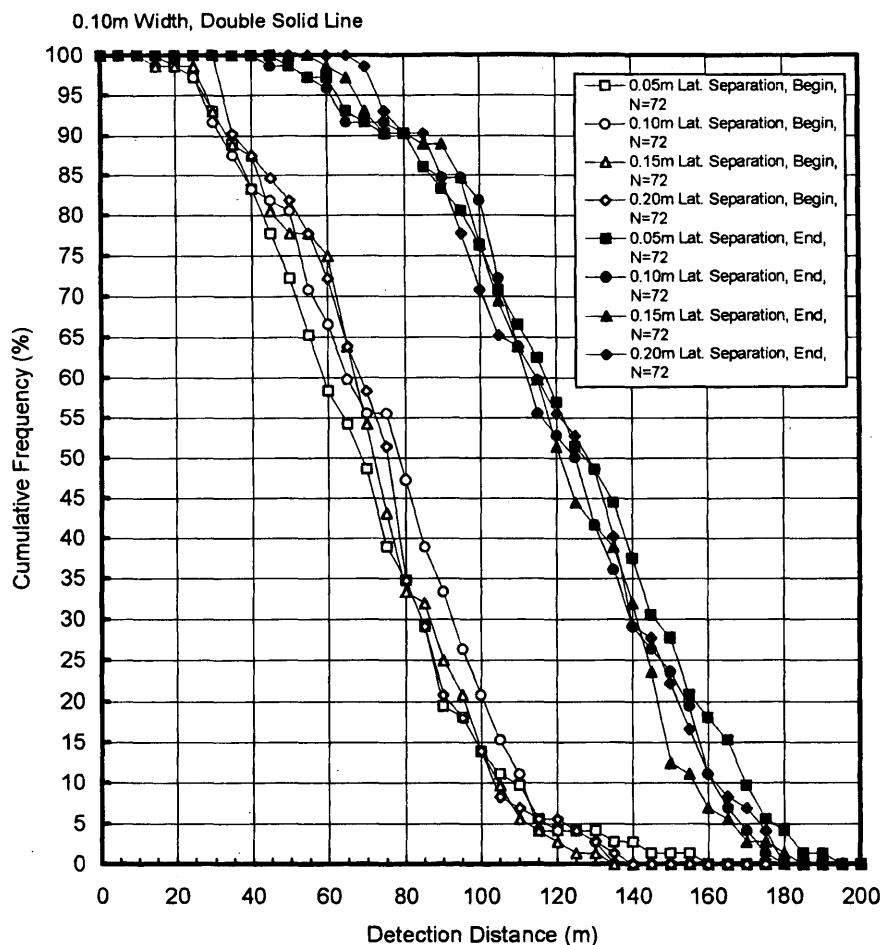


FIGURE 4 Group 2 psychometric curves showing cumulative frequency (percent) for begin and end detection of new yellow 0.1-m-wide double solid center stripes with lateral separations of 0.05, 0.1, 0.15, and 0.2 m on concrete road surface under low-beam illumination at night as function of detection distance (in meters). Begin detection distance values most likely are too short because of limited available approach distance.

was conducted for Group 4, indicated that the factor line type (Types 1 through 4) was significant. However, a close investigation of the Group 4 data with a Scheffe post hoc test again revealed that the significance was against Line 2 (with the exception of a very slight difference between Lines 1 and 4), which is the single solid control line. Overall from the psychometric curves, from the ANOVA and the Scheffe post hoc tests, there appears to be no significant systematic effect caused by the lateral separation between center lines. Figure 7 shows a comparison of the average begin/end, east/west detection distances as a function of lateral separation (0.05, 0.1, 0.15, 0.2 m) for 0.05 and 0.1-m-wide double solid center stripes. The figure again demonstrates that there is no effect caused by lateral separation because the detection distances within one line width and approach direction are almost the same for the 0.05, 0.1, 0.15, and 0.2-m lateral separation. Figure 8 shows a comparison of the average begin/end, east/west detection distances as a function of lateral separation (0.05, 0.1, 0.15, and 0.2m) for 0.05-m-wide double-dashed center stripes with a gap/stripe ratio of 9.15/3.05 m and 10.98/1.22 m. No systematic effect caused by lat-

eral separation can be found. Both Figures 7 and 8 generally show somewhat longer begin-and-end detection distances in the east-bound direction. This observation was confirmed by the ANOVAs that were conducted on data from Groups 1 through 4. The slightly longer east-bound begin-and-end detection distances may be attributed to the darker night horizon background, which was present in the eastbound direction.

Figure 2a shows the effect of available retroreflective area on the 85th percentile detection distance for center stripe Types 1 through 4. The begin-detection distances are not shown in this graph because some subjects have detected some of the lines already at the starting position. This has artificially reduced the begin-detection distances to some degree for some conditions. A more retroreflective area (wider lines or solid rather than dashed lines, or all of these) generally results in somewhat longer detection distances for detection of the end. However, it can be clearly seen from Figure 2(a) that there appear to be severe limitations in terms of increasing the detection distances by increasing the amount of retroreflective material used. The positive effects of using more retroreflective material may be

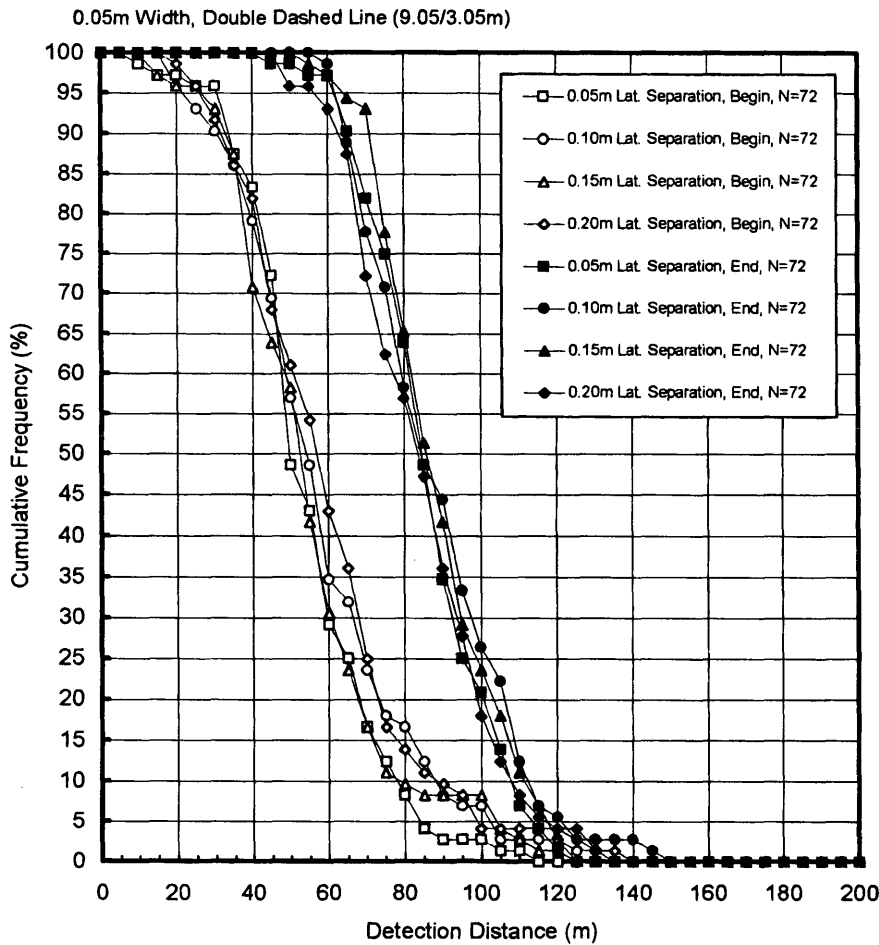


FIGURE 5 Group 3 psychometric curves showing cumulative frequency (percent) for begin and end detection distance of new yellow 0.05-m-wide double-dashed center stripes with lateral separations of 0.05, 0.1, 0.15, and 0.2 m and gap/stripe ratio of 9.15/3.05 m on concrete road surface under low-beam illumination at night as function of detection distance (in meters). Begin detection distance values may be too short because of limited available approach distance.

gradually outdone by the increased cost for the additional material. Further, Figure 2a indicates that the gain in the 85th percentile end-detection distance as a function of retroreflective material area seems to asymptotically approach a maximum of about 85 m. The reason for this asymptotic detection distance curve shape may be found in the limited reach of the low-beam headlamps (80 to 100 m) and the shallow entrance and observation angles that are present at such distances, which generally reduces the photometric effectiveness of the retroreflective material. The amount of retroreflective material (0.05, 0.1, 0.15, or 0.2 m width, double solid versus dashed, 9.15/3.05 m versus 10.98/1.22 m gap/stripe ratio) has a fairly small effect on the 85th percentile end-detection distances, thus indicating a relatively small marginal gain in visibility with a substantially increased retroreflective area. In fact, calculations indicate that an increase in area from 0.122 to 2.44m² for each 12.2-m-long center line segment (20-fold increase, see Table 2) is required to increase the average end-detection distance from about 82 to 128 m, which is an increase of only 56 percent. However, because of logistic constraints, it was necessary to use two experimental vehicles. Some

additional variability caused by differences in headlamps and windshield transmission was likely being introduced.

DISCUSSION AND CONCLUSIONS

A review of the technical literature about the visibility of center stripes has indicated that, with the exception of the data provided by Zwahlen and Schnell (1) there seems to be no availability of pavement marking visibility data in terms of begin-and-end detection distances. Further, the literature does not seem to provide any information about the effect of lateral separation between double center-stripe pavement markings on visibility. This study was conducted to overcome this apparent lack of information. New pavement markings were used in this lateral separation study because no feasible method was available to degrade new pavement markings uniformly to some specified "used" condition. The use of the minimum specified dimension center stripes (0.05 m wide) was intended to somewhat counteract the newness of the used pavement marking

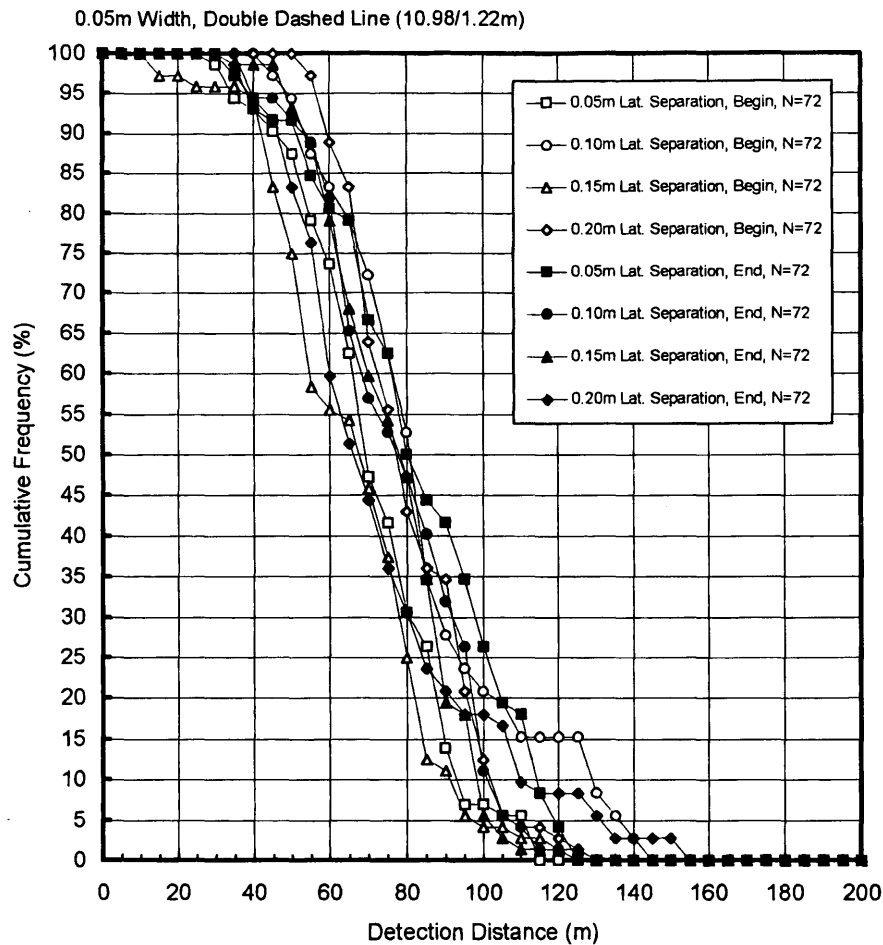


FIGURE 6 Group 4 psychometric curves showing cumulative frequency (percent) for begin and end detection distance of new yellow 0.05-m-wide double-dashed center stripes with lateral separations of 0.05, 0.1, 0.15, and 0.2 m and a gap/stripe ratio of 10.90/1.22 m on concrete road surface under low-beam illumination at night as function of detection distance (in meters).

TABLE 2 Begin and End Detection Distances as Function of Lateral Separation, Approach Direction, Center Stripe Type, and Gap Space

Separation		5 cm			10 cm			15 cm			20cm		
		Avg.	SD.	N	Avg.	SD.	N	Avg.	SD.	N	Avg.	SD.	N
0.1 m Double Solid Line													
Begin	East	88.9	30.5	36	73.1	27.6	36	75.4	29.9	36	83.5	28.2	36
	West	60.1	19.6	36	85.6	28.9	36	77.9	21.1	36	73.3	20.7	36
End	East	146.6	31.3	36	121.1	30.4	36	131.5	29.1	36	136.7	31.7	36
	West	114.6	30.4	36	132.7	32.0	36	121.1	27.3	36	120.5	27.5	36
0.05 m Double Solid Line													
Begin	East	79.6	24.8	36	69.3	18.2	36	81.9	24.1	36	81.5	21.9	36
	West	67.0	18.9	36	76.6	20.7	36	78.6	17.6	36	70.1	13.3	36
End	East	84.1	31.1	36	89.1	36.3	36	101.9	30.2	36	100.5	32.9	36
	West	96.1	22.5	36	106.9	38.4	36	112.1	30.7	36	108.0	28.5	36
0.05 m Double Dashed Line(9.15/3.05)													
Begin	East	63.4	18.5	36	55.8	20.1	36	60.2	23.7	36	67.5	27.4	36
	West	54.5	16.8	36	68.9	25.1	36	58.4	21.2	36	60.2	18.8	36
End	East	99.3	11.8	36	83.6	14.8	36	92.4	15.2	36	97.4	18.3	36
	West	81.6	14.8	36	102.1	19.9	36	94.1	16.4	36	80.6	15.2	36
0.05 m Double Dashed Line(10.98/1.22)													
Begin	East	89.0	15.2	36	73.9	13.6	36	70.7	24.7	36	87.9	18.2	36
	West	62.7	14.3	36	103.5	26.5	36	69.3	18.5	36	82.6	15.4	36
End	East	94.6	18.8	36	78.4	19.0	36	79.6	19.1	36	84.4	32.6	36
	West	79.2	26.3	36	86.4	20.1	36	82.6	16.7	36	71.2	18.8	36

Note: Begin Detection Distance values maybe too short due to limited available approach distance

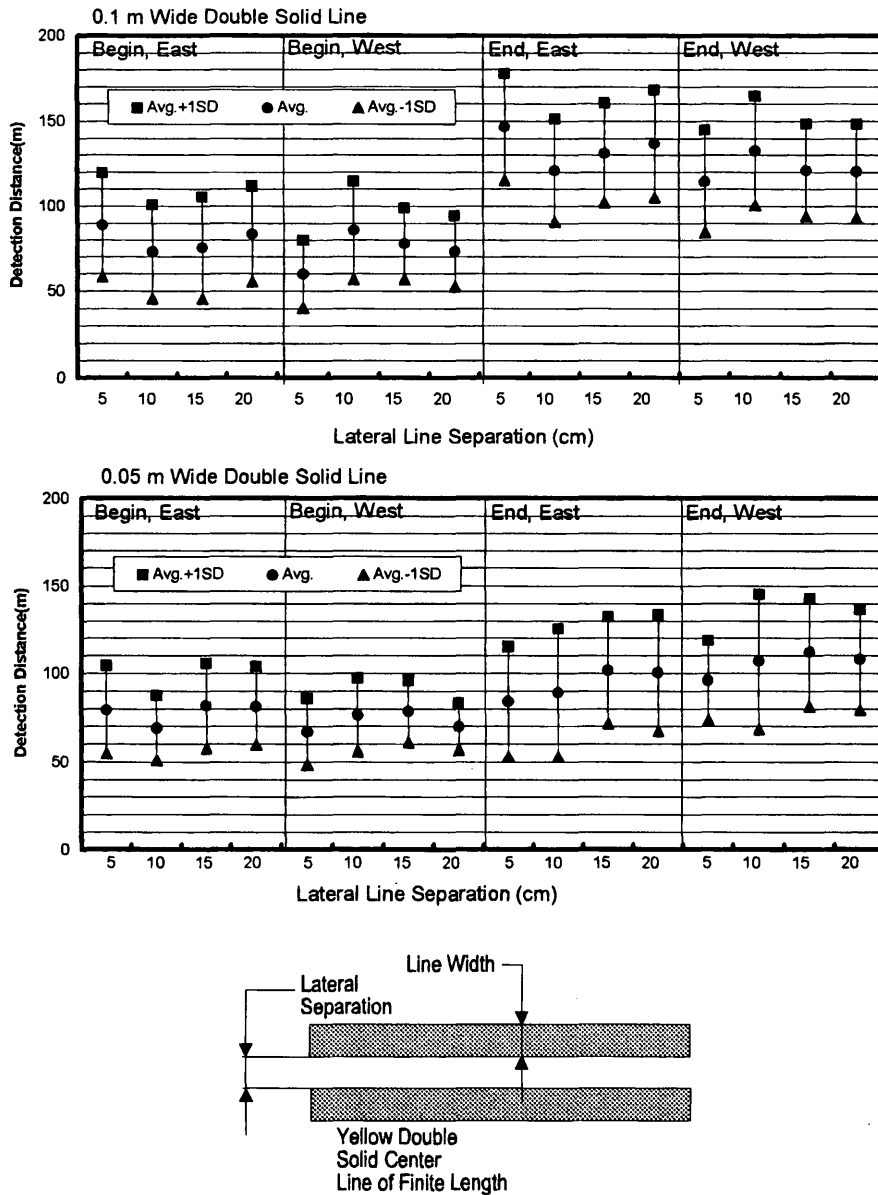


FIGURE 7 Comparison of average begin and end, east/west detection distances as function of lateral separation (0.05, 0.1, 0.15, and 0.2 m) for 0.05- and 0.1-m-wide double solid center stripes. Begin detection distance values for 0.1-m-wide double solid line is most likely too short; begin detection distance values for 0.05-m-wide double solid line may be too short because of limited available distance.

tapes. This research may also have some value for the cost-effective installation of enhanced "coded" temporary center stripes in newly resurfaced zones. It was initially hypothesized that increased lateral separation between double center stripes may increase the detection distance because the human visual system would spatially integrate over the space between the lines to form a more visible target that subtends a greater visual angle. This study investigated the effect of various lateral separations (0.05, 0.1, 0.15, and 0.2 m) for double solid and for double-dashed center stripes with a gap/stripe ratio of 9.15/3.05 m and 10.98/1.22 m. Average begin-and-end detection distances were established and psychometric curves were plotted.

An ANOVA and Scheffe post hoc test failed to find any consistent statistically significant systematic effect caused by lateral separation. On the basis of the findings of this study one may tentatively conclude that the lateral separation between the center stripes (from 0.05 to 0.2 m) under the investigated conditions does not appear to be a useful method to increase driver visibility in a practically significant manner. However, if on the other hand one would want to increase the lateral separation between double center stripes to possibly increase the lateral separation between opposing vehicles on two-lane roads, there appear to be no significant difficulties in terms of driver visibility.

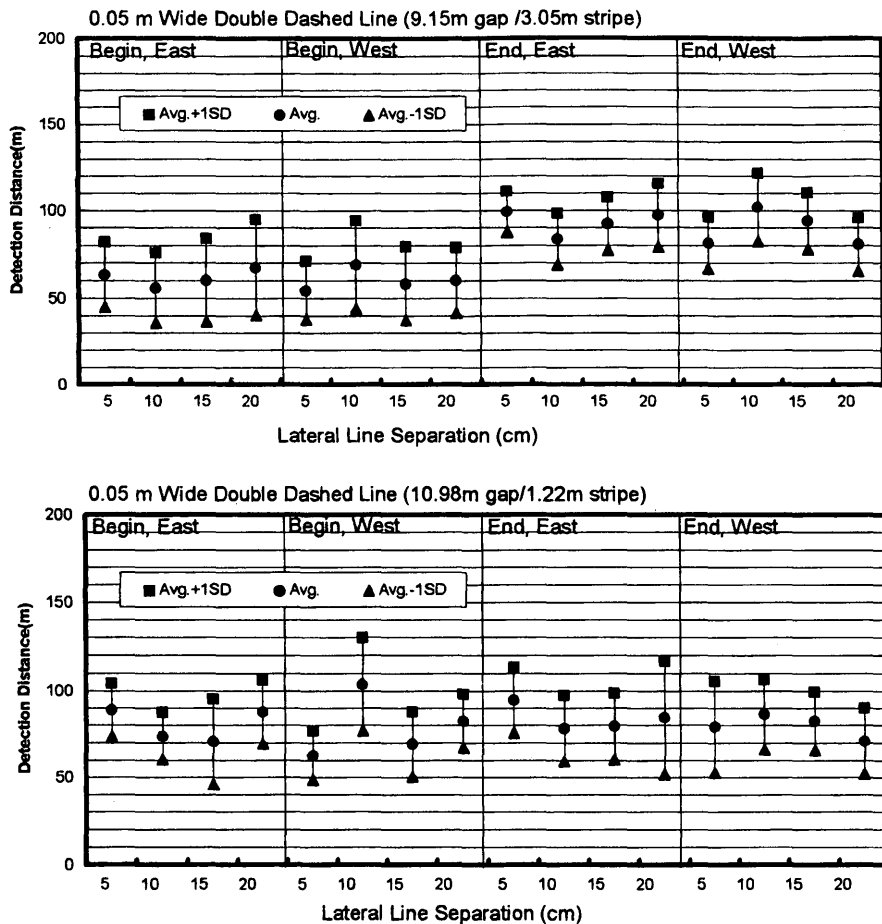
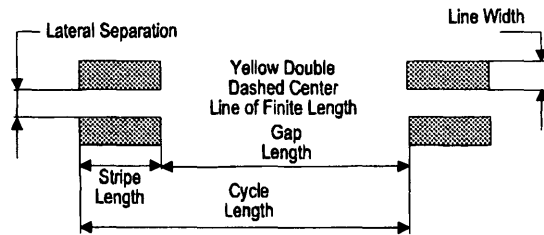


FIGURE 8 Comparison of average begin and end, east/west detection distances as function of lateral separation (0.05, 0.1, 0.15, and 0.2 m) for 0.05-m-wide double-dashed center stripes with gap/stripe ratio of 9.15/3.05 m and 10.98/1.22 m. Begin detection distance values may be too short because of limited available approach distance.



REFERENCES

1. Zwahlen, H. T., and T. Schnell Visibility of New Pavement Markings at Night Under Low Beam Illumination. Paper Presented at 73rd Annual Meeting of the Transportation Research Board, Washington, D.C., Jan. 1994.
2. Dudek C. L., et al. Field Studies of Temporary Pavement Markings at Overlay Project Work Zones on Two-Lane, Two-Way Rural Highways, In *Transportation Research Record 1160*, TRB, National Research Council, Washington, D.C., 1988, pp. 22-31.
3. *Ohio Manual on Uniform Traffic Control Devices for Streets and Highways*, Division of Operations, Bureau of Traffic, Ohio Department of Transportation, Columbus, Ohio, 1972.

4. *Manual on Uniform Traffic Control Devices for Streets and Highways*, FHWA, U.S. Department of Transportation, 1988.
5. Cotrell, B. H., Jr. Evaluation of Wide Edgelines on Two-Lane Rural Roads. In *Transportation Research Record 1160*, TRB, National Research Council, Washington, D.C., 1988, pp. 35-44.
6. *Visual Aspects of Road Markings*. CIE Joint Technical Report 73. CIE/PIARC, Vienna, 1988.
7. Saito, M. N. J., Garber. Lane Markings and Traffic Characteristics on Two-Lane Highways. *ITE Journal*, Aug. 1985.

Publication of this paper sponsored by Committee on Visibility.

Curve Radius Perception Accuracy as Function of Number of Delineation Devices (Chevrons)

HELMUT T. ZWAHLEN AND JIN YOUNG PARK

Monocular and binocular curve radius perception accuracy of ten young drivers under curve approach and nighttime conditions using a 1:50 scaled laboratory setup was investigated. The experiment consisted of a sequential comparison of a 90 degree segment of a right curve with a standard radius equipped with 12 equally spaced 1:50 scaled retro-reflective yellow/black miniature chevron signs with a 90 degree segment of a test curve (right curve), which could have either two, three, four, or eight equally spaced 1:50 scaled retroreflective miniature chevron signs along a curve radius of either 95, 97.5, 100, 102.5, or 105 percent of the standard curve radius. For each experimental presentation the standard curve was presented first to the subjects (black road environment and chevrons illuminated by electrically controlled headlamps) for 2 sec, then the subjects rotated 90 degrees and were presented with the test curve (one of five curve radii, with either two, three, four, or eight equally spaced chevrons) for 2 sec. A forced-choice response (smaller, larger than standard curve radius) was required from the subjects. All experimental conditions five radii, four chevron levels, five replications for each subject) were randomized within a viewing condition for each subject. The curve approach viewing distance from the subject's eyes to the beginning of the 90 degree segment of the curve was 4.57 m (15 ft), which represents 228.6 m (750 ft) in the real world, whereas the curve radius of the standard curve was 0.914 m (3 ft), which represents a curve radius of 45.6 m (150 ft) (38 degrees of curvature) in the real world (moderately sharp curve). All chevrons were within a total visual field of view of about 11 degrees. The overall averages for the percentage of the number of correct responses were calculated for the two, three, four and eight-chevron conditions for each radius of the test curve for binocular viewing and monocular viewing, and these percentages were plotted against the number of chevrons. On the basis of the results of this study, it is safe to tentatively state that the average of correct responses for the 95, 97.5, 102.5, and 105 percent curve radii increases for the binocular viewing conditions from 56 percent for two chevrons, to 62.5 percent for three chevrons, to 82.5 percent for four chevrons, and remains about the same (81.0 percent) for eight chevrons. For monocular viewing, the average correct responses increase from 50 percent for two chevrons, to 64 percent for three chevrons, to 70.5 percent for four chevrons, and remains about the same (72.5 percent) for eight chevrons. Overall, for the five test curve radii and for the four chevron levels, the binocular viewing condition (especially for four and eight chevrons) produces on the average a somewhat higher overall average value for correct responses (70.6 percent versus 64.3 percent monocular). On the basis of analysis of variance, the curve radii, the number of chevrons, and the viewing conditions are all statistically highly significant factors (0.05 level, interactions not significant). Considering the monocular results as more applicable for the real-world curve approach, it is concluded that, for the conditions investigated in this study, four equally spaced chevrons within a total visual field of about 11 degrees provide adequate curve radius estimation cues for unfamiliar drivers approaching a curve at night.

Many run-off-the-road (ROR) vehicular accidents occur on curves, especially at night. Limited advance information about the sharpness of a curve and excessive speed have been identified as primary reasons for these accidents. Initially, when the first roads were built, there was no warning system in place to provide an unfamiliar driver with information about the existence and the sharpness of a curve ahead. Along with the development and the increased paving of the road network, a curve warning sign system was designed and installed on selected curves, which provided a driver with advance information that either a curve or a turn (a very sharp curve) was ahead. At a later time, retroreflective pavement markings were added (center line, edge lines) and advisory speed plates were added to the upgraded retroreflective advance curve-and-turn warning signs. Among others, Zwahlen (1) investigated the effects of advisory speed plates and found no speed-reducing effects. Further, a retroreflective black arrow (on a yellow background) sign was placed in the beginning section of selected curves to indicate to an unfamiliar driver exactly where the curve started. All these devices were helpful, especially to an unfamiliar driver at night, but they did not provide any specific visual curve radius information or cues. Recently, more and more chevrons, or other discrete delineation devices, were placed in selected curves to provide a driver with curve radius information or cues. Also, spacings for curve delineation devices were established by Zwahlen and others (2,3; and in a paper in this Record). These spacings were mainly based on photometric calculations and assumed that four discrete delineation devices should be visible to a driver under low-beam night driving conditions. It is hypothesized that by providing drivers with actual curve radius information before they enter the curve, most unfamiliar drivers will be able to adjust their speeds more appropriately and therefore drive with a larger margin of safety through the curves, especially at night. Further, the Ohio Manual of Uniform Traffic Control Devices [OMUTCD (4)] specifies that the spacing of chevron alignment signs (on the outside of a curve or sharp turn) shall be such that the motorists always have two in view and that they should be visible for at least 152.4 m (500 ft). No research studies were found that could justify the "two-in-view" chevron rule, and there is no quantitative information available for the angular extent of the field of view. It was the objective of this study to find a suitable experimental paradigm and to investigate the binocular and monocular (more realistic for curve approach) curve radius perception accuracy of young drivers under curve approach and nighttime conditions as a function of the number of equally spaced chevrons in a 90 degree segment of a moderately sharp right curve. Since the observation conditions of the stimuli were such that they represented a right curve ahead in a real driving situation as seen from about 228 m (750 ft), it seemed to be reasonable to assume that

the perceptual accuracy would not be influenced by vehicle motion. The initial angular rate of a change per unit time for the displayed chevrons in a driver's visual field, when approaching curves viewed from a relatively far distance ahead is generally small and negligible from a perception point of view.

METHOD

Subjects

Ten young subjects (drivers) were used for both the monocular (preferred, better-eye) viewing condition and the binocular viewing condition. All drivers had valid U.S. driver's licenses, normal vision, and contrast sensitivity.

Experimental Apparatus

A black observation booth was constructed in which the subject was seated on a rotating chair and could view the standard right curve (level surface, outlined with 12 equally spaced miniature chevrons, height 12.2 mm, width 9.1 mm) and after a 90 degree head and body turn to the test curve (level surface, right curve, one of five different radii, with either two, three, four, or eight equally spaced miniature chevrons). Figure 1 illustrates the experimental setup. Two electrically controlled headlamp sets were used to illuminate the

miniature chevrons on the two black presentation tables with black backgrounds. Luminances of the miniature chevrons were measured and adjusted (by voltage and aiming of the lamps) so that the 1:50 scaled laboratory situation provided similar luminances as were found in the real world (see Figure 2). The change in the appearance of the color yellow of the miniature retroreflective chevrons (3M high intensity) caused by the lower operating voltage (lower than 12.8 volts) and subsequent lower-color temperature of the headlamps was not noticeable to the subjects and was not considered to be a significant factor in this study. The total field of view of the 90 degree curve segment containing the chevrons for the investigated curve approach situation was about 11 degrees. Subject eye height with respect to the presentation tables and the miniature chevrons was also adjusted to fit the 1:50 scale.

Experimental Design

The major independent variable was the number of equally spaced chevrons used to indicate the sharpness of a 90 degree curve segment displayed 4.57 m (15 ft) ahead of a subject's eye(s). The other two independent variables were the viewing condition and the radius of the test curve. The dependent variable was the forced-choice response, which indicated whether the test curve radius was perceived as greater or smaller (curve sharpness) than the standard curve radius in the sequential comparison with 2 sec of exposure time for each presentation.

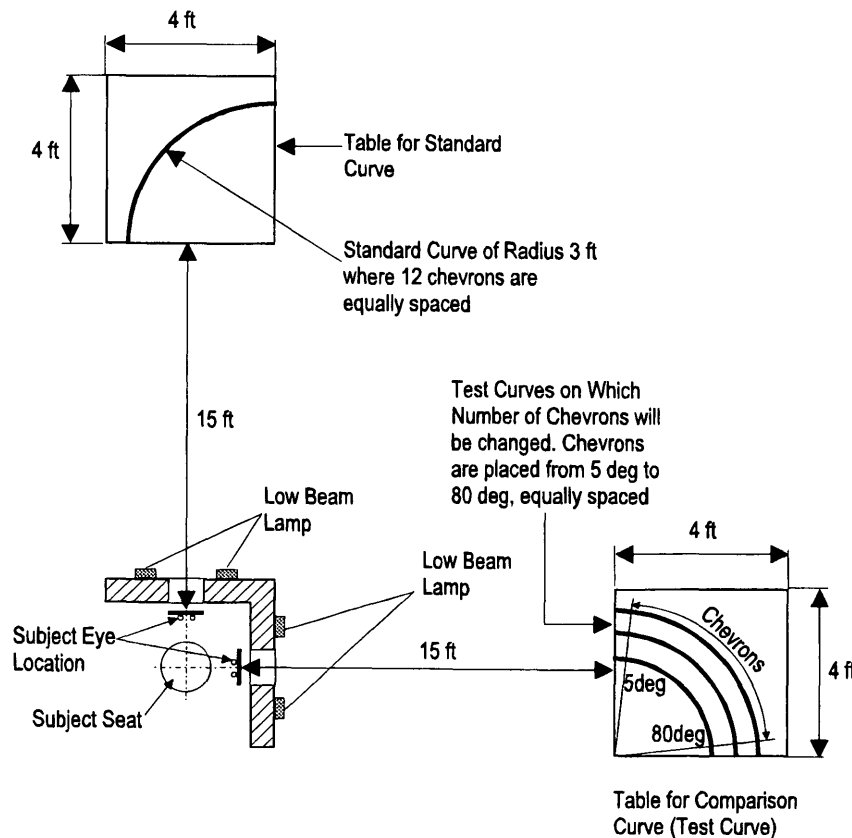


FIGURE 1 Plan view of experimental setup.

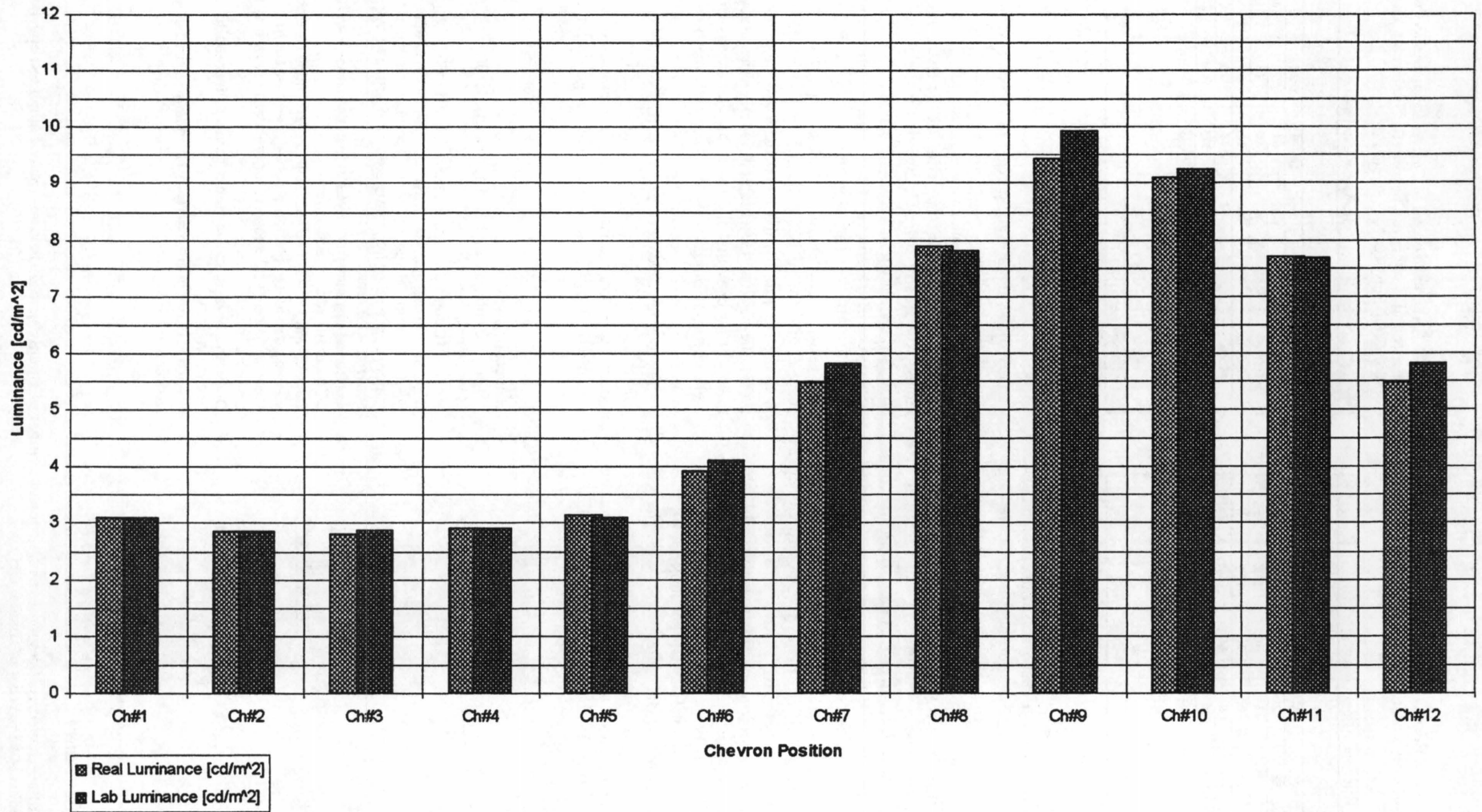


FIGURE 2 Comparison of real luminances (field) and laboratory luminances for 12 equally spaced chevrons (Ch) along standard curve (laboratory headlamps: current = 11A, voltage = 6 V).

TABLE 1 Average percent of Correct Responses as Function of Curve Size and Number of Chevrons for Binocular Conditions (10 Subjects, N = 50 per cell)

Curve Size	Number of Chevrons Level					Average % of C.R.
	Two	Three	Four	Eight	Total	
95%	64	70	88	84	306	76.5
97.50%	50	56	72	76	254	63.5
100%	54	54	46	58	212	53
102.50%	54	56	80	78	268	67
105%	58	68	90	86	302	75.5
Total	280	304	376	382	1342	
Avg. % of C.R., Excluding 100% Curve Size	56.5	62.5	82.5	81	282.5	70.625

C.R. = Correct Responses

TABLE 2 Average Percent of Correct Responses as Function of Curve Size and Number of Chevrons for Monocular Viewing Conditions (10 Subjects, N = 50 per cell)

Curve Size	Number of Chevrons Level					Average % of C.R.
	Two	Three	Four	Eight	Total	
95%	54	66	76	78	274	68.5
97.50%	52	62	64	70	248	62
100%	62	62	44	48	216	54
102.50%	44	56	68	66	234	58.5
105%	50	72	74	76	272	68
Total	262	318	326	338	1244	
Avg. % of C.R., Excluding 100% Curve Size	50	64	70.5	72.5	257	64.25

C.R. = Correct Responses

After an initial learning period, each subject was presented with 100 sequential comparison trials (five curve radii, four chevron Levels 2, 3, 4, and 8, and five replications) for the binocular viewing condition and the monocular viewing condition each. Although it would have been desirable to investigate the intermediate chevron Levels 5 through 7, it was decided that to keep the experimental duration reasonable for the subjects, chevrons Levels 5 through 7 were not of sufficient experimental interest. Further, from an economical point of view, having more than four chevrons within a visual field of about 11 degrees was not considered to be practical. The chevron level of 8 was added to see whether there would be, in fact, a considerable increase in the curve radius perception accuracy when going from four to eight chevrons.

The presentations within a viewing condition were completely randomized. One-half of the subjects started with the binocular viewing condition (total 100 trials per subject) first and then did the monocular viewing condition (total 100 trials per subject), whereas the other half of the subjects were tested in the reverse order. The percentage of correct responses for each test curve radius was then computed for each chevron number level and plotted and analyzed using analysis of variance (ANOVA) and other statistical techniques.

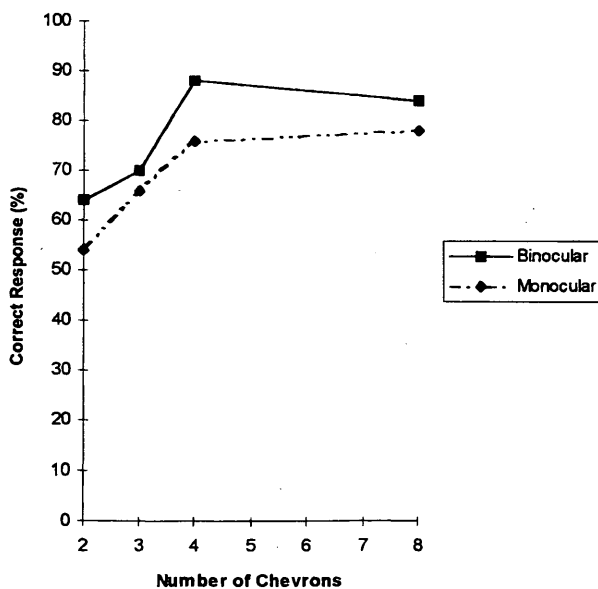


FIGURE 3 Average percent correct responses as function of number of equally spaced chevrons (placed along test curve from 5 to 80 degrees) with curve radius of 95 percent of standard curve.

RESULTS

Table 1 shows the average percent of correct responses as a function of the test curve size and the number of equally spaced chevrons for the binocular viewing condition. The average percent of correct responses as a function of the test curve size and the number of equally spaced chevrons for the monocular viewing condition are shown in Table 2. Figures 3 to 7 show the average percent correct responses as a function of the number of equally spaced chevrons (placed along the test curve from 5 to 80 degrees) for a given test curve radius (expressed in percent of the standard curve radius) for the binocular and monocular viewing condition. With the exception of the 100 percent test curve radius data (Figure 5), the increase in perceptual judgment accuracy from two to three to four chevrons and the rather flat extension from four to eight chevrons holds fairly well for both the binocular and the monocular viewing conditions. Table 3 and Figure 8 show the overall average percent correct responses for all chevron levels as a function of the five different test curve radii for the binocular and monocular (more realistic for curve approach situation) viewing conditions. It can be seen that the average percentage of correct

- Binocular vision
 - 10 subjects each 5 observations, N=50
- Monocular vision
 - 10 subjects each 5 observations, N=50
- Size of equally spaced chevrons (yellow retroreflective material) Width=9.1mm, Height=12.2mm, vertical distance from approximately eye level or from simulated road surface (level) to bottom of chevron = 28.4mm
- Horizontal distance from eyes to begin of curve = 4572 mm
- 95% curve radius = 868.7 mm
- Dark viewing conditions with reflectorized miniature chevrons
- Viewing sequence: Standard curve, then test curve
- Viewing Duration: 2 seconds for standard curve and 2 seconds for test curves
- Chevrons always shown within range 5 degrees to 80 degrees in test curves
- Standard curve delineated with 12 equally spaced chevrons using 0 degrees to 90 degrees.

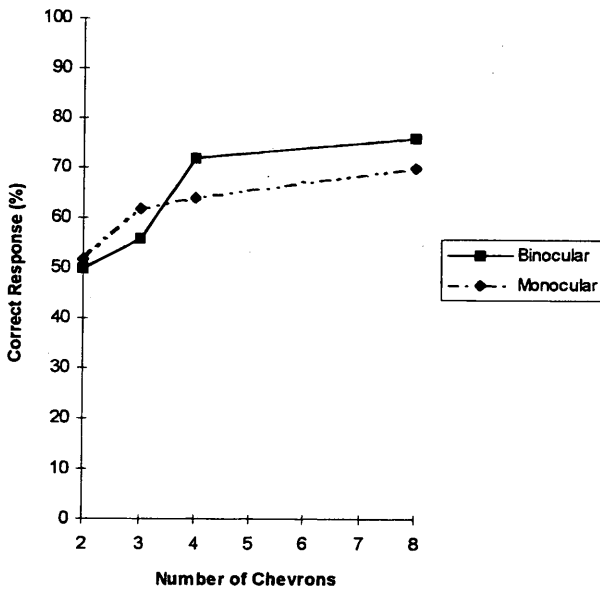


FIGURE 4 Average of percent correct responses as function of number of equally spaced chevrons (placed along test curve from 5 to 80 degrees) with curve radius of 97.5 percent of standard curve.

- Binocular vision
 - 10 subjects each 5 observations, N=50
- Monocular vision
 - 10 subjects each 5 observations, N=50
- Size of equally spaced chevrons (yellow retroreflective material) Width=9.1mm, Height=12.2mm, vertical distance from approximately eye level or from simulated road surface (level) to bottom of chevron = 28.4mm
- Horizontal distance from eyes to begin of curve = 4572 mm
- 97.5% curve radius = 891.5 mm
- Dark viewing conditions with reflectorized miniature chevrons
- Viewing sequence: Standard curve, then test curve
- Viewing Duration: 2 seconds for standard curve and 2 seconds for test curves
- Chevrons always shown within range 5 degrees to 80 degrees in test curves
- Standard curve delineated with 12 equally spaced chevrons using 0 degrees to 90 degrees.

responses increases from 53 and 54 percent (slight bias, 50 percent expected) at the 100 percent test radius almost linearly and fairly symmetrically with increasing or decreasing test curve radius. The steeper slope for the binocular viewing condition indicates its expected superiority over the monocular viewing condition. An ANOVA was performed for the binocular viewing condition for the curve size and the number of chevron factors. Although curve size and number of chevrons of the two factors are statistically highly significant, the interaction at the $\alpha = 0.05$ level is not. An ANOVA was also performed for the monocular viewing condition

for the curve size and the number of chevron factors. Again, the two factors—the curve size and number of chevrons—are statistically significant, although the interaction at the $\alpha = 0.05$ level is not. An ANOVA was performed to compare the binocular versus the monocular viewing condition and the number of chevron factors using 10 replications because each subject participated in both the binocular and the monocular viewing conditions. The viewing condition (binocular/monocular) and the number of chevrons are statistically highly significant, whereas the interaction at the $\alpha = 0.05$ level is not.

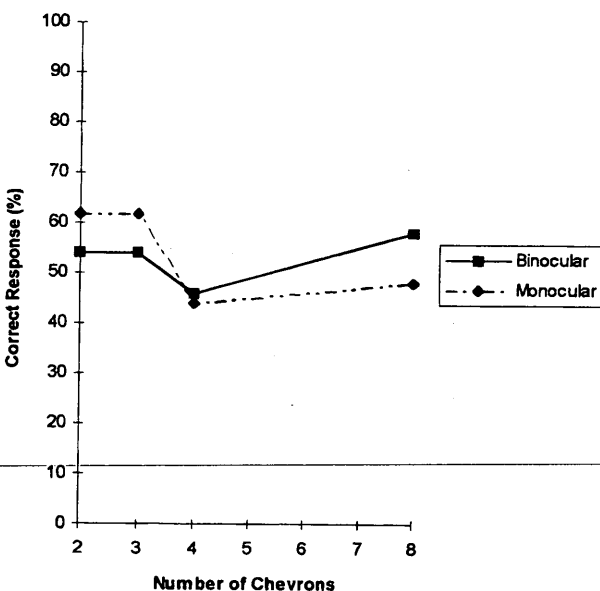


FIGURE 5 Average of percent correct responses as function of number of equally spaced chevrons (placed along test curve from 5 to 80 degrees) with curve radius of 100 percent of standard curve.

- Binocular vision
 - 10 subjects each 5 observations, N=50
- Monocular vision
 - 10 subjects each 5 observations, N=50
- Size of equally spaced chevrons (yellow retroreflective material) Width=9.1mm, Height=12.2mm, vertical distance from approximately eye level or from simulated road surface (level) to bottom of chevron = 28.4mm
- Horizontal distance from eyes to begin of curve = 4572 mm
- 100% curve radius = 914.4 mm (standard curve)
- Dark viewing conditions with reflectorized miniature chevrons
- Viewing sequence: Standard curve, then test curve
- Viewing Duration: 2 seconds for standard curve and 2 seconds for test curves
- Chevrons always shown within range 5 degrees to 80 degrees in test curves
- Standard curve delineated with 12 equally spaced chevrons using 0 degrees to 90 degrees.

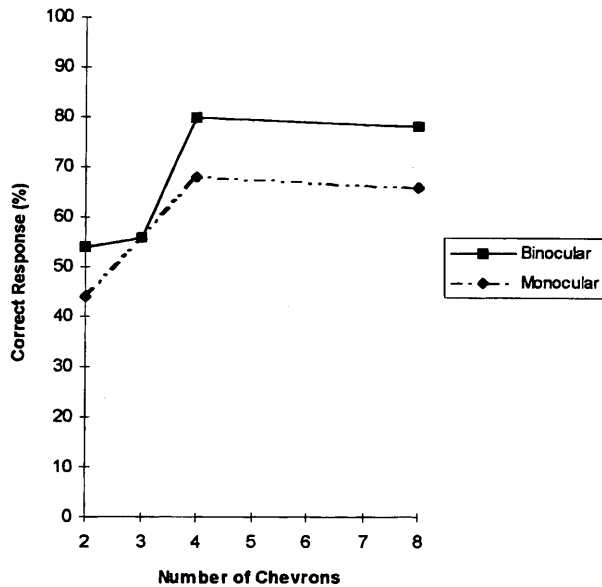


FIGURE 6 Average of percent correct responses as function of number of equally spaced chevrons (placed along test curve from 5 to 80 degrees) with curve radius of 102.5 percent of standard curve.

DISCUSSION AND CONCLUSIONS

An experimental paradigm had to be developed that would allow one to quantitatively assess the influence of the number of discrete delineation devices (within a defined field of view) on the accuracy of curve radius perception. Because a direct and absolute estimation of the curve radius (in meters or feet), or the curvature (in degrees) of a displayed curve (curvature in degrees = 1746.5 divided by radius in meters, or 5730 divided by radius in feet) is a hard task, for which regular subjects have little or no practical experience, an experimental paradigm had to be developed that would simplify a

- Binocular vision
 - 10 subjects each 5 observations, N=50
- Monocular vision
 - 10 subjects each 5 observations, N=50
- Size of equally spaced chevrons (yellow retroreflective material) Width=9.1mm, Height=12.2mm, vertical distance from approximately eye level or from simulated road surface (level) to bottom of chevron = 28.4mm
- Horizontal distance from eyes to begin of curve = 4572 mm
- 102.5% curve radius = 937.3 mm
- Dark viewing conditions with reflectorized miniature chevrons
- Viewing sequence: Standard curve, then test curve
- Viewing Duration: 2 seconds for standard curve and 2 seconds for test curves
- Chevrons always shown within range 5 degrees to 80 degrees in test curves
- Standard curve delineated with 12 equally spaced chevrons using 0 degrees to 90 degrees.

subject's perceptual response as much as possible while providing quantitative data relevant to the actual curve radius estimation task. A sequential comparison procedure (always standard curve presented first, then shortly after the presentation of the test curve) was therefore selected as the experimental paradigm because this method allows a subject to make a forced choice (smaller, larger-than-standard-curve) decision and because it can be argued that a higher perceptual accuracy (more correct responses) in this sequential comparison task would most likely also result in more accurate perceptual absolute judgments of the radii of curves in the real world. Further, if it is assumed that a portion of the ROR accidents

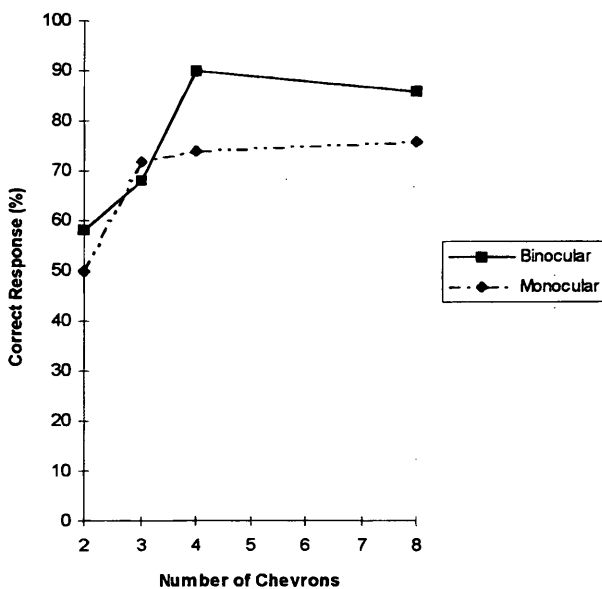


FIGURE 7 Average of percent correct responses as function of number of equally spaced chevrons (placed along test curve from 5 to 80 degrees) with curve radius of 105 percent of standard curve.

- Binocular vision
 - 10 subjects each 5 observations, N=50
- Monocular vision
 - 10 subjects each 5 observations, N=50
- Size of equally spaced chevrons (yellow retroreflective material) Width=9.1mm, Height=12.2mm, vertical distance from approximately eye level or from simulated road surface (level) to bottom of chevron = 28.4mm
- Horizontal distance from eyes to begin of curve = 4572 mm
- 105% curve radius = 960.1 mm
- Dark viewing conditions with reflectorized miniature chevrons
- Viewing sequence: Standard curve, then test curve
- Viewing Duration: 2 seconds for standard curve and 2 seconds for test curves
- Chevrons always shown within range 5 degrees to 80 degrees in test curves
- Standard curve delineated with 12 equally spaced chevrons using 0 degrees to 90 degrees.

TABLE 3 Overall Average Percent of Correct Responses of Each Test Curve Size for all Chevron Levels for Binocular and Monocular Viewing Conditions

Vision Type	Curve Size					Average % of C.R. Excluding 100% Curve Size
	95%	97.50%	100%	102.50%	105%	
Binocular	76.5	63.5	53	67	75.5	70.625
Monocular	68.5	62	54	58.5	68	64.25

C.R. = Correct Responses

in curves occur because drivers have perceptually underestimated the sharpness of a curve ahead (too high-speed for curve); then, providing drivers with an adequate number of discrete curve delineation devices such as chevrons may increase their perceptual judgment accuracy and may encourage them to adjust the speed more appropriately, resulting in a lower curve speed and a reduction in ROR accidents.

The developed experimental paradigm, although executed in the laboratory, is characterized by a high level of visual fidelity based on an accurate miniaturization (sizes, colors, luminances), a true three-dimensional presentation mode (superior over questionable two-dimensional slide, video, or driving simulator display presentations) and appears to provide useful quantitative answers with respect to the accuracy of curve radius perception as a function of the number of equally spaced delineation elements within a specified field of view. Further, the results obtained in this study match fairly well the results obtained in an earlier and similar exploratory study, in which four young subjects (drivers) were tested under monocular viewing conditions and seven young subjects (drivers) were tested under binocular viewing conditions (5). On the basis of these results, it is possible to tentatively conclude that for the conditions investigated four equally spaced discrete delineation devices, such as chevrons, within a total visual field of about 11 degrees provide adequate curve radius estimation cues for unfamiliar

drivers approaching a curve at night. The use of four instead of three discrete delineation devices such as chevrons within the specified visual field not only improves the perceptual accuracy slightly, but more important where one of the discrete delineation devices is missing (because of a collision, vandalism, etc.), the remaining three curve delineation devices will be able to provide a driver with a level of perceptual curve radius estimation cues that most likely produce judgment accuracy levels considerably superior to those where only two discrete delineation devices would remain visible to a driver within a specified visual field. With the recent introduction of continuously illuminated curve guidance sections (3M lighted guidance tubes), it would be interesting to investigate how much the perception accuracy of a curve radius for a curve ahead can be improved when compared with discrete delineation elements. It would also be of interest to conduct further research to investigate the effect of the extent of the visual field within which the discrete or continuous delineation devices are contained, the type, shape, photometric properties of delineation devices, the exposure time duration, and to determine whether the apparent leveling-off of the curve radius perception accuracy from four to eight or more discrete delineation devices is mainly caused by human information processing limitations or by the visual information acquisition limitations (limited exposure time duration of 2 sec to make a sufficient number of eye fixations), or a combination of both.

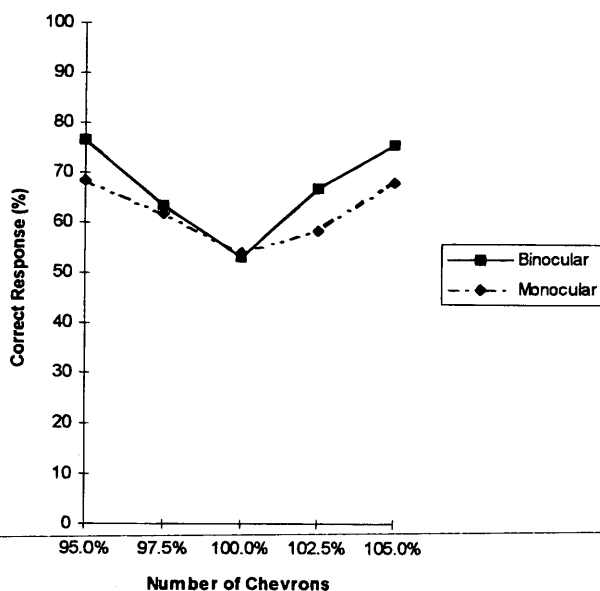


FIGURE 8 Overall average of percent correct responses as function of five different test curve sizes for binocular and monocular viewing conditions.

- Binocular vision
 - 5 different radii for each subject (95%, 97.5%, 100%, 102.5%, 105% radius of standard curve), 5 observations, N=250
- Monocular vision
 - 5 different radii for each subject (95%, 97.5%, 100%, 102.5%, 105% radius of standard curve), 5 observations, N=250
- Size of equally spaced chevrons (yellow retroreflective material) Width=9.1mm, Height=12.2mm, vertical distance from approximately eye level or from simulated road surface (level) to bottom of chevron = 28.4mm
- Horizontal distance from eyes to begin of curve = 4572 mm
- 95% curve radius = 868.7 mm
- 97.5% curve radius = 891.5 mm
- 100% curve radius = 914.4 mm (standard curve)
- 102.5% curve radius = 937.3 mm
- 105% curve radius = 960.1 mm
- Dark viewing conditions with reflectorized miniature chevrons
- Viewing sequence: Standard curve, then test curve
- Viewing Duration: 2 seconds for standard curve and 2 seconds for test curves. (95%, 97.5%, 100%, 102.5%, 105% radius of standard curve)
- Chevrons always shown within range 5 degrees to 80 degrees in test curves
- Standard curve delineated with 12 equally spaced chevrons using 0 degrees to 90 degrees.

REFERENCES

1. Zwahlen, H. T. Advisory Speed Signs and Curve Signs and Their Effect Upon Driver Eye Scanning and Driving Performance. In *Transportation Research Record 1111*, TRB, National Research Council, Washington, D.C., 1987, pp. 110–120.
2. Zwahlen, H. T. Driver Lateral Control Performance as a Function of Delineation. In *Visibility Highway Guidance and Hazard Detection Transportation Research Record 1149*, TRB, National Research Council, Washington, D.C., 1987, pp. 56–65.
3. Zwahlen, H. T., M. Miller, K. Mohammad, and R. Dunn. Optimization of Post Delineator Placement from a Visibility Point of View. In *Transportation Research Record 1172*, TRB, National Research Council, Washington, D.C., 1988, pp. 78–87.
4. *Ohio Manual of Uniform Traffic Control Devices for Streets and Highways*, Revisions 16 and 17. Ohio Department of Transportation, Columbus, 1992.
5. Zwahlen, H. T. *Curvature Perception Experiment Using Discrete Delineation Elements Under Simulated Nighttime Driving Conditions*. Human Factors and Ergonomics Laboratory Report, Ohio University, Athens, Dec. 1992.

Publication of this paper sponsored by Committee on Visibility.

Knowledge-Based Personal Computer Software Package for Applying and Placing Curve Delineation Devices

HELMUT T. ZWAHLEN AND THOMAS SCHNELL

The delineation of curves on rural two-lane highways in Ohio is the responsibility of traffic engineers in the Ohio Department of Transportation (ODOT). The traffic engineers currently use the Ohio Manual of Uniform Traffic Control Devices (OMUTCD) as a guide for the curve delineation planning and implementation. However, the rules that are given in the OMUTCD and the federal MUTCD do not guarantee that the curve delineation provides optimal, uniform information to the driver. OCARD (ODOT computer-aided road delineation), a knowledge-based system running on an MS DOS personal computer assists the user in the delineation task and treats similar or equal curves with the same traffic characteristics in exactly the same, consistent, and uniform way. The basis for the development of OCARD is the idea that an adequate number of roughly equally spaced delineation devices in a curve provides an unfamiliar driver with curvature information that may be helpful in the curve speed selection, thus resulting in fewer run-off-the-road accidents. The computed curve and delineation information can be stored and easily distributed if required. OCARD was carefully developed with regard to easy human-computer interaction. An extensive context sensitive on-line help utility describes the system, the required input data, the handling, all field measurement procedures, and the produced output data in great detail. As with any other software package it would be strongly recommended to use it only after the user has had adequate user training in obtaining the required measurements in the field and running a number of case studies using the system.

The Manual on Uniform Traffic Control Devices MUTCD (1) and the Ohio Manual of Uniform Traffic Control Devices OMUTCD (2) describe the application for a number of roadside delineation devices that may be used in curves on rural two-lane highways to provide drivers with visual cues that indicate the severity of the curve before they enter the curve. However, on the basis of an overall system point of view, there are no application guidelines in the federal MUTCD (1) and in the OMUTCD (2) that explicitly specify the prevalent physical or traffic conditions or both, in which a particular type or combination of types of roadside delineation devices would be optimal to apply from a driver visibility, performance, and safety point of view. Therefore, one can find curves on rural state highways in Ohio that are similar, have similar traffic characteristics, and are equipped with none or any one or any combination of the roadside delineation devices specified in the OMUTCD (2).

A survey of the current delineation practices used in the various states in the United States and provinces of Canada (3) found that the importance of the development of a set of quantitative guidelines seems to be recognized and desired by the surveyed traffic

engineers. Further, the survey indicates that there is no U.S. state or Canadian province that uses computer-assisted methods for the curve delineation task. At the same time 66 percent of the surveyed Ohio Department of Transportation (ODOT) district traffic engineers, 42 percent of the surveyed U.S. state traffic engineers, and 66 percent of the Canadian province traffic engineers expressed the desire and need for a computer-assisted curve delineation package such as OCARD (ODOT computer-aided road delineation).

A photolog analysis (3) of ODOT Districts 5 and 10 was conducted and the information about the delineation of the curves on selected two-lane rural highways was documented. The photologs contained recent frames (one to several years old) for each $\frac{1}{100}$ mi (16 m) of roadway. Surprisingly it was found in both districts that chevron signs are rarely used together with an arrow sign, even though an arrow sign by itself does not provide adequate curvature information, especially at night.

To make certain that there are no unexpected adverse effects caused by the curve delineation and to acquire more knowledge about the way traffic engineers tend to judge curves on rural two-lane highways and to delineate them according to their engineering judgment, an extensive before/after delineation evaluation involving 12 evaluators (ODOT/FHWA personnel) was conducted (3). From the answers of the interviewed evaluators the following can be seen: (a) even experienced evaluators have difficulties recommending the correct type, number, and location of curve delineation devices by just looking at a particular curve when driving through that curve at night with low beams; (b) subjective evaluation of an undelineated curve tends to provide a required number of devices that is too low; (c) the optimal type, number, and location of the delineation devices may be more accurately and more consistently determined by using a set of algorithms, which should be implemented in a computer software package to simplify their use, and (d) the opinion of an experienced evaluator is extremely valuable for the evaluation of a delineated curve. These findings supported the need for the development and use of a knowledge-based interactive delineation package such as OCARD.

In addition to the research mentioned earlier, a series of approach and center-speed measurements before and after installing curve delineation devices were conducted. The measurement results indicate that there is no systematic pattern in speed increase or speed reduction before and after the delineation devices are installed. The sharpness of tight curves may be emphasized by the delineation, thus leading to a speed reduction, whereas somewhat flatter curves may be more easily recognized as such, after the delineation is installed, thus leading to a speed increase. In both instances, it seems that the curve delineation appears to provide the perceptual basis for a more adequate curve speed selection.

From the above research, which was described previously (3), a number of delineation rules and algorithms were developed and implemented into OCARD. The system was carefully developed with respect to easy human-computer interaction. The computed delineation can be previewed both in a perspective view and in a top view. A hard copy of the preview screens can be printed if desired. OCARD not only computes the curve delineation devices but also specifies the type and advance location of the advance curve warning sign. In addition to this, OCARD creates a number of output documents that are used for the delineation material preparation in the warehouse during the actual delineation device installation in the curve and for reference purposes in the archive.

OCARD SYSTEM DESCRIPTION

The personal computer hardware (minimum 386 with math coprocessor) and software requirements have been described previously (3).

Field Tools

For the curve data acquisition in the field use of an electronic car compass to measure the heading change of the curve, an electronic digital level to determine the superelevation and grade in the curve, a distance measuring wheel to measure long distances such as the outside curve length, and a 100-ft tape for measuring the chord height and for measuring shorter distances such as the road width, is recommended. A can of white spray paint is needed to mark the beginning, the center, the location with the minimum curve radius and the end of the curve, as well as the maximum chord height (along the curve center line), which is needed to determine the minimum radius of the curve. The measured distances, superelevations, grades, and angles should be summarized on an empty data collection sheet while the user is in the field.

System Architecture

OCARD consists of a number of programs and control data files embedded in a software environment. Figure 1a illustrates how OCARD interacts with the external programs that are an integral part of the package. The user can operate OCARD with a mouse and a keyboard. The perspective view program and the top view program read the communication data files Persp.DAT and Topv.DAT on activation and display a perspective view or top view of the current curve. Context-sensitive help is provided in all data entry masks. A separate file handler program was required because Level5 Object 2.5 cannot easily access MS Windows common user dialogs (future releases of Level5 Object may offer this capability). The file handler is needed to create the curve data file that stores the curve geometry and other features of the curve and the delineation output files .GEO, .STC, and .DEL, which are generated by OCARD and can be edited or printed, or both. These files contain the geometrical curve data, a bill of materials for the delineation, and an instruction list containing the spacing distances needed to install the devices, respectively.

Level5 Object

A detailed description of Level5 Object V2.5 is found in the User's Guide (4) and the Reference Guide (5). Level5 Object is an

advanced tool to develop object-oriented, knowledge-based applications. During the development of OCARD a number of drawbacks of the Level5 Object 2.5 development system became evident.

1. The MS Windows drop-down menus are completely missing;
2. Access to common dialog boxes of MS Windows is not possible. For this reason it was necessary to build an external file handler;
3. The drawing tools needed to place and design the items of the graphical user interface are difficult to handle;
4. Documenting the code is impossible;
5. Generated code is hard to read because of the many line breaks produced by the output processor;
6. Compiled knowledge bases usually become very big;
7. Bitmap pictures that are used in the application are stored external to the knowledge base. Level5 Object does not purge old or obsolete versions of these bitmap files. This causes the hard disk to fill up quickly during the application development phase. Manually purging the hard disk is time consuming; and
8. Level5 Object requires the user to purchase a run time license.

In spite of these drawbacks (some may actually be eliminated by future releases of Level5 Object), the expert system shell Level5 Object provided the required flexibility to model the curve delineation task, which uses geometric calculations and rule-based knowledge.

CURVE DATA INPUT

Menu Structure

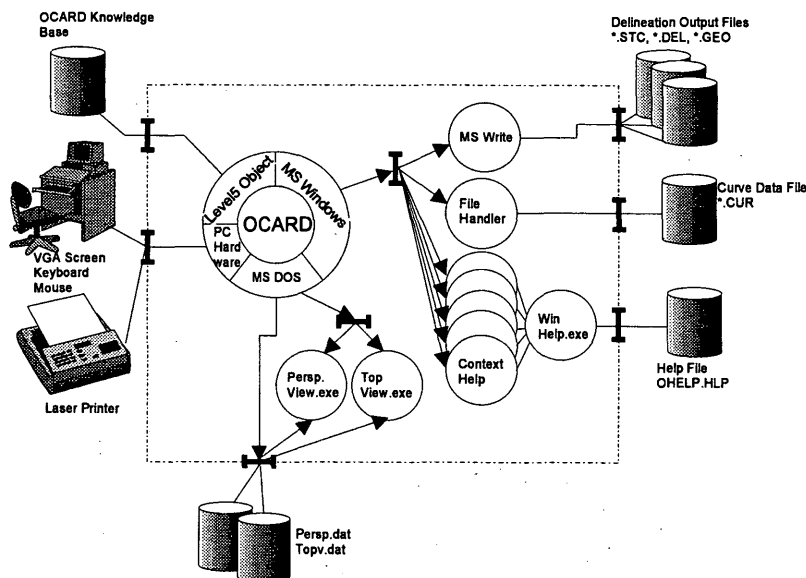
For easy human-computer interaction it was essential to include the standard MS Windows drop-down menus for the flow control of the application. However, as mentioned earlier, Level5 Object 2.5 does not offer this feature. It was therefore necessary to implement a substitute drop-down menu structure using bitmap pictures and hyperregions. The bitmap picture that resembles the drop-down menu is pasted statically on a Level5 Display background.

As shown in Figure 1b, hyperregions are placed over the menu item keywords. As the user clicks with the mouse in such an invisible hyperregion a signal is sent to the attached [S] attribute which has a when-changed method attached that then fires. For each menu item there is a separate menu attribute and when-changed method. If the user changes from one main menu to the other, a Level5 display containing another bitmap picture of a drop-down menu is displayed.

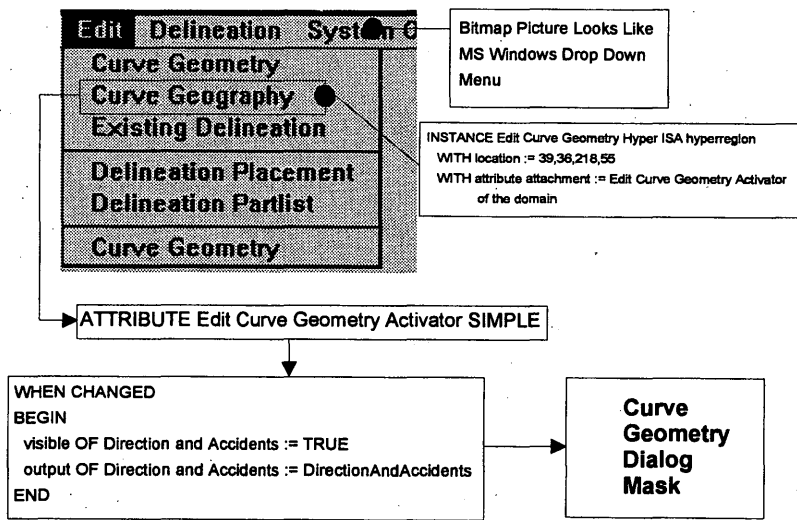
A Sample Session

OCARD is a fairly large application that offers a number of different ways of handling it. In most cases however a typical session with OCARD follows a certain pattern. Figure 2 shows a strongly simplified typical curve delineation session. Note that the figure does not show all features that are offered in OCARD. The numbered steps refer to the numbers in Figure 2.

1. After OCARD is started, the first action a user usually takes is to create a new curve or to open an existing one.



a). OCARD System Borders



b). OCARD Drop Down Menu Technique

FIGURE 1 OCARD Level5 environment.

2. The external file handler calls an MS Windows common dialog box that is needed to enter the filename and the path of the new curve.

3. Then the user switches from the file menu to the edit menu where the curve geometry can be entered or edited, or both. Note that for simplicity there is only one data entry mask shown in Figure 2. Values for distances or speeds may be entered in either metric or English.

4. From the edit menu the user changes over to the compute menu where a data output mask with an empty table is displayed. OCARD first determines whether an arrow sign must be used. After this step OCARD offers the three following device-type selection options:

a. User specifies whether flexible postdelineators, object markers, or chevrons (four different sizes) are to be used by OCARD;

b. OCARD determines the device type solely on the basis of the accident severity (none, minor damage, substantial damage, minor injuries, and fatalities) judged by the user for a given curve; and

c. OCARD determines the device type on the basis of the user-judged accident severity and the accident frequency provided by an automatic computation using an accident prediction model (6) and the ADT (average daily traffic) volume. Alternatively, the user could provide the accident frequency on the basis of accident records or any other applicable method. Then the central device is placed using the central device algorithm (Figure 3). OCARD always places three devices around the central device, all within the driver's functional visual field using another algorithm. Finally OCARD determines the location of the remaining devices (to the end of the curve) using the computed average spacing between the devices. Delin-

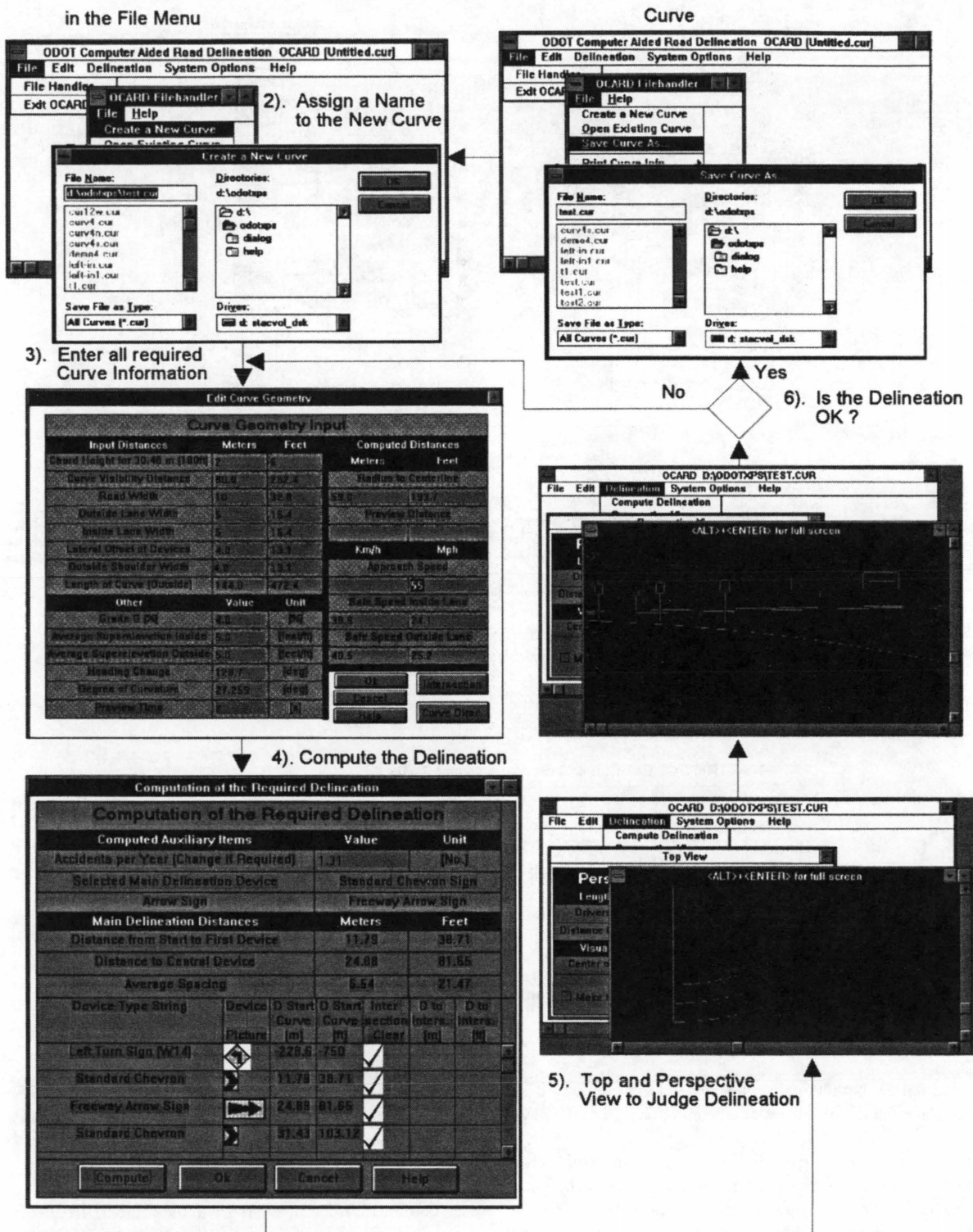


FIGURE 2 OCARD sample session.

ation devices that would interfere with an outside intersection can be deleted or relocated to the intersecting road.

5. The type of the advance warning sign (curve, turn, reverse curve, or reverse turn) and the corresponding approach speed dependent advance location [Table S-1 in the OMUTCD (2)], are displayed in the table on the screen and listed in the delineation output files along with the other devices.

6. The newly computed curve delineation can be previewed with the TopView and the PerspectiveView utility. Users can then judge whether they are satisfied with the appearance of the delineation.

7. The final curve delineation is usually saved to disk. For this the user must change to the file menu and activate the file handler again, this time however to save the curve information. To allow the

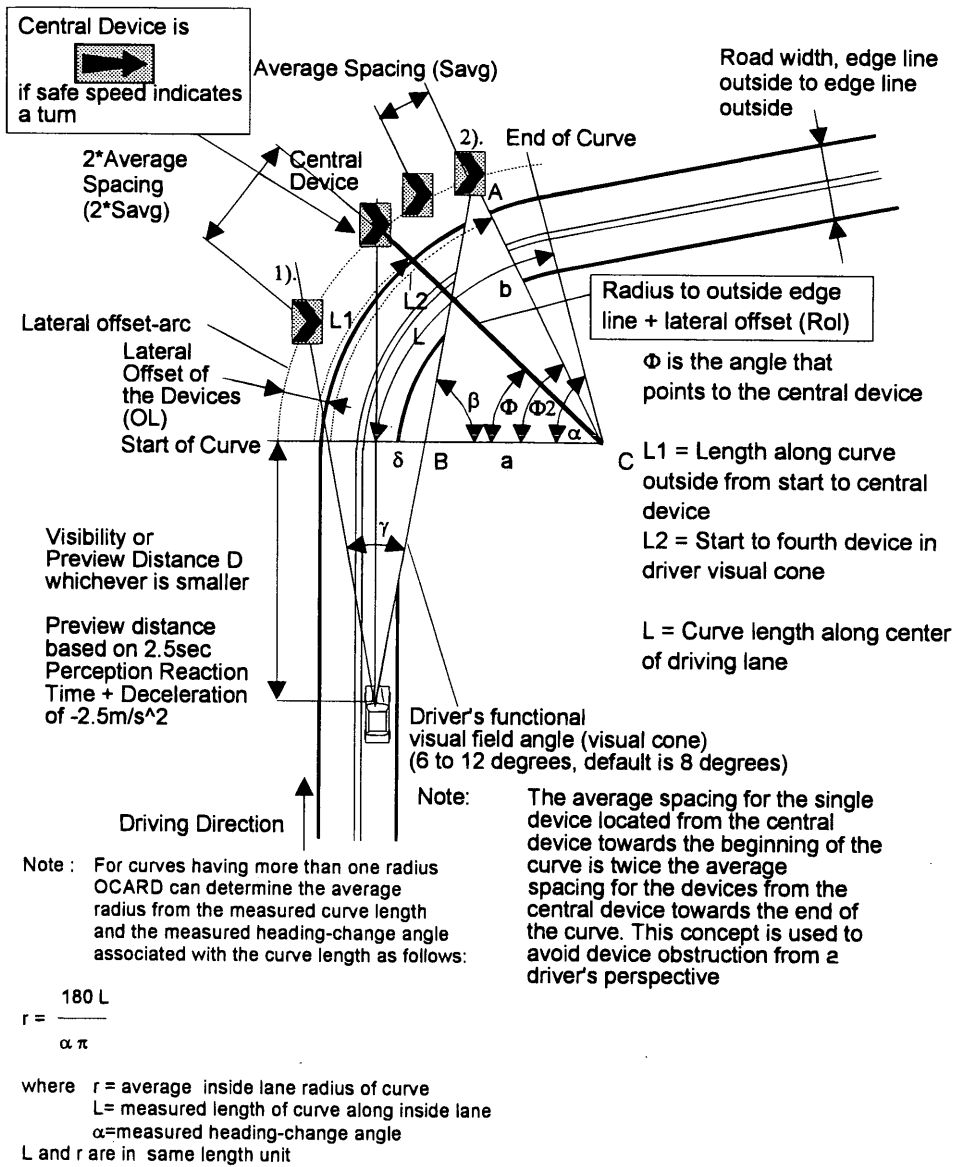


FIGURE 3 Algorithm for placing central device and four devices in driver's visual cone.

user to select the name and path of the curve data file a save dialog box is opened.

DELINEATION COMPUTATION

The delineation is computed on the basis of the curve geometry, which is measured in the field and entered by the user. OCARD V1.0 is suited for curves with fairly long straight approaches with typical approach speeds of approximately 50 mph or more. It is possible to use OCARD for curves with slower approach speeds, but the number of placed delineation devices could be slightly too high. The grade in the curve approach section and in the curve is used in the accident prediction model (δ) only. OCARD contains no rule that directly uses the grade (either positive, going up, or negative, going down) for the selection and the placement of the delineation devices. The delineation algorithms were developed on the basis of the research results that were briefly described in the introduction of this paper.

In general, the following algorithms are used to determine the optimal delineation for a given curve geometry:

- Device-type selection,
- Placing the central device,
- Placing four devices in the driver's functional visual field (central device embedded within three curve delineation devices),
- Placing the remaining devices to the end of the curve,
- Relocating devices to the outside edge line of the intersecting road, if desirable, and
- Computing the location of the advance warning sign from the beginning of the curve.

Device-Type Selection Options

Option 1: User-Specified Device Type

Users can override the automatic device-type selection of OCARD according to their own judgment.

Option 2: OCARD Selects Device Type on Basis of Accident Severity

Users estimate the accident severity (consequences) for a given curve according to their own judgment. OCARD then determines the device type as follows:

- No consequences: Flexible post delineators 1.06 m (42 in.) high with 2.54 × 20.32 cm (1 × 8 in.) white microprismatic sheeting installed on both sides;
- Minor damage: Object marker, 22.8 × 38.1 cm (9 × 15 in.) with yellow high-intensity sheeting, 1.82 m (6 ft) above the road edge;
- Substantial damage: Standard chevron sign ODOT W-33-12, 30.48 × 45.72 cm (12 × 18 in.) with yellow high-intensity sheeting;
- Minor injuries: Major standard chevron sign ODOT W-33-18, 45.72 × 60.96 cm (18 × 24 in.) with yellow high-intensity sheeting;
- Substantial injuries: Large chevron sign ODOT W-33-30, 76.2 × 91.44 cm (30 × 36 in.) with yellow high-intensity sheeting;
- Fatalities: Extralarge chevron sign ODOT W-33-36, 91.44 × 121.92 cm (36 × 48 in.) with yellow high-intensity sheeting.

This list is a tentative, proposed delineation device selection strategy. Other strategies could be implemented into OCARD with a minor programming effort.

Option 3: OCARD Selects Device Type On Basis of Accident Severity and Accident Frequency

OCARD can select the type of delineation devices on the basis of estimated accident severity and the number of accidents in the given curve per year as indicated in Table 1.

If a full guardrail around the outside of the curve is present the selected device is always a guardrail reflector. Users may provide the actual number of accidents per year on the basis of accident records or their own judgment. If desirable, users may also leave the computation of the accident frequency up to OCARD, which uses an accident prediction model for curves on rural two-lane roads, as described in the paper of Kalakota et al. (6).

$$AR = -0.3 + 3.8(L) + 0.37(D)(L) + 0.011 (D)(G) + 0.004 (D)(SWR) - 0.012(L)(G)(D) \tag{1}$$

with an $R^2 = 0.28$

where

- AR = accidents per million vehicles per year,
- D = degree of curvature (degrees),
- L = section length (mil),
- G = percent grade, and
- SWR = outside shoulder width (ft).

The device-type selection algorithm according to Table 1 requires OCARD to compute the number of accidents per year. This number can be obtained from Equation 1, as follows:

$$AYR = \frac{365(ADT)}{10^6} AR \tag{2}$$

where AYR is the number of accidents per year and ADT is the average daily traffic volume.

The accident prediction model given in Equation 1 is tentative because of the apparent lack of fit ($R^2 = 0.28$) and should be replaced by a more efficient model when available. To estimate and enter the correct accident severity (consequences) in case of an ROR (run-off-the-road) incident the user can obtain a detailed description of the various severities from the on-line help utility.

Placing the Central Device

For an optimal delineation it is essential to have one delineation device straight ahead of the vehicle approaching a curve along the tangent section of a highway. This device is called the central device. In cases in which the computed safe speed is less than 45.06 kph (28 mph) this device must always be an arrow sign. Otherwise the central device is of the same type as the remaining devices that were selected with the device-type Selection algorithm. When an arrow sign is required OCARD automatically specifies that a turn or reverse-turn sign must be used as an advance warning sign (with a speed-dependent advance location computed by OCARD). The

TABLE 1 Device Type Selection Based on Accident Severity and Accident Frequency (Excluding Central Device and Reflectors on Outside Guardrail)

Estimated ROR Consequences	Accident Frequency (Number of Accidents per Year)									
	0-1	1-2	2-3	3-4	4-5	5-6	6-7	7-8	8-9	9-10
None	FP	FP	FP	FP	FP	FP	FP	FP	FP	FP
Minor Damage	FP	FP	FP	FP	FP	FP	FP	OB	OB	OB
Subst. Damage	FP	OB	OB	OB	CHS	CHS	CHS	CHM	CHM	CHM
Minor Injuries	OB	OB	OB	CHS	CHS	CHM	CHM	CHM	CHM	CHL
Subst. Injuries	OB	CHS	CHS	CHM	CHM	CHM	CHL	CHL	CHL	CHL
Fatalities	CHL	CHL	CHL	CHL	CHL+	CHL+	CHL+	CHL+	CHL+	CHL+

- FP = Flexible Post Delineator, 1.06 m (42") high with 2.54 cm x 20.32 cm (1" x 8") white microprismatic sheeting
- OB = Object Marker, 22.8 cm x 38.1 cm (9" x 15") with yellow high-intensity sheeting, 1.82 m (6 ft) above the road edge
- CHS = Small Chevron Sign (Standard), 30.48 cm x 45.72 cm (12" x 18") ,yellow high-intensity sheeting
- CHM = Medium Chevron Sign (Major Standard), 45.72 cm x 60.96 cm (18" x 24") with yellow high-intensity sheeting
- CHL = Large Chevron Sign (Freeway and Expressway Exit Ramps), 76.2 cm x 91.44 cm (30" x 36") with yellow high-intensity sheeting
- CHL+ = Extra Large Chevron Sign (Freeway and Expressway),91.44 cm x 121.92 cm (36" x 48") with yellow high-intensity sheeting

arrow and advance turn, or reverse-turn warning sign must always be placed as a pair, together for both approaches to the curve, regardless of whether or not the traffic characteristics for one of the approaches are less severe than for the other approach. When no arrow is placed in the curve, the advance warning sign (again absolutely needed for both approach directions) can be at most a curve, reverse curve, or winding road sign (with a speed-dependent advance location computed by OCARD). If a curve within a winding road section requires an arrow, that curve must be signed with an advance-turn or reverse-turn warning sign. OCARD computes the safe speed in the curve for both travel directions according to the formula given in the OMUTCD (2)

$$V_s = \sqrt{(e + f) 15R} \quad (3a)$$

where

V_s = safe speed of vehicle (mph),
 e = superelevation (ft per 1 ft of horizontal width),
 f = transverse friction coefficient (slightly speed dependent),
 R = radius of curvature (ft)

or

$$V_s = 11.289 \sqrt{(e + f) R} \quad (3b)$$

where

V_s = safe speed of vehicle (kph),
 e = superelevation (m per 1 m of horizontal width),
 f = transverse friction coefficient (slightly speed dependent),
 and
 R = radius of curvature (m).

A field investigation has shown that the computed safe speed is a superior statistical and more stable measure when compared with the Ball Bank method described in the OMUTCD (2). The Ball Bank method has a number of serious shortcomings, including the fairly substantial time required to take a sufficient number of readings, the sensitivity to slight sudden steering corrections and the resulting fairly bad statistical properties, although it provides basically the same values as those in Equation 3.

By finding the angle Φ of the triangle indicated in Figure 3 it is possible to compute the distance L_1 to the central device along the outside road edge. For left curves this angle is given by

$$\Phi = a \cos\left(\frac{R_{ol}}{R_{el} + O_L}\right) \quad (4)$$

and for right curves by

$$\Phi = a \cos\left(\frac{R_{il}}{R_{el} + O_L}\right) \quad (5)$$

where

Φ = angle in radians to central device, as indicated in Figure 3,
 R_{ol} = radius to center of outside lane,
 R_{il} = radius to center of inside lane,
 R_{el} = radius to outside edge line, and
 O_L = lateral offset of devices as indicated in Figure 3.

Using Equation 3 or 4 it is possible to compute the distance to the central device along the outside edge line.

$$L_1 = \Phi R_{el} \quad (6)$$

To install the device later, this distance can be measured from the start of the curve with a distance measuring wheel.

Placing Four Devices in the Driver's Field of View

Previously conducted laboratory experiments (Zwahlen in a paper in this Record) (1:50 scale, three-dimensional model situation under low-beam nighttime driving conditions) indicate that at least four delineation devices should be placed within the driver's functional visual field, assuming that the approach to the curve is fairly straight and the approach speed is approximately 50 mph or more. There appears to be no practically significant increase in the accuracy of curvature judgment if more than four devices within the functional visual field are used, but there is a loss with respect to the accuracy of curvature judgment if fewer than four devices are placed within a driver's functional visual field.

The algorithm first compares the preview distance and the visibility distance. The tip of the driver's visual cone is placed at a distance D away from the start of the curve into the tangent section of the curve approach. D is equal to the visibility or preview distance, whichever is smaller. Then the algorithm attempts to find the location where the sides of the visual cone meet the lateral offset arc. These two locations are marked with 1 and 2 in Figure 3, respectively. The sides a and b of the triangle ABC can be determined as follows:

$$b = R_{el} + O_L \quad (7)$$

For left curves

$$a = R_{ol} - \delta \quad (8)$$

For right curves

$$a = R_{il} - \delta \quad (9)$$

Findings from eye scan research conducted by Zwahlen (7,8) may be used to estimate the extent of the functional visual field angle γ (visual cone) for a driver approaching a curve. The extent of the functional visual field angle is estimated to be between 6 and 12 degrees. Mackworth (9) found in his research that the useful field of view (UFOV) from which a subject can extract accurate visual information, varies between 1 and 4 degrees per eye fixation and that operators search a region so that two adjacent UFOV may touch each other but do not overlap. The extent of the UFOV appears further to be dependent on the density and the conspicuity of the searched-for items against a given background. In the case of yellow or white retroreflective devices at night in typical rural fairly dark and uniform surroundings it would be reasonable to assume a somewhat larger UFOV.

Considering a driver's short-term memory limitations and the dynamics of the driving process, it is safe to tentatively assume that fairly accurate curvature information can be extracted and integrated on the basis of two, maximally maybe three, successive eye fixations of about 0.4 to 0.8 sec duration each. Thus, based on the

basis of the above information OCARD uses a functional field-of-view angle γ of 8 degrees as a default value. The user may select any other angle γ within the range of 6 to 12 degrees. Using γ and the visibility or preview distance D (whichever is smaller), it is possible to determine δ as follows:

$$\delta = D \tan\left(\frac{\gamma}{2}\right) \quad (10)$$

The angle Φ_2 that points to the outermost of the four devices within the visual cone can be computed as follows:

$$\beta = \frac{\pi}{2} - \frac{\gamma}{2} \quad (11)$$

$$c = \frac{1}{2} \{2a \cos(\beta) + \sqrt{[-2a \cos(\beta)]^2 - 4(a^2 - b^2)}\} \quad (12)$$

$$\Phi_2 = a \cos\left(\frac{a - \cos(\beta)c}{b}\right) \quad (13)$$

Using Equation 12 it is possible to compute the distance L_2 from the start of the curve to the outermost device in the driver's visual cone, along the outside edge line of the road.

$$L_2 = \Phi_2 R_{el} \quad (14)$$

The average spacing with which all subsequent devices (from central device to end of curve) are placed can be computed from the position of the central device and the position of the outermost device in the visual cone as follows:

$$S_{avg} = \frac{L_2 - L_1}{2} \quad (15)$$

Placing the Remaining Devices

The remaining devices are placed using the average spacing that was computed for having four devices in the functional visual field of the driver. The algorithm stops when a device would be placed beyond the end of the curve.

Relocating Devices to the Intersection Edge Line

The basic device-placing algorithm of OCARD does not consider outside intersections. With a few geometric calculations it is, however, possible to relocate devices that interfere with the outside intersection along the outside edge of the intersecting road. The approaching driver may not notice such a relocation easily because the algorithm relocates the devices such that the delineation appears as if it would follow the curve. The size and the luminances of the relocated devices, however, may appear slightly smaller, which could result in a reduction of the available perceptual curvature information.

Figure 4 illustrates how the devices that would have been placed on the intersection are projected along the outside edge of the intersecting road. OCARD provides the position for each relocated device in terms of a distance D_{rel} along the outside intersection edge line as illustrated in Figure 4. The following describes the calculations that are performed by OCARD to determine D_{rel} .

Two coordinate systems X_1Y_1 and X_2Y_2 are placed at the beginning and at the end of the intersection, as shown in Figure 4. The inclination angles ϑ_1 and ϑ_2 can be determined by using

$$\vartheta_1 = \omega - \Phi_{is} \quad (16)$$

$$\vartheta_2 = \omega - \Phi_{ie} \quad (17)$$

OCARD can determine the angle Φ_{is} between the start of the curve and the start of the intersection with respect to the origin O from R_{el} and the distance from the start of the curve to the start of the intersection. Likewise, it is possible for OCARD to determine Φ_{ie} by using R_{el} , the distance from the start of the curve to the start of the intersection and with the width W of the intersection. The inside intersection offset line, which is parallel to the inside intersection edge line can be described with respect to X_1Y_1 as

$$F_1(X) = -\tan(\vartheta)X + O_L\{\tan(\vartheta)[1 - \sin(\vartheta)] - \cos(\vartheta)\} \quad (18)$$

The outside intersection offset line, which is parallel to the outside intersection edge line, can be described with respect to X_2Y_2 as

$$F_2(X) = -\tan(\vartheta)X + O_L\{\tan(\vartheta)[1 + \sin(\vartheta) + \cos(\vartheta)]\} \quad (19)$$

Using the radius to the lateral offset arc as shown in Figure 4

$$R_{ol} = R_{el} + O_L \quad (20)$$

it is possible to describe the lateral offset arc as

$$F_3(X) = \sqrt{2XR_{ol} - X^2} \quad (21)$$

To determine whether a given delineation device with its coordinates X_{dev}, Y_{dev} with respect to the coordinate system X_D, Y_D interferes with the outside intersection it is necessary for OCARD to determine the projected start and the projected end of the intersection, including the lateral offset buffer O_L at both sides of the intersection. The distance from the start of the curve to the projected start of the intersection can be determined by searching for the point of intersection of the offset arc $F_3(X)$ with the inside offset line $F_1(X)$.

$$F_1(X) = F_3(X) \quad (22)$$

solving the quadratic Equation 21 with respect to X yields the X -coordinate:

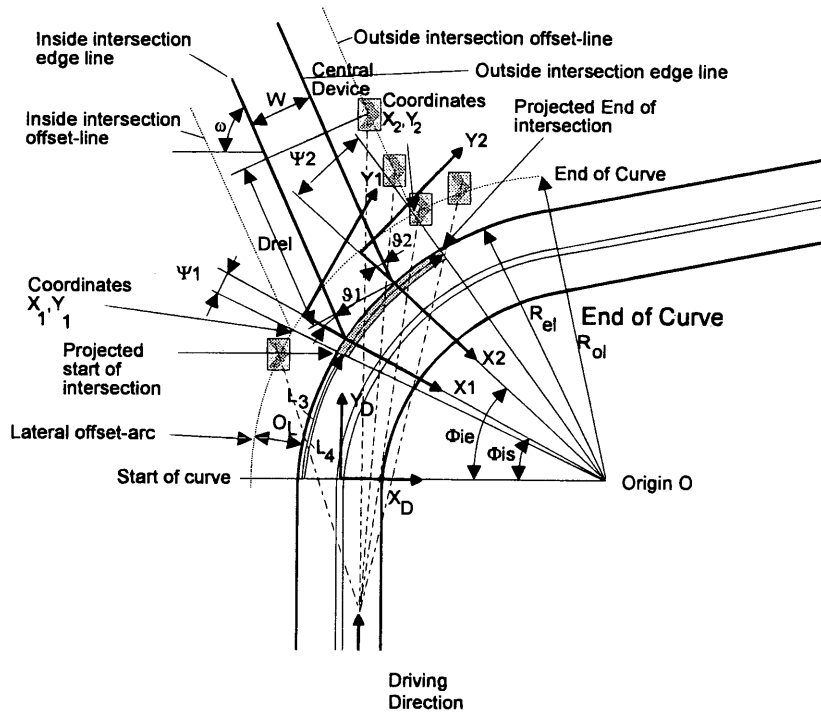
$$X_1 = \frac{R_{ol}\cos^2(\vartheta_1) - \sqrt{R_{ol}^2\cos^4(\vartheta_1) + O_L^2[2\cos^4(\vartheta_1)]}}{2\cos^2(\vartheta_1) - 1} \quad (23)$$

and by inserting Equation 22 into 17 it is possible to obtain the Y -coordinate

$$Y_1 = -\tan(\vartheta_1)X_1 + O_L\{\tan(\vartheta_1)[1 - \sin(\vartheta_1)] - \cos(\vartheta_1)\} \quad (24)$$

The angle Ψ_1 between the start of the curve and the location where $F_1(X) = F_3(X)$ is given by

$$\Psi_1 = 2 \operatorname{asin}\left(\frac{\sqrt{X_1^2 + Y_1^2}}{2R_{el}}\right) \quad (25)$$



Note: Delineation devices cannot be placed within the shaded section of the curve. The user has the following options in OCARD:

- 1). Discard the devices that otherwise would obstruct the intersection
- 2). Relocate these devices to the outside edge of the intersecting road

FIGURE 4 Coordinate transformation for devices that were placed on intersection.

Using this angle it is possible to determine the projected start of the intersection in terms of distance from the start of the curve along the outside edge line. Between the projected start of the intersection and the projected end of the intersection, installation of any delineation devices is not recommended.

$$L_3 = R_{el}(\Phi_{is} + \Psi_1) \quad (26)$$

The coordinates of the projected end of the intersection can be determined by searching for the intersection of the offset arc $F_3(X)$ with the outside offset line $F_3(X)$.

$$F_2(X) = F_3(X) \quad (27)$$

$$X_2 = \frac{R_{ol}^2 \cos^2(\vartheta_2) - \sqrt{R_{ol}^2 \cos^4(\vartheta_2) + O_L^2 [2 \cos^4(\vartheta_2) - 5 \cos^2(\vartheta_2) + 2 \sin(\vartheta_2) - 4 \sin(\vartheta_2) \cos^2(\vartheta_2) + 2]}}{2 \cos^2(\vartheta_2) - 1} \quad (28)$$

$$Y_2 = -\tan(\vartheta_2)X_2 + O_L \{ \tan(\vartheta_2)[1 + \sin(\vartheta_2)] + \cos(\vartheta_2) \} \quad (29)$$

$$\Psi_2 = 2 \operatorname{asin} \left(\frac{\sqrt{X_2^2 + Y_2^2}}{2 R_{el}} \right) \quad (30)$$

The true end of the intersection is finally given by

$$L_4 = R_{el}(\Phi_{ie} + \Psi_2) \quad (31)$$

A delineation device within the projected start and the projected end of the intersection should either be left out or relocated to the outside edge line of the intersecting road as shown in Figure 4. This transformation involves only the Y-coordinate so that for the driver the relocated device appears to be in the same direction ahead. The Y-coordinate is transformed using

$$Y_i = \tan(\omega)X_{dev} + \sin(\Phi_{ie} + \Psi_2)(R_{el} + O_L) + \tan(\omega)[R_{cl} - \cos(\Phi_{ie} + \Psi_2)(R_{el} + O_L)] \quad (32)$$

where

ω = the angle of the intersection,

X_{dev} = the X-coordinate from the base delineation algorithm of a device that is located in the intersection, and

R_{cl} = the radius of the curve to the center line.

The distance D_{rel} (see Figure 4) from the intersection to the relocated device along the outside edge line of the intersection is determined as follows:

$$D_{rel} = \frac{[Y_i - \sin(\omega) O_L] - \sin(\Phi_{ie})(R_{el} + O_L)}{\sin(\omega)} \quad (33)$$

This distance can be measured with the distance measuring wheel. The distances for all relocated devices are displayed in the data out-

put mask indicated in Figure 2. The delineation output file contains the list of all installation distances for the delineation devices.

CONCLUSIONS AND LIMITATIONS OF OCARD

In a number of test cases the delineation designs obtained by the use of OCARD appear to be in fairly close agreement with the designs that are based on the use of extensive and sound traffic engineering judgment. As with any other software package, use of OCARD is strongly recommended only after having completed prior adequate user training. Such a user training would include the following major activities:

1. Train the traffic engineers or route markers responsible for curve delineation in the proper method and procedure to take the few field measurements; and

2. Train the traffic engineers or route markers in the actual use of OCARD on the PC in the office or in the field for the application and placement of curve delineation devices for selected simple curves and for selected curves with an outside intersection that may or may not require the relocation of delineation devices along the intersecting road.

REFERENCES

1. *Manual on Uniform Control Devices for Streets and Highways*, FHWA, U.S. Department of Transportation, 1988.
2. *Ohio Manual of Uniform Control Devices for Streets and Highways*, Division of Operations, Bureau of Traffic, Ohio Department of Transportation, Columbus, 1972.
3. Zwahlen, H. T. *Optimal Application and Placement of Roadside Reflective Devices for Curves on Two-Lane Rural Highways*. Final Report FHWA/OH-93. Ohio Department of Transportation, Columbus, July 1993.
4. *Level5 Object User's Guide*. Documentation for Level5 Object Release 2.2. Information Builders, Inc., New York, 1990.
5. *Level5 Object Reference Guide*, Documentation for Level5 Object Release 2.2. Information Builders, Inc., New York, 1990.
6. Kalakota, K. R., P. K. Seneviratne, M. I. Nazrul. Prediction of Accidents on Rural Two-Lane Highways, Presented at the 72nd Annual Meeting of the Transportation Research Board, Washington, D.C., 1993.
7. Zwahlen, H. T. Advisory Speed Signs and Curve Signs and Their Effect Upon Driver Eye Scanning and Driving Performance. In *Transportation Research Record 1111*, TRB, National Research Council, Washington D.C., 1987, pp. 110-20.
8. Zwahlen, H. T. Conspicuity of Suprathreshold Reflective Targets in a Driver's Peripheral Visual Field at Night. In *Transportation Research Record 1213*, TRB, National Research Council, Washington, D.C., 1989, pp. 35-46.
9. Mackworth, N. H. Ways of Recording Line Of Sight. In *Eye Movements and Psychological Processing* (R.A. Monty and Senders, eds.), Erlbaum, New Jersey, 1976.

The contents of this paper reflect the views of the authors, who are responsible for the facts and accuracy of the data presented. The contents do not necessarily reflect the official views or policies of the Ohio Department of Transportation or FHWA. This paper does not constitute a standard, specification, or regulation.

Publication of this paper sponsored by Committee on Visibility.

Visibility of New Pavement Markings at Night Under Low-Beam Illumination

HELMUT T. ZWAHLEN AND THOMAS SCHNELL

Three independent field studies investigating the nighttime detection distances of yellow and white-painted and taped pavement markings of varying widths under low-beam illumination were undertaken. Different centerline and edge line configurations, typically used on highways, were tested. The objective of Study 1 was to obtain exploratory pavement marking visibility field data for detecting the begin and end of a continuous pavement marking line as a function of line width, material, color, and lateral position of the line. Study 2 was conducted to determine the visibility distance of the onset of a left or a right curve (244-m radius) along a tangent section marked with a continuous white taped edge line placed at approximately 1.83 m to the right of the car, as a function of line width. Study 3 was conducted to determine the detection distances for the begin and end of yellow taped pavement marking configurations having different widths, placed on the left side of the vehicle representing a typical centerline on a two-lane rural highway. The results of Study 1 indicate no statistically significant differences ($\alpha = 0.05$) for the average begin or end detection distances using a line width between 0.1 and 0.2 m. The results for Study 2 indicate that there is a statistically significant difference in the average detection distance ($\alpha = 0.05$) between a 0.1- and a 0.2-m-wide right edge line for a left curve. The results of Study 3 indicate that the double solid line configuration provides statistically significantly ($\alpha = 0.05$) longer average detection distances when compared with the other configurations for all three widths (0.05, 0.1, and 0.2 m). Overall in Study 3, the end detection distances were significantly ($\alpha = 0.05$) longer than the begin detection distances.

The Ohio Manual of Uniform Traffic Control Devices for Streets and Highways (1) defines pavement markings as traffic control devices used on the surface of a roadway to regulate, warn, and guide the motorists. Pavement markings are applied for centerlines, edge lines, no-passing zones, and others as discussed previously (1, 2). Ethen et al. (3) conducted a subjective evaluation in the field using pavement markings with a broad range of retroreflectance. Allen et al. (4) provided basic relationships that related visibility range, stripe-to-skip length, and luminance contrast to the driver's lateral vehicle control. They suggested a minimum pavement marking contrast of 2. Serres (5) developed a correlation between subjective ratings and line retroreflectance. He concluded that a line retroreflectance below 150 cd/m²/lux is unacceptable to the median viewer and that a line should be repainted if a retroreflectance of less than 100 mcd/m²/lux is measured. In addition, a study conducted by Graham et al. (6) found that more than 90 percent of subjects rated a retroreflectance of 93 mcd/m²/lux as adequate or more than adequate for nighttime driving.

None of these studies provide actual nighttime visibility distances for different pavement marking configurations and different

line widths. CIE Publication 73 (7), on the basis of prior research, quotes that a minimum preview time of 5 sec would be a conservative but a safe criterion to allow efficient, anticipatory steering behavior. The publication suggests that a minimum preview time of 3 sec, however, would be more applicable in practice. The publication further states that the visibility distance of continuous pavement marking lines is defined as the distance ahead of the driver at which the luminance contrast between the pavement markings and the road surface is equal to the threshold contrast of the driver. The report then describes a number of mathematical relationships that were developed to calculate the visibility distances of various pavement markings. However, one can question the adequacy of the CIE pavement marking visibility model in terms of (a) the use of a poor threshold contrast approximation; (b) the assumption that the target (pavement marking) is a rectangle (transformed into a circle with equivalent area) rather than a perspective seen line; (c) not accounting for the lateral position of the line with respect to the longitudinal vehicle axis; (d) not considering the color of the line; and (e) not considering pavement marking configurations (double solid lines, solid-dashed combinations, single solid lines, and dashed lines with different stripe and gap lengths).

A study conducted by McLean et al. (8) investigated the driver steering control (tracking) performance for straight-lane driving. It was found that the far-sight distance needed for drivers to adequately steer the car in a traffic-free environment to be about 21.3 m. This preview distance appeared to be independent of the two speeds 32 and 48 kph, that were used in the study.

Sorensen (unpublished data, 1993) evaluated average detection distances of pavement marking edge lines of three different widths, 0.5, 0.3, and 0.15 m under various conditions of illumination. According to Sorensen, an average detection distance of 129 m for a vehicle traveling at 100 kph on the basis of the conservative CIE preview time estimate of 5 sec cannot be achieved, but a preview time of 3 sec may be feasible.

A study conducted by Harkey et al. (9) investigated the effect of permanent and nonpermanent pavement markings on driver performance during the day and night. The study was conducted on a multilane freeway using the following nonpermanent lane line configurations: (a) 0.6-m stripes with 11.6-m gaps, (b) 1.2-m stripes with 11-m gaps and the full complement of markings: 3.1-m stripes with 9.1-m gaps as lane line. This configuration also included edge lines. The first two patterns were temporary markings, whereas the third was a permanent marking used for comparison with the former two types. The effectiveness of the pavement markings was measured in terms of lateral deviation of the vehicle in the lane, vehicle speed within the test segment, number of edge line and lane line encroachments, and number of erratic maneuvers. Harkey et al. (9) concluded that drivers performed better with the 3-m/9.1-m stripe/gap lane line markings including edge lines during both the day and the

night. Because the consecutive adjoining highway sections used in the study were not tangent sections and had different geometric alignments and one section also included edge lines and a bridge structure, it is not clear from the study what influence the various geometric alignments had on the results and whether there was an order of presentation effect in the results caused by the fixed sequential method of data collection.

Hall (10) evaluated the effectiveness of 0.2-m-wide edge lines in terms of their run-off-the-road (ROR) accident-reducing potential. It was concluded that the 0.2-m-wide edge lines do not have a significant effect in terms of ROR accident reduction at night on straight or curve sections with or without opposing traffic.

The superiority of wider edge lines is still inconclusive. All of the studies mentioned earlier used one of the following to investigate the effectiveness of the pavement marking stripes: subjective ratings, photometric retroreflectivity measurements, driver lateral position maintenance performance, preview, or accident analyses. None of the studies has provided average detection distances in terms of detecting the begin or end of a pavement marking line or the begin of a curve ahead. For this reason three exploratory nighttime pavement marking detection studies under low-beam illumination conditions were conducted at Ohio University, Athens, Ohio.

OBJECTIVES OF THE THREE STUDIES

The objective of Study 1 was to obtain exploratory pavement marking nighttime visibility field data for detecting the begin and end of a continuous pavement marking line as a function of line width, material, color, and lateral position of the line. The results will be needed primarily to assist in the development of a pavement marking nighttime visibility model for continuous lines and of an experimental methodology to evaluate the visibility of pavement markings.

The objective of Study 2 was to obtain exploratory pavement marking nighttime visibility data under low-beam conditions to determine the visibility distance to detect the onset of a left or a right curve with a 244-m radius along a tangent section marked with a continuous white edge line placed at approximately 1.83 m to the right of the car as a function of line width.

The objective of Study 3 was to obtain the nighttime average detection distances under low-beam illumination conditions for the begin and end of various yellow centerline pavement marking tape configurations using various widths.

METHOD

Study 1: Detection of the Begin and End of Continuous Pavement Marking Lines

Experiment

The following treatments (independent variables) were used in Study 1:

1. 10-m-wide white pavement marking tape located about 1.83 m to the left and right sides of the longitudinal car axis;

2. 13-m-wide white painted pavement marking located about 1.83 m to the right side of the longitudinal car axis;

3. 13-m-wide yellow painted pavement marking located about 1.83 m to the left side of the longitudinal car axis;

4. 20-m-wide white pavement marking tape located about 1.83 m to the left side of the longitudinal car axis;

5. 20-m-wide white painted pavement marking located about 1.83 m to the left and right sides of the longitudinal car axis; and

6. 25-m-wide white painted pavement marking located at about 1.83 m to the right side of the longitudinal car axis.

The dependent variable was the detection distance of the begin and end of these treatments.

Subjects and Experimental Vehicle

A total of seven young, healthy college students (five men and two women, average age, 23.1 years, normal vision) participated in the experiment of Study 1. A 1976 Datsun B210 with H6054 headlamps was used as experimental car in Study 1.

Experimental Site

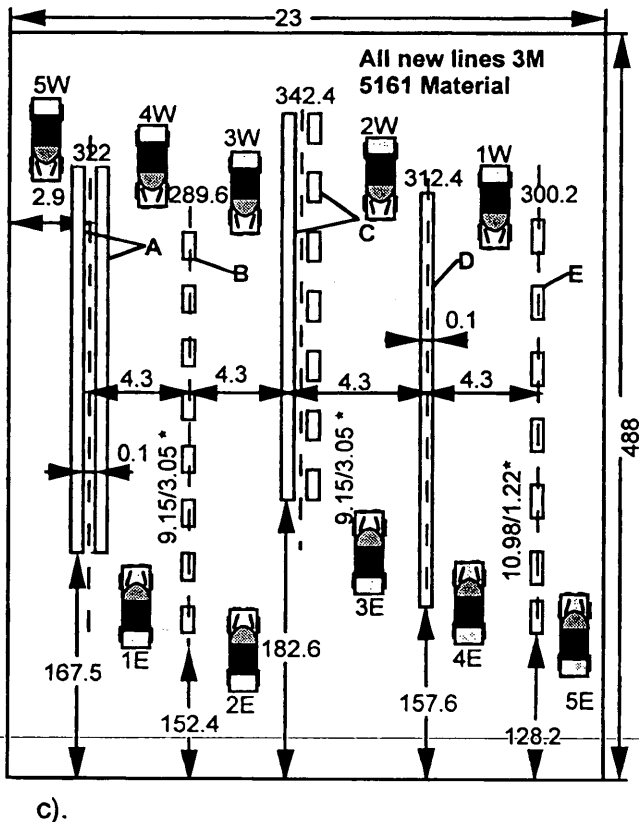
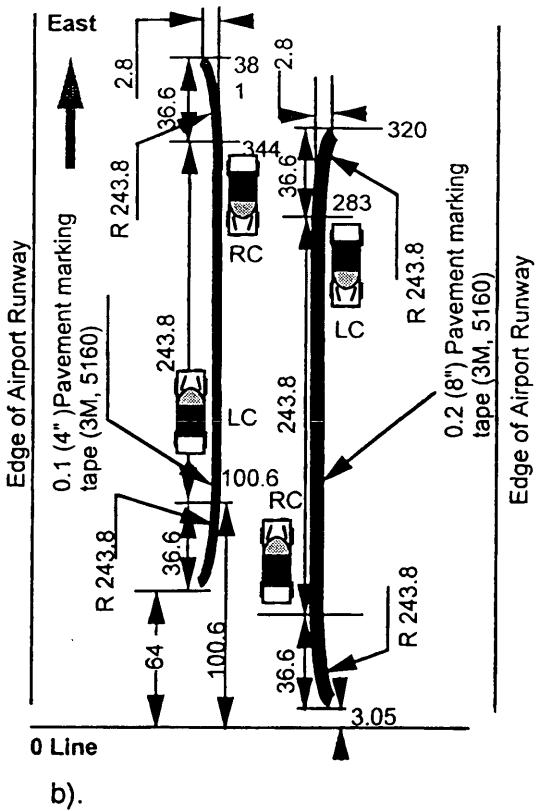
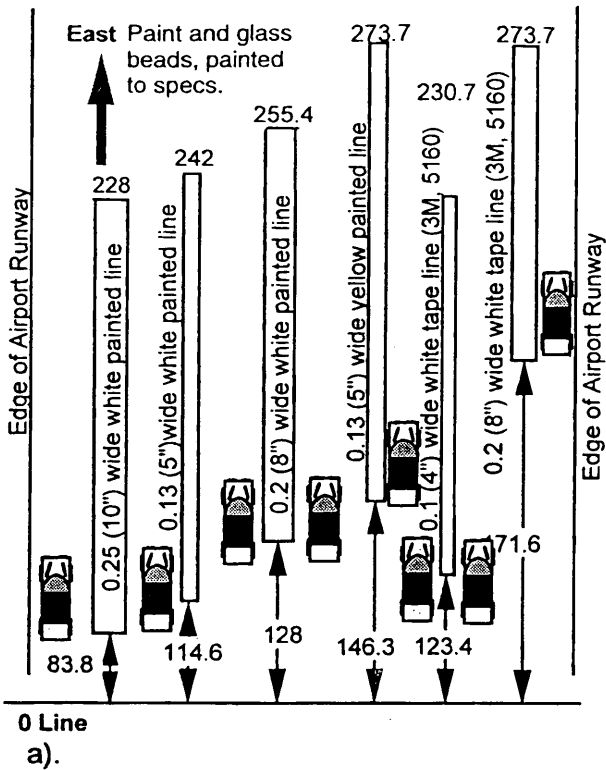
The experiment was conducted on an old unused airport runway in Athens, Ohio. The runway was about 23 m wide and 500 m long. A two-lane state highway with moderate traffic runs parallel about 61 m away from the runway. During the course of the experiment the experimental car was driven in the eastbound direction (relatively dark background). A number of luminaires, a few illuminated advertising signs, and other light sources were within the field of view, especially in the left half of the field of view. Figure 1a shows the site and the layout of the pavement markings for the Study 1 experiment.

Experimental Design

A randomized block experimental design was used in Study 1. Each subject was tested under each condition in four replications. One subject finished only three replications. Each condition was randomized within a block of eight runs in such a way that each condition appeared exactly once within that block. Therefore the total number of observations for each condition was 27 (six subjects with four replications each and one subject with three replications).

Experimental Procedure

The subjects accelerated the car to a speed of about 8 to 16 kph. As soon as the subject reported seeing the begin of the straight single pavement marking line, a sandbag was dropped onto the runway by the experimenter riding in the car. The sandbag distance was then recorded. The same method was used for the detection of the end of the pavement marking lines. As soon as the run was completed, the subject drove back to the west end of the runway to prepare and position the car for another run. The average time needed to complete 32 runs for each subject was about 1 hr 15 min.



Note:

1. 1E, 2E, ..., 4W, 5W represent the number and approach direction of the pavement configurations. These numbers and direction were painted on both ends of the runway at about 6 ft. to the right of pavement configuration to aid the subject to align his/her car.
 2. A - Double Solid Yellow Line, B - Dashed Yellow Line 9.15 m/3.05 m (30 ft./10 ft.)
 C - Solid and Dashed 9.15 m/3.05 m (30 ft./10 ft.) Yellow Line, D - 4" Solid Yellow Line, E - Dashed Yellow Line 10.98 m/1.22 m (36 ft./4 ft.)
- * 9.15/3.05 means a pavement marking configuration with 3.05 m (10 ft.) stripes and 9.15 m (30 ft.) gaps.
 * 10.98/1.22 means a pavement marking configuration with 1.22 m (4 ft.) stripes and 10.98 m (36 ft.) gaps.

All Dimensions in Meters

FIGURE 1 Layout for detection of begin and end of single new retroreflective pavement marking lines in Study 1: (a) begin and end of single new retroreflective pavement marking lines in Study 1; (b) begin of a curve along a single new retroreflective pavement marking tape line in Study 2; (c) begin and end of new pavement marking lines in Study 3.

Study 2: Detection of the Begin of a Right or a Left Curve

Experiments

A left or a right curve with a radius of 244 m along a tangent section was simulated with a continuous white edge line placed at approximately 1.83 m to the right of the car. The pavement marking tape material was white 3M-5160 (Ecolux, 86.5 degrees entrance angle, 1 degree observation angle, RL = 1000 mcd/m²/lux). The experiments investigated three different line widths (independent variables):

1. 0.05 m
2. 0.1 m
3. 0.2 m

Experiments 1 and 2 investigated all three widths, whereas Experiment 3 investigated only the 0.1- and 0.2-m-wide markings. The dependent variable was the detection distance of the onset of the curve marked with the above treatments.

Experimental Site

The three experiments of Study 2 were conducted at the same site as that used in Study 1. Figure 1*b* illustrates the site and the typical layout of the pavement markings for Experiment 3 of Study 2.

Subjects and Experimental Vehicles

Three subject groups, each one of which consisted of 16 (8 men and 8 women) young and healthy subjects were used for the three different experiments conducted as part of Study 2 (average age, 20.9 years, standard deviation 0.77 years, normal vision). A Chevrolet Cavalier (1986) with H9006 low-beam headlamps was used as the experimental car in Study 2.

Experimental Design

A randomized block design was used for the experiments in Study 2. In each of the three experiments, the subjects were tested under each condition in two replications. Every condition was randomized within a block of four runs in such a way that each condition appeared exactly once within a block. Therefore, the total number of observations in an experiment for each condition was 32 (16 subjects, two replications).

Experimental Procedure

The experimental procedure was similar to the one used in Study 1. For each run, the pavement marking line would appear on the right side of the car. Unlike in Study 1, the subjects had to report when they detected the begin of either a left or a right curve (about 1.83 m to the right of the longitudinal car axis).

Study 3: Detection of the Begin and End of Five Different Pavement Marking Line Configurations Placed in the Center of the Road Using Different Line Widths

Experiments

Three independent nighttime field experiments were conducted under low-beam illumination as part of Study 3. The following treatments were used (independent variables):

1. Double solid lines, 0.05, 0.1, and 0.15 m wide;
2. Single solid line and a dashed line with a stripe length of 3.05 m and a gap length of 9.14, 0.05, 0.1, 0.15 m wide;
3. Dashed line with a stripe length of 3.05 m and a gap length of 9.14, 0.05, 0.1, and 0.15 m wide;
4. Dashed line with a stripe length of 1.22 m and a gap length of 10.97, 0.05, 0.1, and 0.15 m wide; and
5. 0.10-m-wide single solid line; baseline comparison between groups.

The treatments were observed in the eastbound and westbound directions. The pavement marking tape material was yellow 3M-5161 (Ecolux, 86.5 degrees entrance angle, 1 degree observation angle, RL = 650 mcd/m²/lux). The dependent variable was the detection distance of the begin and end of these treatments.

Experimental Site

The three experiments of Study 3 were conducted at the same site as that used in Studies 1 and 2. Figure 1*c* shows the site and the layout.

Subjects and Experimental Vehicles

Three different subject groups consisting of 10 young and healthy subjects each (normal vision), were used for the three different experiments conducted as part of Study 3. Eight men and two women participated in Experiment 1, five men and five women participated in Experiment 2, and seven men and three women participated in Experiment 3.

Experimental Design

Study 3 used a randomized block experimental design. Each subject was tested under each condition in two replications. Further, all subsequent configurations were completely randomized for each of the subjects in an experiment. Each condition was randomized within a block of 10 runs in such a way that each condition appeared exactly once within that block of an experiment. Therefore, the total number of observations in an experiment for each condition was 20 (10 subjects, 2 replications each).

Experimental Procedure

The experimental procedure used in Study 3 was similar to the ones used in Studies 1 and 2. The selected pavement marking configura-

tion always appeared to the left of the car. Unlike in Studies 1 and 2, the subjects had to report when they detected the begin and end of the five straight yellow pavement marking configurations from the east as well as from the west.

RESULTS

Study 1

The statistical tests indicate that the average begin and end detection distances for a continuous pavement marking line are not statistically significantly different. However, one can observe a slight tendency of the average begin detection distance to be longer than the end detection distance. Further, it appears that the 0.1-m white pavement marking tape located on the left side of the car does not provide an average end detection distance that is statistically different from the average end detection distance provided by the 0.2-m-wide white tape.

Table 1 shows the average detection distances and the standard deviations for the different pavement marking configurations used in Study 1 for each replication. It can be seen from the table that there is no appreciable difference in the average detection distances among the four replications for any of the configurations tested. This implies that there is no learning effect when the pavement marking configurations were viewed for the second, third, or fourth time. Because of this it is possible to consider the combined data from the four replications in the statistical analysis. Figure 2a shows the average detection distance as a function of the width of the pavement marking lines. It can be seen that there is no significant difference among the distances needed to detect either the begin or end of the 0.13-, 0.20- and the 0.25-m-wide continuous white painted lines located to the right of the car. Moreover, the figure also shows that the average end detection distances are always slightly longer than the average begin detection distances. The results of Study 1 also indicate that the average begin and end detection distances for white continuous taped lines located to the left or right of the car are slightly but not significantly ($\alpha = 0.05$) longer than the average begin and end detection distances for the corresponding continuous white painted lines. The average begin and end detection distances for lines located to the right of the car are slightly but not significantly ($\alpha = 0.05$) longer than the average begin and end detection distances of the corresponding lines located to the left of the car. The average detection distances for the 0.13-m-wide yellow painted pavement configuration are shorter than the average detection distances of all the other pavement marking configurations used in Study 1. Figure 3a shows a typical psychometric curve for the detection distances of the 0.1-m-wide pavement marking tape located 1.83 m to the left of the longitudinal car axis. The figure indicates that 95 percent of the selected drivers can detect the begin of the 0.1-m-wide marking at a distance of about 81 m and the end at a distance of about 73 m. Figure 3a also illustrates that the begin detection distances are relatively close to the end detection distances for the 0.1-m-wide line.

Study 2: Detection of Begin of Right or Left Curve

The statistical tests conducted on the average detection distance data obtained from the three experiments in Study 2 indicate that there is no significant difference between the average detection dis-

tance of a right curve marked with a new 0.1-m-wide line and a right curve marked with a new 0.2-m-wide line placed on the right side of the car. For the left curve, however, there is a significant difference at the 0.05 level. Table 2 indicates the average curve-begin detection distances for Replication 1 using all three new pavement marking configurations (0.05, 0.1, and 0.2-m-wide white tape located about 1.8 m to the left or right side of the car). As indicated in Table 2 and Figure 2b, the average curve-begin detection distances for the left curve are always shorter than the average curve-begin detection distances for the corresponding right curve. Further, it can be seen that by increasing the width from 0.05 to 0.2 m, the average detection distances are longer by about 21 m for the left curve and 22 m for the right curve.

Figure 3b shows a typical psychometric curve for the detection distance of the right and the left curve. As seen in the figure, 95 percent of the selected drivers can detect the onset of a left curve at a distance of about 67 m and the onset of a right curve at a distance of about 81 m. Similar detection distances can be obtained from the psychometric curve for any other selected probability of detection value.

Study 3: Detection of Begin and End of Five Different New Pavement Marking Line Configurations Placed in Center of Road Using Different Line Widths

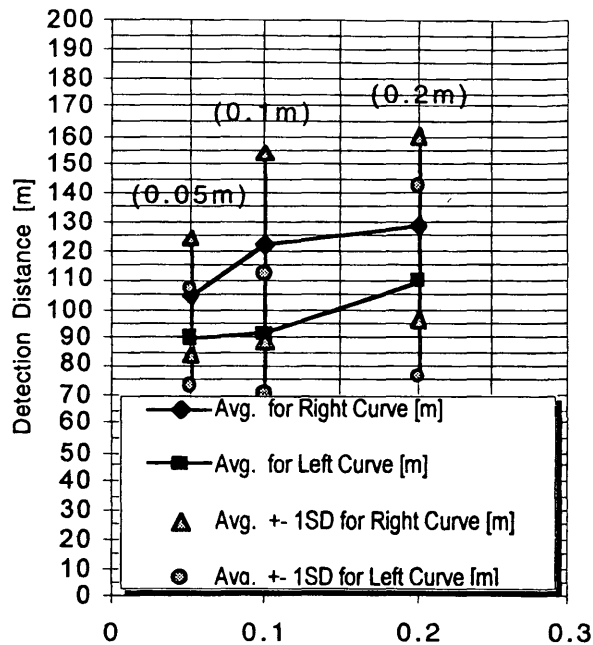
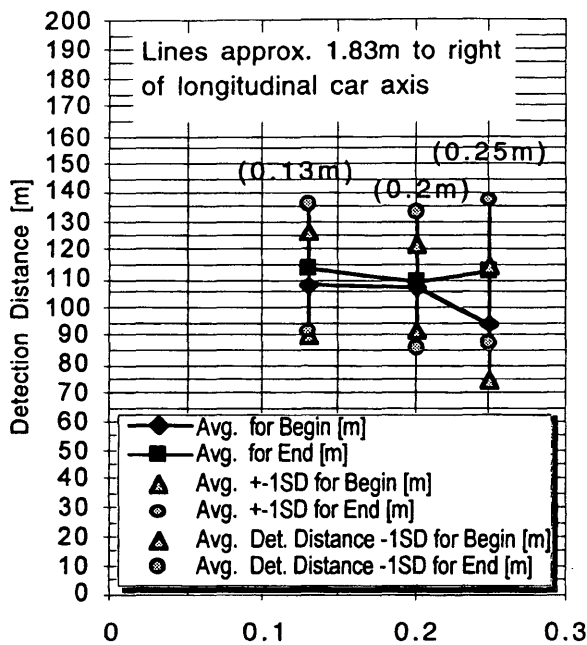
Statistical tests were conducted on the data obtained from the three experiments in Study 3 (0.05-, 0.1-, and 0.2-m-wide centerline configurations). As expected, in all three experiments it was found that the configuration type is significant, with the double solid line configuration having the longest average detection distance in the three experiments. Overall, it can be seen that the average end detection distance for the used pavement marking configurations was significantly longer than the average begin detection distance.

Tables 3 through 5 show the average detection distances for the 0.05-, 0.1-, and the 0.2-m-wide pavement marking configurations used in Experiments 1, 2, and 3, respectively. It can be seen from the tables that, for all three widths, the double solid-line configurations showed the longest average begin and end detection distances. Moreover, for the three widths tested, the dashed-line configuration with a stripe length of 1.2 m and a gap length of 12.27 m shows almost always the shortest average begin and end detection distance. Further, for all three widths tested, the solid-dashed line combination has a longer average detection distance when compared with the average detection distance for the two single dashed line or the single continuous line configurations.

Tables 3 through 5 also show the average detection distances for the 0.1-m solid-line configuration, which was the only common configuration for all three subject groups. This 0.1-m configuration provided average begin and end detection distances, both east- and westbound, across the three different experiments that are fairly close to each other. This would indicate that despite different vehicles with different low beams, no single subject group had a superior detection performance when compared with the other two subject groups, thus allowing a comparison of the results across the three experiments of Study 3. It can be seen from Figure 2c that for both eastbound and westbound traffic, there is a tendency for the 0.2-m-wide pavement marking configurations to provide somewhat longer detection distances than can be obtained with the corresponding 0.05- and 0.1-m configurations. Unlike in Study 1 where new wider painted lines with glass beads did not necessarily

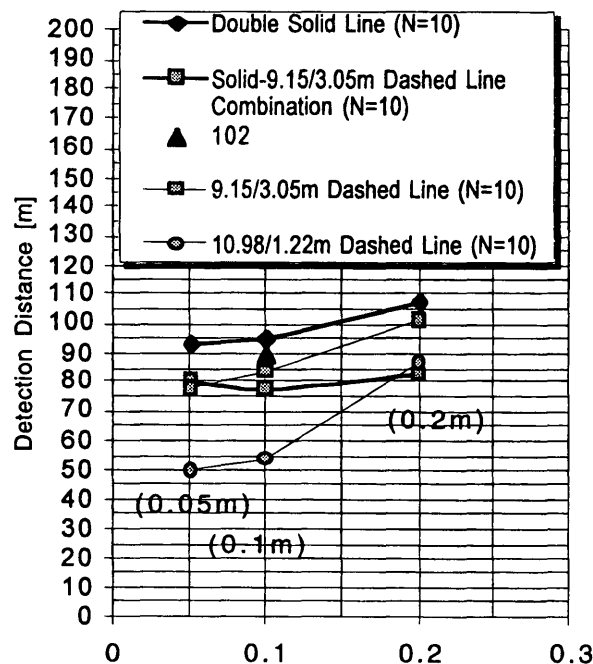
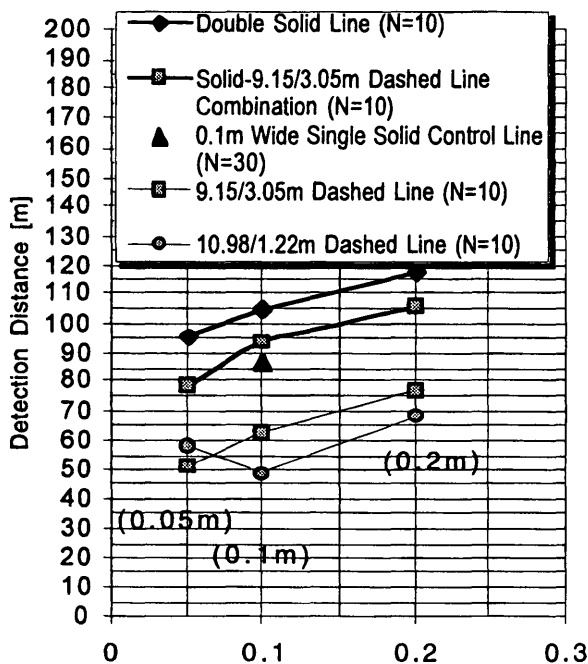
TABLE 1 Average Detection Distances and Standard Deviations for Different New Pavement Marking Configuration and Replication

No.	Pavement Marking Configuration	Replication	N	Average in meters	Std. Dev. in meters
1	0.101 m (4") Left, Begin White Tape	1	7	118.17	21.08
		2	7	119.97	25.06
		3	7	122.64	31.96
		4	6	118.97	29.78
2	0.101 m (4") Left, End White Tape	1	7	118.79	36.15
		2	7	120.07	26.59
		3	7	118.54	23.59
		4	6	110.10	26.54
3	0.101 m (4") Right, Begin White Tape	1	7	114.42	21.54
		2	7	118.66	27.39
		3	7	120.07	22.09
		4	6	112.88	24.06
4	0.101 m (4") Right, End White Tape	1	7	124.22	34.56
		2	7	116.88	23.39
		3	7	120.87	28.82
		4	6	98.36	35.45
5	0.127 m (5") Left, Begin Yellow Paint	1	7	90.64	18.10
		2	7	81.94	20.03
		3	7	93.05	19.86
		4	6	81.45	19.53
6	0.127 m (5") Left, End Yellow Paint	1	7	95.17	29.90
		2	7	89.93	30.03
		3	7	94.42	21.97
		4	6	78.71	22.23
7	0.127 m (5") Right, Begin White Paint	1	7	108.83	21.60
		2	7	103.21	19.94
		3	7	103.68	14.17
		4	6	108.37	27.19
8	0.127 m (5") Right, End White Paint	1	7	123.48	26.24
		2	7	120.00	26.85
		3	7	112.16	17.24
		4	6	98.79	15.63
9	0.203 m (8") Left, Begin White Paint	1	7	95.72	17.02
		2	7	96.99	22.88
		3	7	100.11	21.59
		4	6	96.28	21.30
10	0.203 m (8") Left, End White Paint	1	7	104.98	32.55
		2	7	101.97	29.57
		3	7	105.66	25.13
		4	6	91.20	18.78
11	0.203 m (8") Right, Begin White Paint	1	7	110.21	18.69
		2	7	102.85	19.27
		3	7	100.77	17.88
		4	6	99.92	18.37
12	0.203 m (8") Right, End White Paint	1	7	116.01	27.73
		2	7	110.13	27.30
		3	7	110.48	19.60
		4	6	100.04	22.18
13	0.203 m (8") Left, End White Tape	1	7	119.00	31.39
		2	7	110.45	26.18
		3	7	113.40	24.24
		4	6	99.07	31.99
14	0.254 m (10") Right, Begin White Paint	1	7	95.48	26.72
		2	7	94.67	21.43
		3	7	94.88	20.98
		4	6	93.54	16.52
15	0.254 m (10") Right, End White Paint	1	7	114.13	24.60
		2	7	115.50	33.26
		3	7	116.47	22.75
		4	6	108.42	26.20



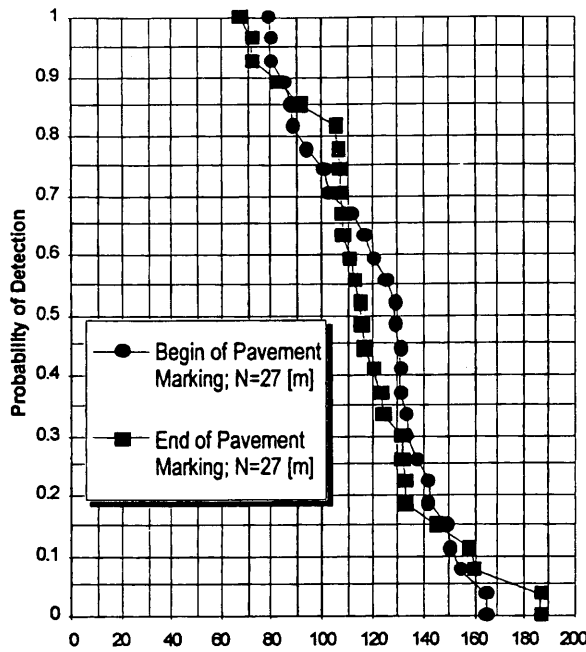
a).

b).

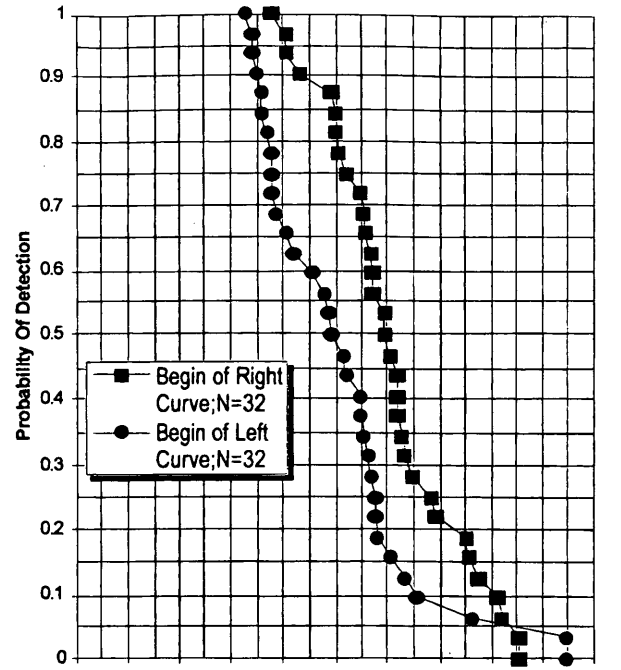


c).

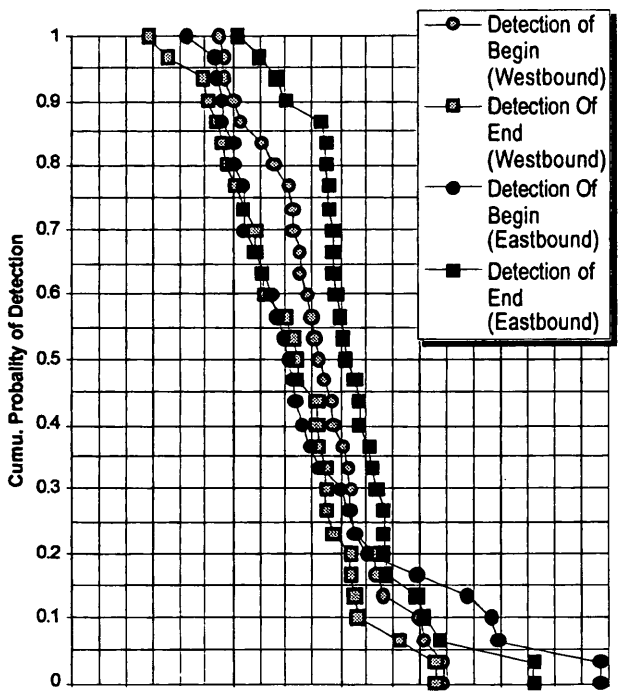
FIGURE 2 Average detection distances and standard deviations as a function of pavement marking width: (a) Study 1—new white continuous painted lines with glass beads; (b) Study 2—new white continuous tape 1.83 m to right of longitudinal car axis; (c) Study 3—new yellow tape 1.83 m to left of longitudinal car axis, eastbound (left) and westbound (right), Replication 1.



a).



b).



c).

FIGURE 3 Psychometric curves (a) for Study 1, (b) for Study 2, (c) for Study 3.

Study 1: Psychometric curves showing the probability of detection as a function of the detection distance for a 0.1m wide, white retroreflective pavement marking line (Adhesive P.M.Tape) located approximately 1.83m to the left side of the longitudinal car axis on a concrete road surface under low beam illumination conditions at night, for 7 subjects, 4 replications each (exception 1 subject, 3 replications)

Study 2: Psychometric curves showing the probability of detection as a function of the detection distance for a 0.1m wide new, white retroreflective pavement marking line (Adhesive P.M.Tape), 243.8m radius, placed on a concrete road surface under low beam illumination conditions at night, pavement marking line located approximately 1.83m to the right side of the longitudinal car axis for left curve and right curve, 16 subjects, 2 replications each.

Study 3: Psychometric Curves showing the probability of detection as a function of the detection distance for a 0.1m wide new, yellow tape pavement marking line on a concrete road surface under low beam illumination conditions at night, located approximately 1.83m to the left of the longitudinal car axis.
 Begin Westbound Avg.=92.08m, StdDev.=22.35m
 End Westbound Avg.=79.94m, StdDev.=25.22m
 Begin Eastbound Avg.=88.79m, StdDev.=36.79m
 End Eastbound Avg.=105.02m, StdDev.=21.22m

provide longer detection distances, the moderate width effect found in Study 3 may be explained by the consistent pavement marking tape quality when compared with the less uniform paint and glass bead application in Study 1. The configuration of the pavement markings, on the other hand, has a much stronger effect on the average detection distance than the stripe width. For the east direction (Figure 2c), the double solid line appears to provide the longest

average detection distance followed by the solid-dashed line combination, the 0.1-m single solid line, and the two single dashed lines. The dashed-line configurations, 9.15/3.05 m and 10.98/1.22 m, are relatively close to one another in terms of average detection distances. Based on Figure 2c, the dashed-line configuration of 9.15/3.05 m does not provide longer detection distances than that of 10.98/1.22 m when using the 0.05-m-wide lines. Also, if one con-

TABLE 2 Average Detection Distance for Begin of a Curve Using Different Pavement Marking Configurations, Replication 1 (N = 16)

Expt. No.	Width and Type of Pavement Marking	Average and Standard Deviation Detection Distances for the Begin of the Curve in Meters			
		Left		Right	
		Avg.	SD.	Avg.	SD.
1 (8M,8F)	2" White Tape	90.00	18.23	105.93	19.97
2 (8M,8F)	4" White Tape	91.40	22.63	121.19	35.78
3 (8M,8F)	8" White Tape	110.74	32.90	128.22	33.65

siders the standard deviations of the average detection distances, it is evident that both dashed-line configurations produce similar results in terms of average detection distances.

For the west direction (Figure 2c), where there are a number of luminaires in the field of view of the drivers, the double solid-line configuration again provides the longest detection distances across all line widths used. The 0.1-m single solid line, the solid-dashed line combination, and the dashed-line configuration of 9.15/3.05 m produce almost the same average detection distance when using the 0.1-m-wide lines. The dashed configuration of 10.98/1.22 m provided average detection distances that are considerably shorter than the ones provided by the other configurations, when stripes 0.05 and 0.1 m wide were used. For 0.2-m-wide stripes the dashed-line configuration of 10.98/1.22 m appears to provide average detection distances that are fairly close to the average detection distances obtained for the dashed-line configuration of 9.15/3.05 m.

Figure 3c shows a typical example of a psychometric curve for the average detection of the begin and end of the 0.1-m-wide configuration for Replication 1. The figure indicates that 95 percent of

the selected drivers can detect the begin of the 0.1-m new yellow taped pavement marking line in the west direction at a distance of about 57 m and the detection of the end at a distance of about 36 m. For the east direction these distances are about 54 m to detect the begin and about 70 m to detect the end.

COMPARISONS, SUMMARY, AND CONCLUSIONS

It was found that the begin of a right curve marked with a 0.1-m-wide continuous white taped line (Study 2) provides an average detection distance that is almost equal to the average begin detection distance of a 0.1-m-wide white continuous taped line (Study 1). On the basis of this observation, it would seem reasonable in a pavement marking visibility model, to use the average detection distance calculations on the basis of the begin of a white line placed to the right side of the car to predict the average detection distance for the begin of a curve. Because there appears to be a significant difference between the average detection distances of a left and a right

TABLE 3 Average Detection Distances and Standard Deviations in Meters for 0.05-m-Wide New Yellow Tape Pavement Marking Configurations

Type of line	Replication 1			Replication 2			Replication (1+2)			East & West (Rep. 1)		
	Avg.	SD.	N	Avg.	SD.	N	Avg.	SD.	N	Avg.	SD	
Double line												
Begin	East	95.55	16.74	10	103.72	25.11	10	99.64	21.19	20	94.37	17.23
	West	93.19	18.52	10	100.11	18.39	10	96.65	18.31	20		
End	East	107.18	25.49	10	103.28	29.79	10	105.23	27.06	20	100.35	23.87
	West	93.52	21.20	10	97.38	31.40	10	95.45	26.15	20		
Solid-Dashed line (9.15/3.05)												
Begin	East	78.13	14.95	10	87.05	21.71	10	82.59	18.71	20	79.25	15.58
	West	80.37	16.92	10	83.33	17.21	10	81.85	16.68	20		
End	East	90.05	19.60	10	101.76	36.42	10	95.90	29.09	20	91.61	19.30
	West	93.17	19.91	10	92.53	26.91	10	92.85	23.04	20		
0.1 m Wide Solid Line												
Begin	East	80.01	28.19	10	81.82	14.49	10	80.92	21.83	20	88.50	24.37
	West	91.77	19.55	10	100.38	22.77	10	96.08	21.12	20		
End	East	99.24	19.11	10	105.24	21.38	10	102.24	19.97	20	90.85	28.01
	West	76.99	31.88	10	81.94	29.28	10	79.46	29.9	20		
Dashed line (9.15/3.05)												
Begin	East	51.12	17.46	10	62.58	26.20	10	56.85	22.45	20	64.93	21.96
	West	78.74	17.02	10	80.49	18.70	10	79.61	17.42	20		
End	East	67.98	27.58	10	66.68	16.24	10	67.33	22.04	20	78.19	26.05
	West	88.41	20.99	10	77.19	29.58	10	82.80	25.61	20		
Dashed line (10.98/1.22)												
Begin	East	58.11	18.92	10	56.38	18.84	10	57.25	18.40	20	54.40	18.33
	West	50.69	17.90	10	60.24	16.41	10	55.46	17.42	20		
End	East	68.23	31.37	10	73.31	40.04	10	70.77	35.11	20	70.97	37.50
	West	73.71	44.36	10	92.31	37.76	10	82.70	41.21	20		

9.15/3.05 means a pavement marking configuration with 3.05 m stripes and 9.15 m gaps.

10.98/1.22 means a pavement marking configuration with 1.22 m stripes and 10.98 m gaps.

West direction has brighter background (luminaires of parking lot, etc.) than east direction

TABLE 4 Average Detection Distances and Standard Deviations in Meters for 0.1-m-Wide New Yellow Tape Pavement Marking Configurations

Type of line		Replication 1			Replication2			Replication (1+2)			East & West (Rep. 1)	
		Avg.	SD.	N	Avg.	SD.	N	Avg.	SD.	N	Avg.	SD
Double line												
Begin	East	105.43	24.89	10	116.41	24.66	10	110.92	24.76	20	100.50	22.49
	West	95.57	19.86	10	109.97	14.13	10	102.77	18.33	20		
End	East	121.02	16.57	10	118.70	18.43	10	119.86	17.10	20	112.27	18.17
	West	103.52	15.88	10	115.31	17.61	10	109.45	17.36	20		
Solid and Dashed line (9.15/3.05)												
Begin	East	94.70	27.43	10	107.89	22.34	10	101.30	25.27	20	92.44	23.41
	West	78.99	16.36	10	88.16	11.33	10	83.58	14.48	20		
End	East	109.28	21.79	10	112.59	15.84	10	110.93	18.61	20	109.41	18.43
	West	106.48	15.43	10	109.28	14.82	10	107.88	14.79	20		
0.1 m Wide Solid line												
Begin	East	77.33	14.63	10	87.1	13.96	10	82.22	14.79	20	83.53	19.42
	West	89.73	22.28	10	108.11	12.78	10	98.92	20.03	20		
End	East	102.19	14.58	10	111.79	9.69	10	106.99	13.01	20	92.96	25.87
	West	83.73	31.79	10	88.4	10.86	10	86.06	23.24	20		
Dashed line (9.15/3.05)												
Begin	East	62.59	18.13	10	75.51	15.65	10	69.05	17.77	20	73.64	20.67
	West	84.69	17.37	10	100.76	17.64	10	92.73	18.93	20		
End	East	69.96	17.03	10	79.17	19.60	10	74.56	18.48	20	76.83	17.30
	West	83.69	15.39	10	88.84	13.67	10	86.26	14.41	20		
Dashed line (10.98/1.22)												
Begin	East	49.58	15.78	10	61.06	7.39	10	55.34	13.37	20	52.55	12.59
	West	55.53	8.12	10	66.81	8.99	10	61.17	10.15	20		
End	East	63.00	15.15	10	74.41	13.93	10	68.70	15.33	20	77.03	25.77
	West	91.05	27.11	10	87.05	23.50	10	89.05	24.78	20		

9.15/3.05 means a pavement marking configuration with 3.05 m stripes and 9.15 gaps

10.98/1.22 means a pavement marking configuration with 1.22 m stripes and 10.98m gaps

West direction has brighter background (luminaires of parking lot, etc.) than east direction

TABLE 5 Average Detection Distances and Standard Deviations in Meters for 0.203-m-Wide New Yellow Tape Pavement Marking Configuration

Type of Line		Replication 1			Replication2			Replication (1+2)			East & West (Rep. 1)	
		Avg.	SD.	N	Avg.	SD.	N	Avg.	SD.	N	Avg.	SD.
Double line												
Begin	East	116.91	21.64	10	132.39	23.73	10	125.61	22.36	20	113.12	18.64
	West	109.34	15.28	10	117.44	11.29	10	113.73	13.12	20		
End	East	135.51	20.49	10	142.40	33.22	10	138.88	26.70	20	125.96	28.02
	West	116.40	32.17	10	134.28	35.65	10	125.27	32.42	20		
Solid and Dashed line (9.15/3.05)												
Begin	East	106.06	22.55	10	117.44	23.23	10	111.75	23.03	20	94.82	24.86
	West	83.58	22.70	10	91.66	15.99	10	87.62	19.55	20		
End	East	120.97	29.44	10	128.76	31.71	10	124.86	30.05	20	123.30	29.03
	West	125.64	30.01	10	140.62	40.42	10	133.13	35.49	20		
0.101 Wide Solid line												
Begin	East	82.61	32.07	10	88.12	31.36	10	85.37	31	20	88.76	29.45
	West	94.91	26.8	10	98.42	29.22	10	96.68	27.35	20		
End	East	113.84	27.26	10	115.62	37.35	10	114.73	31.84	20	109.84	35.18
	West	105.84	42.82	10	97.23	38.92	10	101.45	40.08	20		
Dashed line (9.15/3.05)												
Begin	East	75.85	25.90	10	82.53	23.39	10	79.19	24.26	20	89.56	28.09
	West	103.28	24.02	10	114.98	32.74	10	109.13	28.59	20		
End	East	83.78	24.78	10	89.08	30.19	10	86.43	27.02	20	94.24	32.39
	West	104.70	36.84	10	108.11	35.06	10	106.41	35.04	20		
Dashed line (10.98/1.22)												
Begin	East	68.14	20.66	10	83.13	23.33	10	75.63	22.78	20	77.62	21.31
	West	87.10	18.21	10	88.35	21.62	10	87.73	19.47	20		
End	East	78.30	13.71	10	97.79	34.11	10	88.04	27.22	20	88.50	29.57
	West	98.70	37.77	10	118.02	35.04	10	108.36	36.67	20		

9.15/3.05 means a pavement marking configuration with 3.05 m stripes and 9.15 m gaps.

10.98/1.22 means a pavement marking configuration with 1.22 m stripes and 10.98 m gaps.

West direction has brighter background (luminaires of parking lot, etc.) than east direction

curve, the pavement marking curve visibility model could be calibrated using the field data provided in this paper. A comparison made between the 0.13-m yellow painted line (Study 1) and the 0.1-m yellow taped line (Study 3) indicated that the average detection distance of the 0.13-m line is about 10 m longer.

A comparison made between the average detection distances for the begin and end of a 0.1-m-wide white taped line (Study 1) and a 0.1-m-wide yellow taped line (Study 3) indicated that the average begin and end detection distances of the white line are longer by about 38 and 35 m, respectively. These two comparisons indicate that the color of the pavement markings might have a significant influence on the average detection distances. The longest average detection distance for the begin of a pavement marking configuration found in Studies 1 through 3 is 125.61 m obtained for the 0.2-m double solid centerline configuration (two replications, east direction, detection of begin) used in Study 3. The shortest detection distance found in the studies is 55.46 m, which was obtained using the 0.05-m 10.98/1.22 m dashed centerline configuration (two replications, west direction, detection of begin). The 0.2-m double solid centerline used in Study 3 provides an average detection distance that is significantly longer than the average detection distance determined by Sorensen (unpublished data, 1993), which was about 109 m for a new 0.5-m-wide pavement marking (converted to automobile illumination as described by Sorensen). Most pavement marking configurations and line widths appear to provide average detection distances that are above the minimum required visibility distance value of 80 m recommended by Sorensen.

The visibility distance of 58 m for 2-year-old painted pavement markings under dry, clear weather conditions shown previously (7), appears to be close to the above-mentioned shortest detection distance value of 55.46 m, which was obtained using the new 0.05-, 10.98/1.22-m yellow dashed line.

Harkey et al. (9) found a significant driver performance difference between the 10.98/1.22-m dashed-line configuration and the 9.15/3.05-m dashed-line configuration, including edge lines. The results of Study 3, however, indicate no significant detection distance differences between comparable 10.98/1.22-m and the 9.15/3.05-m dashed-line configurations.

Detection distances have been established for the various configurations of 0.05-, 0.1-m, 0.13-, 0.2-m, and 0.25-m-wide pavement markings. Psychometric curves have been established to show the distances at which a certain percentage of population can detect a given pavement marking configuration. Such curves may have a practical importance in the establishment of minimum retroreflectivity standards for the application of pavement markings on highways and on resurfacing zones.

The generally longer distances for the detection of the end of the pavement markings can be attributed to the fact that the subjects

already have visual contact with the line, which most likely simplifies the search for the end. For the detection of the begin of the markings, however, the subject has to visually search for the begin of the markings, which is a cognitively more demanding task, thus resulting in somewhat shorter visibility distances.

Overall, it appears that the pavement markings located to the right of the car are detected more easily and at distances farther away when compared with the corresponding markings placed to the left of the car. This could be attributed to the alignment of the automobile low beams, which point approximately 2 degrees down and 2 degrees to the right, thus favoring the right side. It also appears from the experimental results that the white pavement markings provide average detection distances that are slightly longer than the average detection distances for the yellow pavement markings, thus indicating that any other color than white for the markings will result most likely in a slight reduction of the detection distance. The results presented in this paper were obtained using young and healthy (those most close to ideal visual capabilities) drivers and should not be generalized to other driver age groups without applying proper visual adjustment factors.

REFERENCES

1. *Ohio Manual of Uniform Traffic Control Devices for Streets and Highways*. Ohio Department of Transportation, Columbus, Ohio, 1980.
2. *Manual on Uniform Traffic Control Devices for Streets and Highways*. FHWA, U.S. Department of Transportation, Washington, D.C., 1988.
3. Ethen, E. L., and H. L. Woltman. Minimum Retroreflectance for Night-time Visibility of Pavement Markings. In *Transportation Research Record 1093*, TRB, National Research Council, Washington, D.C., 1986, pp. 43-47.
4. Allen, R. W., J. F. O'Hanlon, and D. T. McRuer. *Driver's Visibility Requirements for Roadway Delineation, Vol. I: Effects of Contrast and Configuration on Driver Performance and Behavior*. FHWA-RD-77-165. FHWA, U.S. Department of Transportation, 1977.
5. Serres, A. M. The Visibility of Highway Markings (Translation from the French: La visibilité des marques routières). *Lux*, Vol. 112, 1981.
6. Graham, J. R., and L. E. King. Retroreflectivity Requirements for Pavement Markings. In *Transportation Research Record 1316*, TRB, National Research Council, Washington, D.C., 1991, pp. 43-47.
7. *Visual Aspects of Road Markings*. Joint Technical Report CIE/PIARC. Publication CIE 73, 1988.
8. Mclean, J. R., and E. R. Hoffman. The Effects of Restricted Preview on Driver Steering Control and Performance. *Human Factors*, Vol. 14, No. 4, 1973, pp. 421-430.
9. Harkey, D. L., R. R. Mera, S. R. Byington. Effect of Non-Permanent Pavement Markings on Driver Performance. In *Transportation Research Record 1409*, TRB, National Research Council, Washington, D.C., 1993.
10. Hall, J. W. Valuation of Wide Edge Lines. In *Transportation Research Record 1114*, TRB, National Research Council, Washington, D.C., 1987, pp. 21-30.

Publication of this paper sponsored by Committee on Visibility.

Loss of Visibility Distance Caused by Automobile Windshields at Night

HELMUT T. ZWAHLEN AND THOMAS SCHNELL

The Technical literature was reviewed with respect to the loss of visibility distance caused by automobile windshields or other optical filters. A series of nighttime luminance measurements in the field provided baseline data for a visibility distance computer model that was developed to investigate nighttime visibility of diffusely reflective targets under low-beam illumination conditions seen through automobile windshields having different transmittances. The computer model offers three alternative luminance contrast threshold models: (a) Adrian's target visibility algorithm, (b) PCDETECT, and (c) Blackwell's 1946 contrast threshold data. The new model, which is based on Blackwell's 1946 data, considers the effects of age and observation time and determines the actual contrast from the target luminance, which depends on the target reflectance, the selected headlamps, and the current observation distance. Percent visibility distance loss graphs, as a function of the initial visibility distance D_0 (using no windshield) were established. A tentative field factor of 2.28 for the Blackwell data was determined. The obtained percent visibility distance loss data were compared with those published earlier by Haber in 1955. This comparison indicates that the percent distance loss functions shown by Haber are misleading and wrong because they are proposed to apply for a target with a constant mean linear dimension of 91.4 cm (3 ft) over the entire initial visibility distance range. Furthermore, the data presented by Haber are conservative and too high. On the basis of the results of this investigation, it would appear to be of benefit to further validate the results in the field and to review the appropriateness of established minimum luminous transmittance standards.

Visibility considerations are highly important in the driving task, as most of the information a driver needs for keeping the vehicle on the road, to drive through curves, to stop at intersections and so forth, is acquired visually. The visual information that is acquired from outside the vehicle must typically pass through the automobile windshield, which may act like an optical filter. Target visibility ahead of an automobile mainly depends on the transmittance characteristics of the windshield, the reflectance properties and linear dimensions of the target, the observer's visual performance, and to a large degree the intensity distribution of the headlamps. The investigation described here examines the loss of visibility distance caused by automobile windshields at night.

REVIEW OF TECHNICAL LITERATURE

Roper (1) and Heath and Finch (2) conducted nighttime visibility distance experiments to assess the effects of tinted windshields on visibility distance. Roper used square targets with a side length of 40.64 cm (16 in) and the same uniform reflectance of $R = 0.075$. The

experiment was conducted using (a) a clear safety plate windshield with a transmittance of $T = 0.883$ and (b) a tinted windshield with a transmittance of $T = 0.73$. Initial target visibility distances ranging from 76 to 123 m (250 to 400 ft) were established with the clear safety plate windshield. The tinted windshield resulted in a visibility distance loss of about 5 percent. Heath and Finch (2) used targets of different sizes, shapes, and reflectances. Heath and Finch found a reduction in visibility distances of up to 22 percent caused by tinted windshields. On the basis of the results of their study, they concluded that it does not appear to be feasible to assign an overall percent loss value to account for the difference in transmittance between two windshields. However, Heath and Finch pointed out that tinted windshields may significantly reduce the visibility distance.

Haber (3) attempted to theoretically analyze the effects of various tinted media on the percent loss of the initial visibility distance D_0 (no windshield) for a target having a mean linear dimension of 91.4 cm (3 ft) and a reflectance of $R = 0.15$ under low-beam illumination conditions. Haber used the data from Roper (1) and Heath and Finch (2) to validate, by extrapolation, the loss percentage of visibility distance as a function of the initial visibility distance D_0 . However, Haber's approach to extrapolate and validate his percent loss curves into ranges below 61 m (200 ft) and beyond 137 m (450 ft) without having one single field data point available appears to be questionable. The method used by Haber (3) to obtain the visibility distance appears to be incorrect and provides visibility distances that are too short. Haber presented percent loss curves for a target having a constant mean linear dimension of 91.4 cm (3 ft) and a constant reflectance. Under illumination from a pair of headlamps having a constant intensity, such a setup will provide 1 percent loss point rather than a functional relationship. To obtain losses of a magnitude given by Haber (3) and subsequently published previously (4), it would be necessary to shrink the target to a mere 3 cm (0.1 ft) when using a tinted windshield with a transmittance of $T = 0.359$. Such a small target no longer represents a pedestrian and would not likely have to be considered as a major or important road hazard for the establishment of minimum transmittance standards.

Waetjen et al. (5) investigated the influence of windshields with different transmittances under various angles of inclination. It was found by the researchers that the windshield angle of inclination only marginally influenced the transmittance $T = f(\text{angle})$. However, at large angles more and more light was found to be reflected specularly off the windshield. Therefore, it was expected that large angles and tinted windshields would provide the shortest legibility distances [they used a Landholt ring with a stroke width of 8.7 cm (3.42 in.) as the target]. The researchers found legibility distances (mean, and standard deviation) of (a) 32.2 ± 5.5 m (105.64 \pm 18.04 ft) when no windshield was used and (b) 26.9 ± 5.1 m (88.25 \pm 16.73 ft) for the tinted windshield at the maximum angle of inclination of 70 degrees. This would result in an average loss percent

Human Factors and Ergonomics Laboratory, Department of Industrial and Systems Engineering, College of Engineering and Technology, Ohio University, Athens, Ohio 45701-2979.

legibility distance of 16.45 percent because of a transmittance of T (70 degrees) = 0.6. Waetjen et al. concluded, on the basis of their findings, that tinted windshields reduce driver visibility such that they might impose a road hazard, especially if the target is a pedestrian. However, it is unclear why the legibility of a Landholt ring with a stroke width of 8.7 cm (3.42 in.) is brought into relationship to the detection of a pedestrian. A Landholt ring with a gap size of 8.7 cm (3.42 in.) and a height of 43.5 cm (17.12 in.) certainly does not represent a pedestrian.

Freedman et al. (6) investigated the visibility of targets, seen through automobile rear windows, of various transmittances using six slide projectors to subsequently present five common roadway objects on screens located about 3 m (9.84 ft) to the rear and side-rear of a simulated vehicle. The results indicate that the probability of detecting the target strongly depends on the target type. Older subjects generally showed a considerably smaller probability of detection. All age groups appeared to have more difficulties detecting the seated child and the bicyclist. On the basis of their findings, Freedman et al. (6) concluded that the safety of backing maneuvers may be significantly reduced for all drivers in cars having rear windows with a transmittance of less than $T = 0.35$. These findings appear to be reasonable, considering the typically low illumination of targets in the rear visual search zone of an automobile. It should be noted, however, that the objective of the current study is the visibility of targets in the search zone ahead of an automobile.

Derkum (7) conducted a dynamic perception laboratory experiment under simulated nighttime low-beam illumination conditions to determine the minimum permissible transmittance level for automobile windshields. The lowest transmittance without significant decrease in visibility was determined as 68 percent when no glare source was present and 63 percent when glare was present.

Kessler (8) investigated the degradation of driver visibility under consideration of the light-scattering properties of worn optical media. Theoretical models that were based on the physics of light scattering were developed. Kessler pointed out that the negative influence of scattered light should be considered in driver visibility.

Hazlett and Allen (9) investigated the effects of pedestrian clothing, reflectorization, and driver intoxication on the ability to detect pedestrians at night. The obtained visibility distances for grey, non-reflectorized pedestrians were short. Reflectorization dramatically increased the visibility distances.

Shinar (10) studied the nighttime pedestrian visibility, considering the influence of driver expectancy and pedestrian clothing. It was found that the visibility distance increased with expectancy. It was also found that pedestrian reflectorization significantly influenced visibility.

Strickland et al. (11) investigated the effects of hyperopia, myopia, and increased optical scatter on the detection of roadway obstacles under low-beam and high-beam illumination conditions. Visibility impairments were found with ametropia and increased optical scatter. High beams appeared to be helpful in improving visibility.

Austin et al. (12) studied pedestrian visibility under standard headlamp illumination. On the basis of their analysis, they proposed applicable retroreflective treatments as safety countermeasures.

Zwahlen (13) developed a geometric model to analyze reflectorized targets along a tangent-curve and curve-tangent section of a highway. The model demonstrated that unknown or unexpected reflectorized targets may initially appear at moderately large peripheral angles up to 15 degrees away from the foveal fixation point or line of sight. On the basis of a peripheral detection field study, it was

found that the detection distance at a peripheral detection angle of 10 degrees was only about one-half of the foveal detection distance.

OBJECTIVES

On the basis of information mentioned earlier, the objectives of this study were as follows:

1. To examine each step in Haber's theoretical visibility distance analysis;
2. To conduct exploratory field luminance measurements involving targets of different reflectances;
3. To develop an independent visibility distance prediction software package written in the C-language, providing the user with the following three luminance contrast threshold models:
 - (a) Adrian's target visibility algorithm (14),
 - (b) PCDETECT (15) algorithm, and
 - (c) Two-dimensional, 3rd-order polynomial Lagrangian interpolation (16) of Blackwell's 1946 contrast threshold data (17) (positive contrast, 6 sec exposure time);
4. To compare the outputs of the newly developed visibility model with the findings of Haber (3);
5. To conduct a small target visibility field experiment under low-beam nighttime driving conditions to obtain a tentative field factor. This field factor is required to account for the average performance of a normal observer in a driving situation; and
6. To provide visibility distances and percent loss curves as a function of the initial visibility distance D_0 , as they can be expected by a typical headlamp pair (6054 headlamps in a 1981 VW Rabbit).

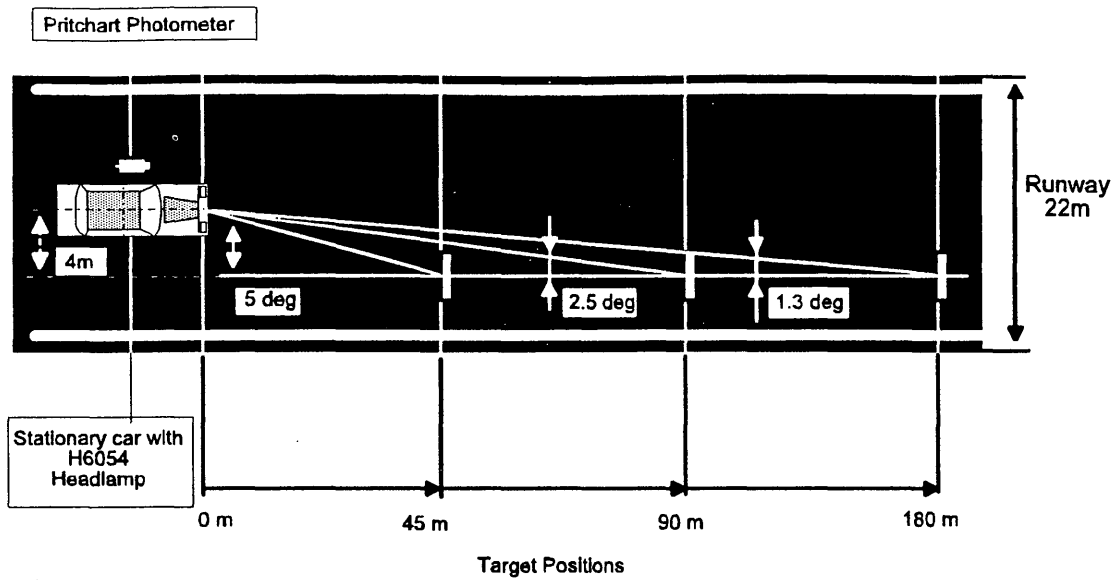
EXPLORATORY FIELD LUMINANCE MEASUREMENTS

Objective and Method

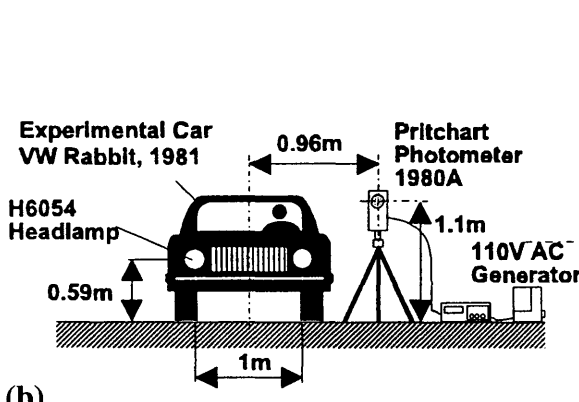
The exploratory field luminance measurements were required to provide a basis of reliable target and background luminances, measured on eight different nonretroreflective targets under low-beam illumination conditions at night. The measured luminances were used to validate the algorithms during the development of the visibility distance software package. Note that no glare source was present. A spray-painted black plywood board, a spray-painted reddish dark brown plywood board, a spray-painted blue plywood board, a spray-painted dark yellow-beige plywood board, a spray-painted dark green plywood board, dark brown clothing attached to plywood board, light blue (jeans) clothing attached to plywood board, and a plain plywood board served as targets.

Figure 1C illustrates the target setup. The targets 0.6096×0.6096 m (1 × 1 ft) were installed 0.3048 m (1 ft) above the pavement. Luminance values were obtained at the positions marked 0 to 5, as indicated in Figure 1C, using a Pritchard photometer model 1980A, which was located as close to the vehicle as possible (see Figure 1A and B.) The photometer aperture was selected such that the measured area was about 60 percent of the target area. Note that the photometer was not measuring through the automobile windshield and provided therefore the luminance values that were needed to determine the initial seeing distance D_0 .

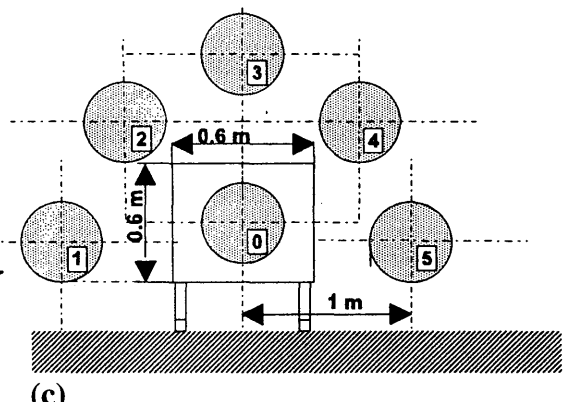
Figure 1A shows the setup of the targets and experimental car on the runway of an old, unused airport in Athens, Ohio. Each one of



(a)



(b)



(c)

FIGURE 1 Layout of experimental site (a) setup of the experimental vehicle (b); and Pritchard photometer measurement positions (c).

the eight targets was measured at a distance of 45, 90, and 180 m away from the car. The setup of the experimental vehicle is shown in Figure 1B.

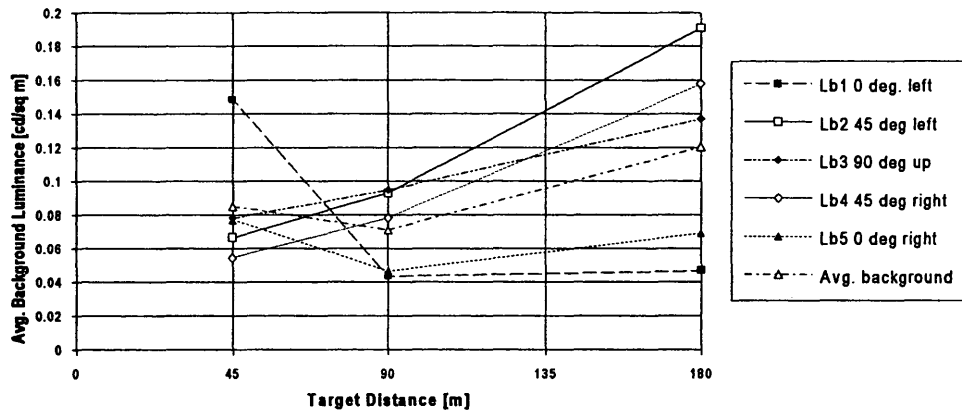
Experimental Results and Conclusions

From Figure 2A, it appears that most background luminances are fairly close to one another regardless of the measurement location. At close distances (45 m), however, there seems to be an increase in background luminance to the left of the target. An analysis of variance on the background luminance values was used to determine whether it is adequate to take an average background luminance over all five measurement locations for further model development and validation. Because $F_{\alpha} = 0.05$ $v_1 = 2$ $v_2 = 10 > F_0$, one fails to reject H_0 , and therefore it is adequate to use an average taken over all five measurement locations as background luminance. Figure 2B shows the target luminance, the background luminance, and the contrast for the eight nonretroreflective targets as a function of the target distance. The exact values can be found in Tables 1-3. From

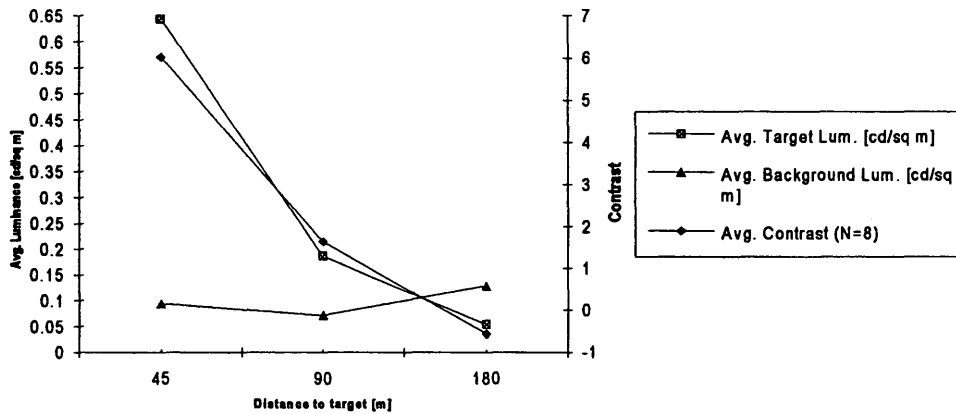
these results it can be seen that the average background luminance lies within the range of 0.0939 and 0.1288 cd/m^2 , that is, the background luminance remains almost constant over the entire range of the target distances used in the experiment. The target luminance, on the other hand, ranges from 0.0535 to 0.644 cd/m^2 , that is, the target luminance increases considerably for smaller target distances. The resulting actual average contrast drops from 6.02 for a target distance of 45 m to -0.558 for a target distance of 180 m.

EXPLORATORY TARGET DETECTION FIELD EXPERIMENT

A small visibility distance field experiment was conducted to determine a field factor (contrast multiplier) that must be used to account for average observers under nighttime driving conditions. The experiment was conducted on the runway of the old, unused airport in Athens, Ohio. A blue spray-painted target 60.96 x 60.96 cm (2 x 2 ft) with a reflectance of $R = 0.155$ was placed at the right edge of the runway. Two women with an average age of 22.5 years



A. Average Background Luminance At Different Measurement Locations For All Non-Retroreflective Targets (N=8) As A Function Of Target Distance



B. Average Target Luminance, Average Background Luminance and Average Contrast (N=8) As A Function of Target Distance

FIGURE 2 Average background and target luminances for all nonretroreflective targets (N=8) as a function of target distance.

TABLE 1 Target Luminances Averaged over Five Different Measurement Positions of Eight Nonretroreflective Targets Under Low-Beam Illumination at Night

Target Number	Material and Color	Target Luminance [cd/sq m]					
		45m		90m		180m	
		Avg	Std.Dev	Avg	Std.Dev	Avg	Std.Dev
1	S.P.Black	0.1371	2.40E-04	0.0408	1.03E-04	0.0243	2.40E-04
2	S.P. Reddish Dark Brown	0.5413	6.85E-04	0.1206	3.43E-04	0.0449	2.06E-03
3	S.P. Blue	0.7778	6.17E-03	0.2957	1.37E-03	0.0658	6.85E-04
4	S.P. Dark Yellow Beige	0.7915	1.71E-03	0.1912	6.85E-04	0.0589	2.40E-04
5	S.P. Dark Green	0.6990	4.11E-02	0.2837	2.06E-03	0.0617	3.43E-04
6	Dark Brown Clothing	0.1018	3.43E-04	0.0305	3.43E-04	0.0185	1.03E-03
7	Light Blue Clothing	0.6030	2.40E-03	0.1552	1.37E-03	0.0521	2.06E-03
8	Plain Plywood	1.5007	1.95E-02	0.3700	6.85E-04	0.1021	6.85E-04
Average		0.6440		0.1860		0.0535	

TABLE 2 Background Luminances Averaged over Five Different Measurement Positions of Eight Nonretroreflective Targets Under Low-Beam Illumination At Night

Target Number	Material and Color	Background Luminance [cd/sq m]					
		45m		90m		180m	
		Avg	Std.Dev	Avg	Std.Dev	Avg	Std.Dev
1	S.P.Black	0.0634	8.84E-03	0.0829	3.40E-02	0.1593	7.95E-02
2	S.P. Reddish Dark Brown	0.0822	3.84E-02	0.0805	2.96E-02	0.1333	5.24E-02
3	S.P. Blue	0.0850	3.67E-02	0.0819	2.98E-02	0.1466	8.70E-02
4	S.P. Dark Yellow Beige	0.0815	3.04E-02	0.0829	3.28E-02	0.1124	7.67E-02
5	S.P. Dark Green	0.0874	4.69E-02	0.0692	3.03E-02	0.1566	1.55E-01
6	Dark Brown Clothing	0.0939	5.52E-02	0.0541	1.45E-02	0.1110	7.67E-02
7	Light Blue Clothing	0.1624	4.25E-02	0.0517	1.63E-02	0.1151	5.07E-02
8	Plain Plywood	0.0949	4.28E-02	0.0665	2.30E-02	0.0963	3.77E-02
Average		0.0938		0.0712		0.1288	

were used as subjects in this experiment. The experimental vehicle was a 1981 VW Rabbit with 6054 headlamps (low beams) and a windshield transmittance of $T = 0.72$. Because of the limited runway length, the subjects had to wear dark sunglasses ($T = 0.0568$) to provide useful visibility distances. Earlier attempts to use sunglasses with a greater transmittance failed because the subjects were often able to detect the target from the beginning of the runway [distance > 400 m (1,312 ft)]. Overall, the transmittance was $T_{tot} = 0.72 \cdot 0.0568 = 0.040896$. Each subject performed five runs. After each run the target was moved to another location along the right edge of the runway to avoid learning. Subject order and target location were completely randomized.

The average visibility distance was 104 m (342 ft) with a standard deviation of 16.6 m (54 ft). This data point was used to obtain a field factor (contrast multiplier) of 2.28, which must be applied to Blackwell's threshold contrast values (17), during the computation of C_{th} in the computer model.

DEVELOPMENT OF A VISIBILITY DISTANCE PREDICTION SOFTWARE PACKAGE

Introduction

The visibility distance of a target as seen through an automobile windshield or other similar optical filters with different transmittances can be determined by using representative human visual

threshold contrast data (17). Threshold contrast data provide a better basis for visual task performance studies than can be obtained using visual acuity measures (18). Visual acuity can be compensated in most cases with corrective glasses or lenses, whereas the threshold contrast function cannot be influenced.

The underlying algorithm of the program is based on the fact that a target is just visible at a given distance if the threshold contrast C_{th} and the actual contrast C_{act} are the same. For simplicity it is assumed that a driver's eyes are at the same longitudinal position as the headlamps. If no optical filter is present in the visual path from the headlamps to the target to the observer, one can determine the initial visibility distance D_0 as described by Haber (3). Now assume that an optical filter is inserted into the visual path of the observer. This reduces the light that reaches the retina of the observer, leaving the actual contrast C_{act} unaffected but increasing the threshold contrast C_{th} according to Blackwell's data (17) or that of other threshold contrast models, or both (14,15).

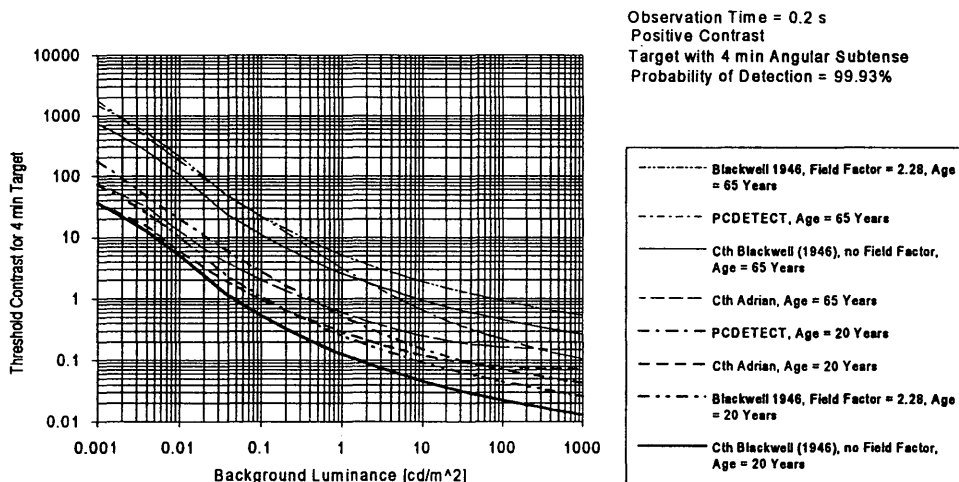
The visibility distance algorithm varies the distance of the observer and the headlamps to the target until C_{th} and C_{act} are equal. The same approach was also used by the Ford Motor PCDETECT (15) program. However, the CIE 19/2.1 (19) threshold contrast model used in PCDETECT does not appear to be in close accordance with the most comprehensive source of threshold contrast data as provided by Blackwell (17). In his experiment Blackwell (17) attempted to determine the threshold contrast of the human eye by conducting a large-scale experiment involving 19 subjects for an

TABLE 3 Contrasts Averaged over Five Different Measurement Positions of Eight Nonretroreflective Targets Under Low-Beam Illumination at Night

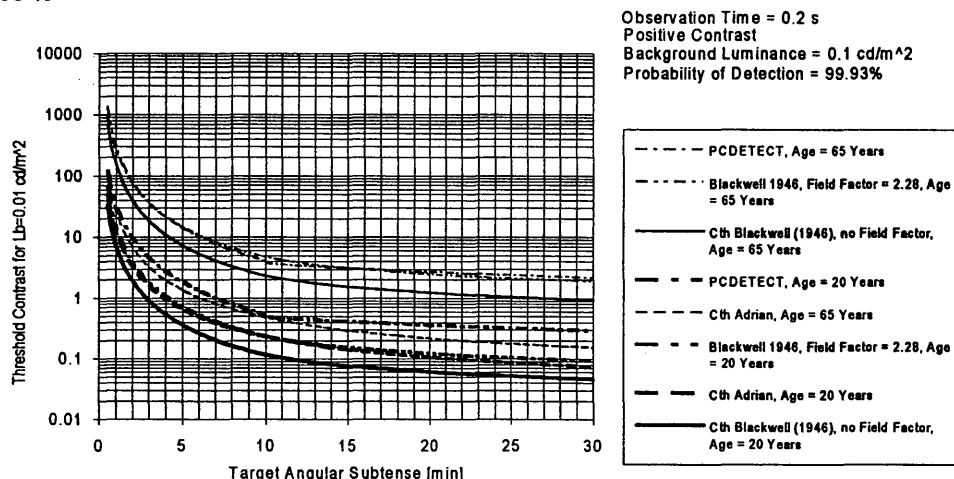
Target Number	Material and Color	Actual Contrast		
		45m	90m	180m
1	S.P.Black	1.16	-0.51	-0.85
2	S.P. Reddish Dark Brown	5.58	0.50	-0.66
3	S.P. Blue	8.15	2.61	-0.55
4	S.P. Dark Yellow Beige	8.70	1.31	-0.48
5	S.P. Dark Green	7	3.10	-0.61
6	Dark Brown Clothing	0.084	-0.44	-0.83
7	Light Blue Clothing	2.71	2	-0.55
8	Plain Plywood	14.81	4.57	0.06
Average		6.028	1.64	-0.56

extended period of up to 2.5 years. The subjects had to report whether they could detect a projected circular spot of a given angular subtense and a given luminance on a screen with a given background luminance as seen from about 60 ft away. Young women, aged 19 to 26, served as subjects with a visual acuity for both eyes of about 20/20. Stimulus size, stimulus brightness, and the background luminance were systematically changed. The subjects provided more than 2 million responses, some 450,000 of which were statistically evaluated.

On the basis of the statistical quality of Blackwell's experiment (17) it appears reasonable to use his data for the development of a visibility distance prediction software package. PCDETECT (15) on the other hand uses the CIE 19/2.1 (19) model because it is analytically derived from the vision theory and can therefore easily be implemented using a programming language. The PCDETECT model appears to produce threshold contrasts that are different (see Figure 3) from those that Blackwell (17) found in his experiments.



A : Threshold contrast comparison over a selected range of background luminances, for a target angular subtense of 4 min, observer age 20 years and 65 years, and a probability of detection of 99.93 %



B : Threshold contrast comparison over a selected range of target angular subtenses, for a background luminance of $0.1 \frac{cd}{m^2}$, observer age 20 years and 65 years, and a probability of detection of 99.93 %

FIGURE 3 Comparison between Adrian's threshold contrast model (14), PCDETECT (15), and the newly developed threshold contrast model based on data from Blackwell (17) with and without field factor.

THRESHOLD CONTRAST ALGORITHMS

Precise Two-Dimensional Third-Order Polynomial Lagrangian Interpolation (16) Using Blackwell's Data (17) as Tabular Points

Any point between the cells of Blackwell's tabulated threshold contrast data can be found with

$$C_{th}(\alpha, L_b) = \sum_{r=i}^{i+n} \sum_{s=j}^{j+n} \left(\prod_{\substack{k=i \\ k \neq r}}^{i+n} \frac{\alpha - \alpha_k}{\alpha_r - \alpha_k} \right) \cdot \left(\prod_{\substack{l=j \\ l \neq s}}^{j+n} \frac{L_b - L_{bk}}{L_{bs} - L_{bk}} \right) \quad (1)$$

where n is the order of the polynomial (order 3 seems to be sufficient). The interpolation in the newly developed computer model is based on Equation 1, implemented with Neville's algorithm (16) using 16 tabulated threshold contrast points around the point of interpolation. Using this method, it is possible to interpolate Blackwell's data (17) with a maximum relative error of, at the most, 5 percent for background luminances ranging from 3.4262×10^{-5} to 3426.2 cd/m^2 and target angular subtenses ranging from 0.595 to 360 min of arc. Thanks to the high precision of the interpolation method it is possible to compare the visibility distances that can be obtained by using the PCDETECT (15) model and by using Adrian's model (14) with the visibility distances obtained by using Blackwell's data (17) adjusted with a field factor of 2.28.

Adrian's Threshold Contrast Model

Adrian (14) describes a threshold luminance model based on the luminous flux function (Φ) characteristic for the Ricco process

$$\Delta L_{\alpha \rightarrow 0} = \Phi(L_b) \alpha^{-2} \quad (2)$$

and the luminance function (L) characteristic for Weber's law

$$\Delta L_{\alpha \rightarrow \infty} = L(L_b) \quad (3)$$

where α is the visual angle subtended by the target.

Adrian describes the threshold luminance function over the entire range of α as

$$\Delta L = k \left(\frac{\sqrt{\Phi}}{\alpha} + \sqrt{L} \right)^2 \quad (4)$$

Adrian gives the flux and luminous functions as follows

- On the basis of data from Adrian (20), for higher luminance levels of $L_b \geq 0.6 \text{ cd/m}^2$

$$\sqrt{\Phi} = \log(4.1925 \cdot L_b^{0.1556}) + 0.1684 \cdot L_b^{0.5867} \quad (5)$$

$$\sqrt{L} = 0.05946 \cdot L_b^{0.466} \quad (6)$$

- On the basis of data from Aulhorn (21) for very low luminance levels of $L_b \leq 0.00418 \text{ cd/m}^2$

$$\sqrt{\Phi} = 10^{0.028 + 0.173 \cdot \log(L_b)} \quad (7)$$

$$\sqrt{L} = 10^{-0.891 + 0.5275 \cdot \log(L_b) + 0.0227 \cdot (\log(L_b))^2} \quad (8)$$

- On the basis of Blackwell (17) for medium luminance levels of $0.00418 \text{ cd/m}^2 \leq L_b \leq 0.6 \text{ cd/m}^2$

$$\sqrt{\Phi} = 10^{-0.072 + 0.3372 \cdot \log(L_b) + 0.0866 \cdot (\log(L_b))^2} \quad (9)$$

$$\sqrt{L} = 10^{-1.256 + 0.319 \cdot \log(L_b)} \quad (10)$$

To account for an observation time t of less than 2 sec, Adrian (14) uses the following relationship:

$$\Delta L_t = \Delta L_{t=2s} \cdot \frac{a(\alpha, L_b) + t}{t} \quad (11)$$

where

$$a(\alpha, L_b) = \frac{\sqrt{a(\alpha^2 + a(L_b)^2)}}{2.1} \quad (12)$$

and

$$a(\alpha) = 0.36 - 0.0972 \times \left\{ \frac{[\log(\alpha) + 0.523]^2}{[\log(\alpha) + 0.523]^2 - 2.513 [\log(\alpha) + 0.523] + 2.7895} \right\} \quad (13)$$

$$a(L_b) = 0.355 - 0.1217 \times \left\{ \frac{[\log(L_b) + 6]^2}{[\log(L_b) + 6]^2 - 10.4 [\log(L_b) + 6] + 52.28} \right\} \quad (14)$$

In Adrian's model, the influence of observer age is given as follows:

$$\begin{aligned} 23 < \text{Age} < 64 & \quad AF = \frac{(\text{Age} - 19)^2}{2160} + 0.99 \\ 65 < \text{Age} < 75 & \quad AF = \frac{(\text{Age} - 56.6)^2}{116.3} + 1.43 \end{aligned} \quad (15)$$

According to Adrian (14) the probability of detection is 99.93 percent. The contrast threshold is then given by inserting Equations 5 through 11 into 4 and dividing the threshold luminance difference by the background luminance

$$C_{th} = \frac{2.6}{L_b} \left[\left(\frac{\sqrt{\Phi}}{\alpha} + \sqrt{L} \right)^2 \cdot \frac{a(\alpha, L_b) + t}{t} \cdot AF \right] \quad (16)$$

The model, as illustrated, should be used for positive contrasts only because Adrian's contrast polarity factor F_{cp} was not considered here. Adrian found a relatively strong contrast polarity effect, whereas a close investigation of Blackwell's data (17) reveals almost no contrast effect.

PCDETECT Model

The PCDETECT threshold contrast algorithm (15) is based on the CIE 19/2.1 (19) model. Unlike in the earlier model DETECT, which was based on the empirical data from Blackwell, the programmers decided to use a slightly modified version of the analytical CIE 19/2.1 model. The threshold contrast in PCDETECT is given by

$$C_{th} = cx \cdot \frac{0.0923}{n} \cdot \left[\left(\frac{S}{t \cdot L_e} \right)^{0.4} + 1 \right]^{2.5} \quad (17)$$

where the background luminance and the veiling luminance are used to express the effective background luminance present

$$L_e = L_b + B_v \quad (18)$$

and

$$n = \left[\left(\frac{S}{100 \cdot t} \right)^{0.4} + 1 \right]^{2.5} \quad (19)$$

and cx is a size factor introduced by the developers of PCDETECT

$$\begin{aligned} d \leq 10 \text{ min} & \quad cx = 3 \cdot (0.37)^{\log_{2d}} \\ d > 10 \text{ min} & \quad cx = 0.106 - 0.0006d \end{aligned} \quad (20)$$

This factor seems to cause an irregularity in the threshold contrast function at a target visual angle of 10 min (see Figure 3B).

The S -parameter in Equation 19 is a function of the target size d and the observer age in s

$$S = 10^{0.5900 - 0.6235 \log(d) - s} \quad (21)$$

where s is given by

$$\begin{aligned} 20 \leq \text{Age} \leq 44 & \quad s = 0 \\ 45 \leq \text{Age} \leq 64 & \quad s = 0.00406 \cdot (\text{Age} - 44) \\ 65 \leq \text{Age} \leq 80 & \quad s = 0.0812 + 0.00667 \cdot (\text{Age} - 64) \end{aligned} \quad (22)$$

the function for t in Equation 17 is given by

$$\begin{aligned} 20 \leq \text{Age} \leq 30 & \quad t = 1 \\ 31 \leq \text{Age} \leq 44 & \quad t = 10^{-0.01053 \cdot (\text{Age} - 30)} \\ 45 \leq \text{Age} \leq 64 & \quad t = 10^{-0.1474 - 0.0134 \cdot (\text{Age} - 44)} \\ 65 \leq \text{Age} \leq 80 & \quad t = 10^{-0.4154 - 0.0175 \cdot (\text{Age} - 64)} \end{aligned} \quad (23)$$

Another age-related factor is the contrast multiplier m_1

$$\begin{aligned} 20 \leq \text{Age} \leq 42 & \quad m_1 = 1 + 0.00795 \cdot (\text{Age} - 20) \\ 43 \leq \text{Age} \leq 64 & \quad m_1 = 1.175 + 0.0289 \cdot (\text{Age} - 42) \\ 65 \leq \text{Age} \leq 80 & \quad m_1 = 1.811 + 0.1873 \cdot (\text{Age} - 64) \end{aligned} \quad (24)$$

To account for the increased variability of the threshold contrast for older observers and to apply the threshold contrast function at any probability of detection, PCDETECT uses

$$\begin{aligned} \text{Age} \leq 35 & \quad \sigma_{\log} = 0.124 + 0.001133 \cdot \text{Age} \\ \text{Age} > 35 & \quad \sigma_{\log} = 0.064 + 0.002850 \cdot \text{Age} \end{aligned} \quad (25)$$

and a factor cf to correct the log standard deviation in Equation 25 to account for the influence of the background luminance on the variability of the threshold contrast:

$$\begin{aligned} \log L_b \leq -0.5 & \quad cf = 1.0875 - 0.065 \cdot \log(L_b) \\ \log L_b > -0.5 & \quad cf = 1.012 - 0.216 \cdot \log(L_b) \end{aligned} \quad (26)$$

Equation 27 is used to correct the standard deviation given in Equation 25 as follows:

$$\sigma_{\log C_{th}} = \sigma_{\log} \cdot cf \quad (27)$$

A contrast multiplier is introduced to allow evaluation of the threshold contrast function at any given probability of detection

$$\log(\text{cmp}) = Z_p \cdot \sigma_{\log C_{th}} \quad (28)$$

where Z is the standardized normal variable associated with the desired probability P . The threshold contrast function C_{th} can be obtained by inserting equations 18 to 23 into Equation 17 and by applying the multipliers given in Equations 24 and 28 as follows:

$$C_{th} = cx \cdot m_1 \cdot \text{cmp} \cdot \frac{0.0923}{n} \cdot \left[\left(\frac{S}{t \cdot L_e} \right)^{0.4} + 1 \right]^{2.5} \quad (29)$$

Comparison and Discussion Of Threshold Contrast Models

The three previously described threshold contrast models were implemented in a computer program using the C-language. The computer program was used to plot the threshold contrast curves indicated in Figure 3A and B. Figure 3A illustrates the comparison of the three threshold contrast models for a background luminance range of 0.001 (cd/m²) to $L_b \leq 1000$ (cd/m²), a positive contrast target having a constant angular subtense of a 4-min arc, an observation time of 0.2 sec, and a probability of detection of 99.93 percent. As indicated in Figure 3A, the lowest threshold contrasts were obtained from Blackwell's 1946 data (17), which is no surprise, considering that the involved subjects were young women who were highly skilled observers. A previously described exploratory target visibility field experiment was conducted under automobile low-beam illumination conditions to provide a field factor (contrast multiplier) for Blackwell's 1946 data. A field factor of 2.28 seemed to be adequate to account for average observers under such conditions. The adjusted Blackwell threshold contrast values shown in Figure 3A have the same overall shape as the original data from that work (17) but are higher in magnitude, indicating that normal observers would provide shorter visibility distances. Adrian's model (14) provides threshold contrast values that seem to match Blackwell's data (17) relatively closely for background luminances below 0.01 cd/m². For higher luminances, Figure 3A shows that Adrian's model (14) deviates more and more from Blackwell's data (17). This may be attributed to the fact that the model uses the three independent threshold contrast data bases from Adrian (20), Aulhorn (21), and Blackwell (17), as a function of the background luminance. From Figure 3A it is also evident that the age function in Adrian's model (14) does not seem to adequately account for observer age. PCDETECT, on the other hand, provides threshold contrast values that are considerably higher in magnitude than the adjusted Blackwell data (field factor = 2.28). This would indicate that PCDETECT generally provides visibility distances that are somewhat shorter.

Figure 3B illustrates the comparison of the three threshold contrast models for an angular subtense ranging from 0.5 min $\leq \alpha \leq 30$ min, a positive contrast target, a background luminance of 0.1 (cd/m²), which is the approximate average background luminance obtained in the field measurements, an observation time of 0.2 sec, and a probability of detection of 99.93 percent. As seen in Figure 3B, the lowest threshold contrast values are obtained for Black-

well's 1946 data (17). Under the given conditions, it seems that Adrian's model (14) and the adjusted Blackwell data (field factor = 2.28) produce similar threshold contrasts. PCDETECT, on the other hand, provides threshold contrast values that are significantly higher than both Adrian's data and Blackwell's adjusted data. From Figure 3B it can be seen that PCDETECT has an irregularity in its threshold contrast function at a visual angle of 10 min of arc. This may be attributed to the size factor cx in Equation 20. For visual angles greater than 10 min of arc the PCDETECT model produces threshold contrast values that are considerably higher than the ones obtained from Adrian's model (14) and both the adjusted and unadjusted data from Blackwell (17). From the comparison of the algorithms it can be concluded that only the adjusted Blackwell threshold contrast values appear to be adequate for use in visibility distance models where extended ranges of both the angular subtense and the background luminance may be present and normal observers are considered. Adrian's model (14) seems to provide adequate results for background luminances below 0.1 (cd/m²), given that young observers are used. Adrian's age function appears to be too gentle for older observers. PCDETECT generally provides threshold contrasts that are too high when compared with those of the other models. This may lead to rather short visibility distances. The PCDETECT model should be used carefully, with a lot of caution, for visual angles above 10 min of arc.

EXAMINATION OF LOSS IN DRIVER VISIBILITY CAUSED BY TINTED OPTICAL MEDIA

Visibility Distance Prediction Software Package

The newly developed visibility distance software package, based on Blackwell's threshold contrast data (17), adjusted with a field factor of 2.28 was used for a critical examination of the statements made in Haber's paper (3). The program was implemented in the C-language and is executable on IBM (or compatible) personal computer running under MS DOS 5.0 or newer. The user must provide the target reflectance, the physical target size (size corresponds to the size of a Blackwell disk), the background luminance that will be kept constant over all iterations, the optical filter transmittance in percent, the observer age, the observation time, the probability of detection (50, 90, 95, and 99.93 percent, and the headlamp type (Haber lamp A, Haber lamp B, Taurus low beam, Taurus high beam, 6054 low beam)

Using this input, the program determines the Blackwell threshold contrast (17) adjusted with a field factor of 2.28, by applying the two-dimensional third-order polynomial Langrangian interpolation given in Equation 1. The actual contrast is determined from the target luminance, which depends on the target reflectance, the selected headlamp data (two low-beam headlamps), and the current observation distance, and from the background luminance, which has been found to remain almost constant over the entire visibility range. If the actual contrast C_{act} is greater or equal to the threshold contrast C_{th} , then the target is still visible and can be moved farther away one step. The step size is reduced by 50 percent in case a threshold crossing from visible to invisible or vice versa has occurred. The iteration process continues as long as the step size is greater than 1 cm. When this final condition is reached the program returns the current distance D as the visibility distance under the entered conditions. The implemented solver-algorithm basically

determines the point where the actual contrast function $C_{act} = f(D)$ intersects the threshold contrast function $C_{th} = f(D)$.

Examination of Statements Made by Haber (1)

Figure 4A illustrates how a target placed at the initial visibility distance D_0 (target just visible without optical filter), ahead of the observer in an automobile, produces a given luminance contrast C_{act1} between the target and the background under low-beam illumination. The actual contrast C_{act1} at the initial visibility distance D_0 is then equal to the threshold contrast C_{th1} from Blackwell (17), adjusted by a field factor of 2.28, because the target is just visible at a given probability of detection. Inserting an optical filter of a given transmittance $T < 1$ at the initial distance D_0 does not change the actual contrast C_{act1} . However, because the background luminance L_b is reduced by the optical filter, the threshold contrast C_{th} is increased according to the adjusted Blackwell data. The target therefore becomes invisible at the current distance because of insertion of a tinted optical filter. The target can be made visible again by moving the automobile (with the observer) closer to the location of the target (or vice versa). This changes the angular subtense α and the target luminance L_t , and to some degree the background luminance L_b . Therefore, moving the observer in the automobile and the target closer together also changes the actual contrast C_{act} and the threshold contrast C_{th} . As indicated in Figure 4A, the target becomes visible again when $C_{th2} \leq C_{act2}$. In his analysis, Haber (3) incorrectly stated that this will occur at the same contrast level as the initial contrasts $C_{th1} = C_{act1}$. This would require the background luminance L_b to vary synchronously with the target luminance L_t , which is extremely unlikely. The previously described exploratory field luminance measurements have clearly indicated that the background luminance L_b remains almost constant over the visibility range, causing the actual contrast C_{act} to decrease with increasing distance. This fact is also illustrated in Figure 4A. Under Haber's incorrect assumption (3) that the actual contrast C_{act} does not change as a function of distance, one generally obtains a visibility distance (D_{Haber}) that is too short (Figure 4A.) This in turn leads to an unreasonably high percent loss of the visibility distance when an optical filter of a given transmittance is inserted. The correct percent loss, based on the example shown in Figure 4A is given by

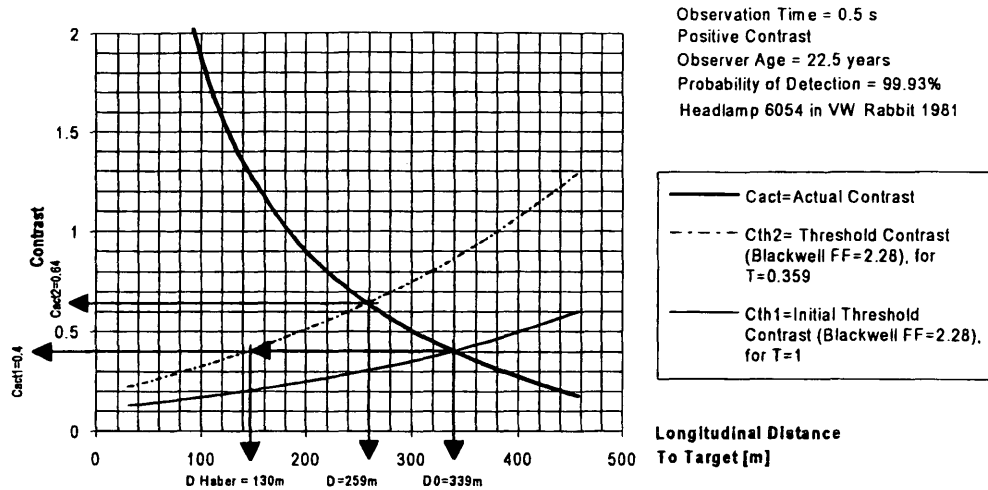
$$PL = 100 \cdot \left(1 - \frac{D}{D_0}\right) = 100 \cdot \left(1 - \frac{259m}{339m}\right) = 23.59 \text{ percent} \quad (30)$$

The incorrect percent loss in visibility distance for the example shown in Figure 4A, based on Haber's incorrect assumption is given by

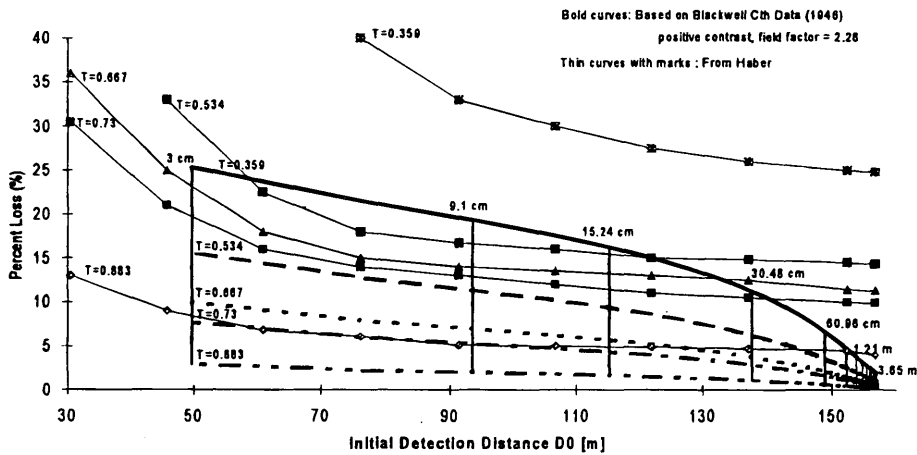
$$PL = 100 \cdot \left(1 - \frac{130m}{339m}\right) = 61.65 \text{ percent} \quad (31)$$

This would indicate that the statements made by Haber (3) about the reduction in driver visibility caused by tinted optical media are incorrect and misleading.

It is also evident from Figure 4A that a target of a given physical dimension and reflectance always provides the same average initial visibility distance D_0 , given that the intensity of the headlamps, the filter transmittance ($T = 1$), and the ambient background luminance L_b are not varied. Haber (3), however, presented percent loss curves for a target having a constant mean linear dimension of 91.4 cm (3 ft) over the entire distance range. These incorrect percent loss



A: The initial distance D_0 in the above example is found at the point where $C_{act1}=0.4$ intersects with $C_{th1}(T=1)$. When a filter of $T=0.359$ is inserted, the visibility distance D is found where $C_{act2} = 0.64$ intersects with $C_{th2}(T=0.359)$. Haber (3) incorrectly proposed that D can be found at the point where $C_{th2}(T=0.359)$ intersects with $C_{act1}=0.4$. However, this would lead to unreasonably short visibility distances.



B: Percent loss of visibility distance curves provided by model for various filter transmittances and target sizes, and incorrect percent loss of visibility distance curves provided by Haber for a target having a constant mean linear dimension of 91.4 cm (3 ft) over the entire distance range. Target reflectance $R=0.15$, headlamp Haber type A, probability of detection $P=99.93\%$, observer age = 22.5 years, exposure time $T=0.5$ sec.

FIGURE 4 Loss of visibility distance because of tinted optical media.

curves are shown in Figure 4B, superimposed on the size-dependent percent loss curves provided by the newly developed computer model. For a target having a constant mean linear dimension and a constant reflectance, Haber's curves are incorrect because at a given initial visibility distance D_0 , there is only one given target luminance L_t , only one given background luminance L_b , and only one given angular subtense α . Therefore there is only one actual contrast $C_{act} = (L_t - L_b)/L_b$ and only one threshold contrast C_{th} . Figure 4B illustrates how Haber incorrectly assumed an entire range of D_0 for a single-size 91.4-cm (3-ft) target with a reflectance of $R = 0.15$.

Figure 4B also illustrates that the magnitude of the percent loss curves from Haber's (thin lines with marks) grossly overestimates the true percent loss obtained with the computer model (bold lines). According to the computer model, a motorist can detect a 91.4-cm (3-ft) target ($R = 0.15$) at $D_0 = 157$ m (515 ft) when no windshield is used ($T = 1$). Even with a filter having a transmittance $T = 0.359$ the motorist can detect the same target at $D = 149.4$ m (490.15 ft) which is equivalent to a 4.81 percent loss. The incorrect percent loss at $D_0 = 157$ m (515 ft) given by Haber is about 25 percent. To obtain such high losses, it would be necessary to shrink the target to

a mere 3 cm (0.1 ft) when using a tinted windshield with a transmittance of $T = 0.359$. Such a small target no longer represents a pedestrian and would not likely have to be considered as a road hazard for the establishment of minimum transmittance standards.

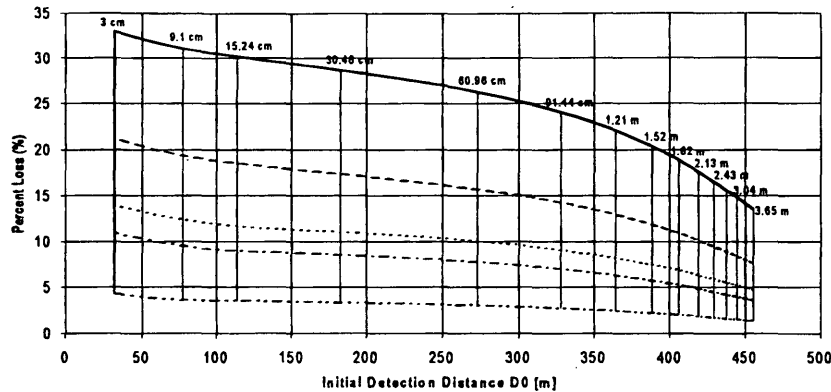
Figure 5A indicates the output of the computer model for various windshield transmittances and target sizes for data from the 6054 headlamps that were used in the field target visibility experiment, a constant background luminance of 0.1 cd/m^2 , and an observer age of 22.5 years. Figure 5B indicates the percent loss when the observer age is increased to 65 years. By comparing Figure 5A with 5B it can be seen that the magnitude of the percent loss does not considerably change with age, but the initial visibility distances are reduced significantly. On the basis of the literature (5,6), further research with older drivers may be required to quantify the influence of observer age with an even-higher accuracy.

CONCLUSIONS

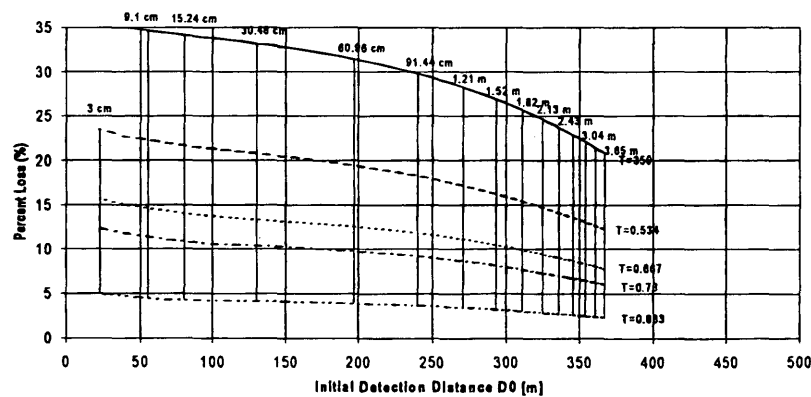
The exploratory field luminance measurements indicate that the background luminance remains almost constant over the entire

visibility range. The actual contrast C_{act} therefore decreases as the distance to the target increases. A target visibility field experiment has indicated that even with a transmittance as low as $T=0.0408$, young subjects can detect a blue spray-painted target $60.96 \times 60.96 \text{ cm}$ ($2 \times 2 \text{ ft}$) under low-beam illumination on the average at 104 m (342 ft).

It was found that Adrian's model (14) provides threshold contrast values that seem to match those of Blackwell (17) for background luminances below 0.01 cd/m^2 . PCDETECT (15) provides threshold contrast values that are considerably higher in magnitude than both the adjusted Blackwell data (field factor = 2.28) and the threshold contrast values obtained from Adrian's model (14). This would indicate that PCDETECT provides visibility distances that are generally somewhat too short. PCDETECT should be used with a lot of caution for visual angles above 10 min of arc. From the comparison of the algorithms it can be concluded that only the adjusted Blackwell threshold contrast values (field factor = 2.28) appear to be adequate for use in seeing distance models, where extended ranges of both the angular subtense and the background luminance may be present and normal observers are considered.



A: Percent loss visibility distance as a function of initial visibility distance D_0 (transmittance $T=1$) for various filter transmittances and target sizes. Target reflectance $R=0.155$, headlamps 6054 in VW Rabbit 1982, probability of detection $P=99.93\%$, observer age = 22.5 years, exposure time $T=0.5 \text{ sec}$.



B: Percent loss visibility distance as a function of initial visibility distance D_0 (transmittance $T=1$) for various filter transmittances and target sizes. Target reflectance $R=0.155$, headlamps 6054 in VW Rabbit 1982, probability of detection $P=99.93\%$, observer age = 65 years, exposure time $T=0.5 \text{ sec}$.

FIGURE 5 Percent loss visibility distance as a function of initial visibility distance.

The graphical method to determine the visibility distance proposed by Haber (3) was closely examined and appears to be ambiguous and incorrect because it assumes a constant actual contrast C_{act} . It was shown with a newly developed computer model that the magnitude of the percent loss visibility distance is much smaller than that stated by Haber, even for windshields with a relatively low transmittance. Haber (3) presented incorrect percent loss curves for a target having a constant mean linear dimension of 91.4 cm (3 ft) and a constant reflectance. It was demonstrated in this investigation that for a constant headlamp intensity, only 1 percent loss point can be obtained for one given filter transmittance. Haber's percent loss curves are therefore unclear and misleading. To obtain losses of the magnitude given by Haber (3) and subsequently published (4), however, it would be necessary to shrink the target to a mere 3 cm (0.1 ft) when using a tinted windshield with a transmittance of $T = 0.359$. Such a small target no longer represents a pedestrian and would not likely have to be considered as a major or important road hazard for the establishment of minimum transmittance standards. However, tinted windshields will reduce not only foveal but also peripheral detection distances. Therefore, despite the much smaller percent visibility distance losses found in this study when compared with Haber's (3) percent loss values, the authors are in no way suggesting that darker tints on windshields should be permitted or that drivers should be driving with sunglasses at night. Any changes in windshield transmission standards should be based on tradeoffs between factors such as visibility, thermal comfort (infrared deflection), and glare reduction and on additional field validation studies that include older drivers and peripheral target detection.

Further field experiments using a wider range of transmittances (less tinted optical media) would be beneficial to further validate the developed computer model. After additional validation, the output of the computer model could assist in the review of the appropriateness of the established minimum transmittance standards.

REFERENCES

1. Roper, V. J. *Bulletin 68.*, HRB, National Research Council, Washington, D.C., 1953.
2. Heath, W., and D. M. Finch. The Effect of Tinted Windshields and Vehicle Headlighting on Night Visibility. *Bulletin 68.*, HRB, National Research Council, Washington, D.C., 1953, pp. 1-15.
3. Haber, H. Safety Hazard of Tinted Automobile Windshields at Night. *Optical Society of America*, Vol. 45, No. 6, June 1955, pp. 413-419.
4. Henderson, R. L. (ed.). *Driver Performance Data Book*. Final Report DOT-HS-807-121, NHTSA, April 15, 1986.
5. Waetjen, R., U. Schiefer, A. Gaigl, and E. Aulhorn. Der Einfluss von Windschutzscheiben "-Toenung" und "-Neigung" auf den Erkennungsabstand unter mesopischen Bedingungen. *Zeitschrift für Verkehrssicherheit* (in German), Vol. 39, No. 1, 1993.
6. Freedman, M., P. Zador, and L. Staplin. Effects of Reduced Transmittance Film on Automobile Rear Window Visibility. *Human Factors*, Vol. 35, No. 3, 1993, pp. 535-550.
7. Derkum, H. Effects of Various Transmission Levels in Windshields on Perception. *Vision in Vehicles-IV*, Elsevier Science Publishers B.V., 1993.
8. Kessler, F. R. Light Diffusion Characteristics and Visibility Interferences in Automobile Windshields. *Vision in Vehicles -IV*, Elsevier Science Publishers B.V., 1993.
9. Hazlett, R. D., and M. J. Allen. The Ability to See a Pedestrian at Night: The Effects of Clothing, Reflectorization and Driver Intoxication. *American Journal of Optometry and Archives of American Academy of Optometry*, Vol. 45, No. 4, 1968.
10. Shinar, D. The Effects of Expectancy, Clothing Reflectance, and Detection Criterion on Nighttime Pedestrian Visibility. *Human Factors*, Vol. 27, No. 3, 1985, pp. 327-333.
11. Strickland, J., B. Ward, and M. J. Allen. The Effect of Low vs. High Beam Headlights and Ametropia on Highway Visibility at Night. *American Journal of Optometry and Archives of American Academy of Optometry*, Vol. 45, No. 2, 1968.
12. Austin, R. L., D. J. Klassen, and R. C. Vanstrum. Driver Perception of Pedestrian Conspicuousness Under Standard Headlight Illumination. 3M Company, St. Paul, Minn.
13. Zwahlen, H. T. Conspicuity of Suprathreshold Reflective Targets in a Driver's Peripheral Visual Field at Night. In *Transportation Research Record 1213*, TRB, National Research Council, Washington, D.C., 1989.
14. Adrian, W. Visibility of Targets. In *Transportation Research Record 1247*, TRB, National Research Council, Washington, D.C., 1989, pp. 39-45.
15. Farber E., and C. Matle. PCDETECT: A Revised Version of the DETECT Seeing Distance Model. In *Transportation Research Record 1213*, TRB, National Research Council, Washington, D.C., 1989, pp. 11-20.
16. Press, W. H., W. T. Vetterling, S. A. Teulkowsky, and B. P. Flannery. *Numerical Recipes in C*, 2nd ed. Cambridge University Press, Cambridge, England, 1992.
17. Blackwell, H. R. Contrast Thresholds of the Human Eye. *Journal of the Optical Society of America*, Vol. 36, No. 11, 1946.
18. Ginsburg, A. P. Contrast Sensitivity, Driver's Visibility, and Vision Standards. In *Transportation Research Record 1149*, TRB, National Research Council, Washington, D.C., 1989, pp. 32-39.
19. An Analytic Model For Describing the Influence of Lighting Parameters Upon Visual Performance. *Publication CIE 19/2.1 (TC-3.1)*, Commission Internationale de L'Eclairage, Paris, France, 1989.
20. Adrian W. *Lichttechnik* (in German), Vol. 21, 1969.
21. Aulhorn, E. *Graefes Archiv für Klinische und Experimentelle Ophthalmologie* (in German), Vol. 167, No. 1, 1964.

Publication of this paper sponsored by Committee on Visibility.

Traffic Sign Reading Distances and Times During Night Driving

HELMUT T. ZWAHLEN

Videotaped eye fixations and saccades (30 frames per second) were analyzed for 32 young, healthy unfamiliar drivers along rural two-lane highways in Ohio under low-beam illumination conditions at night for the approach to a curve/turn warning sign (curve/turn symbol) for two selected curves. The first-look distance (longitudinal distance measured from the sign to a driver's eyes at which a driver foveally fixates the sign for the first time), last-look distance (the distance measured from the sign to a driver's eyes where he or she moves the eyes away from the sign for the last time before reaching the sign), number of looks and durations of looks at the warning sign were of main interest in this study. Cumulative last-look distance, first-look duration, and last-look duration graphs were established. The results of this study and a previous similar study indicate that drivers look on the average about two times at a warning sign during a nighttime low-beam approach. It was found that between the first look (information acquisition) and the last look (confirmation) at a sign there was usually at least one eye fixation on the roadway ahead. Using cumulative eye fixation duration data obtained for straight road driving under low-beam nighttime conditions published in another study and an average saccade duration of about 0.03 sec, a sign reading distance model was developed that determines the distance (minimum required legibility distance, MRLD) at which a simple bold symbol on a warning sign must be recognized. The model provides for a given speed the overall cumulative probability distribution function for the MRLD in terms of distance or in terms of time. The advantage of this model, which is applicable to warning signs with simple symbols under low-beam illumination at night, is that it is totally based on observed, recorded, and analyzed driver eye scanning and information-seeking behavior in the field.

The minimum distance away from the sign at which the message or a symbol on a sign must be legible or recognized by a driver under nighttime low-beam driving conditions is important, if one wants to determine the minimum required sign luminance, or the minimum retroreflective requirements of a sign sheeting material. A recent FHWA report on minimum retroreflectivity requirements for traffic signs (1) and a software package called CARTS, discussed in Paniati and Mace (1) make use of such a minimum required distance (minimum required visibility distance, MRVD), which has been described by Mace and Gabel (2). The MRVD values used in CARTS were found to be unsatisfactory for the following reasons:

1. A total of 95 out of 164 (58 percent MRVD distances used for signs in CARTS) have a value of about 61 m (200 ft) for an approach speed of 88 kph (55 mph). This results in a preview time of only 2.5 sec when a driver's sign-reading process starts. According to a number of technical sources such as CIE report 73 (3) a minimum preview time of 3 sec is recommended, which would indicate that the sign-reading process would have to be completed when a driver's eyes are 3 seconds away from a warning sign.

2. In the case of side-mounted signs an arbitrary horizontal out-of-view angle of 10 degrees is used; it is not speed dependent and results in a constant out-of-view distance of about 34 m (111 ft) for a typical sign placed on the right side of the road. This results in a minimum preview time of 1.4 sec at a speed of 88 kph (55 mph).

3. There is only one MRVD value given in CARTS for a given sign and speed without reference to a population percentile value or information whether it is an average value, a median value, or a percentile value. Any human factor design in the field of traffic safety should always be based on a selected population percentile value (i.e., 85 or 95 percent). Furthermore, most MRVD values given in CARTS appear to be extremely short, especially for signs with symbols, when compared with actual driver eye-scanning behavior data.

4. There is no transparent mathematical formula or logical structure given in CARTS that would identify, for each sign and speed case, the factors and their values used to arrive at the MRVD distance. Some MRVD distances are also not speed dependent.

5. Some of the MRVD model components are most likely based on average values only, which are based on laboratory studies using young subjects in a nondriving situation under relatively high luminance conditions (4,5).

OBJECTIVE

It was the objective of this study to develop a model for driver sign reading behavior for warning signs or similar signs with simple bold symbols and limited information content, which is based on actual observed symbolic sign reading behavior of young drivers at night under low-beam conditions on two-lane rural roads in the real world. Further, the model must be capable of providing minimum required legibility distance (MRLD) values for selected population percentiles (i.e., 50, 85, and 95 percent).

REQUIREMENTS OF THE MRLD MODEL

The following requirements had to be met by the MRLD model:

1. The MRLD model should be based on actual driver eye-scanning behavior recorded under nighttime, low-beam driving conditions on two-lane rural roads;

2. The MRLD model should be valid for a speed range of 48 to 105 kph (30 to 65 mph) and for warning signs, regulatory signs with either bold simple symbols or 1- or 2-word simple text (well-known; large character height; short words, e.g., EXIT, LEFT, RIGHT);

3. The MRLD model should provide not only an average MRLD value for a selected speed but also MRLD values for different driver population percentile values such as 50, 85, and 95 percent;

4. The model should be simple and easy to use.

DESCRIPTION OF MRLD MODEL

The MRLD model is based on the fact that drivers almost always try to confirm the information they have acquired in a first or previous eye fixation on a sign with an additional eye fixation. One could argue that a driver should have a right to be given enough time to make at least two eye fixations on a warning sign or a regulatory sign, which contains text information that is either simple bold symbolic or limited, or has well-known or short words and large character height. It is further observed and generally agreed on that a driver should look at the roadway ahead as frequently as driving conditions permit (almost always at least once or twice every second). In addition, for carrying out the information acquisition and the driving task in an efficient, safe, and comfortable manner a preview time of at least 3 sec or more is usually required (3). Therefore, the MRLD is given by the last-look distance plus the last-look duration times speed, plus the saccade duration times speed, plus the road-look duration times speed, plus the saccade duration times speed plus the first-look duration times speed. All of the three durations and the last-look distance are probability distribution functions and are assumed to be independent of each other, with the exception of the two saccade durations (0.03 sec each), which are assumed to be constants. The saccade distance when moving the gaze away from the sign, after the last look, is assumed to be part of the last-look distance.

DEVELOPMENT OF MRLD MODEL KNOWN, SHORT WORD TEXT INFORMATION

The following assumptions were made during the development of the MRLD model for warning signs containing either simple bold symbolic or limited large-character-height well-known short-word text information:

1. Drivers make an average of about two eye fixations on a warning sign (first look, information acquisition and processing; second look or last look, confirmation of information) (6,7).

2. Between the first look and last look on the sign there is usually at least one eye fixation on the road or the road environment ahead of the vehicle.

3. The duration of an individual eye fixation on the sign or on the road is long enough that a driver can acquire and process the information available from that fixation, make a decision, and initiate a control action, if any is required.

4. Foveal or near-foveal eye fixations away from the road to the sign are required to recognize the symbol or text, or both, on the sign.

5. The eye fixation times to recognize a simple bold symbol or simple, large-character-height text on a road sign are not constant within a driver, are somewhat different from driver to driver, and can best be described by a probability distribution (cumulative time distribution).

6. During a given approach to a sign, the first-look (eye fixation) duration, the road-look (eye fixation) duration, and the last-look (eye fixation) duration are assumed to be independent of each other.

7. The last-look distance (distance away from sign when the driver no longer looks foveally at the sign, until he or she passes the sign) within a driver is not a constant. The last-look distances are also somewhat different between drivers. They can be best described by a probability distribution (cumulative distance distri-

bution). The last-look distance can also be called the "true" preview distance, because from that distance to the sign the driver looks most often on a roadway section, or a road environment section, that is beyond the sign.

8. The average saccade time between the first look at the sign and the subsequent look at the road or road environment is assumed to be a constant of 0.03 sec (8). The saccade involved at the end of the last look moving the gaze away from the sign has been assumed to be part of the last-look distance.

9. The average saccade time between the road look and the subsequent last look at the sign is also assumed to be a constant of 0.03 sec (8). The saccade involved at the end of the last look moving the gaze away from the sign has been assumed to be part of the last-look distance.

10. The distance obtained by the sum of the three look durations times the driving speed and the two saccade durations times the driving speed is best represented as a probability distribution. This distance is independent of the last-look distance (which is also a probability distribution).

11. For the MRLD Model 1 it is assumed that the three look durations and the last-look duration (obtained by dividing the last-look distance by the approach speed) within a speed range from 48 to about 105 kph (30 to 65 mph) are constant for all speeds. In this case the sum of the durations (including the two saccades) by a selected speed can be multiplied and the overall distance for that selected speed can be acquired.

12. For the MRLD Model 2 it is assumed that the three look durations are constant and that the last-look distance is constant regardless of the speed within the speed range from 48 to 105 kph (30 to 65 mph). In this case the overall distance is obtained by multiplying the sum of the three durations (including the two saccades) times the selected speed and adding to this distance the constant last-look distance.

13. When a driver looks at a single bold traffic sign symbol, a large character height, well-known short word, a large-number-height two or three-digit number, or at two large-character-height, well-known simple words, it is assumed that the information acquisition and processing time is roughly the same for all these situations.

14. Acquiring and processing the information obtained by an eye fixation on familiar bold symbols or large-character-height short messages on traffic signs, or both, making the correct decision, and initiating the proper action, is assumed to be a highly overlearned task. It is further assumed that this task is completely executed during the duration of that particular eye fixation (usually 0.3 to 0.8 sec).

15. Whether warning signs or regulatory signs are placed on the left or on the right side of the road, the look durations and the last-look distances are assumed to be the same.

16. Because of the much lower sign luminance values found at night, the legibility or recognition of the message on a warning or similar sign such as a regulatory sign during nighttime is more important than the legibility or recognition during daytime.

17. It is assumed that a warning sign, or another similar sign with a limited message content, such as a regulatory sign is always placed in such a way that the action or maneuver, if any is required, can be carried out by the driver in due time (enough distance provided for action or maneuver) from the point of the last-look distance to wherever the action or maneuver needs to be completed. For this to apply, the size of the symbol or the character height of the legend, or both, must be large enough to allow the

reading and processing of the message before the last-look distance is reached.

STUDY DESCRIPTION

A rural two-lane highway was used to conduct the nighttime eye-scanning study under low-beam conditions. Two warning sign approaches (curve sign, with and without advisory speed plate, turn sign with and without advisory speed plate) were used. The speeds ranged from 69 to 78 kph (43 to 48 mph). A total of 32 young, healthy subjects were used. These previously collected video eye-scanning records were further analyzed with respect to first-look (not used in MRLD model), last-look distances, and first-look and last-look durations to obtain cumulative time duration and distance distribution functions.

Figure 1 shows the different stages of the detection and legibility/recognition process for a driver approaching a traffic sign on a long, straight, level highway at night with low beams. Figure 2 shows the cumulative frequency of first-look durations, the cumulative frequency of last-look durations, both at night for an average speed of 73 kph (45.44 mph), and the cumulative frequency of road-look durations at night (8) for an average speed of 84.2 kph (52.3 mph). Figure 3 shows the cumulative frequency of last-look distances at night for an average speed of 73 kph (45.44 mph). The data from a tunnel approach driver eye-scanning behavior study by Zwahlen (9) was used to determine the average saccade duration between two successive eye fixations and was found to be 0.03 sec. Since the saccade durations are short, they were assumed to be constant. Research has shown that drivers on the average look about two times at a warning sign (6,7). The MRLD is considered the sum of four independent distance random variables (three eye fixation durations multiplied by selected speed): first look, road look, last look, and the last-look distance or the last-look duration times speed, plus two constant saccade durations times speed (0.03 sec each, small overall effect). Because the driver eye scan data were collected over a fairly narrow speed range, no reliable data are available at this point to determine whether the last-look distance is

speed dependent within the range of 48 to 105 kph (30 to 65 mph), or whether the last-look distance expressed as a time duration is speed dependent over the speed range mentioned earlier. Therefore, two MRLD models are proposed. Figure 4 shows MRLD Model 1 and Figure 5 shows MRLD Model 2. In Figures 4 and 5 the saccade distance when moving the gaze away from the sign after the last look is assumed to be part of the last-look distance.

The sum of four independent distance random variables is also a random variable and the distribution of the sum can be obtained by applying the techniques of probability modeling. In the first approach it was assumed that all four independent variables are distributed normally each with a specific mean and a specific standard deviation. Using a transform such as the moment generating function (10) defined next and the convolution property (11) it can be shown that the sum of the four independent normal random variables will also be normally distributed with a mean equal to the sum of the individual means and with a variance that is the sum of the four variances. The moment generating function is defined as

$$M(s) = E(e^{st}) = \frac{1}{\sqrt{2\pi\sigma}} \int_{-\infty}^{\infty} e^{st} \cdot e^{-1/2 \left[\frac{x-\mu}{\sigma} \right]^2} dx \tag{1}$$

$$M(s) = e^{\left(s\mu + \frac{\sigma^2 s^2}{2} \right)} \tag{2}$$

If four independent normals are added using transform notation and the convolution property (11)

$$\begin{aligned} T(f * g * h * i) &= T(f) \cdot T(g) \cdot T(h) \cdot T(i) \tag{3} \\ &= e^{\left(\frac{s\mu_1 + \sigma_1^2 s^2}{2} \right)} \cdot e^{\left(\frac{s\mu_2 + \sigma_2^2 s^2}{2} \right)} \cdot e^{\left(\frac{s\mu_3 + \sigma_3^2 s^2}{2} \right)} \cdot e^{\left(\frac{s\mu_4 + \sigma_4^2 s^2}{2} \right)} \\ &= e^{\left(s(\mu_1 + \mu_2 + \mu_3 + \mu_4) + \frac{s^2}{2}(\sigma_1^2 + \sigma_2^2 + \sigma_3^2 + \sigma_4^2) \right)} \end{aligned}$$

$$\text{Sum} = \text{Normal} (\mu_1 + \mu_2 + \mu_3 + \mu_4, \sigma_1^2 + \sigma_2^2 + \sigma_3^2 + \sigma_4^2) \tag{4}$$

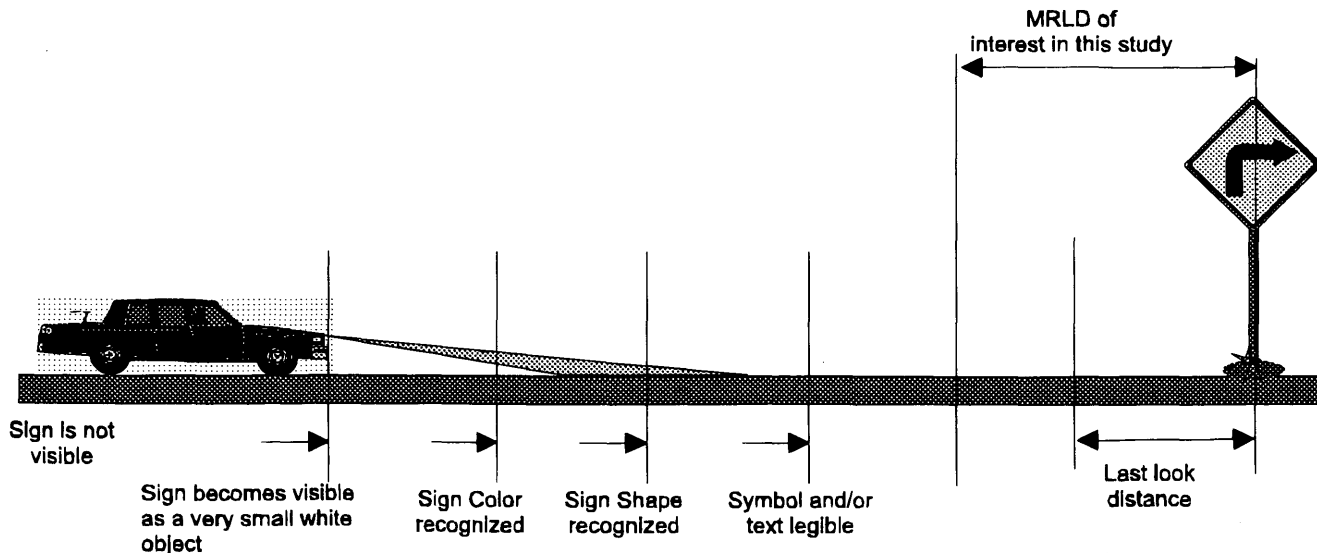


FIGURE 1 Approach to a traffic sign on a long, straight, level highway at night with low beams.

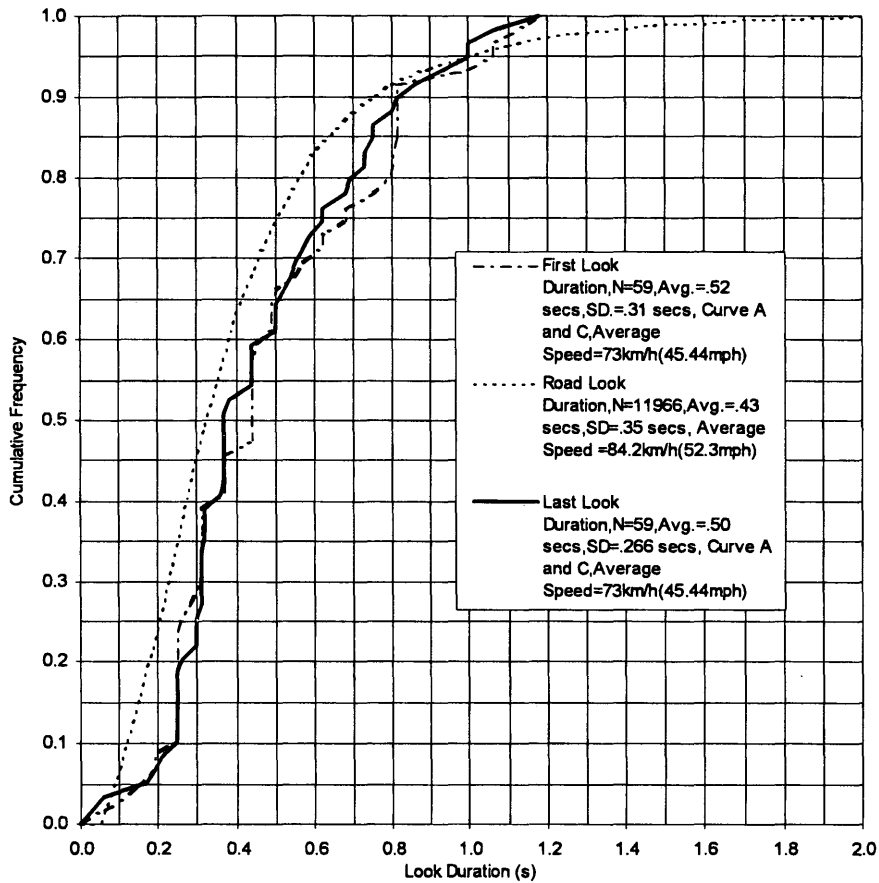


FIGURE 2 Cumulative frequency of first-look duration, road look duration, last-look duration, and nighttime.

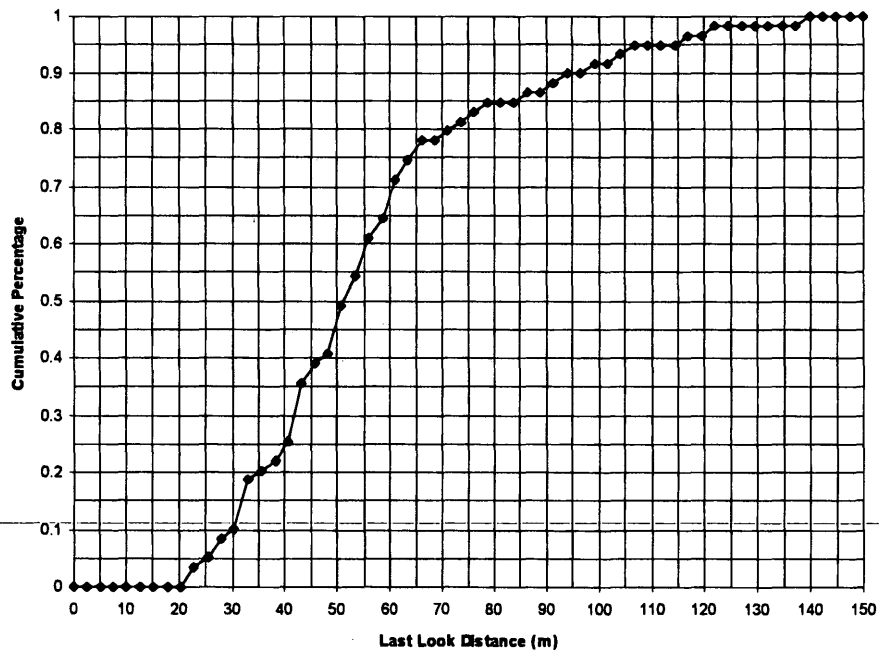
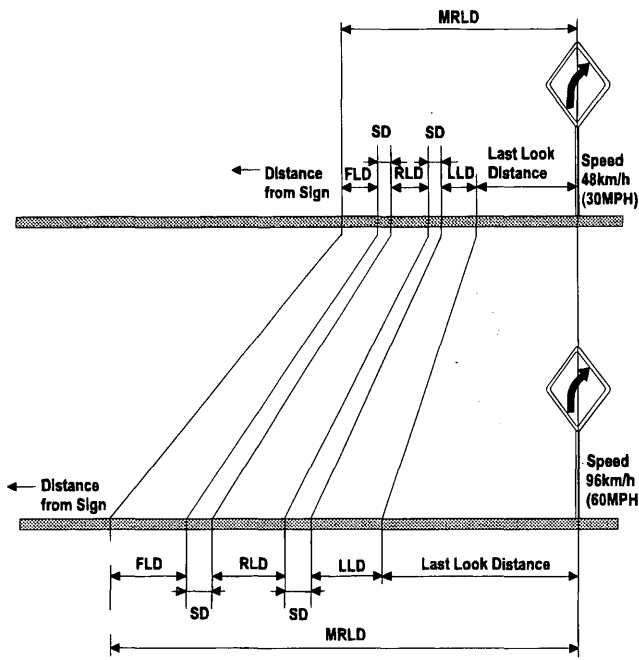
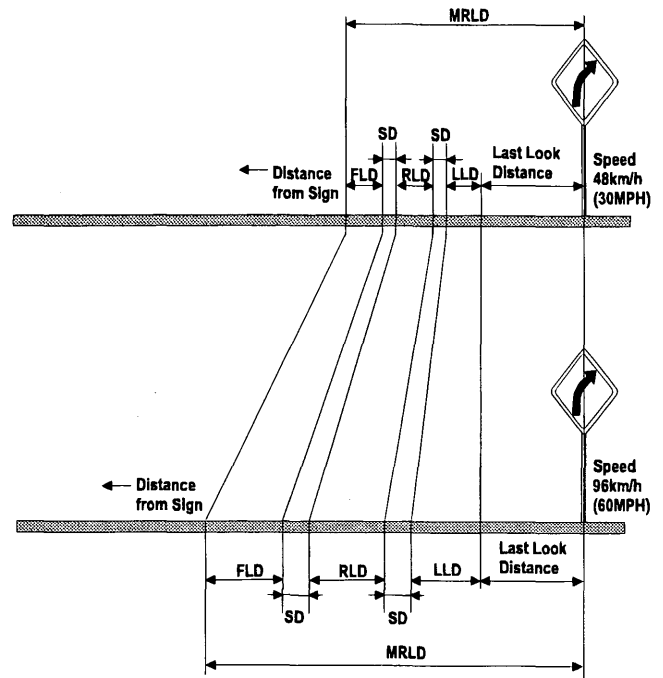


FIGURE 3 Cumulative frequency of last-look distance, nighttime, curves A and C, average speed 73 kph (45.44 mph).



FLD : First Look Duration Distance
 RLD : Road Look Duration Distance
 LLD : Last Look Duration Distance
 SD : Saccade Duration Distance
 The saccade distance when moving the gaze away from the sign after the last look is assumed to be part of the last look distance.

FIGURE 4 MRLD Model 1 for a speed of 48 kph and for a speed of 96 kph.



FLD : First Look Duration Distance
 RLD : Road Look Duration Distance
 LLD : Last Look Duration Distance
 SD : Saccade Duration Distance
 The saccade distance when moving the gaze away from the sign after the last look is assumed to be part of the last look distance.

FIGURE 5 MRLD Model 2 for a speed of 48 kph and for a speed of 96 kph.

The resulting MRLD distance is at the most an approximation because each individual distance probability distribution was approximated with a normal distribution. In the second approach it is again assumed that all four random distance variables are independent of each other but a Monte Carlo simulation program for a personal computer (PC) was written and used along with the actual obtained cumulative distance distributions to obtain the MRLD distribution function. Using a sample size of 10,000 cases in the simulation this approach provides a slightly more accurate MRLD probability distribution function when compared with the transform and convolution approach using normals. Both approaches have been used in this study, although the latter approach was preferred and finally selected because of the increased accuracy.

RESULTS

Figure 6a shows the cumulative frequency of MRLD values for a speed of 73 kph (45.44 mph) for Model 1, the basis of transform and convolution calculations and simulation. Figure 6b shows the cumulative frequency of MRLD values for a speed of 73 kph (45.44 mph) for Model 2 on the basis of transform and convolution calculations and simulation. Figure 7 shows the cumulative frequencies of MRLD values obtained by simulation for 48, 88.5, and 104.6 kph for Models 1 and 2. Figure 8 shows the comparison of average, 50 percent (median), 85 and 95 percent MRLD values

obtained by simulation (based on the GPSS/PC simulation, $N = 10,000$) for MRLD Models 1 and 2. The figure also shows the average MRVD values for 95 out of 164 (58 percent) signs used in CARTS.

DISCUSSION AND CONCLUSIONS

The average MRLD distances obtained with the Monte Carlo simulations, on the basis of the symbol signs investigated using either Model 1 or Model 2 and for a speed range of 48 to 105 kph (30 to 65 mph) are given in Figure 8. One can see that the obtained MRLD values are considerably higher than the corresponding MRVD values used in CARTS for at least 58 percent of all signs in the CARTS sign inventory. The MRLD value is one of the major factors in determining the minimum retroreflectivity requirements. On the basis of typical headlamp candlepower distributions, the geometry of car headlamp, driver, and sign, and retroreflective material characteristics, the short MRVD values will invariably result in low minimum retroreflectivity requirements, whereas the longer MRLD values will result in substantially higher, minimum retroreflectivity requirements. If a symbol is neither bold nor simple, or if the character height of a legend is small, the recognition or legibility distances and the last-look distances observed in the field as well as the

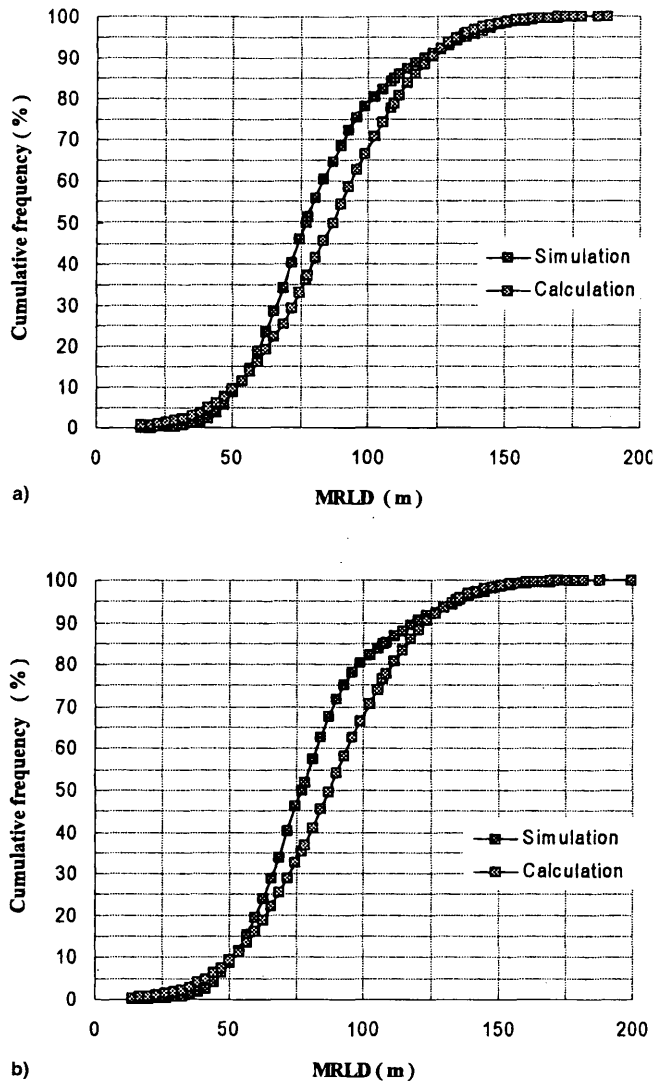


FIGURE 6 Cumulative frequency of MRLD for a speed of 73 kph (45.44 mph): (a) Model 1 and (b) Model 2.

derived MRLD distances could be so short and the minimum retroreflectivity values so low that inadequate preview and driver safety conditions may exist. The advantage of the MRLD model is that it is based on actual driver eye-scanning behavior data, collected in the field at night when driving with low beams and that the MRLD values are available not only as moments (average, variance, standard deviation), but also for any population percentile value a user might want to select. The MRLD model has a number of limitations:

1. Limited sign population (curve/turn signs, bold symbols only, with and without advisory speed plates);
2. Limited vehicle population (only one low-beam pattern);
3. Limited approach speed range (only one average approach speed);
4. Two-lane rural dark road environment only;
5. Practically no other traffic; and
6. Relatively young and healthy, nonimpaired driver population.

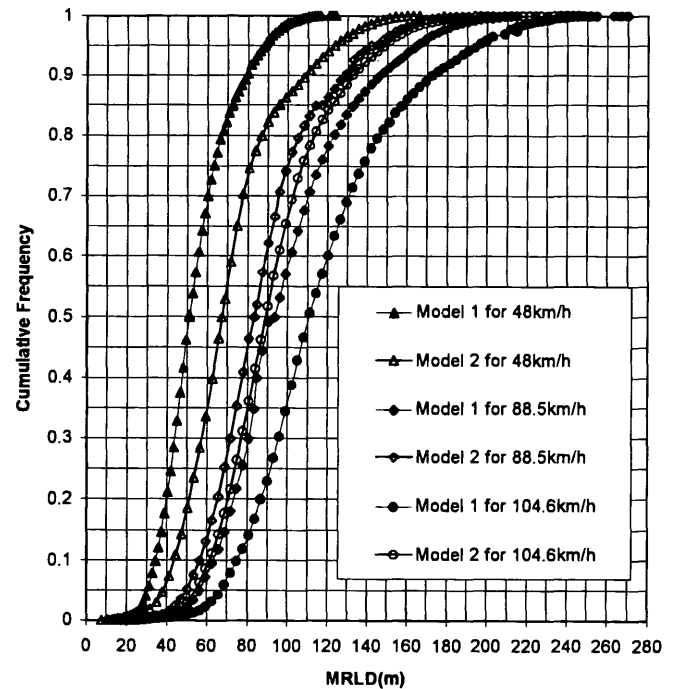


FIGURE 7 Cumulative frequency of MRLD for a speed of 48, 88.5, and 104.6 kph for Models 1 and 2.

It is not known how well the obtained time durations and distances would apply to older drivers. More driver eye-scanning behavior research, using wider ranges of the variables mentioned earlier or factors, or both, would be desirable. Also, more complex and less bold sign symbols and smaller legend character heights and multi-word messages may require two or more first-look eye fixations (information acquisition) to acquire the desired information and may possibly also require more than one confirmation look. Driver eye-scanning behavior studies would also be beneficial to determine whether a number of the stated assumptions, on which the MRLD model is based can be supported and justified. Further eye-scanning behavior studies also would likely provide information about which one of the two MRLD models more closely matches the real-world data. In the meantime, although not knowing which one of the MRLD models more closely matches the real-world data, and to simplify matters, one could always use an average MRLD value based on the two MRLD models and express such a value as a function of the speed using a simple linear relationship, that is, $MRLD(m) = \text{constant} + \text{slope} * \text{speed}$. It is also conceivable that a set of MRLD models, either of Type 1 or Type 2, could be applicable and used, which would be more sensitive and apply specifically to certain maximum symbol recognition or character legibility distances. It is reasonable to assume that depending on the character height of the message or text or the size, complexity, and stroke widths used in a symbol, different first-look and last-look distances and durations may be required (i.e., small character heights or small, thin-stroke width symbols on a sign may result in somewhat shorter MRLDs than were found in this study, which are based on fairly large and bold symbols and large advisory speed numerals). Additional driver eye-scanning behavior studies investigating the sensitivity of the MRLD models and distance values with regard to the

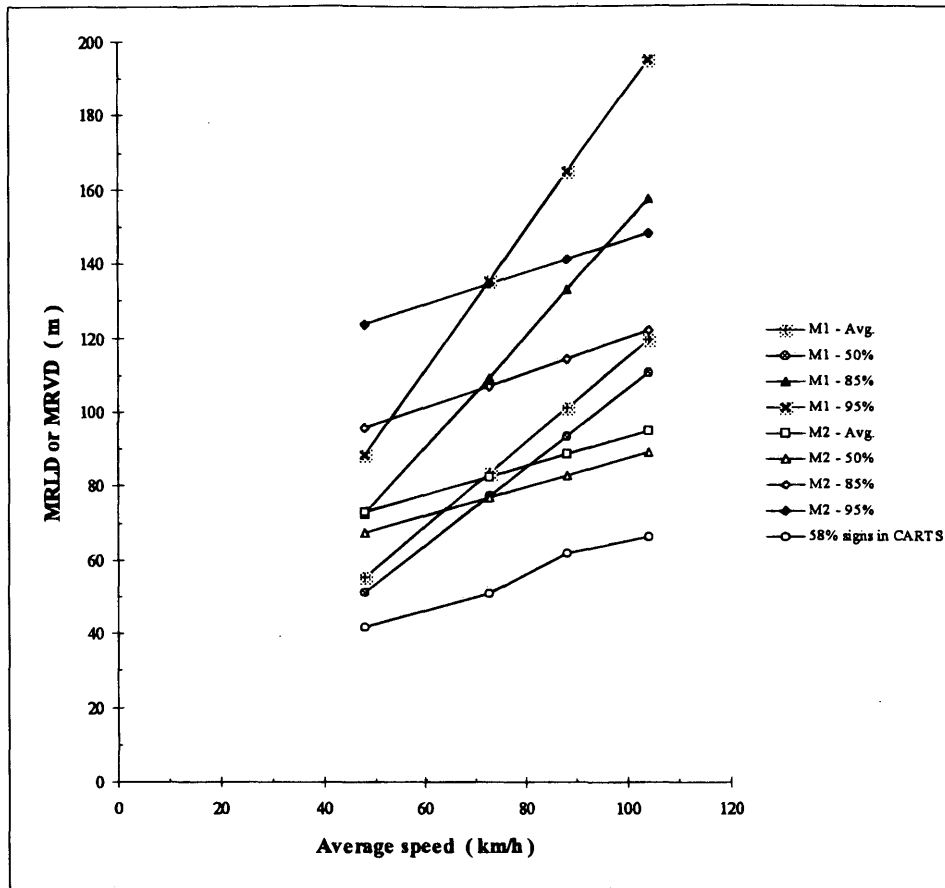


FIGURE 8 Comparison of average, 50, 85, and 95 percent MRLD values based on GPSS/PC simulation, $N = 10,000$ for MRLD Models 1 and 2 and average MRVD value for 95 out of 164 (58 percent sign in CARTS).

maximum recognition and legibility distances would, therefore, also be helpful.

REFERENCES

- Paniati, J. F., and D. J. Mace. *Minimum Retroreflectivity Requirements For Traffic Signs*. Report FHWA-RD-93-077, U.S. Department of Transportation, Oct. 1993.
- Mace, D. J., and R. Gabel. *Modeling Highway Visibility Minimum Required Visibility Distance*. Paper Presented at 71st Annual Meeting of the Transportation Research Board, Washington, D.C., 1992.
- Visual Aspects of Road Markings*. Joint Technical Report CIE/PIARC. Publication CIE 73, CIE, 1988.
- Cole, B. L., and R. L. Jacobs. A Resolution Limited Model for the Prediction of Information Retrieval from Extended Alphanumeric Message. *Proc., 9th Conference of the Australian Research Review Board*, No. 5, 1978.
- Cole, B. L., and R. L. Jacobs. Acquisition of Information from Alphanumeric Road Signs. *Proc., 9th Conference of the Australian Research Review Board*, No. 5, 1978, pp. 390-395.
- Zwahlen, H. T. Driver Eye Scanning Of Warning Signs On Rural Highway. *Proc., 25th Annual Meeting of the Human Factors Society*, 1981, pp. 33-37.
- Zwahlen, H. T. Advisory Speed Signs and Curve Signs and Their Effect on Driver Eye Scanning and Driving Performance. In *Transportation Research Record 1111*, TRB, National Research Council, Washington, D.C., 1987, pp. 110-120.
- Zwahlen, H. T. Eye Scanning Rules For Drivers—How Do They Compare With Actual Observed Eye Scanning Behavior? In *Transportation Research Record 1403*, TRB, National Research Council, Washington, D.C., 1993, pp. 14-22.
- Zwahlen, H. T. *Driver Eye Scanning Behavior at Tunnel Approaches*. Final Report, Franklin Institute Research Laboratories, Feb. 1979.
- Meyer, P. L. *Introductory Probability and Statistical Applications*. Addison-Wesley, Reading, Mass., 1965.
- Giffin, W. C. *Transform Techniques for Probability Modeling*. Academic Press, New York, 1975.

Publication of this paper sponsored by Committee on Visibility.

Yellow Pavement Markings with Yellow Nighttime Color

GREGORY F. JACOBS AND NORBERT L. JOHNSON

Human observers were used to assess the apparent nighttime color of a range of pavement marking products. A total of 24 different materials were viewed at night from an automobile using low-beam illumination with vehicle-to-target distances ranging from 12 to 36 m. The samples were viewed as isolated center lane lines with a parallel white edge line in place for all viewings. Observers rated the color on a scale of 1 to 5 from white to yellow. The results showed significant color differences between pavement marking materials. At shorter distances, more of the materials appeared yellow than at longer distances. At longer distances observer ratings showed greater separation of color distinction between the materials. Retroreflective color was measured at geometries corresponding to 12 and 36 m. Brightness did not appear to correlate with color. Color measurements for the different distances also showed the dependence of color on test conditions. Measured colors with a higher color saturation were reported by observers to have a more yellow appearance. Daytime and nighttime color are not the same. Some yellow pavement markings having acceptable daytime color were white in retroreflective color. Different "yellow" products can have varying nighttime color performance. The feasibility of specifying nighttime color using instrumental methods that can correlate with the human visual experience is demonstrated.

Yellow and white pavement markings are commonly used on roadways to display traffic lanes. A yellow pavement marking typically will have a different meaning to an automobile driver than a white pavement marking. For example, in the United States, a yellow pavement marking is used on a roadway to separate traffic lanes where the traffic moves in opposite directions, whereas a white pavement marking is used to mark the roadway's border at the shoulder and to separate traffic lanes where the traffic moves in the same direction (1,2). In many parts of Europe yellow pavement markings are used to indicate construction workzones or potentially hazardous driving situations. In view of these different functions, it is important that yellow and white pavement markings are discernible to automobile drivers, particularly at nighttime when visibility is limited.

With increased regulation to eliminate the use of lead-based pigments, the development of yellow traffic markings free of such "hazardous" colorants has received significant effort. It has been found that control of the reflective brightness (3) and nighttime color (4) in desirable ranges for yellow pavement markings using organic colorants is not trivial.

With the availability of pavement marking systems having varying reflective performance, the question of the reflective color of road-surface markings providing safe and effective guidance has remained undefined. A part of this in-use appearance variability stems from the lack of meaningful measures of nighttime reflective color of pavement markings that correlate with what drivers see.

The object of this work was to compare pavement marking materials that differ in their nighttime reflective performance using human observers and laboratory test methods for the measurement of nighttime color of retroreflective materials. The observer's color ratings of a range of markings at night were compared with color characterization obtained through photometric measurements of the marking materials.

FIELD OBSERVATION OF PAVEMENT MARKING COLOR

Seven color-normal human observers (based on Ishihara test results) were used to assess the apparent nighttime color of new unworn pavement marking materials with white and yellow daytime colors. All of the viewers had "normal" visual acuity and were licensed drivers in the state of Minnesota. Their ages were 27, 37, 38, 39, 48, 48, and 56 years. One viewer was a woman.

A total of 24 different pavement marking materials were viewed. Of these, five were white and the rest were yellow in daytime color. Each marking was applied to aluminum test panels 0.2 cm thick, 1.52 m in length, and 0.10 m in width. Leading edges of the test panels were masked with matte finish black tape.

Viewings were held in a parking lot well after dark on an overcast night. The pavement was recently surfaced black asphalt. Viewers were seated in a 1989 Pontiac Bonneville 4-door sedan with low-beam headlamps illuminated. The layout of the test area is indicated in Figure 1. Lane width for the viewing area was approximately 4 m. Samples were presented as isolated center lines 1.52 m in length and 0.10 m in width. A length of white pavement marking 12 m in total length was present as a right edge line beginning 9 m closer to the vehicle than the test sample area and continuing 1.5 m beyond it throughout the viewing experiment as a control reference. Vehicle-to-target distances were 12, 24, and 36 m (one to three skip lengths in front of the vehicle).

Before beginning the test, observers in the vehicle were allowed to view five different samples spanning the range of colors in the experiment from white to yellow for about 30 sec to develop an idea of the range of colors they would see during the test. The white edge line control was in full view during this learning period. The viewers were instructed that they would be presented with an isolated centerline marking for a period of 2 to 3 sec. After viewing the sample they would be asked to rate the night color of the sample from 1 to 5, with 1 being white and 5 being yellow. Each viewer had a response form on which, after making a color judgment, they circled the rating number adjacent to the sample number. They would then be presented with another sample and continue through the sample set until the test was completed.

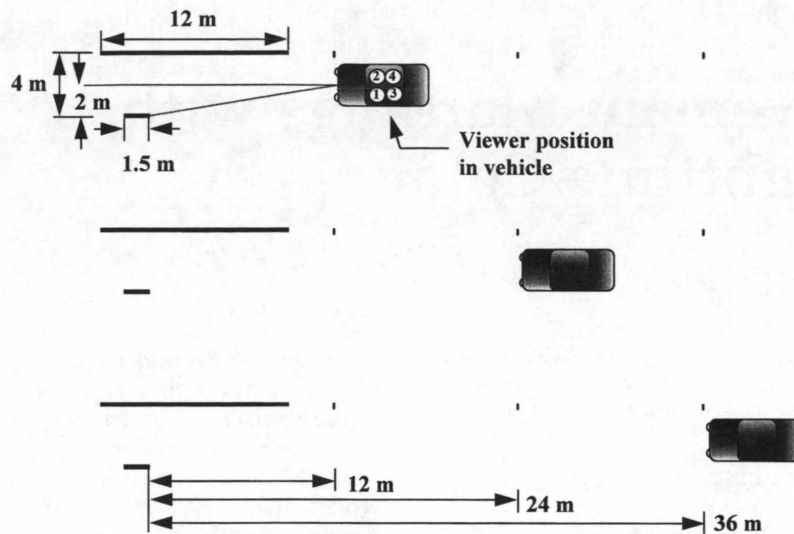


FIGURE 1 Night viewing experiment layout.

During the actual field observations, the test samples were presented to the viewers in the vehicle for the same period of 2 to 3 sec. Twenty-two of the materials were viewed twice and two were viewed three times each for each of three vehicle-target distances. Sample viewing order was randomized. No sample was viewed twice in a row. The overall data collection included 1,050 points [(22 × 2 + 2 × 3) samples × 3 distances × 7 observers].

Figure 2 shows a set of histograms of the distribution of observer night color rating responses for one of the yellow products, *T*, at each of the three viewing distances. Figure 3 shows a similar data set for a white marking material, *A*. Figure 4 shows observer night color rating data for another yellow marking, *X*. It can be seen that the distribution of observer night color rating and the effects of viewing distance for sample *X* differ from the response for sample *T* shown in Figure 2.

Figure 5 shows the mean observer night color ratings for each product at each distance. Samples *A* through *E* had white daytime color, whereas samples *F* through *X* had yellow daytime color. Table 1 presents the mean observer color rating for each marking

material at each of the viewing distances and a pooled standard deviation for each distance.

Significant differences among the marking materials were observed. Distance had an effect on the apparent night color of the pavement markings. At shorter distances, more of the materials appeared yellow than at longer distances. At longer distances, there was greater separation of color distinction between the materials. Also, at longer distances, yellow materials were rated less yellow and white materials were rated less white than at shorter distances. No effect of position in the vehicle or of an individual viewer (of those with normal color vision) on apparent color could be determined in this experiment.

DETERMINATION OF TEST GEOMETRY

The laboratory test measurement geometries were calculated to correspond with 12- and 36-m viewing distances from the Pontiac Bonneville. The vehicle-observer-sample geometries were calculated

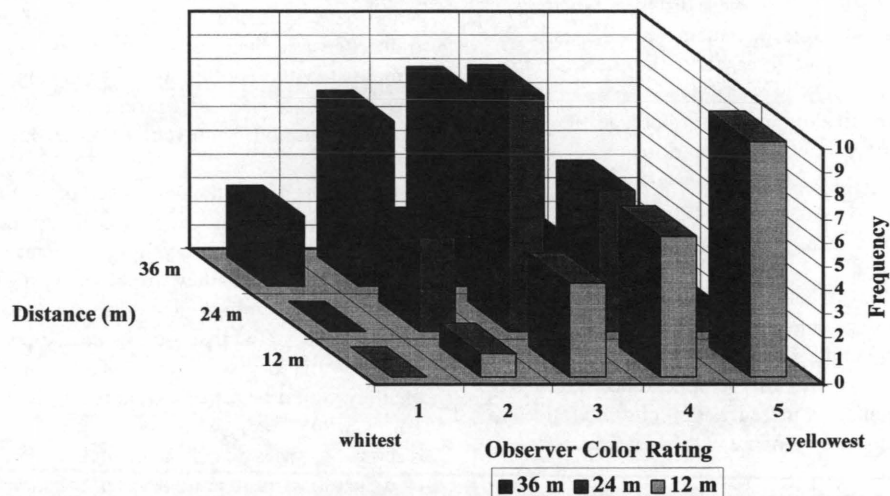


FIGURE 2 Night color of *T*.

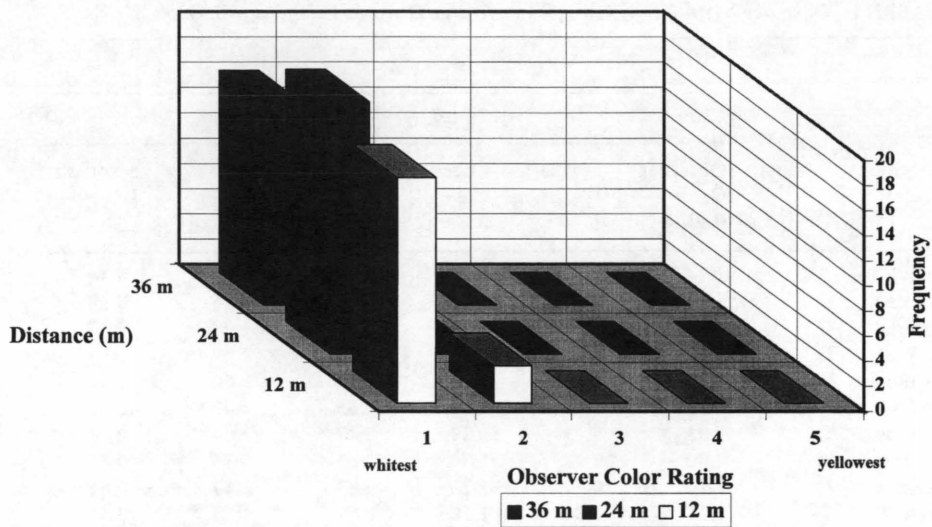


FIGURE 3 Night color of A.

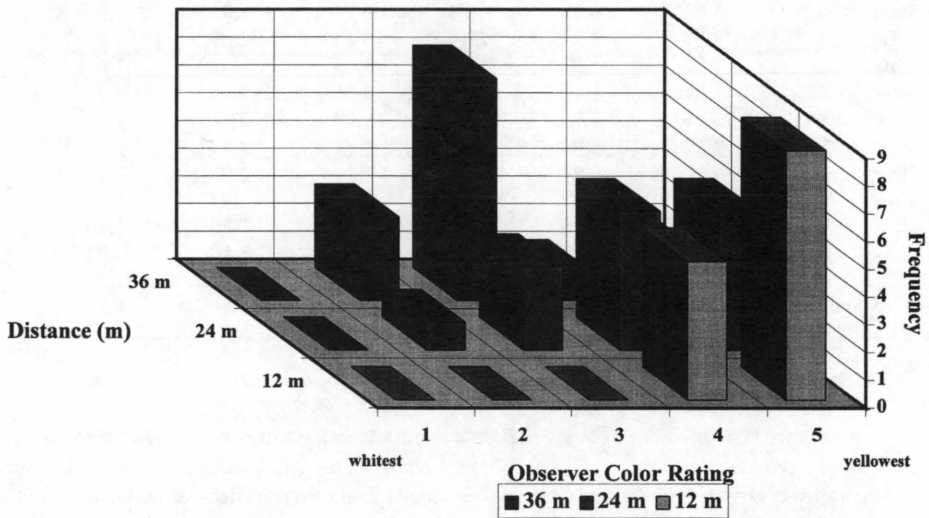


FIGURE 4 Night color of X.

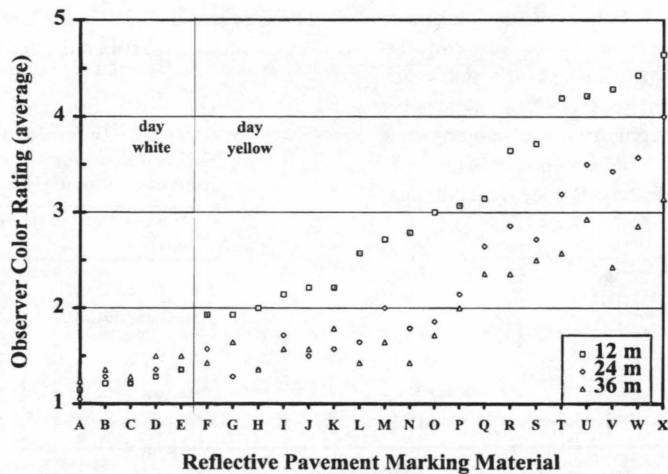


FIGURE 5 Observer night color rating by material.

TABLE 1 Observer Night Color Ratings of Pavement Marking Products A through X

Daytime Color	Product	Distance From Vehicle to Marking					
		12 m		24 m		36 m	
		Observer Color Rating	Standard Deviation	Observer Color Rating	Standard Deviation	Observer Color Rating	Standard Deviation
white	A	1.14	0.36	1.05	0.22	1.24	0.44
white	B	1.21	0.43	1.29	0.47	1.36	0.50
white	C	1.21	0.43	1.21	0.43	1.29	0.47
white	D	1.29	0.47	1.36	0.50	1.50	0.65
white	E	1.36	0.63	1.36	0.50	1.50	0.52
yellow	F	1.93	0.73	1.57	0.65	1.43	0.65
yellow	G	1.93	0.73	1.29	0.47	1.64	0.63
yellow	H	2.00	0.78	1.36	0.63	1.36	0.50
yellow	I	2.14	0.77	1.71	0.83	1.57	0.65
yellow	J	2.21	0.80	1.50	0.52	1.57	0.65
yellow	K	2.21	0.80	1.57	0.76	1.79	0.70
yellow	L	2.57	0.85	1.64	0.74	1.43	0.65
yellow	M	2.71	0.83	2.00	0.68	1.64	0.93
yellow	N	2.79	0.98	1.79	0.70	1.43	0.65
yellow	O	3.00	0.88	1.86	0.77	1.71	0.91
yellow	P	3.07	1.27	2.14	0.53	2.00	0.88
yellow	Q	3.14	1.03	2.64	0.63	2.36	1.01
yellow	R	3.64	1.15	2.86	0.95	2.36	0.74
yellow	S	3.71	0.99	2.71	1.07	2.50	1.16
yellow	T	4.19	0.93	3.19	0.81	2.57	1.03
yellow	U	4.21	0.98	3.50	1.29	2.93	1.07
yellow	V	4.29	0.83	3.43	0.76	2.43	1.28
yellow	W	4.43	0.65	3.57	0.85	2.86	1.10
yellow	X	4.64	0.50	4.00	0.96	3.14	0.95
Pooled Standard Deviation		0.81		0.73		0.81	

Color Ratings: 1 = Whitest, 5 = Yellowest

for all observer positions at each distance. The in-vehicle coordinate system measurements are found in Table 2.

On the basis of measurements of the vehicle and driver position and the spatial layout of the viewing experiment, the angles of illumination and observation were calculated as indicated in Figure 6. The angles corresponding to each viewing condition are shown in Table 3.

For purposes of simplification of the geometries for color measurements, a two-dimensional approach was used, ignoring the effects of presentation and orientation angle and assuming left headlight illumination and viewing from the driver position of the vehicle. With these simplifications, the geometry corresponding to a viewing distance of 12 m was 87.0 degree entrance angle/1.5-degree observation angle and for 36 m, 89.0 degree entrance angle/0.7 degree entrance angle.

LABORATORY MEASUREMENT OF NIGHTTIME BRIGHTNESS OF PAVEMENT MARKINGS

Assessment of the nighttime brightness in the laboratory is usually through measurement of the coefficient of retroreflected luminance, R_L , using the test method described in ASTM D-4061. This is also described as the relative method in CIE Publication 54 (5). In this

method the measured quantities are the reflected light, m_r , the incident light, m_i , the distance, d , and the area of the test surface, A . The coefficient of retroreflected luminance is determined by the following equation:

$$R_L = m_r d^2 / (m_i A \cos v) \quad (1)$$

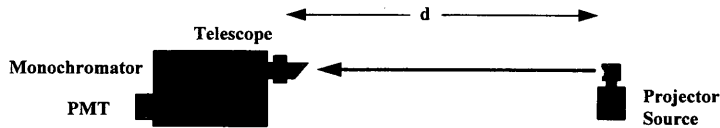
The viewing angle, v , is the angle between the direction of observation and the specimen normal.

TABLE 2 In-Vehicle Coordinate System Measurements for 1989 Pontiac Bonneville Four-Door Sedan

	X	Y	Z
Left Headlamp	0.0	-0.635	0.635
Right Headlamp	0.0	0.635	0.635
Viewer 1	2.235	-0.508	1.143
Viewer 2	2.235	0.508	1.143
Viewer 3	2.997	-0.508	1.143
Viewer 4	2.997	0.508	1.143

measurements are reported in meters

Step 1. Measure Relative Spectral Values of Incident Radiation.



Step 2. Measure Relative Spectral Values of Reflected Radiation.

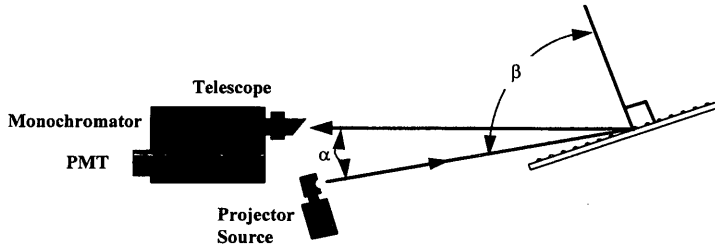


FIGURE 6 Diagram of relative method for measurement of nighttime color.

LABORATORY MEASUREMENT OF NIGHTTIME COLOR OF PAVEMENT MARKINGS

Measurement of the nighttime color (NTC) using the direct spectral method (ASTM E 811-936) is similar to the procedure for measurement of the coefficient of luminance, R_L , using the relative method (5). However for NTC, a telespectroradiometer is used and the measurements can be made with an uncalibrated source. Figure 7 shows a diagram of the NTC measurement method. The spectral distribution of the incident light was measured at 10-nm intervals. Then the spectral distribution of the retroreflected light from pavement marking materials was also measured at 10-nm intervals. Averages of multiple scans and a shortened measurement distance

of 6 m were required because of the relatively low level of energy available.

Calculation of the spectral coefficient of luminous intensity as a function of wavelength, λ , was as follows:

$$R_l(\lambda) = \frac{m_r(\lambda) d^2}{m_i(\lambda)} \tag{2}$$

where

- m_r = the reflected spectral value,
- m_i = the incident spectral value, and
- d = the test distance.

TABLE 3 Calculated Observation and Entrance Angles for Night Viewing Conditions for Leading and Trailing Ends of Test Sample Illuminated by Left and Right Headlamps Viewed from Each Viewer Position at Each Distance

Distance	Viewer	Observation Angle (deg)				Entrance Angle (deg)			
		left		right		left		right	
		begin	end	begin	end	begin	end	begin	end
12.2 m	1	1.61	1.48	6.47	5.71	87.0	87.4	87.1	87.4
	2	3.79	3.55	2.79	2.41	87.0	87.4	87.1	87.4
	3	1.52	1.38	6.70	5.90	87.0	87.4	87.1	87.4
	4	3.26	3.11	3.10	2.65	87.0	87.4	87.1	87.4
24.4 m	1	0.97	0.92	3.11	2.92	88.5	88.6	88.5	88.6
	2	2.38	2.27	1.24	1.16	88.5	88.6	88.5	88.6
	3	0.90	0.86	3.17	2.98	88.5	88.6	88.5	88.6
	4	2.22	2.23	1.29	1.20	88.5	88.6	88.5	88.6
36.6 m	1	0.69	0.67	2.04	1.95	89.0	89.0	89.0	89.0
	2	1.71	1.65	0.81	0.78	89.0	89.0	89.0	89.0
	3	0.66	0.64	2.07	1.98	89.0	89.0	89.0	89.0
	4	1.63	1.58	0.82	0.79	89.0	89.0	89.0	89.0

"begin" indicates the end of the test sample closest to the vehicle.
 "end" indicates the end of the test sample farthest away from the vehicle

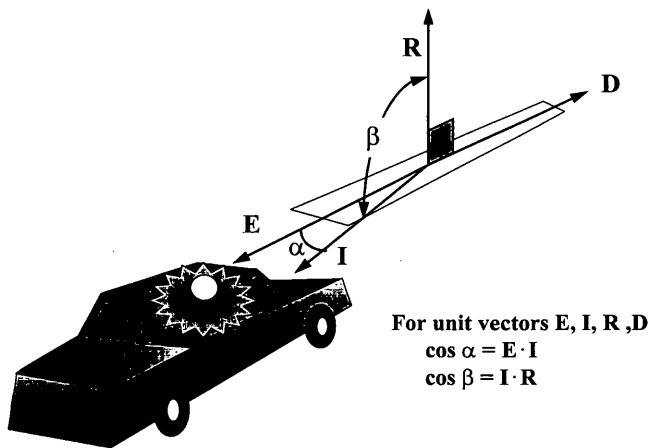


FIGURE 7 Calculation of observation angle and entrance angle.

Calculation of tristimulus values was as follows:

$$X = k \int_{\lambda} S(\lambda) R_r(\lambda) \bar{x}(\lambda) d\lambda \quad (3)$$

$$Y = k \int_{\lambda} S(\lambda) R_r(\lambda) \bar{y}(\lambda) d\lambda \quad (4)$$

$$Z = K \int_{\lambda} S(\lambda) R_r(\lambda) \bar{z}(\lambda) d\lambda \quad (5)$$

These calculations use the usual symbols of CIE Publication 15.2 (6) using Illuminant A and the 2 degree observer.

PHOTOMETRIC DATA

Figure 8 shows an example of the spectral retroreflectance curve of a yellow pavement marking (Sample V) with yellow nighttime color and a marking (Sample A) with white nighttime color for test samples measured at the 36-m geometry. The chromaticity coordinates for the retroreflected light when this material is illuminated using standard Source A are $x = 0.511$, $y = 0.447$ for the yellow and $x = 0.452$, $y = 0.413$ for the white marking. Illuminant A falls at $x = 0.448$, $y = 0.407$ on the CIE 1931 2 degree observer chromaticity diagram. Table 4 presents chromaticity coordinates of retroreflected light from Illuminant A and the coefficient of retroreflected luminance, R_L , at geometries corresponding to 12- and 36-m viewing distances for pavement markings rated for color in the night viewing experiment.

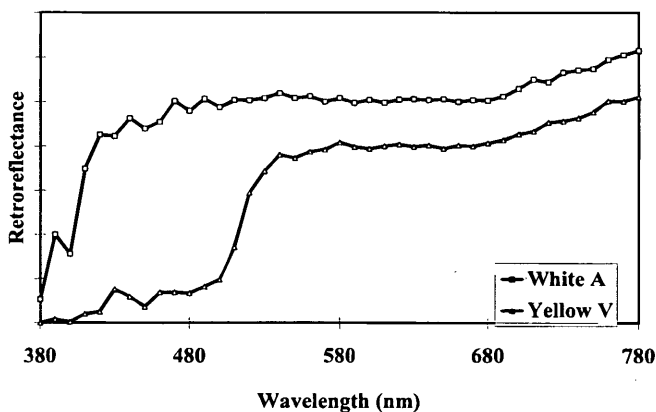


FIGURE 8 Example of spectral wavelength distribution of retroreflected light from white and yellow pavement marking.

Figure 9 shows the measured values of R_L of markings A through X are mapped onto the chromaticity coordinates for the data at 89.0 degree entrance/0.7 degree observation angles corresponding to a viewing distance of 36 m. The brightness of the pavement marking materials appears to be independent of the reflective color of the stripe.

CORRELATION OF VISUAL OBSERVATIONS WITH PHOTOMETRIC MEASUREMENTS

Figure 10 shows the observer night color ratings from the viewing experiment at 36 m mapped onto chromaticity space at 89.0 degree entrance/0.7 degree observation angles. There appears to be a correlation between the color ratings of the observers and the measured chromaticities of retroreflected light from pavement markings. Markings with a higher color saturation, closer to the edge of chromaticity space, were rated to have a yellower appearance than white markings.

Figure 11 shows color value ratings from the viewing experiment at 12 m mapped onto chromaticity space at 87.0 degree entrance/1.5 degree observation angles. Again it is apparent that there is a correlation between the ratings of the observers with measured retroreflective chromaticities.

As noted earlier, viewing distance had an effect on the apparent color of the pavement markings, with more of the materials appearing yellow at shorter distances than at longer distances. Comparison of Figures 10 and 11 shows a measurable color shift with viewing condition. Some pavement markings become more "washed out" in visual appearance at farther distances. The chromaticities of the reflected light of these materials move closer to the chromaticity of the illuminant (i.e., they become more "white").

There were also yellow marking samples (daytime color) that received ratings close to those of the white materials, for example, marking samples L and N at 36 m. From Figure 5 it can be seen that the observer color ratings of some of the yellow markings are essentially the same as those for the white markings, particularly at farther distances. The chromaticities of the light retroreflected from these samples are in fact close to the chromaticity of the light source Illuminant A. It is possible to have markings with acceptable yellow daytime appearance, yet have a nighttime retroreflected color similar to white markings.

For perspective of the location of the nighttime retroreflected colors of the materials used in this study, the chromaticities at the 36-m geometry found in Table 4 are plotted in chromaticity space for the 1931 2 degree observer along with Illuminant A in Figure 12. Figure 13 indicates the same data plotted on the 1976 CIE u' , v' diagram.

Figure 12 shows the measured values of R_L of markings A through X are mapped onto the chromaticity coordinates for the data at 89.0 degree entrance/0.7 degree observation angles corresponding to a viewing distance of 36 m. The brightness of the pavement marking materials appears to be independent of the reflective color of the stripe.

SUMMARY

Human observers were used to assess the apparent nighttime color of a range of pavement marking products. A total of 24 different materials were viewed at night from an automobile using low-beam illumination with vehicle-to-target distances ranging from 12 to

TABLE 4 Chromaticity and Coefficient of Retroreflected Luminance of Pavement Marking Products A through X

Product	Viewing Distance for Measurement Geometry					
	12 m			36 m		
	Chromaticity		R_L	Chromaticity		R_L
	x	y	(mcd/m ² /lx)	x	y	(mcd/m ² /lx)
A1	0.453	0.412	1120	0.452	0.412	937
A2	0.454	0.411	---	0.452	0.414	---
A3	0.454	0.412	---	0.454	0.416	---
A4	---	---	---	0.455	0.417	---
B	0.454	0.416	517	0.454	0.421	586
C1	0.443	0.406	353	0.440	0.406	376
C2	---	---	---	0.452	0.414	---
D	0.457	0.416	741	0.456	0.418	708
E	0.444	0.410	462	---	---	576
F	0.493	0.449	192	0.458	0.416	91
G	0.493	0.459	297	---	---	426
H	0.494	0.456	420	0.478	0.444	445
I	0.487	0.446	438	0.456	0.419	290
J	0.487	0.446	492	0.477	0.442	462
K	0.483	0.446	207	0.472	0.447	122
L	0.494	0.452	434	0.478	0.446	397
M	0.499	0.445	682	0.491	0.447	778
N	0.500	0.455	618	---	---	708
O	0.513	0.456	306	0.486	0.436	252
P	0.502	0.451	605	0.490	0.448	500
Q	0.519	0.445	337	0.494	0.426	277
R1	0.523	0.455	378	0.504	0.449	470
R2	0.524	0.454	---	0.506	0.451	---
S	0.530	0.454	235	0.511	0.441	199
T1	0.524	0.452	648	0.517	0.452	401
T2	0.525	0.454	---	0.518	0.452	---
T3	0.526	0.455	---	0.522	0.457	---
U	0.526	0.447	630	0.517	0.447	1029
V	0.526	0.452	766	0.511	0.447	616
W	0.537	0.449	282	0.534	0.453	291
X	0.549	0.441	287	0.531	0.429	272

Number designation with product letter indicates multiple measurements of that sample. "---" indicates that measurements of that sample were not available.

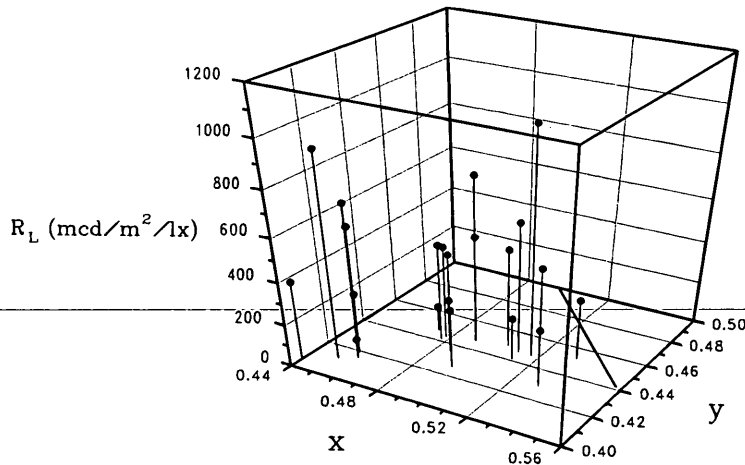


FIGURE 9 Brightness as function of chromaticity at 36-m geometry.

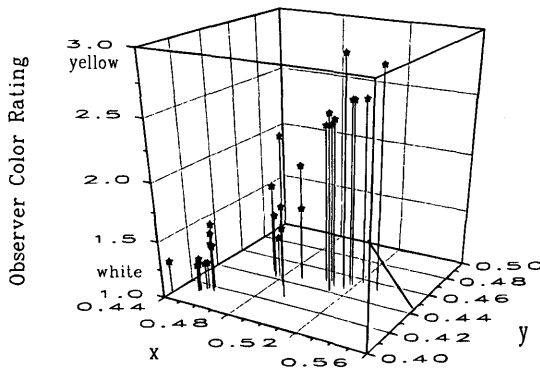


FIGURE 10 Observer night color ratings for 36-m viewing mapped on chromaticity.

36 m. The samples were viewed as isolated center lane lines with a parallel white edge line in place for all viewings. Observers rated the color on a scale of 1 to 5 from white to yellow.

The results showed significant color differences between pavement marking materials. At shorter distances, more of the materials appeared yellow than at longer distances. At longer distances observer ratings showed greater separation of color distinction between the materials.

Retroreflective color was measured at geometries corresponding to 12- and 36-m viewing conditions. Brightness did not appear to correlate with color. Color measurements for the different distances also showed the dependence of color on test conditions. Measured colors with a higher-color saturation were reported by observers to have a more yellow appearance.

CONCLUSIONS

Daytime and nighttime color are not the same. Some pavement markings having acceptable yellow daytime color were white in retroreflective color. Different "yellow" products can have varying nighttime color performance.

This work demonstrates the feasibility of specifying nighttime color using instrumental methods that can correlate with the human

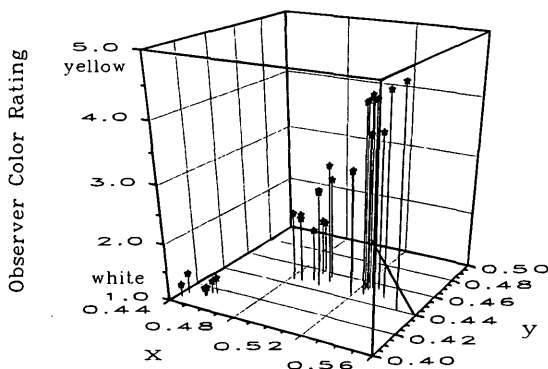


FIGURE 11 Observer night color ratings for 12-m viewing mapped on chromaticity.

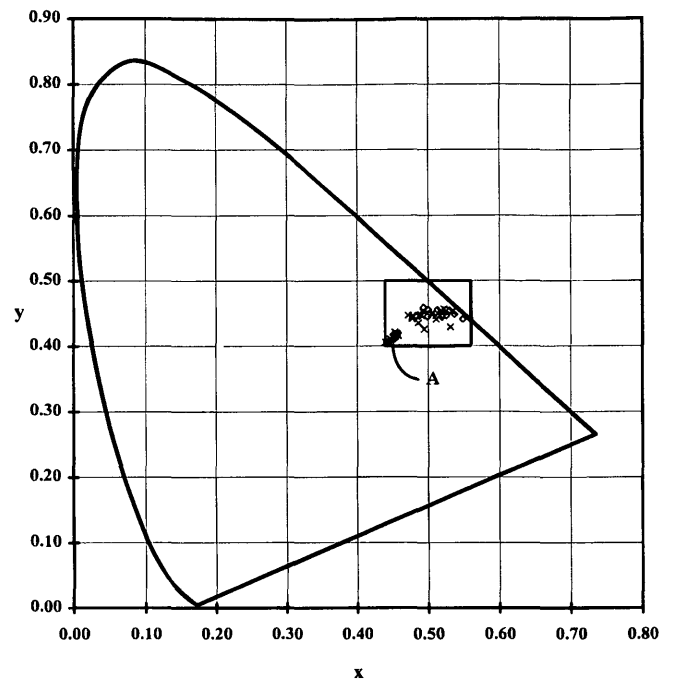


FIGURE 12 Retroreflective chromaticity of pavement markings A through X at 12- and 36-m geometries plotted on chromaticity diagram using CIE 1931 standard observer.

visual experience. However, more effort will be required to make such measurements routine and to define more precisely acceptable color zones. These retroreflective color requirements for pavement markings are subject to the safety needs of the driving environment in question.

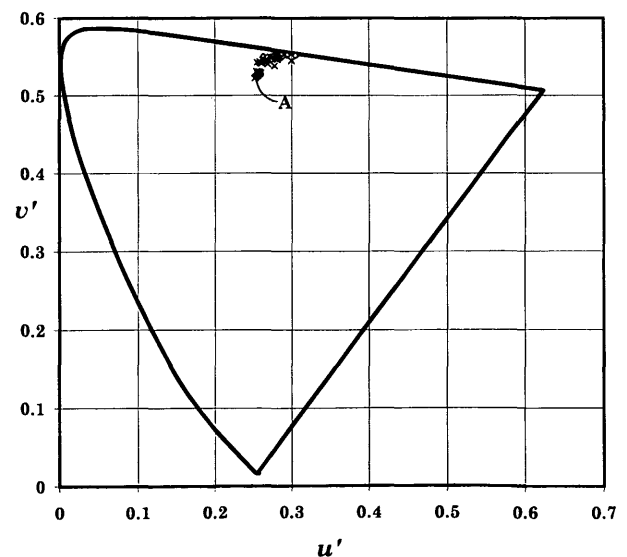


FIGURE 13 Retroreflective color of pavement markings A through X at 12- and 36-m geometries plotted on CIE 1976 u', v' diagram.

REFERENCES

1. *Manual on Uniform Traffic Control Devices for Streets and Highways*. FHWA, U.S. Department of Transportation, 1988, Section 3A-5, p. 3A-2.
2. *Traffic Control Devices Handbook*. FHWA, U.S. Department of Transportation, 1983, Section 3A-4, p. 3-7-3-8.
3. Banov, A. The Markets, This week's developments: Colorants and pigments. *American Paint & Coatings Journal*, Vol. 77, No. 15, Oct. 19, 1992, pp. 19-20.
4. Waldron, D. Advances in Retroreflectivity of Yellow Traffic Striping. Presented at 73rd Annual Meeting of the Transportation Research Board, Washington, D.C., Jan. 1994.
5. *Retroreflection, Definition and Measurement*, CIE Publication 54. Central Bureau of the CIE, A-1033, Vienna, 1982.
6. *Colorimetry*, 2nd ed. CIE Publication 15.2. Central Bureau of the CIE, A-1033, Vienna, 1986.

Publication of this paper sponsored by Committee on Visibility.

Application of Geographic Information Systems to Rail-Highway Grade Crossing Safety

ARDESHIR FAGHRI AND SRIRAM PANCHANATHAN

The application of geographic information systems (GIS) is especially relevant to transportation-related fields because of the spatially distributed nature of transportation-related data. The application of GIS to the management of transportation data can result in reduced costs and time savings. The development of a GIS application for management of safety-related data for public at-grade rail-highway crossings in the state of Delaware is discussed. The objective was to develop a GIS application that would enable better management of safety-related data for rail-highway grade crossings by integrating data from various sources and referencing data to their actual spatial location on the base map. The GIS application enables analysis and interpretation capabilities such as visual access and display, spatial analysis, query, thematic mapping and classification, and statistical and network-level analysis. The work was a continuation of an ongoing project that resulted in the integration of rail-highway grade crossing safety data from various sources, such as the Federal Railroad Administration and the Delaware Department of Transportation into a data base management system and the selection and implementation of the U.S. Department of Transportation (USDOT) accident prediction model into the system. The development of the rail-highway grade crossing safety GIS application is described and the creation of the spatial base map; conversion of existing rail-highway crossings attribute data into a GIS acceptable format; the interface with the USDOT model; and the prioritization, query, manipulation, analysis and editing features of the GIS application are presented.

Developments in the rapidly changing field of information technology have resulted in the availability of better hardware and software, more computing power with faster processing speeds, higher information storage capacity, higher-level queries and operating systems, and more efficient communication of data. All of these advances, including better graphics capabilities as a result, are having a direct and positive impact on the use and development of geographic information systems (GIS).

The application of GIS is especially appropriate to transportation-related functions because of the ability of GIS to provide a coordinated methodology to draw together a wide variety of information resources under a single, visually oriented umbrella and make them available to a diverse user audience (1). The benefits of GIS application lie not only in the integration and availability of diverse information within an integrated system, but also in the analysis, interpretation, and query facilities developed to suit specific needs of the diverse elements of the user community.

Many transportation agencies are investigating the applicability of GIS as a cost-saving and decision support tool. GIS applications can increase productivity through better availability and processing of

data in functions such as map drafting, infrastructure maintenance, cost estimations, inventory management, operational safety and hazard analysis, demand forecasting, land use and rezoning impact studies, and environmental impact analysis, as well as others (2).

Most GIS softwares and systems are equipped with the available analysis, processing, query, and interpretation functions of conventional data base management systems. The feature that distinguishes GIS from conventional data base management systems is the ability to perform spatial analysis. Spatial analysis, mainly in the form of overlaying and buffering, allows the user to explore relationships between different layers of data by referencing and the display of features and their attributes in one layer to the features and attributes contained in other layers. It is also possible to run several algorithms and models that are commonly used for such transportation-related applications as shortest-path, origin-destination tables, traveling salesman, and routing models. The facility to link up to several other packages and procedures for planning and statistical analysis also give access to more data-processing capability. A better perception of results is the result of the visual display and query facilities found in GIS.

Because they are essentially spatially distributed, rail-highway grade crossing safety data are suitable for GIS analysis. Development of a GIS application would allow for not only query and visual display of crossings but also analysis of the relationships between crossing location, land use, population density, and proximity to other features in the vicinity of the crossing. The development of a GIS application would ultimately result in an aid to resource allocation for accident reduction at crossings.

This paper discusses the development of a GIS application for safety evaluation at rail-highway grade crossings in the state of Delaware. The development of the application includes location referencing of the current safety attribute data base for public at-grade rail-highway crossings in Delaware and the linkage of the GIS to an empirical model that determines the accident hazard index for individual crossings on the basis of attribute information. Location referencing of the current data base, linkage to the empirical model, analysis, interpretation and query facilities created, and benefits of the application are discussed.

SAFETY ANALYSIS FOR RAIL-HIGHWAY GRADE CROSSINGS: A REVIEW

The responsibility for inventory and management of public at-grade crossings in Delaware lies in the hands of the Delaware Department of Transportation (DelDOT). In Delaware there are 548 rail-highway crossings of which 265 are public at grade. During a period

of 9 years, from 1981 to 1991, there were 71 train-automobile accidents, of which 10 resulted in fatalities (3). An earlier part of the ongoing study resulted in the identification of the most feasible empirical model for determining the accident hazard index; the development of a computerized data base that includes all safety-related inventory information; and the calculated accident hazard index for all public at-grade rail highway crossings in Delaware.

Data related to safety analysis of rail-highway crossings in Delaware comes from a variety of sources. One source of data is the Federal Railroad Administration, which maintains information on the city and county codes, railroad code, highway number, crossing type, and position of the crossings. Each crossing is assigned a unique DOT-AAR (Association of American Railroads) crossing identification number that is based on the milepoint on the approach road. This is basic information pertaining to the type of the crossing and its actual location.

Other significant information fields include the type of protection device, number of day and night trains passing through, crossing surface, maximum timetable speed, number of traffic lanes, estimated annual average daily traffic (AADT), and accident information. All this information can be obtained from several sources, including inventory records of railroad companies and field studies. The additional information required is the number of accidents, and this was obtained from the DelDOT Bureau of Traffic.

Other information required for resource allocation at crossings includes site-specific and qualitative information such as sight distance along the road and the track, number of school buses and hazardous materials carriers using the crossing, actual speeds on roads, and land use. Because most of the information is subject to frequent change, data must be constantly updated. Some of the data exist in the form of spreadsheets and others exist manually in the form of inventory sheets and tables.

The previous work resulted in collecting the statistically significant information necessary for applying the U.S. Department of Transportation (USDOT) accident index and storing the calculated accident index in an American National Standard Code for Information Interchange (ASCII) format file. The resulting integrated data base consists of 25 different fields of information. The form of the computer data base is indicated in Table 1.

Shortcomings in the Existing Program for Rail-Highway Grade Crossings Safety in Delaware

The first part of the study resulted in the integration of crossings-related safety data from various sources into a single accessible file format and linked the data base to the USDOT model (4) for assessing the hazard potential at the crossings.

Before the development of the GIS application, the user, when presented the data in a text file output could not have a perception of the actual spatial situation of the crossing, which is also crucial to the resource allocation decision-making process. The user had to go through the manual process of looking into a hard copy map to relate the information to the spatial location, which for a large data base of several hundred crossings can be time consuming. Additional information, such as land use, proximity to schools, and other qualitative information, was also not readily available to the user. Furthermore, the data base was not location referenced in a form that is compatible for access into GIS.

TABLE 1 Format of Computer Data Base Developed for Rail-Highway Crossings Safety Data in Delaware

COLUMN	CONTENTS
1-7	DOT-AAR Inventory Number
8	County Code
9-10	City Code
11-27	Street or Road Name
28-33	Milepost
34-35	Number of Day-through trains
36-37	Number of Day-switch trains
38-39	Number of night-through trains
40-41	Number of night-switch trains
42-44	Maximum timetable speed
45	Number of Main tracks
46-47	Number of Other tracks
48	Protection class at crossing
49	Is highway paved?
50	Pavement marking
51	RR advanced warning signs present
52	Crossing surface
53	Number of traffic lanes
54-55	Highway system code
56-61	Estimated AADT
62	Is highway divided?
63	Number of accidents in last 9 years
64	Number of fatalities

BRIEF REVIEW OF GIS

Several definitions have been coined for GIS. One of the appropriate definitions by Dueker and Kjerne (5) describe GIS as "geographic information system—a system of hardware, software, data, people, organizations, and institutional arrangements for collecting, storing, analyzing, and disseminating information about the areas of the earth."

A GIS is basically an integrated, computer-based, spatially referenced data base management system. The components of a typical GIS system include a data base component, a hardware component, and a software/interfaces component. The data base component in GIS is in the form of two distinct data bases: one is the graphic data base and the other is the nongraphic or attribute data base.

The graphic data base is a description of the map features and is composed of geo-coded spatial data that define objects on a two- or three-dimensional surface and identify their relationships by categorizing and defining them either as points, lines, or polygons that are tied to a common referencing system (6).

Spatial data can be obtained from various sources. One is the scanning or digitizing of hardcopy maps, satellite imagery, and photogrammetric sources (7). There are also primary sources of digital data, such as the topographically integrated graphical encoding and referencing (TIGER) files of the U.S. Census Bureau and other digital data bases that are commercially available.

The U.S. Census Bureau developed the TIGER files, which identify every road segment in the United States along with information on street labels and census information, county partitions, statisti-

cal information, national partitions, and geographic catalogs, all referenced in a latitude-longitude coordinate system (8).

The nongraphic, or attribute data bases, refer to data elements that describe the characteristics of features on the spatial maps or those of events occurring at spatial locations.

The crux of the GIS system is the linkage between the nongraphic data and their graphic position or location. The most common way to achieve this linkage is to have an identifier stored with each nongraphic data record that corresponds to the identifier stored with its actual spatial location in the graphic data base. The management of nongraphic data bases can also be done using any of the commercially available data base management software that are compatible in input and output format for import and processing in GIS.

Two distinct components can be seen in GIS software packages: one is the main component that performs the basic functions of data base management, graphic, and mapping functions. The other is a need-specified set of functions that provide geographic and attribute data analysis, manipulation, edit, and query functions. This component varies according to the type of application package. Transportation-related application packages will be likely to have network analysis, routing, and optimization algorithms linked up and provided for manipulation and analysis.

POTENTIAL FOR GIS TECHNOLOGY APPLICATION

The limitations of the current rail-highway program can be eliminated to a great extent by the application of GIS technology. The main benefits can be perceived in the better perception of the problem because of the presentation of crossings data on a map format in reference to its actual position. Resource allocation decision making would be more accurate because the user also gets a visual input, along with the ability to make spatial and textual queries on the data base.

The present crossings safety data base in Delaware allows only limited manipulation, analysis, or query of the data base. The user is limited in the textual queries and selections that can be made. Viewing and processing crossings attribute data with respect to spatial and topological attributes and relationships are not possible. This limits the user, typically the local crossings expert/railroad division engineer, from considering the area-specific qualitative information that is crucial to sound decision making and which would be available in spatial format in a GIS application.

GIS provides a powerful tool in the form of spatial analysis, which is the characteristic that distinguishes it from other data base management systems. Accessing data from several different layers and exploring the relationships between them—for example, the relationship between crossing safety and proximity of the crossing to a school—is one of the powerful and unique features of GIS.

The ability to perform conditional queries and statistical analysis, create thematic maps, and provide charting and statistics enhances the functional ability of the crossings safety program. The ability to link up to external programs and procedures for user-specific functions, such as interfacing the USDOT model to the location referenced attribute data base, also would be possible. This would allow the data base to use specific external packages such as those for statistical analysis and data base management and then view and query the processed data. Linkage with a knowledge-based expert system that considers site-specific and qualitative

information in addition to the statistically significant data to provide decision support to the user is also possible.

Source of Spatial Data

For the development of the rail-highway safety application, the graphic data base requires all rail and intersecting road segments to be labeled, which in effect means road and rail segments, for the state of Delaware. The availability of other attribute information such as land use, population density, and census geography is not actually required for applying the DOT model, but these are significant qualitative factors and are important to sound resource allocation decision making toward mitigation of accidents.

The TIGER data base for Delaware was found to be appropriate and sufficient for all the requirements of the current application. TIGER consists of all city and county and road and rail segment information, and it also has street labels associated with it. This makes possible the identification of the spatial location of crossings and the location referencing of attribute data. In the current data base these attribute data are not in a location referenced form acceptable for building a GIS application. Figure 1 indicates the Delaware base map for the GIS application consisting of rail and road segments.

TIGER has the additional advantage of being in a standard latitude-longitude referenced form, which makes geocoding possible. The availability of census geography information is also helpful, and the ability to append and import data from other sources into most GIS softwares makes TIGER even more versatile for this application.

Selection of GIS Software

Several commercially available GIS application software packages could be used for developing such an application. However, because each of these software packages is designed for specific applications, the needs of the current application were appraised, and the package required was selected on the basis of these identified requirements. The functional capabilities required, in general, for GIS software are described in Spear (9).

Some of the basic functional capabilities required for the rail-highway application were identified to be as follows:

- Basic GIS textual and geographic query and selection functions;
- Geographic and attribute editing functions enabling editing and updating of the attribute data and changing the location coordinates of entities, if required;
- GIS windowing display, zoom in/out, selection and creation of data base layers, display of features and highlighting;
- Ability to import and export referenced data, ability to operate on ASCII, availability of worksheet format files, ability to translate and accept TIGER files; and
- Ability to link with external procedures, provided there are specific programs and statistical software packages.

The requirements were focused more toward the manipulation and handling of the attribute data. Such graphic processing functions as geographic editing, mapping, feature modification, and

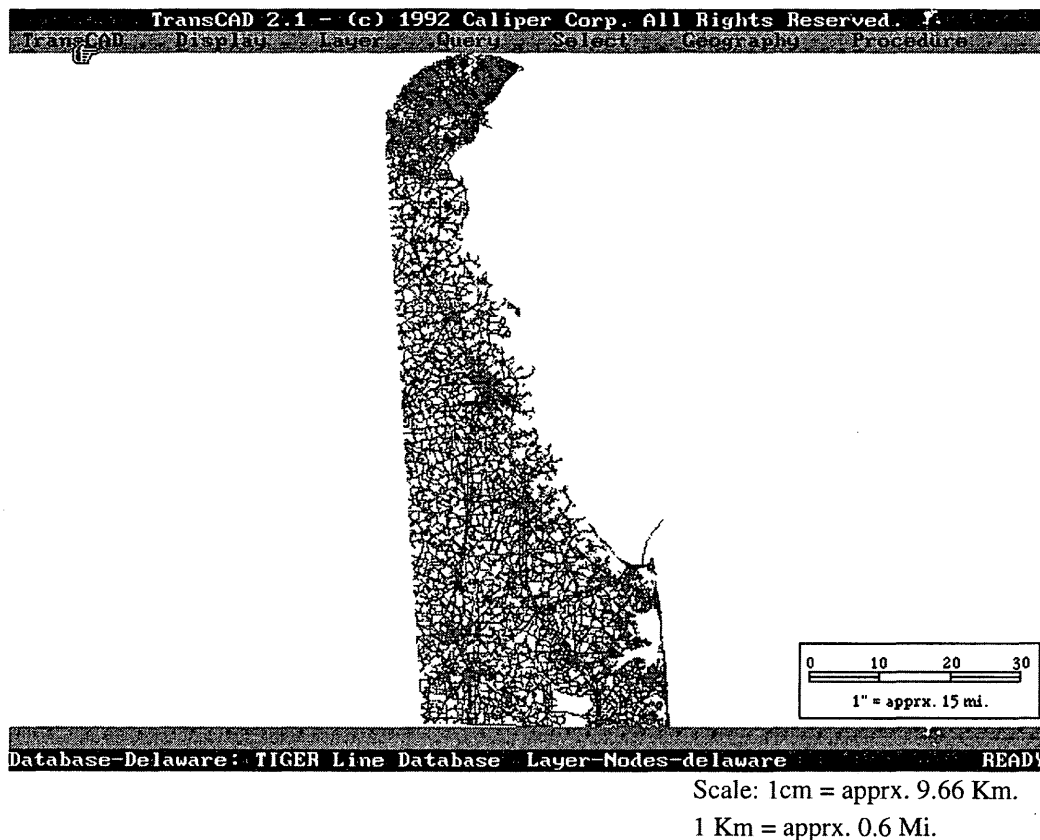


FIGURE 1 Base map with rail and road segments created for Delaware using TIGER data.

interactive digitizing largely are not required for the application. Several UNIX-based software packages that could be run on a workstation had the required functions and, additionally, graphic processing capabilities, and multiuser and windows operation capability at a much higher cost.

While considering the requirements of attribute data representation, external linkage, and manipulation and processing, the objective was to identify a low-cost, microcomputer-based GIS software, which need not require advanced graphic processing functions. TransCAD (10) transportation GIS software was found to be suitable and was selected for building the application.

DEVELOPMENT OF RAIL-HIGHWAY GIS APPLICATION

The first step in developing the GIS application was creation of the base map for Delaware. TIGER files were used to create the base map on which the crossings locations could be displayed. The features included in this base map, which are indicated in Figure 1, are the rail and road links for the entire state.

Once the base map was developed, the next step involved creating the location referenced attribute data base that contains safety-related attribute information for public, at-grade, rail-highway crossings in Delaware. A program was then developed to execute the USDOT model on the crossings safety data and estimate the accident index of each crossing. This program was interfaced to the GIS application to enable it to directly access data from the geocoded attribute data base and pass the results back to the GIS to

enable display and analysis with respect to the crossing location. The last two steps in the development of the GIS application are the analysis and interpretation of data and the presentation of results in the form of charts, tables, thematic maps, and hard-copy generation of the same. All these steps are described in the following sections.

Location Referencing of Attribute Data

The existing data base had location reference information only in the form of city, county description, road labels and milepoint on approach, apart from the DOT-AAR identification number. For the GIS, the data records need to be in one of the standard coordinate systems.

If the information is in latitude and longitude coordinates, the input data for a point data base needs to be in a single file. If it is in some other coordinate system, the GIS has the ability to convert to the latitude-longitude system on provision of the local and world coordinates of any three points on the data base (10).

The only location reference information available consisted of the crossing city, county, street, and railroad names and railroad milepoint information. The milepoint data could not be effectively used because it was inaccurate and inconsistent.

Some of the crossings records were location referenced by a simple program that searched for a match in the strings consisting of the railroad and street names for a crossing record with the respective fields in the node layer data base for Delaware. If a match was found the coordinate information from the node layer record was attached to the crossing record in question. Many of the records could not be

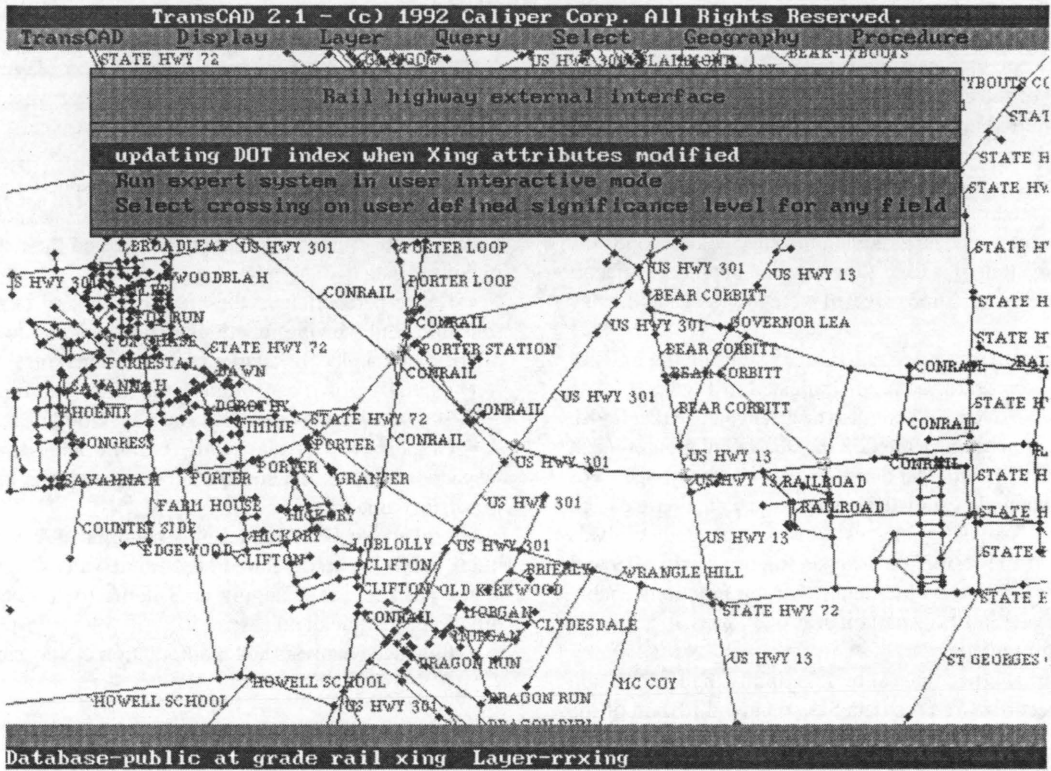


FIGURE 3 Linkage to external procedures (USDOT model).

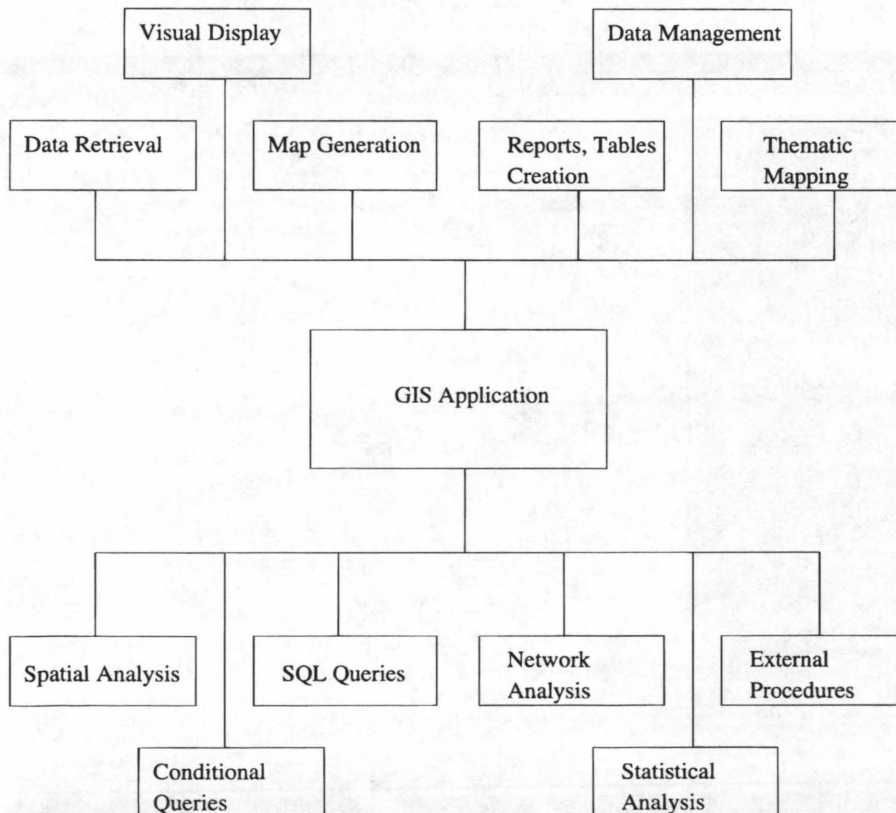


FIGURE 4 General capabilities of rail-highway grade crossing safety GIS application.

objects of a specific type that lie within a specified distance of the crossing—for example, the number of schools within a mile of the crossing. The user can also perform overlaying to assess the land use in the vicinity of the crossing.

The user can query into any crossing and view the attribute data associated with it as indicated in Figure 5. Some of the query conditions created are shown in the menu created in Figure 6. Conditions are created to reflect the strategies for identification of deficient, significant, and hazardous attribute values, and the resource allocation strategies used to reduce the potential for accidents. In this case, the conditions created were to select and display crossings.

Thematic maps were created to classify crossings on the basis of traffic, accidents, or hazard index, as indicated in Figure 7. Data records based on any given field can also be arranged and displayed. Statistical analysis functions in the GIS include calculation of mean values and variances of particular data items over spatial ranges. For more detailed and complex statistical analysis, the data base can be linked to statistical analysis packages such as Statistical Analysis System (SAS), and the results of analysis imported into GIS and viewed and presented on the base map. Charting functions enable the production of pie and bar charts in various forms, a sample of which is shown in Figure 8.

Linkage to external procedures allows flexibility in manipulation and selection of records from the data base on identification of the specific nature of the requirements. A program was developed that enabled selection of records on the basis of a user-specified level of significance, expressed as a percentage, for any field, and display of the selected records/crossings in the digital base map.

RESULTS

A GIS application for integration, graphic display, and processing of rail-highway crossings-related safety data was developed. The features of the GIS application are as follows:

- Possibility of interfacing with need-specific procedures and analysis. Integration of relevant and significant safety-related data from various sources into one data base and the location referencing of the data.
- Better perception of the crossings hazard because of query, selection, and viewing functions in GIS, leading to less possibility of error and neglect of factors in decision making.
- Spatial analysis capability in the form of buffering.
- Statistical analysis of data and generation of results in charts.
- Graphic map display with zooming and scaling allows the inspection of data at a specific crossing and in a quick and easily understandable form.
- Linkage to DOT model gives automated updating of hazard index values on modification of attribute values.
- Updating and changing data items for crossings using edit functions are quick and easy.
- Enhanced analysis and manipulation are possible.

SUMMARY AND CONCLUSIONS

The development of a GIS application for safety evaluation at rail-highway crossings demonstrates the benefit of GIS in the form of

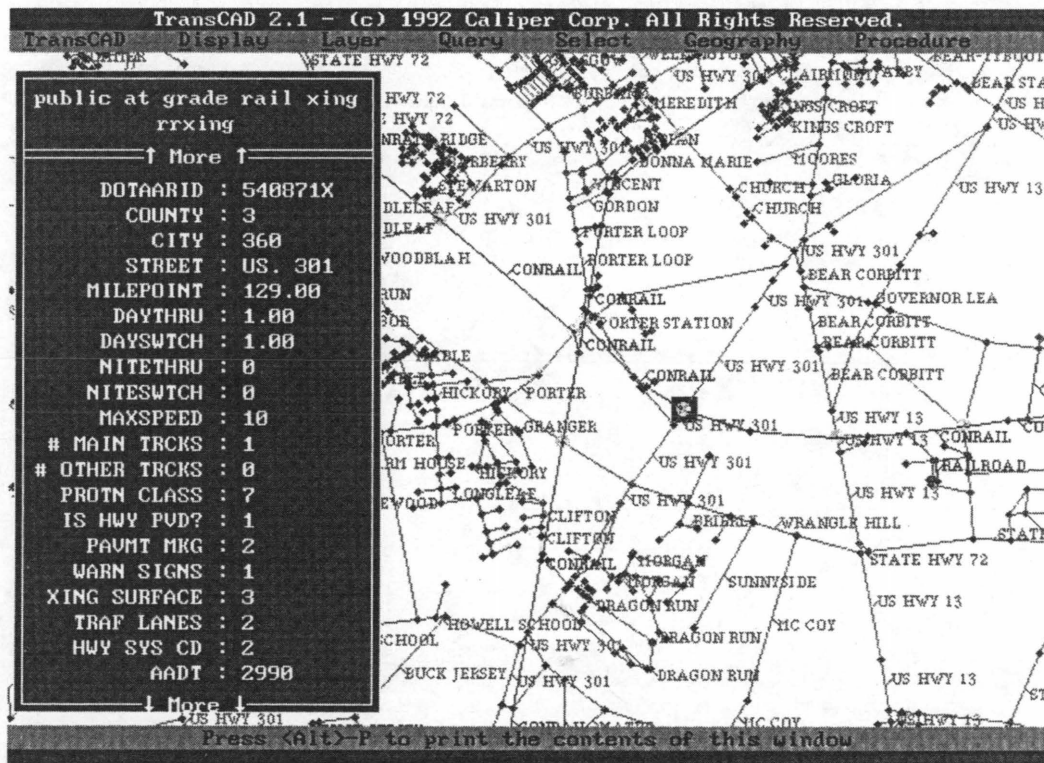


FIGURE 5 Query into crossing showing safety attribute data.

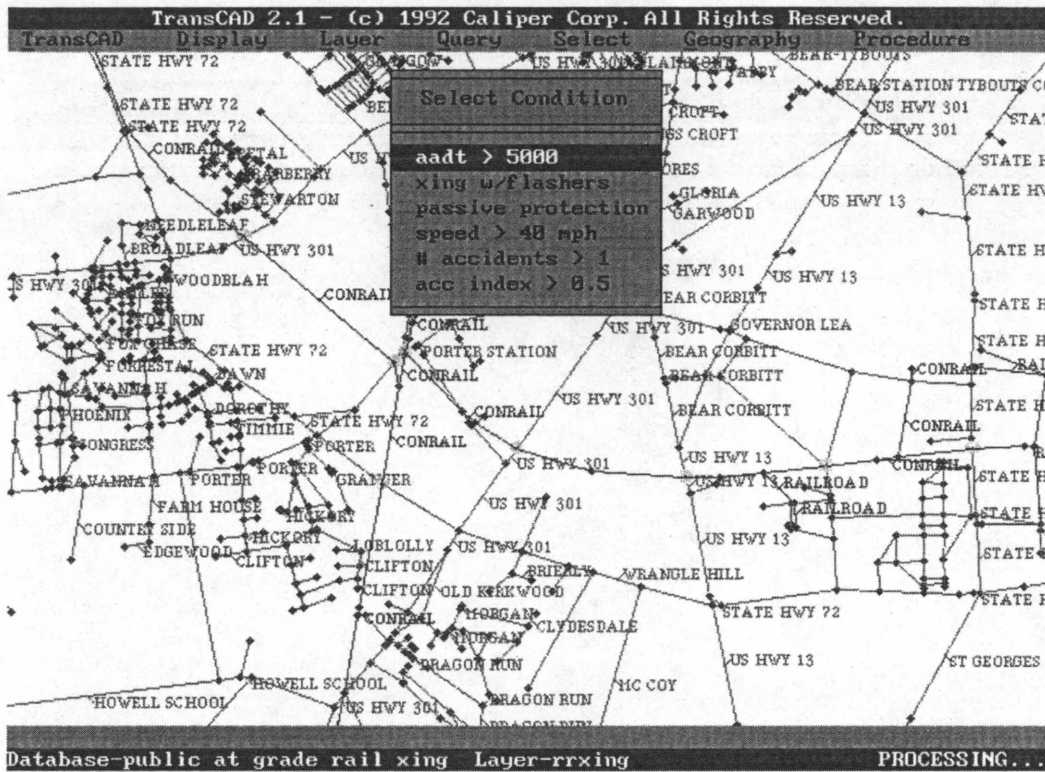
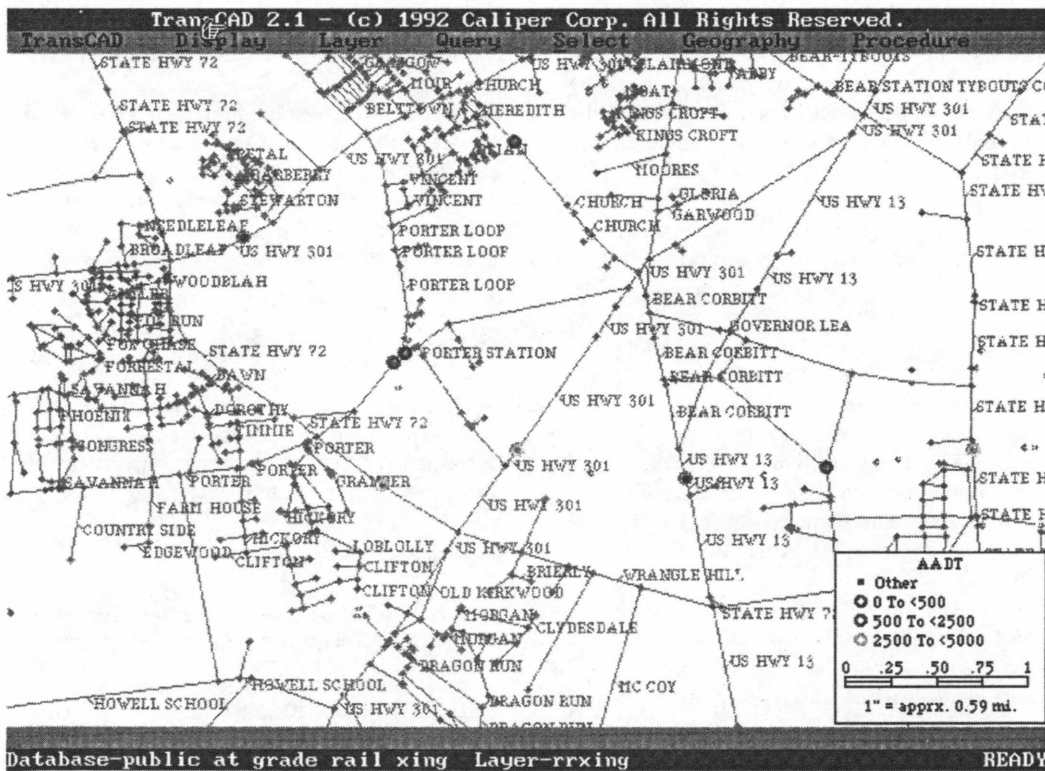


FIGURE 6 Conditions created for display of crossings with attribute values according to nature of queries.



Scale: 1cm = apprx. 0.38 Km.

1 Km = apprx. 0.6 Mi.

FIGURE 7 Sample of thematic map created for display of crossing data according to desired nature of classification.

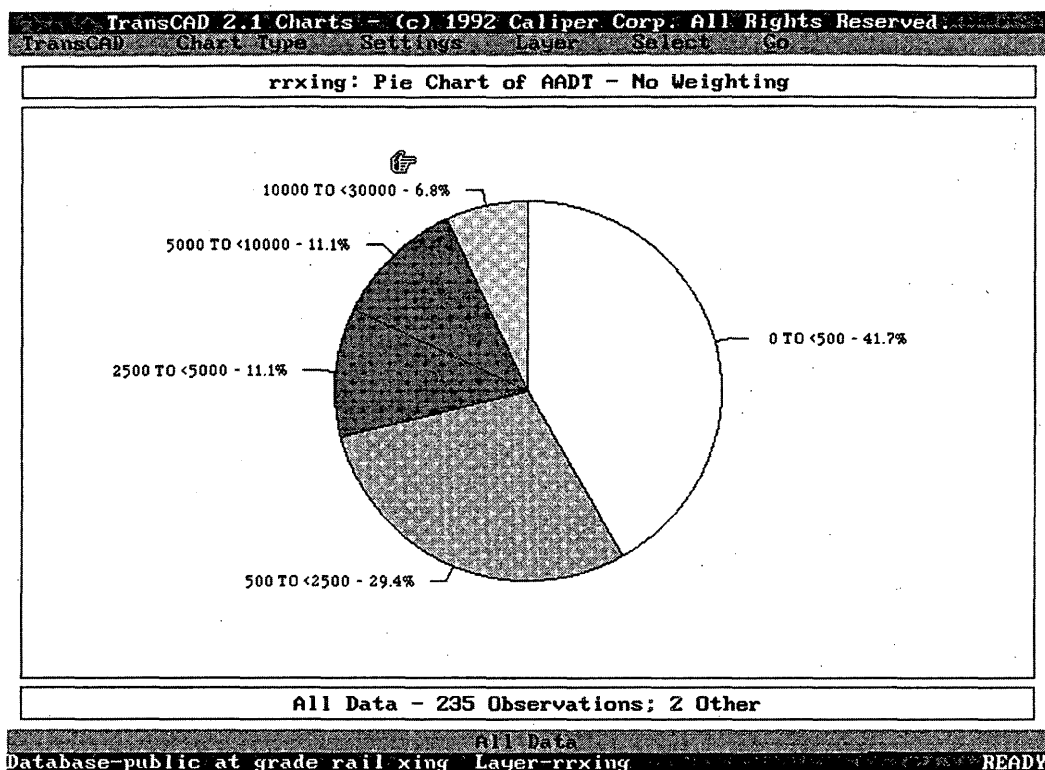


FIGURE 8 Sample pie chart of presentation of results of processes on data.

savings in time and costs through the availability of data from one source and better decision making as a result of better perception and analysis. The location referenced attribute data base could be incorporated into a multiuser, client-server system, making the application and the data base available to a wide variety of users and applications.

The GIS application developed here is a low-cost application developed on a stand-alone 80486 processor-based personal computer. The bulk of the effort involved was in location referencing and keying in attribute data. The system thus developed is a low-cost one. The costs involved are the cost of procuring hardware and software and the labor cost associated with developing the application. For the Delaware data base of 265 public, at-grade rail-highway crossings, the effort involved 200 to 250 person-hours of work. For a larger state, with a few thousand crossings, the effort involved in data conversion would be much more unless there were sufficiently accurate information, such as railroad milepoints, which would enable automation of the entire process of location referencing and thus save a considerable amount of effort in the process.

The project demonstrates the benefits of integration and availability of safety-related information for resource allocation strategy development at a single source and in a user-friendly display form. Integration of rail-highway crossing safety data from diverse sources was achieved. The availability of analysis, manipulation, and result presentation capabilities in the form of an interface to the USDOT model; the statistical analysis functions of the software; the need-specific conditional query; the presentation of attribute data and hazard potential in charting; and thematic map forms all result in cost and time savings through quick and effective analysis of the safety data base.

Because transportation-related data are spatially distributed it is compatible with and benefits from representation in a GIS. The application of GIS to transportation network data, as in this application, results in quantifiable benefits in efficiency through automation of data handling, integration of disparate but application-related data, and expanded capabilities for analysis and manipulation. The savings in the form of reduced labor requirements compared with manual processing can outweigh the costs of developing a GIS system.

ACKNOWLEDGMENT

Funding for this project was provided by the Delaware Department of Transportation through the Delaware Transportation Institute, Department of Civil Engineering, University of Delaware.

REFERENCES

1. Petzold, R. G., and D. M. Freund. Potential for Geographic Information Systems in Transportation Planning and Highway Infrastructure Management. In *Transportation Research Record 1261*, TRB, National Research Council, Washington, D.C., 1980, pp. 1-9.
2. Faghri, A., and N. Raman. *Evaluation of Geographic Information Systems (GIS) Applications in Delaware*. Report 92-DTC-6. Delaware Transportation Center, University of Delaware, Nov. 1992.
3. Faghri, A., and N. Vukadinovic. *Evaluation of Rail-Highway Grade Crossings Safety*. Report 91-DTC-1. Delaware Transportation Center, University of Delaware, Sept. 1991.
4. Hitz, J., and M. Cross. *Rail Highway Crossings Resource Allocation Procedure*. Volpe National Transportation Systems Center, U.S. Department of Transportation, Cambridge, Mass., 1982.

5. Dueker, K. J., and D. Kjerne. Multipurpose Cadstre: Terms and Definitions. *Proc., Annual Convention of ACSM-ASPRS*, Vol. 5, 1989, pp. 94-103.
6. Simkowitz, H. J. Using Geographic Information Systems for Enhancing the Pavement Management Process. In *Transportation Research Record 1261*, TRB, National Research Council, Washington D.C., 1980, pp. 10-19.
7. Antenucci, J. C., et al. *Geographic Information Systems—A Guide to the Technology*. Van Nostrand Reinhold, New York, 1991.
8. *NCHRP Report 359: Adaptation of Geographic Information Systems for Transportation*. TRB, National Research Council, Washington, D.C., 1993.
9. Spear, B. D. Issues and Considerations in Procuring GIS-T Software. *Proc., of The 1991 GIS for Transportation Symposium*. Orlando, Fla., 1991.
10. *TransCAD—Transportation GIS Software, Version 2.0*. Reference Manual. Caliper Corporation, Newton, Mass., 1990.

Publication of this paper sponsored by Committee on Railroad-Highway Grade Crossings.

Evaluation of Accuracy of U.S. DOT Rail-Highway Grade Crossing Accident Prediction Models

M.I. MUTABAZI AND W.D. BERG

Several versions of the U.S. Department of Transportation rail-highway grade crossing accident prediction models have been developed and recommended for use in resource allocation procedures. The objective of this research was to test and evaluate the ability of these models to accurately predict future accident experience at individual grade crossings. Accident history and inventory data were assembled for 1,798 grade crossings in Wisconsin for the period from 1975 through 1989. Differences between the actual and predicted accident rates for 5- and 10-year forecast periods were evaluated using both the basic accident prediction models and the 5-year accident history adjustment to the basic model. It was found that the basic model from the first and third versions provided the best estimate of the long-run accident rate at individual grade crossings and were, therefore, recommended for use in resource allocation procedures.

The U.S. Department of Transportation (DOT) has developed a resource allocation procedure to assist the railroad and highway industry in developing a cost-effective program of improvements at rail-highway grade crossings. A critical component of the procedure is the accident prediction model that is used in estimating the expected number of accidents at a crossing under a given set of physical and operating characteristics. Several versions of the model have been developed and recommended for application (1-3). A critique of two of the earlier versions indicated significant inconsistencies in predicted accident rates, with a resulting potential bias in the implied cost-effectiveness of candidate improvements (4). It was shown that these problems can, as a consequence, lead to a misallocation of limited resources.

The developers of the several DOT accident prediction models had evaluated the relative effectiveness of their models using a parameter called a power factor. The power factor indicates the percentage of all crossing accidents that occur at a selected percentile of the most hazardous crossings as ranked by the accident prediction models. For example, if the power factor for the fifth percentile of ranked crossings is 4, then on the average, each 1 percent of the most hazardous 5 percent of all crossings is contributing 4 percent of the total accidents for the entire population of crossings.

The power factor is useful when comparing two or more hazard-ranking models (be they absolute or relative accident prediction models) that are not expected to be applied in a benefit-cost analysis framework. For example, if there are resources available for upgrading warning devices at 5 percent of the crossings in a population, the exact number of accidents expected to be reduced is

immaterial because what is important is to maximize the expected total number of accidents reduced at crossings in the population. One only need identify that group of crossings expected to experience the greatest number of accidents, regardless of actual number.

However, when the accident prediction models are to be used in a resource allocation or benefit-cost analysis framework, such as the recommended DOT procedure (3), then an estimate of the actual magnitude of expected accident experience at individual crossings is a prerequisite. This is true whether the expected accident reduction is estimated by using the DOT procedure by first predicting the accident rate under existing conditions and then applying an effectiveness ratio to the proposed upgrade or if the expected accident reduction is estimated by simply calculating the difference in predicted accident rates for the alternative warning devices. Preference for the latter approach has been presented and discussed in a previous paper (4). The objective of the research reported herein was to test and evaluate the ability of the three different versions of the DOT accident prediction model to accurately predict future accident experience for a large sample of individual rail-highway grade crossings (5.)

CHARACTERISTICS OF THE MODELS

The first of the three accident prediction models to be evaluated was developed during the late 1970s using 1975 accident and inventory data for all public grade crossings in the United States (1.) The model consists of three sets of equations, one for each of three categories of warning devices: passive (including cross bucks and STOP signs), flashing light signals, and gates. Independent variables used in the equations are indicated in Table 1.

The second set of accident prediction models was released in 1982 and was intended as an upgrade and improvement to the first set of models (2.) A principal change in the structure of the models was the incorporation of a two-stage computational procedure. The first stage consists of a basic accident prediction formula similar to that found in the original models, but with minor changes in the independent variables as indicated in Table 1. The second stage is referred to as the general accident prediction formula, and computationally represents a weighed average of the predicted accident rate from the basic formula and the observed accident rate for the immediately preceding 5-year period. The third set of accident prediction models to be evaluated was released in 1987 and is similar to the second set of models (3.) Some of the independent variables were changed, as shown in Table 1, and the models were recalibrated using 1981 through 1985 accident data and 1986 inventory data.

M. I. Mutabazi, Department of Civil Engineering, Kansas State University, Manhattan, Kans. 66506. W. D. Berg, Department of Civil and Environmental Engineering, University of Wisconsin-Madison, Madison, Wisc. 53706.

TABLE 1 Independent Variables Used in U.S. DOT Accident Prediction Models

Variable	Passive			Flashing Lights			Gates		
	1980	1982	1987	1980	1982	1987	1980	1982	1987
Trains per day	X	X	X	X	X	X	X	X	X
Number of day-through trains	X	X	X	X	X	X			X
Number of main tracks	X	X		X	X	X	X	X	X
Maximum timetable speed		X	X						
Average daily traffic	X	X	X	X	X	X	X	X	X
Number of lanes				X	X	X	X	X	X
Highway paved?	X	X	X						
Highway type	X	X		X					
Area population	X			X					

The inclusion of a 5-year accident history in the second and third models was intended as a method for accounting for the general effect of important influencing factors not included in the models, such as available sight distance. Even if this approach is considered reasonable, there was no reported test of the goodness of the accident predictions that result from the application of this weighting procedure.

METHODOLOGY

The Office of the Transportation Commission (OTC) for the state of Wisconsin maintains rail-highway grade crossing accident history and warning device upgrade information in a card file system for every crossing in the state. In addition, the OTC has microfiche copies of the DOT inventory data for the years 1979, 1982, 1983, 1987, and 1989. This represented a unique data base that could be used for testing the predictive abilities of the three DOT accident prediction models.

A total of 1,798 crossings found on two railroads operating in Wisconsin were selected as an evaluation data set. There were 1,000 crossings equipped with crossbucks, 680 with flashing light signals, and 118 with gates. This sample data base was then compared to the national inventory data base to determine whether it was reasonably representative of grade crossing characteristics found nationwide. As illustrated in Figures 1 through 3, the distribution of crossings by type of warning device, average daily traffic volume, and average trains per day are similar. As a result, it was concluded that the study findings should be applicable to those of other states as well as to Wisconsin.

The 1,798 sample grade crossings were initially analyzed on the basis of 1980 conditions. This included actual knowledge of accident experience during both the prior 5-year period from 1975 through 1979 and the post 10-year period from 1980 through 1989. Each of the three DOT models was applied to the 1980 conditions for each of the 1,798 grade crossings. Five predicted rates were calculated for each crossing using the following model formulations (identified hereafter as Models 1 through 5):

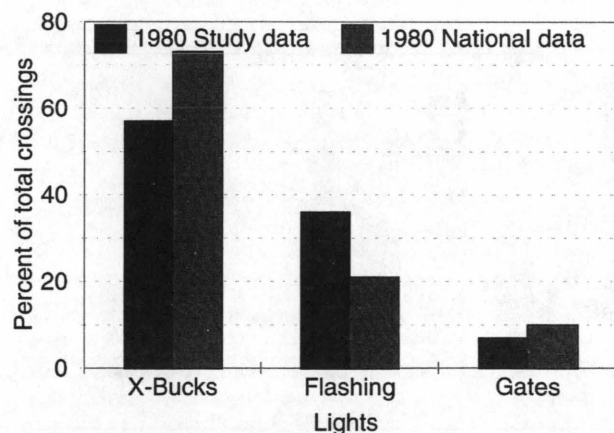


FIGURE 1 Comparison of sample versus national data: type of warning device.

1. First model (1);
2. Second model without accident history: basic formula (2);
3. Second model with accident history: general formula (2);
4. Third model without accident history: basic formula (3); and
5. Third model with accident history: general formula (3).

Each predicted accident rate was compared with the observed rate for post-5- and 10-year periods from 1980 through 1984, and 1980 through 1989, respectively. The questions of interest were: (a) Are the models significantly different from each other; and (b) Which model(s) are better predictors of actual accident rates at individual grade crossings.

DIFFERENCES BETWEEN MODELS

A null hypothesis that all five predicted accident rates were the same was tested against the alternative that at least two were different. A two-way analysis of variance in the predicted rates for the five models was performed for each of the three warning device classes. Crossings were considered as a blocking factor to eliminate crossing-to-crossing variation.

Because the calculated *F*-ratio exceeded the critical ratio at the 5 percent significance level for the models factor for each warning device category, it was concluded that at least two models were significantly different from each other at the 95 percent level of confidence. As expected, it was also found that the sample crossings were significantly different from each other within each warning device class. The same analysis was repeated using only Models 1, 3, and 5. The same conclusions were drawn as those in the previous analysis, thus indicating that at least two of the three versions of the general DOT accident prediction models were significantly different from each other at the 95 percent level of confidence.

Because the *F*-test did not indicate whether there was any pair of models whose difference was statistically insignificant, confidence intervals for the difference between all pairs of models were constructed. The upper and lower limits were calculated at the 95 percent level of confidence. When the range between the upper and lower limits contained zero, it was concluded that the two models were not significantly different from each other. The results revealed that the predicted accident rates from Model 5 were not significantly different from those produced by Models 1 and 4,

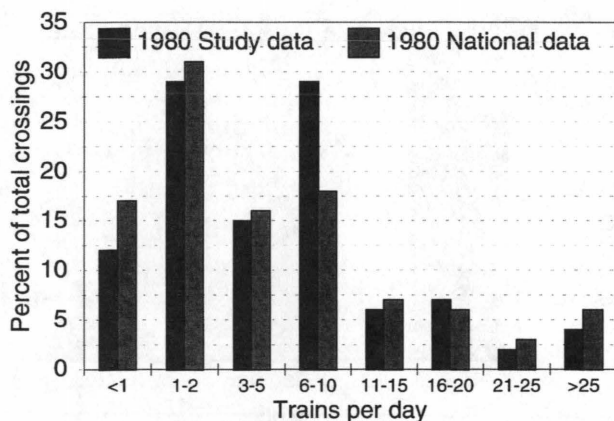


FIGURE 2 Comparison of sample versus national data: average daily traffic.

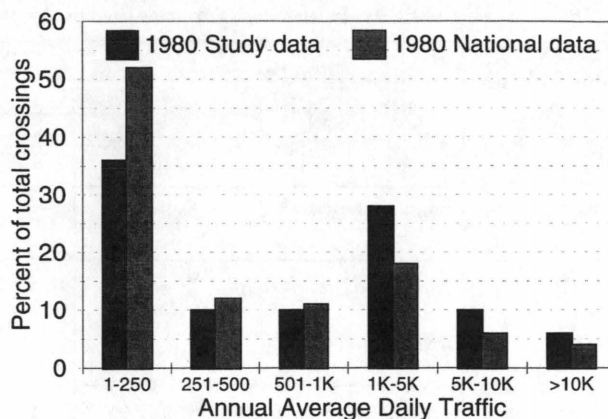


FIGURE 3 Comparison of sample versus national data: average trains per day.

although Models 1 and 4 yielded predicted rates that were significantly different from each other.

Determination of a preferred model was approached by analyzing the absolute deviations from a comparison of observed and predicted accident rates for each model. The preferred model would be the model having the minimum sum of deviations. Comparisons were undertaken for observation periods of 5 and 10 years, first assuming that prevailing physical and operating conditions remained constant and then accounting for any actual changes that occurred during the observation period.

Table 2 illustrates the results of this analysis. It is clear that Models 2 and 3 are inferior to Models 1, 4, and 5 under all conditions. The latter models appear to be of approximately equal relative effectiveness with respect to predicting the accident rate at an individual grade crossing for a 5- to 10-year observation period. In addition, the predictive ability of the models improves as the length of the observation period increases. This implies that observed accident rates based on short time periods (such as 5 years) do not offer good estimates of the true mean accident potential at a grade crossing. This should probably not be unexpected given that the average accident rate for all grade crossings as a whole is about one accident every 30 years.

ACCIDENT HISTORY AS A HAZARD PREDICTOR

For any given grade crossing, there is a true mean accident rate that is unknown. Any observed rate over a given time period is simply an estimator for that true mean rate. However, the 5-year accident history period used in the second and third versions of the DOT models is usually not long enough to assess a true trend for the actual accident rate at a specific grade crossing.

For example, consider a crossbuck-equipped grade crossing with a true accident rate of 0.04 accidents per year, or one accident every 25 years. Further assume that the basic DOT accident prediction formula (without the accident history adjustment) is able to accurately predict the true accident rate at this crossing. If by chance no accidents had occurred during the 5-year accident history period selected for application of the general DOT model, then the weighted predicted accident rate would be 0.028 accidents per year, or one accident every 36 years. This would suggest that the crossing is 43 percent safer than it actually is. The observation of no acci-

TABLE 2 Comparison of Observed with Predicted Accident Rates: Sum of Absolute Deviations

Model	Changes in Prevailing Conditions			
	Accounted For		Not Accounted For	
	5-yr Period	10-yr Period	5-yr Period	10-yr Period
1	116	95	115	95
2	153	136	156	134
3	146	123	144	125
4	116	94	115	93
5	112	90	111	91

dents in the 5-year history period does not necessarily mean that the predicted rate of 0.04 accidents per year was incorrect because the assumed average of one accident every 25 years could occur in any year with the 25-year return period. Had that one accident occurred during the 5-year observation period, then the weighted predicted accident rate using the general DOT model would be 0.09 accidents per year, or one accident every 11 years. This would suggest that the crossing is 125 percent more hazardous than it actually is.

Even if the true accident rate is assumed to be unknown, the predicted rate from the general DOT model in this example can vary from one accident every 11 years to one accident every 36 years, depending on whether one vehicle-train accident had occurred during the previous 5 years. The 5-year observation period is only 14 to 45 percent as long as the average return period on the basis of the predicted accident rate (assuming a 5-year accident history of 0 or 1 accident, respectively). As a result, a 5-year observation period should not be expected to provide a good indication of the general trend or true accident potential at a rail-highway grade crossing.

These observations suggest that regression-to-the-mean phenomena may need to be considered. This statistical concept characterizes a situation in which, if a random deviation from the mean occurs, it is expected that the next observation will be closer to the population mean. For example, if a 10 percent sample of grade crossings having the highest 3-year accident history were selected from a given region, then it would be expected that during the next 3 years the accident rate at these crossings would decline, even if no safety measures were implemented.

Use of the accident history adjustment to the basic accident prediction formula in the second and third versions of the DOT models is tantamount to an approximation for regression to the mean. By virtue of the way in which the basic formula was statistically calibrated, it provides a direct estimate of the true mean or long-run accident rate for a specific set of crossing characteristics. However, if the observed accident rate during the previous 5 years is greater or less than the basic predicted rate, then the DOT procedure adjusts the observed rate toward the basic predicted accident rate. Thus, the resulting adjusted rate presumably approximates the trend expected

during the next short-run observation period, with the basic formula still providing the best estimate of the long-run mean accident rate.

To test this hypothesis, the 1,798 sample grade crossings were first grouped according to the number of vehicle-train accidents actually observed during the 1975 through 1979 time period. The observed accident rates for the subsequent 5- and 10-year periods of 1980 to 1984 and 1980 to 1989 were also determined for each crossing and then averaged within each group. Similarly, the predicted accident rates for each crossing from Models 1, 4, and 5 were averaged within each group.

Figure 4 illustrates the results of this analysis. Models 1 and 4, which do not incorporate any accident history adjustment, suggest a similar expected long-run accident potential. The expected rates from these models were lower than the observed rates during the preceding 5-year period when that observed rate was greater than

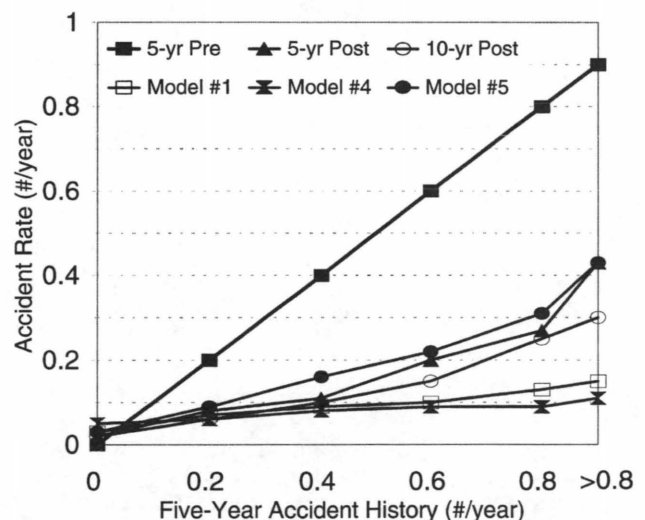


FIGURE 4 Comparison of observed and predicted accident rates for crossings grouped by 5-year accident history.

about 0.05 accidents per year, or one accident every 20 years. Similarly, the predicted rates are greater than the observed rates when the observed rate was less than about 0.05 accidents per year. These patterns imply that the observed accident rate will regress toward the predicted rate during the forecast period. This observation is reinforced by noting that the actual accident rates during the post-5 and 10-year observation periods are regressing toward the predicted rates estimated by Models 1 and 4 and away from the accident rates observed during the immediately preceding 5-year period.

CONCLUSIONS AND RECOMMENDATIONS

On the above findings, it was concluded that the basic accident prediction model (either 1 or 4) is the preferred model for use in the DOT resource allocation procedure because it provides the best estimate of the true long-run accident rate at a specific rail-highway grade crossing. Although some acknowledged hazard influencing variables (such as available sight distance) do not appear in the models, the regression coefficients indirectly reflect the average impact of these factors.

An assertion might be made that, given real-world constraints on decision making and the current confidence in the selection and programming of proposed grade crossing safety improvements, the engineering community should be using the best available models. The authors believe that this research offers a reasonable basis for modifying the recommended DOT resource allocation procedure by deleting the accident history adjustment step and using only the basic accident prediction model (1 or 4) to estimate the expected accident reduction associated with a candidate safety improvement.

Furthermore, the accident history at a grade crossing provides useful information in both the determination of whether a specific crossing is unreasonably hazardous and in the selection of a candidate safety improvement. Because accident history data are gener-

ally available in the national data base beginning with the year 1975, all of this information should be considered, not just that for the immediately preceding 5-year period. If the actual accident rate at a specific grade crossing dramatically exceeds the predicted rate, as estimated by DOT Model 1 or 4, there is clear indication of a unique problem that cannot be accounted for on the basis of a model structure that is limited to a few crossing characteristics.

The prior accidents will also often show a pattern of similarity that can point to a specific deficiency of the crossing that is adversely affecting driver performance. This knowledge will be of help in determining what is causing the problem and how to correct it. In many cases, the appropriate countermeasure will be something other than simply upgrading the type of warning device.

REFERENCES

1. Mengert, P. *Rail-Highway Crossing Hazard Prediction Research Results*. Report FRA-RRS-80-02. U.S. Department of Transportation, March 1980.
2. Hitz, J., and M. Cross. *Rail-Highway Crossing Resource Allocation Procedure User's Guide*. Report FHWA-IP-82-7. Transportation Systems Center, U.S. Department of Transportation, Cambridge, Mass., Dec. 1982.
3. Farr, H. E. *Summary of the DOT Rail-Highway Crossing Resource Allocation Procedure-Revised*. Report DOT/FRA/OS-87/05. U.S. Department of Transportation, June 1987.
4. Berg, W. D. Critique of Rail-Highway Grade Crossing Effectiveness Ratios and Resource Allocation Procedure. In *Transportation Research Record 1069*, TRB, National Research Council, Washington, D.C., 1986, pp. 88-100.
5. Mutabazi, M. I. *Testing Department of Transportation Models for Accident Prediction at Railroad-Highway Grade Crossings*. M.S. thesis, Department of Civil and Environmental Engineering, University of Wisconsin-Madison, Aug. 1991.

Publication of this paper sponsored by Committee on Railroad-Highway Grade Crossings.